Alma Mater Studiorum – Università di Bologna

DOTTORATO DI RICERCA IN

Informatica

Ciclo XXVII

Settore Concorsuale di afferenza: 01/B1 - INFORMATICA

Settore Scientifico disciplinare: INF/01 - INFORMATICA

TITOLO TESI
Cooperative Cognitive Wireless Networks over TV White and Gray Spaces

Presentata da: Luca Bedogni

Coordinatore Dottorato   **Relatore**

Prof. Paolo Ciaccia   **Prof. Luciano Bononi**

Esame finale anno 2015

Abstract

Wireless networks rapidly became a fundamental pillar of everyday activities. Whether at work or elsewhere, people often benefits from an always-on connection. Moreover, this trend is likely to increase in the future, and hence actual technologies struggle to cope with the increase in traffic demand. To this end, Cognitive Wireless Networks have been studied. These networks aim at a better utilization of the spectrum, by understanding the environment in which they operate, and adapt accordingly. In particular recently national regulators opened up consultations on the opportunistic use of the TV bands, which became partially free due to the digital TV switch over. In this work, we focus on the indoor use of of TVWS. Here, interesting use cases like smart metering and WiFI like connectivity arise, and are studied and compared against state of the art technology. New measurements for TVWS networks will be presented and evaluated, and fundamental characteristics of the signal derived. Then, building on that, a new model of spectrum sharing, which takes into account also the height from the terrain, is presented and evaluated in a real scenario. The principal limits and performance of TVWS operated networks will be studied for two main use cases, namely Machine to Machine communication (M2M) and for wireless sensor networks (WSN), particularly for the smart grid scenario.

The outcome is that TVWS are certainly interesting to be studied and deployed, in particular when used as an additional offload for other wireless technologies. Seeing TVWS as the only wireless technology on a device is harder to be seen: the uncertainity in channel availability is the major drawback of opportunistic networks, since depending on the primary network channel allocation might lead in having no channels available for communication. Thus, TVWS can be effectively exploited as offloading solutions, and most of the contributions presented in this work proceed in this direction.

1

Nomenclature

AMI   Advanced Metering Infrastructure

AP   Access Point

BER   Bit Error Ratio

BS   Base Station

CBP   Coexistence Beacon Protocol

CCH   Common Control Channel

CDF   Cumulative Distributive Function

CE   Coexistence Enabler

CM   Coexistence Manager

CPE   Consumer Premise Equipment

CR   Cognitive Radio

D2D   Device-to-Device

DBS   Dynamic Band Switching

DSA   Dynamic Spectrum Access

DSA   Dynamic Spectrum Access

EIRP Effective Isotropic Radiated Power

FEC   Forward Error Correction

FFD   Fully Functional Device

FSK   Frequency Shift Keyring

4

GDB Geolocation Database

GDDDS Geolocation Database Dependent Dependent Station

GDDES Geolocation Database Dependent Enabling Station

LAN Local Area Network

LR-WPAN Low Rate Wireless Personal Area Network

LTE-MTC LTE- Machine Type Communication

M2M Machine-to-Machine

MAC Medium Access Control Layer

MCS Modulation and Coding Scheme

MCS Modulation and Coding Scheme

NB-OFDM Narrow Band Orthogonal Frequency Division Multiplexing

NC-OFDM Non Contiguous Orthogonal Frequency Division Multiplexing

OFDM Orthogonal Frequency Division Multiplexing

PAN Personal Area Network

PANC Personal Area Network Coordinator

PDR Packet Delivery Ratio

PER Packet Error Ratio

PHY Physical Layer

PU Primary User

QEF Quasi Error Free

REM Radio Environment Map

RFD Reduced Functional Device

RLQP Registered Location Query Protocol

RLSS Registered Location Secure Server

RSU Road Side Unit

SCH   Service Channel

SDR   Software Defined Radio

SINR Signal to Interference and Noise Ratio

SSA   Spectrum Sensing Automation

SSF   Spectrum Sensing Function

SU   Secondary User

UHF Ultra High Frequency

VANET Vehicular Ad Hoc Network

VHF Very High Frequency

WLAN Wireless Local Area Network

Acknowledgments

Once you finish a trip, you look at the photos you did, and think about the places you visited and the emotions you had. Once you finish a journey like a PhD, you think at all the effort you put in something in which you believe, at all the discussions you had with people coming from around the world, and the places you visited to talk at conferences and meet professors and researchers. It is a path that changes you, and teaches you to open your mind and try to learn something in all situations. I loved it, and I will start again immediately.

First of all, I would like to thank Professor Luciano Bononi, who has been an invaluable reference for me, both professionally and personally. He guided me through these years, always suggesting and advising me on the best things to do both for my PhD as well as for my professional career.

I strongly thank the reviewer of this thesis, Professor Björn Landfeldt, Lund University, Sweden, and Professor Serge Fdida, Université Pierre et Marie Curie (UPMC), Paris, France, for their invaluable comments that contributed and completed this work.

I would also like to thank Dr. Fabio Malabocchia and all his staff, and Telecom Italia. Having an industry tutor like him, who was always willing to point me to the most interesting topics from an industry point of view, helped me to focus on the hottest and most prominent research areas. Someone once said to me: "It is not important to know the answer. It is instead important to know the question you are answering to". I strongly believe that he always tried to make me think not only on the research, but also on the purposes and on the objectives to pursue.

I would also like to put another special word for Dr. Marco Di Felice, which was always keen to review my research ideas, and who always made me think about my work. I think that the meetings with him contributed consistently in my professional growth.

I'd like to thank Prof. Petri Mähönen, Prof. Marina Petrova, Dr. Andreas Achtzehn, Dr. Nikos Perpinias, Dr. Alexandros Palaios, Dr. Peng Wang, and all the people from iNETS, Aachen University, Germany, for the opportunity

that they gave me. The months that I spent working with them have been amazing, and the advices they gave me, along with the ideas I developed working in a different context, completed my PhD. I really hope to continue to have the possibility to work with them in the future.

I thank Dr. Angelo Trotta for the talks we had during the workdays, and for the brainstorming we had during these years. I wish him the best for his PhD.

I also thank Prof. Tullio Salmon Cinotti. Dr. Alfredo D'Elia, Dr. Francesco Morandi, and Dr. Fabio Vergari, from ARCES, University of Bologna, which have been great colleagues. Their enthusiasm is a constant motivation to come out with new ideas and solutions to the problems we faced.

I also like to thank all the people that I met at conferences and which have been important for my professional growth, speaking and comparing ideas together. Naming them individually would be nearly impossible, so i simple say a thank you all.

I'd really like to spend a few words for my family. Pursuing a PhD is not an easy path, and you really have to rely on a strong support when you switch off the notebook to come home. Having someone that helps you to think at something else, and sustain you when you had a bad day, is fundamental. Papers get accepted and rejected, you can win or lose, but if you have a fix point on which you can rely, you will always have a good day. So I'd like to thank Serena, my fiancee, for her love, and Stefania and Claudio, my parents, which travelled this path with me, and supported me when I mostly needed it. Their help was of paramount importance to me, and most probably it is one of the reasons for which I succeeded in completing the PhD.

Contents

II   Contributions   69

4   Spectrum Measurements for TVWS and TVGS   71

5   Comparison to other wireless technologies   95

6   Per-Floor spectrum sharing   117

List of Figures

List of Tables

Part I

Introduction and Related Work

Chapter 1

Introduction

Wireless communications rapidly became one of the fundamental pillars of today's life. Smartphones, tablets, along with laptops and many different devices, typically communicate wireless. Certainly, new services have been built to ease modern daily routines, and to enhance the possibility each human being has. However, new services and new applications constantly require new wireless spectrum, that it is increasingly difficult to be found, due to a static spectrum allocation. Over the past years, several technologies have been proposed and currently used, like 2G, 3G and, more recently, LTE. However, it is likely to think that as these services will continue to grow, the available spectrum will not be sufficient anymore to cover the spectrum demands. When looking at wireless communication, we are also facing a heterogeneous world, in which several standards and wireless technologies do exist. The coexistence between them is challenging too, since they generally share some spectrum bands, and thus it is important, for the upcoming generation of wireless standards, to focus also on mechanisms that allow the simultaneous presence of a number of heterogeneous devices.

To tackle this problem, cognitive radio technologies have been identified as a possible solution. Cognitive radios (CR) sense the environment in which they operate, and adapt their transmitting parameters accordingly. One of the most studied and appealed features of CR relies on Dynamic Spectrum Access (DSA) , which devices leverage to access portions of frequencies left unused or underutilized by licensed users. To this end, typically it is common to call Primary User (PU) the holder of the rights to transmit on a frequency band, and Secondary User (SU) who access to it opportunistically. .

One band of particular interest, due to their renowned propagation characteristics, is the UHF band, in which it is currently allocated, among the other services, the digital television broadcasting. These spectrum bands, however, present scarce utilization after the digital TV switch over, when

television switched from analog transmission to digital, thus freeing some bands. These spectrum holes are commonly referred to as TV White Spaces (TVWS), and are the main topic of this work.

Several national regulators around the world have already shown interest in these frequencies: for instance, in the U.S. the FCC has published its document about secondary access to TV white spaces [43] back in 2009. In the U.K., also Ofcom has proposed the operational characteristics devices should have to access the TV white spaces [89]. Other regulations are on their way in Singapore, Canada, and other countries in the world.

Even if some differences between the different regulations apply, some points are shared among the proposals, one of which is that secondary devices will need to access a remote database in order to get the list of available frequencies in a given area. The spectrum database has the responsibility to store the list of available channels in all the areas of interest, given the position of the digital TV transmitter. This solution is seen as highly conservative from the SU point of view. Cognitive networks have in fact the ability to sense the spectrum to identify free channels, but since the hidden node problem might end up in marking some channels as free, while instead they are used, regulators prefer to cut off the problem by replacing the spectrum sensing process with a query to the database.

However, the spectrum database could rapidly become a bottleneck for the usage of TV white spaces, given the high number of queries devices can send. In addition, an outdated database could result in a suboptimal usage of white spaces, and a slow responsiveness could make the user to query it again. For these reasons, collaboration through users could alleviate the spectrum database maintenance, allowing at the same time to have more updated information.

In this study we identify some of the key challenges that opportunistic networks in TVWS have to cope with, and analyze them both with theoretical work, as well as with small testbeds and experiments, that show some fundamental aspects that communication in these frequency bands face.

This work is divided in two parts: Part I focuses on the state of the art, analyzing related literature work in Chapter 2, and reviewing standards operating in TVWS in Chapter 3.

Part II is instead focused on the contributions of this work. In particular, new measurements are presented in Chapter 4, carried out in Italy and Germany. Here, we analyzed the differences between indoor and outdoor signal reception.

A comparison between different wireless technologies, with similar use-cases as TVWS, is discussed in Chapter 5. This part is needed in order to understand the boundaries and the limits each technology has, and thus

where TVWS operated networks can be mostly beneficial. In addition, a novel Cognitive Modulation and Coding Scheme adaptation between IEEE 802.11n and IEEE 802.11af networks is presented an evaluated in different challenging scenarios.

Then, specific use-cases are analyzed, like Indoor 3D spectrum sharing, presented and analyzed in Chapter 6. Here we present a novel spectrum sharing model, which also takes into account the height of the device from the terrain. We carry out the analysis both to study the coexistence of SU, and for the TV Gray Space scenario (TVGS). TVGS represent occupied frequencies at the rooftop, possibly free indoors due to shadowing effects. While this behavior is currently not envisioned by regulators, finding communication constraints might free some channels in the future, particularly in dense populated areas, where finding TVWS is challenging. This also represents one of the main drawbacks of TVWS, and most probably one of the key factors that slows the development of TVWS solutions.

M2M communication is studied in the context of TVWS networks in Chapter 7. In particular, the newly published IEEE 802.15.4m is analyzed, and performance figures and constraints are presented and discusses, both for TVWS as well as for TVGS.

Chapter 8 presents the framework of Mobile Femto Databases, built to enhance the availability of Master devices to Slave devices. Simulation results show the benefits that Slave devices gain from multi-hop communication for remote database spectrum queries, and replies caching by master devices to improve the overall latency.

Finally, cognitive networks are also studied in the context of Vehicular Ad Hoc Networks. In particular, an enhanced version of the IEEE 802.11p protocol is presented in Chapter 9, and performance improvements over the classical version are discussed.

Chapter 2

State of the art

In this section, a comprehensive review of the current state of the art is given. The main areas reviewed are concerning the spectrum measurements reports, discussed in Section 2.2, whiel field trials reports are presented in Section 2.3. Coexistence work is taken into account in Section 2.4, while spectrum sharing and spectrum sensing works are reviewed in Sections 2.5 and 2.6, respectively. Finally, two particular use cases are reviewed: one is relative to the smart grid paradigm, and the communication within. The state of the art presentation is given in Section 2.7. Finally, a report on offloading techniques of other technologies to TVWS is given in Section 2.8

2.1   Preliminaries

With the digital TV switch over now finished in most parts of the world, several channels on the UHF and VHF bands are now underutilized and thus available to be reused, constituting the so-called TV White Spaces. National and international regulators such as the FCC [42][43] in the U.S. and Ofcom[88][89] in the U.K. have now published their official statements about the access to TV white spaces (from now on referred to as TVWS) by secondary users.

TVWS is a valuable kind of spectrum, having good propagation characteristics, good penetration through obstacles and house walls, and significantly lower energy needed to transmit data. For these motivations, transmissions carried on TVWS could travel farther than, for instance, Wi-Fi in the 2.4 GHz band.

With TVWS, new applications and services will be deployed, ranging from Super Wi-fi (or Wi-fi on Steroids) [5], to M2M communication [14], smart metering [10], and many others. One case of particular interest is

the use of TVWS for fixed wireless services on area characterized by digital divide, like rural ares. Operators often choose not to install base stations that could make this areas connected to the Internet, and this is usually done for high costs, since installing and maintaining a whole infrastructure is expensive compared to the potential revenues. TVWS could instead bring reliable, low power and low cost connectivity even in those areas, with fewer base stations built by operators and thus with lower expenses.
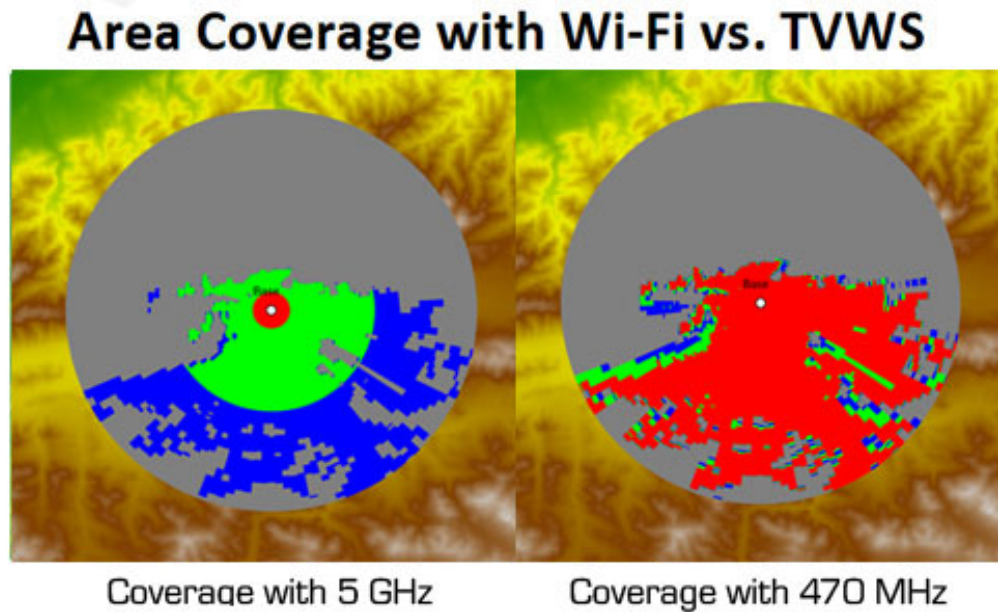
Figure 2.1: Coverage density between 5 GHz Wi-Fi and TVWS Wi-Fi. Image courtesy of Carlson Wireless http://www.carlsonwireless.com/solutions/tv-white-space-rural-broadband.html

In figure 2.1 it is shown how different TVWS are compared to existing wifi technologies in the 5 GHz band in terms of coverage. The Figure shows a propagation radius of 25 miles, highlighting the covered areas, where red areas show better coverage compared to blue and green areas. It is straightforward to note that TVWS propagate better through buildings and obstacles compared to higher frequencies. In rural areas, this is not a fundamental issue, as there is a lower density of buildings compared to urban and sub urban areas. Still, TVWS can achieve a higher range than other technologies, and thus can transmit farther than, for example, WiFi. In addition, rural areas usually experience a higher availability of TVWS [30] [111], given the fact that less primary users are typically involved in transmissions. Using higher frequencies would require the installation of many high base stations, while

using TVWS it is possible to leverage the advantages of lower frequencies and propagate signals even in irregular terrains and through foliage and buildings.

In recent studies [12] [87] it is shown that using TVWS, it is possible to cover a large area even with low transmission power, thus improving in-house coverage. Several studies have also been conducted on coexistence in the TVWS [4] [22] [51] [113]. Coexistence means not interfering with others in the same band as well as not interfering with other users in adjacent bands, by adjusting each one transmitting power.

The FCC and Ofcom also stated that opportunistic users of TVWS should not interfere with incumbent licensed users of the spectrum. This is to prevent interferences and thus transmission problems to tv broadcaster that have payed for the use of the spectrum. TV broadcasters transmit signals at very high power, covering a large area. Since they are stationary, there are mainly two approaches that could be used and are proposed to detect their signals. The first is a Listen Before Transmit approach, in which opportunistic users should sense the channel before transmitting on it, and if they sense a licensed communication, they should immediately move to another channel and run again the sensing part. The second option take advantage of the fact that these transmitters are static, and thus a geolocation database containing all the positions and ranges of these transmitter could help in identifying and preserve their signals [4] [23] [35].

Another kind of device that should be protected by interferences are wireless microphones, that typically transmit on the same bands. This kind of devices are usually hard to identify, since they could transmit in a sporadic way, at low powers, and thus making harder the task of recognizing their signal. Wireless microphones can also register in the database, to gain protection from the secondary transmission. However, this might become unhandy for sporadic operations, but can be a viable option for theaters, sport events, and public meetings. Apart from being registered in the database, two different approaches have been proposed for detecting wireless microphone signals, and they are the Listen Before Transmit, in which a white space device need to sense the spectrum, and if and only if it doesn't detect a microphone transmission, then the channel is free, and the other method is by beaconing, by which microphones should periodically transmit at higher power a short message, to indicate that a channel is being used, thus avoiding opportunistic users to interfere with their transmission [6] [26] [50] [52] [54].

Finally, some medical telemetry devices use channel 37 to transmit data [103], and thus this kind of communication should be protected. The industry and the FCC have agreed on preserving this kind of communication by limiting the usage of channel 37 for opportunistic use, and posing severe restrictions on adjacent channels 36 and 38 [37].

Several protocols have already been proposed for operating in the TVWS, including the IEEE 802.22, IEEE 802.11af, IEEE 802.15.4m, Weightless, Sigfox, and the ECMA 392.

To operate in those frequencies, several constraints and considerations should be taken into account. The major constraints come from the regulators, which impose a plethora of different restrictions on how devices should operate in TVWS. The first and most important of these restrictions is that unlicensed devices should not cause harmful interference to the band licensee. In fact, even if most of the frequencies are underutilized, several TV operators still transmit in these frequencies, and thus this communications should be preserved by devices which will access the spectrum in an opportunistic manner. In addition, also microphones and medical equipment transmits on the same frequencies, and have different powers so their communications are harder to spot and recognize.

To overcome this problem, a proposal is to use a geolocation database which contains all the available frequencies for every location. An unlicensed device which wants to access the spectrum in an opportunistic manner should firstly contact the database and retrieve the list of available frequencies in that area, and then it can transmit on one of those available frequencies. Having to contact an external database means that devices should be connected to the Internet to access this information, something that is not possible everywhere. Thus, another option is to rely on spectrum sensing, listening to the spectrum and deciding if a PU (Primary User, a frequency licensee) is actually transmitting on that frequency. If not, then the device marks that frequency as white space and could eventually transmit on it. With spectrum sensing other problems come out, like the hidden terminal. It is also important to note that the hidden node problem in TVWS is experienced in a different manner compared to other wireless technologies. TV antennas are highly directional, thus with a high gain, and this contributes to the ability to decode signal received at low powers. Thus, sensing those signals for devices with isotropic antennas becomes even more challenging.

Another major issue in accessing the TVWS frequency spectrum is about the MAC layer. It is not sufficient to determine which frequencies are free and then transmit on these. Coordination among the unlicensed devices is advisable, since these devices are not registered in the database and could decide to transmit at any time, thus resulting in interferences and worse communications. By coordinating, the whole system could benefit in terms of throughput and interference mitigation.

Other considerations and further studies should be done on the mobility side, given to the fact that many of the TVWS devices might be mobile, and

thus spectrum sensing and spectrum decision should consider mobility related issue while working. For instance, devices near in the space could experience different sensing results, caused by obstacles, fading and shadowing effects. It is then important to cooperate accounting the mobility, resulting in higher probabilities of successfully detecting PUs signals.

One possible application for TVWS is the M2M paradigm, in which the communication happens between two devices, and not between a device and a base station. This kind of communication is well suited for applications like smart metering and short data messages. M2M devices should usually last several years, and thus energy efficiency is crucial in designing protocols and applications. Nowadays, M2M communication is usually realized using cellular technology. One possible example is the smart metering, in which utilities monitor the consumptions of customers by it to in-home smart meters. However, cellular communication relies on an existing infrastructure which may not be always present. M2M communications over white spaces don't need any kind of infrastructure but the one needed for the provider, and thus are one valuable alternative to cellular M2M communications. For these reasons, M2M communications without using any cellular infrastructure are commonly referred to as capillary M2M networks. Another major reason to switch M2M devices from cellular to TV white spaces is for scalability reasons. Given the predicted growth of M2M communications in the next year, the global thought is that cellular technologies will be overcrowded and consequently not able to deliver the same services as before. By offloading M2M communications to the UHF band, both the cellular operators and M2M devices will benefit from a consistent amount of precious spectrum with better propagation and also less energy consuming.

2.2 Spectrum Occupation

Much work regarding TVWS is devoted to spectrum measurements. Estimating the effective utilization of TV bands is mandatory to assess the economic viability and technical feasibility of secondary networks operating in TVWS.

Even though in Cognitive Networks over TVWS the spectrum utilization, which translates into the available channels, is given by the remote spectrum database, it is still important to determine their accuracy, and possible additional spectrum holes. Thus, to determine the spectrum usage, and quantify the benefits deriving from the introduction of TVWS, two kind of works can be found in literature, namely `Spectrum Measurements` and `Analytic Studies`.

2.2.1   Spectrum Measurements

Spectrum measurements are realized by identifying an area of interest, and by performing one or more measurement in the bands of interest. This is done to obtain the spectrum utilization, and thus assess the communication opportunities. They are typically costly, given the expensiveness of the measurement instrumentation to use to sense potentially low powers, and the cost of the specialized personnel to employ, and also time consuming, since they can last for days. Nevertheless, they are precise, and highly considered in the research community, which rely on the measurement results to perform economical studies, feasibility researches, and testbeds.

Generally speaking, it is hard to find works that study large areas, since it is easier and more beneficial to have detailed measurements in a small area, rather than having coarse readings over larger areas, where analytical studies with propagation model can be employed.

2.2.1.1   Europe

Table 2.1: Spectrum Occupancy for cities in Europe

Area	Band	Scenario	TVWS Free percentage	Reference
Bucharest	25 MHz-3.4 GHz	Outdoor	40%	[75]
Aachen	20 MHz-6 GHz	Outdoor	nearly 100%	[117]
Aachen	20 MHz-6 GHz	Indoor	32%	[117]
Barcelona	75 MHz-7.075 GHz	Indoor	33.7%	[93]
Barcelona	75 MHz-7.075 GHz	Outdoor	61.81%	[93]

In [75], the authors perform a spectrum measurement campaign in the city of Bucharest, Romania. The examined spectrum band is quite wide, but for the TVWS case they report a usage of 40.02% between 470 MHz and 766 MHz, and 12.30% between 766 MHz and 880 MHz. To be conservative, we can say that the occupation is roughly 40%, although certainly lower.

[117] reports the results from a spectrum measurement campaign performed in the city of Aachen, Germany, where the authors focus on a wide band of interest, both indoors as well as outdoor. Unfortunately, they report spectrum occupancy percentages only for the whole band, which is nearly 3 GHz, and thus it is hard to understand the TVWS availability. The values reported are nearly 100% for the outdoor scenario, reduced to 32% while indoors. However, we note that these results should not be considered specifically for TVWS, since the examined band is too wide, and consequently is

impossible from the data provided to assess the numbers restricted to TVWS.

Other measurements are contained in [93], which reports the results of a measurement campaign carried out in Barcelona. Here, both indoor as well as outdoor measurement location are reported. However, the blocks in which the authors divided the measured frequency span are wider compared to the TVWS scenario, and the nearest one is the 75 MHz-1 GHz, which reports a utilization of 42% for the outdoor scenario, and 33.7% indoors. Other 10 measurement points are presented in the paper, which show an average channel occupancy of 63.8%, with a minimum of 16% and a maximum of 85%. Thus, the overall outdoor utilization is 61.81%. The heavy differences experienced are due to the building displacement, which shadows the signal in some locations, where other points have LOS with the transmitter.

2.2.1.2   North America

Table 2.2: Spectrum Occupancy for cities in North America

Area	Band	Scenario	TVWS Free percentage	Reference
Chicago	30 MHz-3 GHz	Outdoor	6% (check)	[79]
Chicago	30 MHz-3 GHz	Outdoor	nearly 40 %	[108]
Dallas	450 MHz	Outdoor	25 %	[28]

In [79] and [108], two measurements studies for Chicago are shown. The spectrum band of the experiment covers the TVWS range, and one of them reports a 6 % of free channels in the explored area.

In [28], the authors perform a study while driving on a highway near Dallas, and measuring the received signal strength in different spectrum bands. They show that the spectrum utilization is directly proportional to the population density, ranging from a higher utilization in Dallas downtown, to a greatly reduced occupation in the visited rural area. Then, they use this data to calculate the number of needed access points to cover an area with a given population density, showing that when the population density is low (i.e. 20, 50, and 100 People per km^2 in the paper), the use of TVWS can greatly reduce the number of deployed APs.

2.2.1.3   Asia

In [122], the authors perform several measurements in Hong Kong. They find more than 50% of free channels in their measurement campaign, although they experience several variations in different areas of the city.

They also perform indoor measurements, and find more than 72% of free channels. This is mainly due, as also identified by the authors, to the high shadowing experienced by indoor signals, which lowers the signal to undetectable levels. They report a 18.4% increase of free channels indoors compared to their outdoor measurements, or 7.7 more channels, a total of 62 MHz of additional spectrum.

In [121] the authors report measurements done in the province of Guangdong, China, in a total of 4 locations. For three of them, results for the TV bands are reported, which are 92.1% for a urban area, and 44.5% and 41.9% for the two suburban areas, thus averaging at 43.2%.

In [62], the authors study the case for Singapore, and perform wide-band spectrum measurements, from 80 MHz to 5850 MHz. They find out that the spectrum occupancy in Singapore is quite low, 49.05% between 174 MHz and 230 MHz, and 52.35% between 490 MHz and 614 MHz.

Measurements from [64], performed in Selangor, Malaysia, report results in the 174 MHz-2.2 GHz band. Low utilization of the tv band is showed, with a 10.92% utilization for the VHF band, and 13.36% for the UHF band. Given the fact that the measured VHF spectrum is 56 MHz, and the UHF measured band is 328 MHz, we compute the overall availability as $\frac{56 \cdot 10.92 + 328 \cdot 13.36}{384} =$ 13%, which is a very scarce utilization of the spectrum.

Table 2.3: Spectrum Occupancy for cities in Asia

Area	Band	Scenario	TVWS Free percentage	Reference
Hong Kong	470 MHz-806 MHz	Outdoor	50%	[122]
Hong Kong	470 MHz-806 MHz	Indoor	72%	[122]
Guangdong	20 MHz-3 GHz	Outdoor	92.1%	[121]
Guangdong	20 MHz-3 GHz	Outdoor	43.2%	[121]
Singapore	80 MHz'5.85 GHz	Outdoor	nearly 50%	[62]

2.2.1.4   Africa

Not many studies reports measurements in the TVWS in Africa. In [78], the authors perform spectrum measurements between 50 MHz and 1 GHz, in three different cities, two of which are in rural areas. Unfortunately, the authors do not report the actual occupancy. However, looking at the charts they provide, it is evident the scarce spectrum utilization experienced.

Table 2.4: Spectrum Occupancy for cities in Africa

Area	Band	Scenario	TVWS Free percentage	Reference
Pretoria	50 MHz-1 GHz	Outdoor	medium	[77]
Philipstown	50 MHz-1 GHz	Outdoor	high	[77]
Macha	50 MHz-1 GHz	Outdoor	high	[77]

2.2.2 Analytical Studies

Analytical studies are realized with wireless propagation models, applied to the position and radio characteristics of the transmitters in the area of interest. They become important when no extensive measurements are to be found, or when the area of interest is too big, and measurements become unpractical.

Here, two works emerge, presented in [55] for the U.S.A., and [111] for Europe.

2.2.2.1 U.S.A.
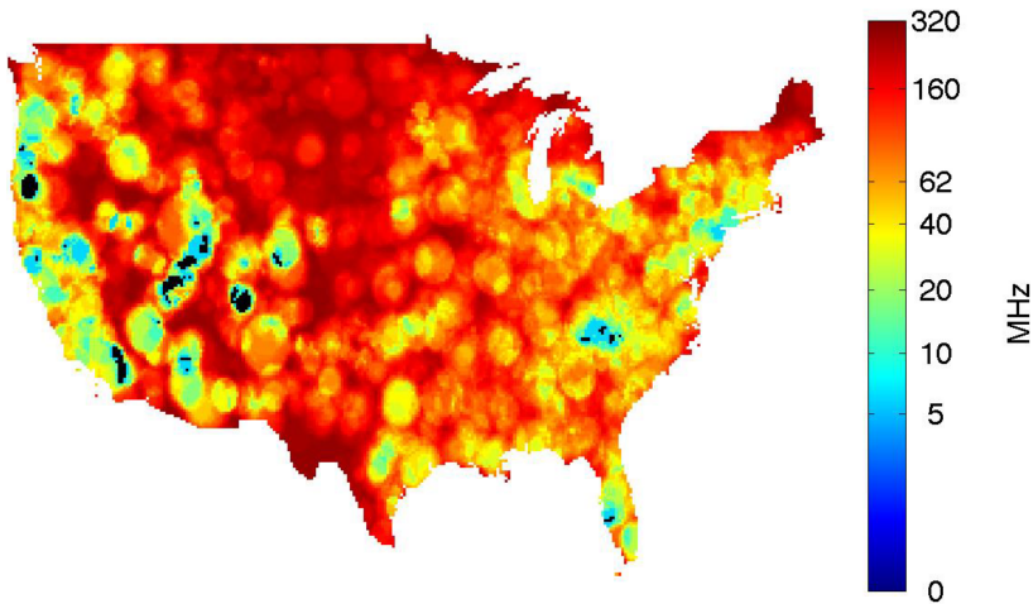
Figure 2.2: U.S.A. TVWS Availability. Image Taken from [55].

In [55] it is contained a wide study for the case of the United Stated of America. The analysis is twofold: at first, they determine the system wide

Table 2.5: Available channels, taken from [57]

Device Type	LVHF	HVHF	LUHF	Total
Total	2.36	2.59	21.77	26.73
Fixed devices	2.36	2.59	15.2	20.17
Portable/Personal	0	0	18.79	18.79
Microphone	2	0	2	4
Busy channels	0.45	2.22	10.43	13.11
Unused	2.18	2.19	4.67	9.05
Percentages	56%	68.7%	87.4%	81.5%

capacity and characteristic of secondary networks on TVWS for the U.S.A..
Then, they focus on a user-centric perspective, by computing the Mbps per
person that can be achieved when operating in the TV bands. The outcome
of the study is that TVWS can be effectively utilized in rural areas, which
experience *"ridiculously high capacities possible for a single link"* [55]. When
focusing on the single person, however, it is possible to see that very few
people can get the highest data rates. Thus, in denser populated ares TVWS
can be utilized only for low data-rate connections. The concluding remark
from the authors is that it would be greatly beneficial from a communication
point of view if the tv channels are taken out from the DVB-T providers, and
allocated to telecom operators, instead of be used in an opportunistic way
and with different available channels. However, this would need a complete
refarm of all the frequencies, which is expensive and technically hard.

[57] contains a similar analysis, using the Longley Rice propagation model,
for the U.S.A.. An interesting result provided by the authors is the percentage
of available channels based on the device type, which we report in Table 2.5.
Mobile/Portable devices cannot use the VHF band, which is reserved for
Fixed devices. Thus, they experience a lower number of available channels,
compared to Fixed devices, even though they experience about 3.5 more
available channels in the UHF band, mostly tanks to the reduced transmission
power.

If we compare these results with the one offered by Google, which is one of
the licensed database provider, we can see how reliable the analytical studies
are, since no enormous differences can be found. In Figure 2.3 we plot the
results of a query to the remote spectrum database concerning the whole
U.S. area, and it is possible to see the similarities between Figures 2.2 and
the latter.
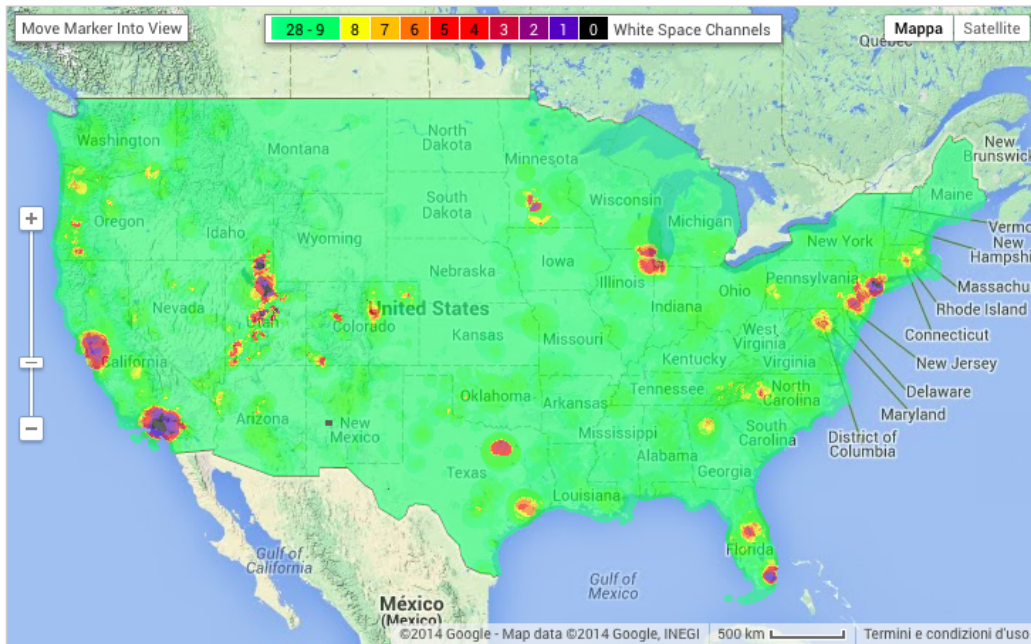
Figure 2.3: U.S.A. TVWS Availability. Image Taken from the Google Spectrum Database.

2.2.2.2 Europe

In [111], the authors focus on finding the occupancy in the TV bands for the European scenario. They perform a quantitative analysis on the network performance that can be obtained in different European countries. Then, they focus on the case for Germany, in which they show additional performance metrics and case studies. Europe differs from the U.S.A. scenario, in which there are vast rural areas that can greatly benefit from TVWS, since few channels are occupied, and thus more spectrum is available for secondary operation. One of the results of the study is that in the 11 European countries taken into considerations, which are Austria, Belgium, Czech Republic, Denmark, Germany, The Netherlands, Luxembourg, Slovakia, Sweden, Switzerland, and United Kingdom, an average of 56% of TVWS can be found, compared to a much bigger 79%, as found in [81]. The concluding remarks of the authors states in fact that in Europe TVWS are less abundant compared to the U.S.A., and this is due to the different population density. Another analysis carried out in [111] is on the protection distance, which plays a major role in the availability of spectrum for secondary access.

A smaller study, focused on the Peloponnese region in Greece, shows the possible TVWS performance in the region [73]. Mostly interesting here
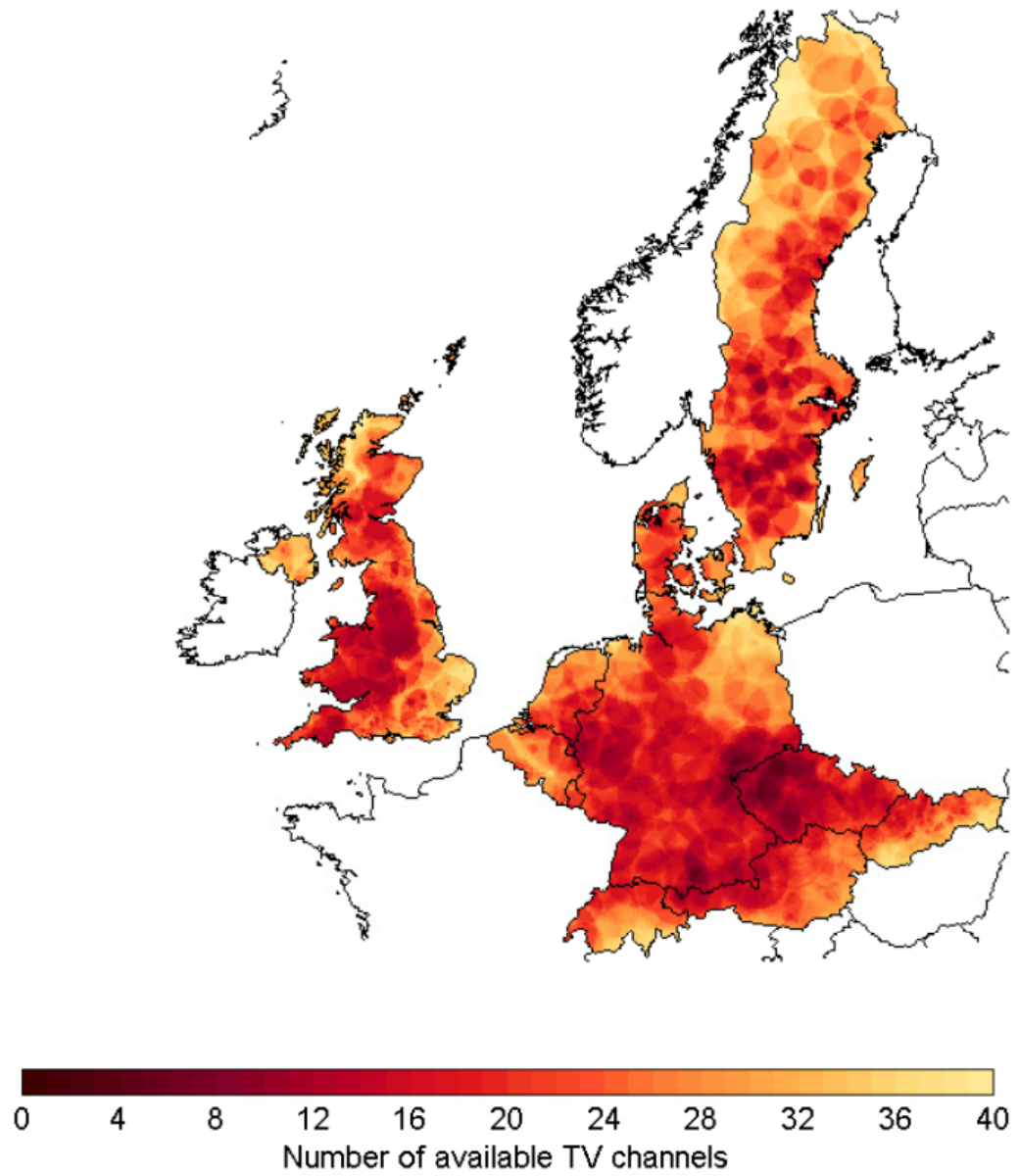
Figure 2.4: Europe TVWS Availability. Image Taken from [111].

is the explanation of a step-by-step methodology to analytically assess the availability of TVWS in a given region. The outcome of the study is the average of available spectrum in the studied region, which is reported as 125 MHz.

Focusing on the U.K., the study reported in [83] reports an average of 150 MHz. Moreover, another interesting result is the fact that in more than the 90% of locations, there would be at least 100 MHz of spectrum available for cognitive networks.

2.3 Field Trials

Figure 2.5: Worldwide TVWS Trials

Trials anticipate a real network deployment in a target scenario. In the past years, an increasing number of tests have been performed through the world, particularly in the U.S, U.K., and Africa, targeting key use-cases such as the rural broadband. They are typically run by private companies and regulators, sometimes with the help of universities. Although specialized, they can give a real idea of the potentials of the network deployment, and focus on real usage patterns. Thus, they are highly representative of the achievable performance of a possible utilization of TVWS.

Figure 2.5 shows the worldwide trials, planned and completed. As it can be seen, there are several ongoing projects, focused on different scenario, ranging from rural areas to M2M, and broadband service extension. Trials activity coincide with the standardization and regulation efforts, since most

of them are located in the U.S.A., U.K., Africa, and Singapore, which are the pioneering countries in developing TVWS networks.

2.3.1   Field Trials in the U.K.

In June 2011, several telecommunication companies, media industries, and global partners, organized a consortium to test the effectiveness of TVWS network deployments. The targeted use-cases were:

- Broadband wireless access in rural and low-populated areas

- Data offloading in urban areas

- Applications related to the smart city concept

The trail took place in Cambridge, UK, which experience a high number of vacant TV channels, and a relatively flat terrain. One of the key reasons that gave birth to the consortium and to the trial was to assist and help Ofcom in issuing the regulation on opportunistic usage of the TV bands.

The key finding of the trial, as also summarized in [24], are as follows:

- TVWS is flexible, in the sense that it meets the requirements of a number of applications, and can thus be adapted to cope with the different communication constraints and QoS requirements.

- There is a high TVWS capacity that can be exploited, dependant on the scenario and on the target application.

- The geolocation database can be effectively used as a secure method to obtain channel availability information. It is practical, it can incorporate PMSE information, and is relatively simple to implement and to access. The database can also help in performing frequency switching, by changing the relevant information in it, and accommodate temporary changes in the frequency plans. It is also foreseen as a secure method to offer protection to the primary users.

- DVB-T receivers experienced some problems regarding the interference generated by TVWS devices, and this should be taken into account when calculating protection contours. However, no serious reports by nearby houses are reported.

2.3.2 Field Trials in Africa

Africa experienced a vast set of pilots and trials, one of which was performed over a six month period, from March 2013, in the Western Cape [71]. One of the main objectives and results was the provision of broadband Internet access to ten schools in Tygerburg to the Stellenbosch University Faculty of Medicine and Health Sciences' hospital. Three BS were attached to the hospital, and one terminal was installed in each one of the ten schools. The network deployment can be seen in Figure 2.6.
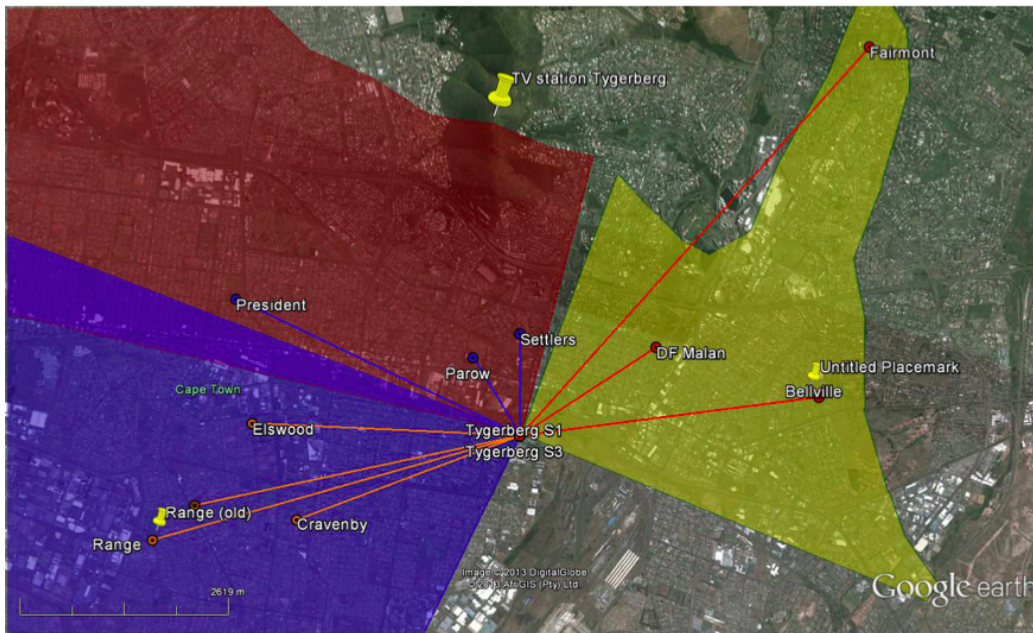
Figure 2.6: Tygerburg trial network deployment

The most notable outcome of the trial from a technical point of view is the estimation of the protection distances between secondary and primary networks. To summarize the results:

- The interference from any WSD devices, the schools of the trial, is contained between 50-200 meters from the position of the WSD.

- If large scale TVWS deployments are used, mesh-like network deployments should be planned, to allow the use of repeaters and thus reduce the EIRP of each WSD.

- Low power and short range device can be effectively deployed and used without noticing any significant interference to the primary network, given the shadowing and the relatively low emission powers.

2.4   Coexistence

Over the past years, several work has been carried out regarding IEEE
802.11af, and WLAN over TV White Spaces. In [101], the authors present a
study in which they show the benefits WLAN on TVWS can have. Basically,
they show that there is a tradeoff between range and throughput. Clearly,
WLANs operating in the TV bands have attractive characteristics, like the
coverage range, and less energy needed to transmit. However, this directly
lead to more devices in the same coverage area, which eventually results in
a more challenging interference environment. In particular, the study of co-
existence mechanisms gained a lot of attention by industry and academia in
the recent years. Since different standards for opportunistic communication
in the TV White Spaces are now published, like IEEE 802.22 [104], IEEE
802.15.4m [47], Weightless [115], and of course IEEE 802.11af, methods to
guarantee the coexistence of different devices, operating on several protocols
in the same bands, must be deployed. We highlight here [9] [51] [65] [112]
[114], which focus on the coexistence between different technologies operating
in the same bands. In particular, [65] studies the performance degradation
of IEEE 802.22 when a 802.11af network is operated in the same area. The
problem becomes even bigger when the 802.11af network is located near a
802.22 user equipment, since both networks perceive a strong interference
from the other one, and thus network synchronization becomes mandatory.
One possible solution is the Coexistence Beacon Protocol [56], studied for
802.22 networks, which foresees the exchange of a periodic beacon to retrieve
the neighboring and possibly interfering networks.

The IEEE also proceeded to standardize the IEEE 802.19.1, which aims
at developing methods to enable coexistence between different technologies.
The standard defines the Coexistence Manager (CM), which can be seen as
the central entity of the whole standard, in charge of discovering other CMs
and provide information to the TVWS devices. Another entity is put be-
tween the CM and the secondary network, called Coexistence Enabler (CE),
which should translate the instructions received by the CM into operational
parameters to be fed to the network.

2.5   Spectrum Sharing

Wireless communication are shared by nature. The wireless channel is the
same for everyone, and thus it is mandatory to find methods to share the
spectrum. In cognitive networks, this becomes even more important, as there
are at least two classes of users, primary and secondary, and the frequency

spectrum is usually wide.

Two general architectures emerge, and those can be `centralized` or `distributed`.

- **Centralized Spectrum Sharing** - In Centralized Spectrum Sharing architectures, the spectrum is managed by a central entity, often referred to as the `Spectrum Coordinator`. The spectrum can be leased to clients in a competitive way, in the sense that the same channel information is given to all the clients, or controlled, meaning that the `Spectrum Coordinator` grants access to a specific channel for a certain amount of time.

- **Distributed Spectrum Sharing** - Each node performs decision based on local information and observations, and optionally cooperate with other nodes. Cooperation is better in terms of recognized spectrum holes and communication opportunities, but involve more messages exchange, and thus overhead and energy consumption by the nodes.

2.6 Spectrum Sensing

Even though in Cognitive Wireless Networks over TVWS the spectrum sensing step is not mandatory, replaced by the database, the research community did a lot of work on efficient and reliable techniques to determine the presence of other networks. This has effects on the detection of other secondary networks, which can thus be protected by the interference, and the detection of wireless microphones, which share the same bands. It is not mandatory for wireless microphones to register in the database, but they should be treated as primary users by any secondary network. Thus, it is also important to recognize whether a microphone is transmitting, and protect it.

In literature it is possible to find two main solutions that address this problem, namely `Energy Detectors`, and `Eigenvalues Detector`. A particular case is for Wireless Microphones, which have a smaller bandwidth and are generally not registered in the remote spectrum database.

2.6.1 Microphones

Wireless Microphones sensing represent one of the most challenging task for networks in TVWS. The transmit over a bandwidth of 200 kHz, in the UHF bands, even though most of the energy is typically concentrated in a 40 kHz bandwidth. The maximum power is rather low, but with such a narrow bandwidth the coverage can reach up to 500 meters.

2.6.2   Energy Detectors

The energy detector decides whether a microphone is transmitting based on the amount of energy received. These algorithms typically have a threshold, above of which the presence of the microphone is detected. They are very simple to realize, but present several issue.

The first problem is the fact that it is impossible to actually detect a PU signal, but only see the channel as occupied. As a consequence, it is impossible to distinguish between a PU signal and a (competing or cooperating) SU signal. However, if both networks share the same protocol, it is possible to use beaconing to announce the presence of a secondary network, with the introduction of additional overhead.

The second problem is how to set the threshold at which a microphone is detected. Low threshold would make the system more safe, in the sense that it is easier to find microphones, but at the same time it would increase the number of false negatives, due to noise and fading. On the inverse, a higher threshold might fail to recognize far microphones, or struggle in dense scenarios with obstacles.

The third problem comes from the fact that it might be hard to reach a decision in short times. Thus, longer sensing times or multiple iterations need to be used, which might significantly reduce the time devoted to data transmission, eventually reducing the throughput of the network.

2.6.2.1   Definition of Energy Detectors

Given a signal defined as $y(n) = x(n) + w(n)$, where $x(n)$ is the signal component and $w(n)$ the additive White Gaussian noise, it is possible to define the test statistic T as [100]:

$$T = \frac{1}{M} \sum_{m=1}^{M} y(m)y*(m) \tag{2.1}$$

The test statistic T is then compared with a threshold, picked to meet the false positives and false negatives constraints of the application.

The energy detector module, however, relies on the previous knowledge of the noise power. Not knowing a priori the noise power on the bandwidth M is called noise uncertainty, and its effects are depicted in Figure 2.7 taken from [100].

The probability of missed detection P_{MD} falls rapidly when the noise uncertainty is $0\,\text{dB}$, but when it is higher it is more challenging to correctly detect the sensed signal.
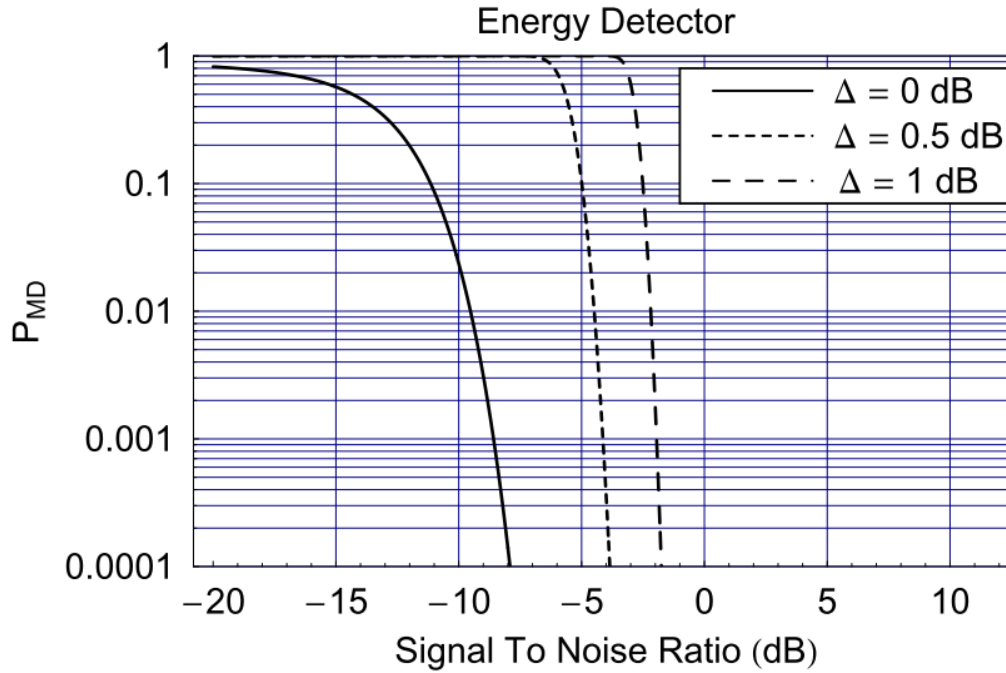
Figure 2.7: Effect of noise uncertainty in Energy Detectors. Image taken from [100].

2.6.3 Eigenvalues Detectors

Another technique utilized is to use the Eigenvalues of the correlation matrix. As a first step, the detector determines the autocorrelation function of the received signal. Then, after the Eigenvalues are detected, they can be used with different techniques, such as the ratio between the highest and the smallest one.

2.6.4 Cyclostationary Detectors

Cyclostationary Detectors exploit the periodicity and repetitiveness of the received signal, in terms of pilot tones, hopping sequences, and sinusoidal carriers. Cyclostationary detectors can effectively distinguish between noise, which is non periodical, and signal, which instead shows high degrees of correlation between consecutive measurements, and some unique characteristics that make it easier to be recognized. Thus, when experiencing low SNRs, cyclostationary detectors usually perform better compared to energy detectors, at the cost of an increased complexity and to know a priori the characteristics of the signal to recognize.

2.6.5 Cooperative Spectrum Sensing

To mitigate the hidden node problem, and to speed up the sensing times, cooperative spectrum sensing is foreseen as a viable alternative. Here, nodes exchange information about their measurements, and each one takes a decision on the channel condition. Compared to other local detectors, cooperative spectrum sensing involves more overhead, since message have to be exchanged by nodes. This also translates into an increased delay for the communication, and more energy consumed by each node that participates in the process. However, all the approaches for cooperative spectrum sensing face the problem that nodes should not be spatially correlated, and at least one of them should be in a favorable position with respect to the signal coming from the PU, to report a more reliable sensing result compare to the others.

Three main architectures for cooperative sensing are identified in [4], shown in Figure 2.8:

- Centralized Cooperative Sensing

- Distributed Cooperative Sensing

- Relay Cooperative Sensing
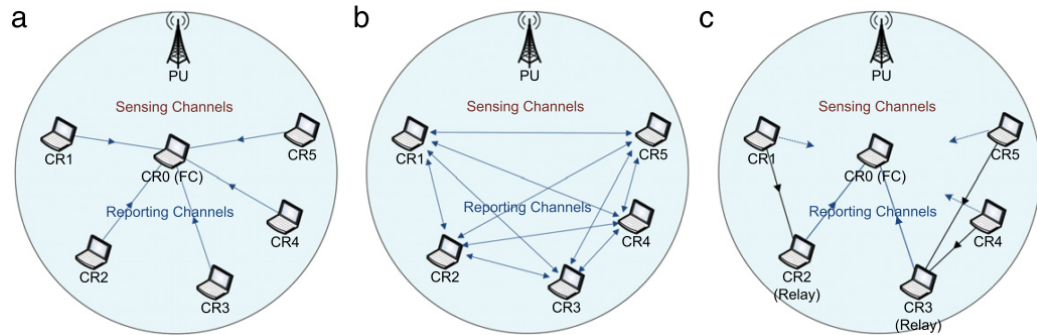
Figure 2.8: Cooperative Sensing Architectures: (a) Centralized, (b) Distributed, (c) Relay. Image taken from [4].

2.6.5.0.1 Centralized Cooperative Sensing In Centralized Cooperative Sensing, it is foreseen the presence of a centralized entity, that manages the spectrum sensing process. It instructs the other devices on which channels to sense, merge the readings together, and communicate the decision. Here, two different decision schemes emerge, namely the `Hard Decision` and `Soft Decision`. When using the `Hard Decision` scheme, the central entity

decides based on the local decision of the nodes. Basically, each node decides whether any given channel is occupied or not, and reports this to the central entity. Finally, the central entity, given all the local decisions, decides whether the channel is occupied or not, based on some voting rule such as the majority rule, AND rule, OR rule and so on.

2.6.5.0.2 Distributed Cooperative Sensing In Distributed Cooperative Sensing, no central entity exist, and everything is left to the devices, which must exchange information and reach a global consensus on the presence of a PU.

2.6.5.0.3 Relay Cooperative Sensing A third architecture is Relay Cooperative Sensing, in which not all the nodes can communicate between each other, and consequently a multihop communication is used. This can become an advantage in noisy environments, where it might be hard to find a common control channel to send the reports, and thus relay nodes can be used.

2.6.5.1 User selection

In cooperative sensing, it is not mandatory that all the users should take part in the sensing process. For instance, when experiencing correlated shadowing, it is better to select independent user to take part in the process. Generally speaking, it is possible to select users either in a centralized manner, or distributively. In centralized user selection, a centralized entity selects the best users for the next round or sensing, based on the measurements received in the last iteration [99]. When performing distributed user selection, clusters emerge, and user are bind together based on any given metric, like their spatial correlation, or to maintain similar cluster sizes.

2.7 Smart Grid and Smart Metering

Although not specifically related to telecommunication research, the new and upcoming scenario of the smart grid is considered to become one of the most promising communication network for WSN and M2M. Up to now, smart meters only rely on cellular communication to report their readings to a central coordinator, but in the future, however, more sophisticated network architecture can be planned. Here, TVWS can find a prominent use-case, given the fact that typically smart meters are indoors, in cellars or in the basement, where shadowing effects highly degrade the transmitted signal.

Moreover, the cellular deployment is scarce in rural areas, and thus it might be difficult to have a good coverage. In addition, M2M are envisioned, and those are difficult to be realized on cellular networks, where it is always envisioned that the communication should be relayed by the macrocell, even though LTE-A introduces Machine-type communication (LTE-MTC [1]) [120].

Still, one of the main advantages that TVWS communication would bring to the communication in the smart grid is the so-called last-mile coverage, because it would be larger compared to the already mentioned cellular communication. As a consequence, less infrastructure would be needed. Depending on the frequency used, and the propagation environment, the advantages can be up to 40 times more coverage compared to other solutions [91]. However, recently cellular communication also foresee the use of frequencies in the 700 MHz range, which will bring the benefits also for this kind of wireless technology.

[86] points out that new protocols need to be deployed, since the traditional TCP/IP communication is shown to be inefficient for M2M communications, given their redundancy which translates into higher energy consumptions. M2M communication typically demand few data to be transmitted, and thus specific protocols that leverage on this assumption must be defined and evaluated.

In [125], the authors also state that M2M communication devices should be implemented with self-x capabilities, meaning that they have to self-organize, self-configure, self-manage, and self-heal. Since they don't need human intervention, they must also be able to perform network operations and repairs on their own, without maintenance by the network operator or by the installer. This would raise the cost and make M2M communication unattractive to industry. Instead, they must operate autonomously, and also have the possibility to repair the network if any breaks would occur.

In [1] it is reported that in the coming years, the data generated by smart grid related communication would be in the order of thousands of terabytes. Even more, that would be fragmented into millions of devices, bringing up challenges for network synchronization and spectrum access.

Still in [125] it is also pointed out that generally M2M devices are envisioned to be simple, low cost, and their battery (if any) must last for years, possibly tenths of years. This collides with the cognitive paradigm, which is instead more complex than communicating in ISM bands. Thus, heterogeneous networks, composed both by cognitive devices as well as simpler ones are envisioned and could be effectively deployed. The cognition can reside in devices with higher computational power, that can serve simpler devices,

---

[1]http://www.huawei.com/ilink/en/download/HW_259010

in the classical Master/Slave paradigm foreseen in Cognitive Networks over TVWS.

In [105] it is proposed WISEMEN, which stands for White Space for Smart Metering. Clearly, one of the pillars of the communication in the smart grid is the Advanced Metering Infrastructure (AMI), composed of millions of smart meters connected together, exchanging information in order to balance and improve the stability of the network.

2.8 Offloading

TVWS have been actively studied to offload traffic from other networks into unlicensed bands. When experiencing overwhelmed bands, or increasing traffic demands, TVWS can be effectively used to bring additional spectrum and mitigate the spectrum scarcity problem.

More in detail, it is actually foreseen the offload of LTE traffic in the TV bands, to increase the range both in terms of coverage holes and spatial extension. Also, in public events such as music concerts, sport matches, and political debates, having additional spectrum on-demand is actually identified as one of the most promising use cases for TVWS. In these scenarios, there is a high density of users, and data intensive applications like video streaming are typically used. TVWS correlate well mainly due to the better propagation characteristics of TV bands, and the considerably larger number of channels that can be used.

In [74] the authors present an architecture to offload LTE traffic to TVWS. TVWS are presented as promising solution to offload uplink connections, which typically require less bandwidth compared to downlink, and thus free resources at the base station to be allocated for downlink. The authors report peak uplink throughputs ranging from $110\,\mathrm{kb/s}$ to $940\,\mathrm{kb/s}$, depending on the bandwidth used and on the traffic load.

The solution proposed in [107] is to dynamically create hotspots that can tether data over TVWS. This is studied in the case of dense areas, where it is hard to find available bandwidth for cellular communication, and where installing more BS is expensive, and where the communication demands scale with the population density. Although TVWS cannot match the data rates of LTE communication, it can still be beneficial to offload some types of traffic onto it, such as web browsing and user-intensive applications, where the data rate is not important as in video streaming, for instance.

An EU-FP7 project, COGEU, focused on the LTE offloading to TVWS [18] [97]. The project is concluded, and in one of the final deliverables (D 6.4), the project's participants show a study performed in Germany, in the city

of Ramersdorf-Perlach, which has a population density of 5160 person/km^2. They calculate the number of LTE users, and provide quantitative results on the benefits of the LTE extension to TVWS, by using both a conservative database as well as a less conservative one. Clearly, the conservative database provides less channels, but the benefits are still tangible, and show that when communication peaks are experienced, supplying additional bandwidth for opportunistic communication can greatly relief the burden on the licensed band.

In [48] it is proposed an architecture for LTE offloading, based on a study made with REMs, under the EU-FP7 project FARAMIR. The proposal leverages the utilization of REMs to build the spectrum opportunities, and in the paper it is also presented the implementation of the whole architecture on real devices. In the paper is is also shown how REMs can effectively enlarge the availability of TVWS for LTE offloading.

Chapter 3

Background

In this chapter, a fundamental background on regulations and TVWS is given. More precisely, in Section 3.1 a comprehensive review of the two most known regulations is given, namely for the U.S. [43] and for the U.K. [89]. Then, in Section 3.2 the standards currently envisioned for operations in TVWS are described.

3.1 Regulations

In this Section we present and discuss two of the most cited regulations for TVWS: the first one has been written by the FCC for the U.S., and it is going to be presented in Section 3.1.1. The other one has been written by Ofcom, and it is referred to the U.K.. The latter is presented in Section 3.1.2. Both regulations specify that the user need to access to a database before starting to communicate on a TV channel.

3.1.1 FCC

Back in 2004, in the U.S. the FCC published [42] its national plan for opportunistic access to tv frequency bands by unlicensed users. In 2009 [43], further regulations have been made available by the FCC to regulate access by unlicensed users to the TV frequency band.

The FCC defines two different kind of devices: fixed and personal/portable. Fixed devices are static, and can operate up to 4 W using outdoor antennas. They need to be registered in the TVWS database and the antenna height from terrain must not exceed 30 metres. The U.S. regulatory framework allows other than UHF also communication in some portions of the VHF band, but only for static devices . For those devices it is also mandatory to be able

to access the TVWS database before communicating on any tv channel. They can operate in any channel ranging from 2 to 51, except channels 3 and 4, to protect video cassette recorders and digital video recorders, and channel 37, which is reserved for medical telemetry and astronomy. Restricting access to channel 37, there are also strict requirements for using adjacent channels 36 and 38, which also applies in general to any other free channel adjacent to an occupied one.

Personal/portable devices can use channels from 21 to 51, except channel 37, with a maximum power limit of 100 mW. However, the transmission power limit falls to 40 mW if a primary user transmission is detected in an adjacent channel. These kind of devices could operate independently, and in this case they should be aware of their geolocation and they should access the TVWS database prior to beginning any transmission too. If a device is not capable of accessing the database, it could rely on sensing only but it could transmit at 50 mW of maximum power. The FCC classify devices with geolocation capabilities and able to access the database as Mode II devices, while devices that need a Mode II devices prior to access the TV spectrum are classified as Mode I devices.

The sensing threshold is fixed at -114 dBm. This means that if a device sense a primary user signal up to -114 dBm, then the channel should not be used for opportunistic transmission since its occupied by a licensee. Every device should sense the spectrum for 30 seconds before transmitting on any channel, and when the transmission starts it needs to sense the channel once every 60 seconds during its normal operations. At this point, if it detects a primary user transmission, it should leave the channel in less than 2 seconds.

3.1.2   Ofcom

In the U.K., the Office of Communications (Ofcom) is the independent regulator of telecommunications. On the 1st of July 2009 Ofcom published [88] the official statement about opportunistic use of TVWS. Another document by Ofcom came out in 2012 [89], with further policies and improved devices specifications, and is currently under discussion.

Like the FCC regulates in the U.S., also Ofcom stated that they will firstly rely on a database access by secondary users to protect interferences to primary user. For this purpose, each device should have geolocation capabilities, with a minimum accuracy of 50 meters.

However, Ofcom also considered sensing only devices, that is, devices that will not access the database before starting to transmit on a channel. Opposed to the FCC, where the sensing threshold is -114 dBm, Ofcom fixed this threshold at -120 dBm. This is also due to the different channels widths,

with 6 MHz channels in the U.S., opposed to 8 MHz channels in Europe.

Ofcom also reported that devices could eventually rely on cooperative sensing in order to spot primary users' transmission [89]. Cooperative sensing means that devices could collaborate and cooperate between each other in order to exchange information about the current channels status. These techniques focus on reducing the impact that the hidden node problem have on the detection of free channels.

3.2 Standards

In this Section a selection of the most prominent standards for opportunistic networks in TVWS is presented. Several standards have already been proposed to efficiently use the TV bands. These include the IEEE 802.22 WRAN (Wireless Regional Area Networks), the IEEE 802.15.4m for Wireless Sensor Networks, the IEEE 802.11af for WiFi hotspots, ECMA-392, and other standards for M2M communication like Weightless and Sigfox.

3.2.1 IEEE 802.11af

To accommodate WiFi-like transmissions over TVWS, IEEE proceeded to standardize the IEEE 802.11af amendment, specified for opportunistic operations in the tv bands.

The Physical layer of IEEE 802.11af devices is inspired by IEEE 802.11ac networks, in the sense that it uses OFDM, multi-user beamforming, channel bonding, and packet aggregation. An interesting feature of IEEE 802.11af networks is NC-OFDM, which permits to aggregate together channels not contiguous between each other. This feature permits to aggregate together a maximum of four channels, in a maximum of two non contiguous blocks. The channel bandwidth can be either 6 MHz, 7 MHz, or 8 MHz, depending on the telecommunication region in which the network is deployed [46]. This has been done to adhere with the characteristics of the TV band, where it is likely to find multiple channels but not contiguous between each other in the frequency band.

To cope with the requirements imposed by regulators, IEEE 802.11af introduces a channel acquisition method, which describe the queries to be done to the remote spectrum database, which will eventually reply with the channel availability list.

3.2.1.1   Architecture of IEEE 802.11af

From an architectural point of view, IEEE 802.11af defines different entities, which are described in the following:

3.2.1.1.1   Geolocation Database   IEEE 802.11af networks foresee the presence of a remote spectrum database, which can be reached through a data connection, able to provide the list of available channels at a given position. Database operators must firstly register and guarantee several security and operational constraints before being certified as a database provider.

3.2.1.1.2   Geolocation Database Dependent Enabling Station   The GDDES can be seen as an evolved Access Point, capable of accessing the GDB. The GDDES is thus in charge of getting the list of available channels, and provide them to other stations via a white space map (WSM).

3.2.1.1.3   Geolocation Database Dependent Dependent Station   The GDDDS is a normal device, which must act under the control of a GDDES, to which it rely on the list of available channels to use. Thus, it needs to get a white space map (WSM) from a GDDES before starting any communication.

3.2.1.1.4   Registered Location Secure Server   The RLSS can be seen as a small local database, which contains the list of available channels for a limited set of networks.

3.2.1.1.5   Registered Location Query Protocol   The RLQP is the protocol used to communicate between entities in an IEEE 802.11af network, particularly between GDDES and GDDDS to exchange WSMs.

3.2.1.2   Use cases

IEEE 802.11af networks can cover some specific scenarios in which traditional IEEE 802.11 a/b/g/n networks struggle to deliver optimal performance. Penetration losses are less severe in the TV bands, making IEEE 802.11af networks the ideal candidate to deliver high speed connections in dense scenarios, such as large houses, or to offer WiFi connectivity in campus or public events [5] [21].

3.2.1.2.1   Coverage holes   In addition, IEEE 802.11af networks are also a good candidate to cover coverage holes in houses [87]. Here, the better propagation characteristics, as well as the superior penetration through obstacles, can significantly extended the WiFi service where other networks in the ISM bands fail to deliver satisfactory performance. Still, it is harder to think at indoor-to-outdoor networks, since the shielding of the walls degrade the signal, although less compared to ISM bands [10] [12].

3.2.1.2.2   HDTV streaming   More recently, also HDTV streaming has been considered as a possible use cases for WLAN networks operating in the TV White Space [40]. The main reason behind this is the fact that the data rate of IEEE 802.11af networks is more than enough to deliver HD videos, thus the higher data rate of IEEE 802.11n or IEEE 802.11ac networks is not strictly necessary. Moreover, it is easier to achieve such data rate through the house using IEEE 802.11af networks, and thus less repeaters are needed. Finally, HDTV streaming on ISM bands also suffers from nearby IEEE 802.11 networks on ISM bands, which can partially and temporally break the streaming, which is less likely to happen if other less used bands are involved.

3.2.1.3   Non-contiguous channel bonding

Due to the characteristics of the TV bands, it is hard to find contiguous free channels. Moreover, given the small channel size, the capacity of the network would is lower compared to other 802.11 networks for WLAN. Thus, 802.11af leverages the utilization of NC-OFDM, which permits to aggregate together up to 4 channels in 2 different spectrum chunks. Technically, this feature is realized by erasing the transmitting power of the OFDM subcarriers in the occupied channels between the two free blocks. Thus, only the subcarriers of the free bands are effectively used to transmit power, and the primary network is protected.

3.2.2   IEEE 802.22

The IEEE 802.22 is a standard made by IEEE for Wireless Regional Area Network (WRAN) using white spaces in the TV frequency spectrum. 802.22 uses cognitive radio technology to opportunistically access the TV spectrum, to bring broadband access in rural areas, with low densities of people. IEEE 802.22 networks are designed to protect primary users such as TV broadcasters and wireless microphones. In Figure 3.1, it is possible to see a comparison of IEEE 802.22 against other popular well known standards and technologies.
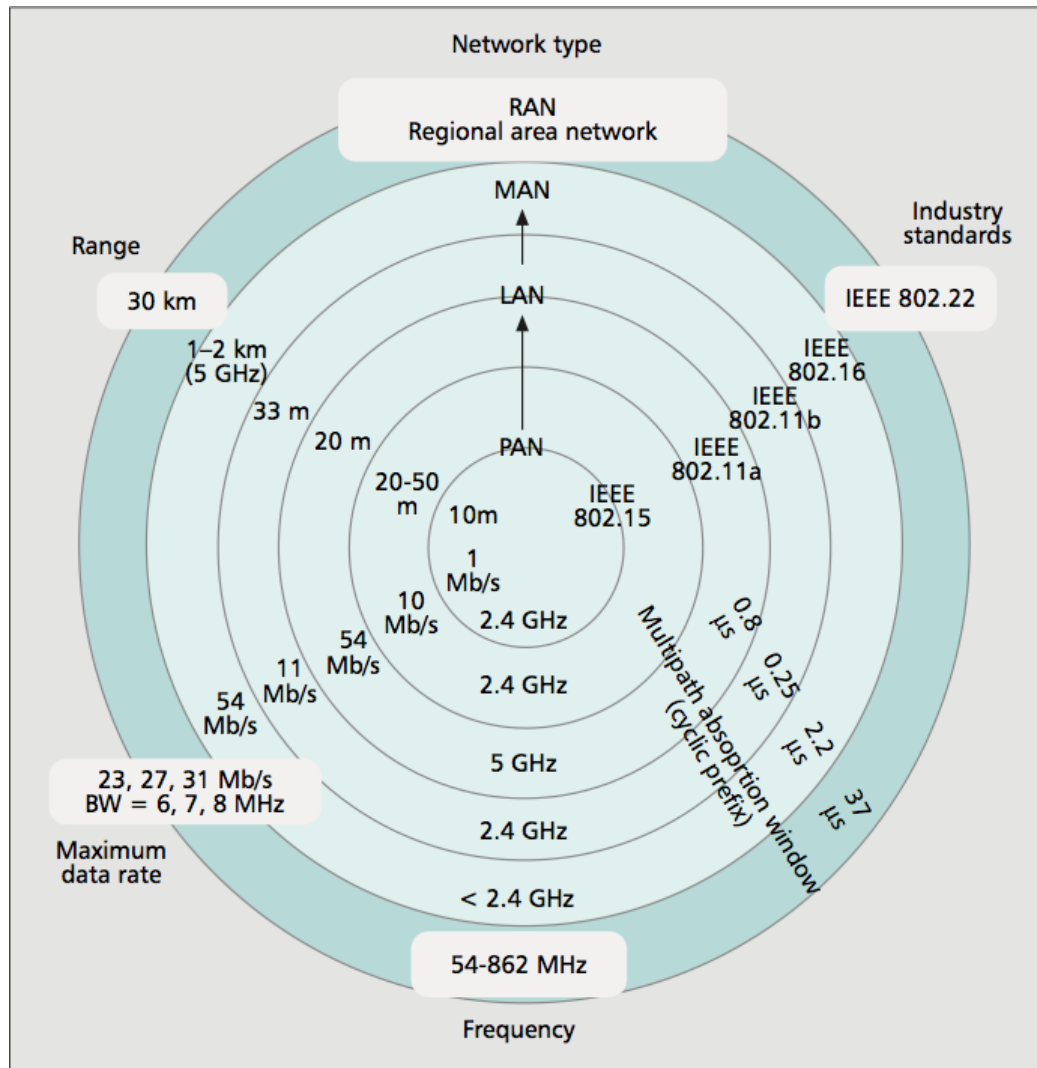
Figure 3.1: IEEE 802.22 in comparison to other technologies. Image credits to [104].

3.2.2.1 Architecture

IEEE 802.22 networks are typically identified to bring wireless coverage to rural areas, with ranges of 17 km to 33 km, up to 100 km in some specific scenario. From an architectural point of view, it is mainly composed of two different devices: a base station (BS) , and one or more Consumer Premise Equipment (CPE) . Technically, a single BS can serve up to 255 CPE.

3.2.2.1.1 Base station The BS is the Master device in terms of TVWS terminology. It is thus responsible to allocate the channels to Slave devices, and gather the information on their availability.

3.2.2.1.2 Consumer/Customer Premise Equipment The CPE is a device operated by the user, which must attach to a BS before starting to communicate.

3.2.2.2 Point-to-Multipoint Topology

The topology used in IEEE 802.22 networks is based on a Master/Slave relationship, in which the BS performs all the management and allocation operations, and the CPEs attach and use the network. Thus, all the CPEs have to attach to a BS before starting to communicate, and receive the operational parameters from it. No Device-to-Device communication is actually allowed, and all the transmission should be routed by the central BS. This architectural choice fits well with the current regulations, in which it is foreseen the presence of a Master device, which acts as coordinator of the network, and multiple devices that have to attach and to which the Master has to grant permission to communicate.

3.2.2.3 Physical Layer

The IEEE 802.22 Physical Layer is designed to use vacant TV channels. The coverage range have been declared to be between 33 km and 100 km. It is based on OFDMA, and the downstream achievable data rate is around 20 Mb/s, to be divided for all the CPE attached to the base station, depending on the MCS and on the bandwidth. Concerning upstream traffic, the achievable data rates are smaller, with a a peak of 384 kb/s. The EIRP for CPEs is 4 W, which translates into a maximum range of 33 km. This also copes with the regulations, and can be seen as a municipal wifi-like service.

Table 3.2 show all the MCSs for IEEE 802.22 for different channel bandwidths. A total of 14 MCS are identified, to accommodate the huge diversity

Table 3.1: IEEE 802.22 parameters

Parameter	Specification
Frequency Range	54-862 MHz
Bandwidth	6,7,8 MHz
Modulation	16-QAM, 64-QAM
EIRP	4W
Access	CSMA

Table 3.2: IEEE 802.22 MCS

Modulation	Coding Rate	Data rate (Mb/s)		
		6 MHz	7 MHz	8 MHz
BPSK	-	4.54	5.29	6.05
QPSK	1/2 - 3	1.51	1.76	2.01
QPSK	1/2	4.54	5.29	6.05
QPSK	2/3	6.05	7.05	8.06
QPSK	3/4	6.81	7.94	9.08
QPSK	5/6	7.56	8.82	10.08
16-QAM	1/2	9.08	10.59	12.1
16-QAM	2/3	12.1	14.11	16.13
16-QAM	3/4	13.61	15.87	18.14
16-QAM	5/6	15.13	17.65	20.17
64-QAM	1/2	13.61	15.87	18.14
64-QAM	2/3	18.15	21.175	24.2
64-QAM	3/4	20.42	23.82	27.22
64-QAM	5/6	22.69	26.47	30.25

that IEEE 802.22 networks must support, given the heterogeneity of TV
bands. The BPSK modulation is used to exchange management informa-
tion, and the first QPSK modulation is for the coexistence beacon protocol
(CBP). Every other MCS can be used for data transmission.

3.2.2.4   Features

3.2.2.4.1   Incumbent Detection   In IEEE 802.22, bot the BS as well as
all the CPEs are able to detect the presence of an incumbent on the channels,
but only the BS can make decisions on the channels to use. Clearly, the
devices need to know the location in which they are, and this is typically
realized by using the GPS. Moreover, it is foreseen the presence of a remote
spectrum database, which contains the list of all the free channels at the

device location. IEEE 802.22 also supports spectrum sensing, to detect TV transmission as well as microphone users, even though this method has been partially discarded by regulatory bodies.

3.2.2.4.2 Spectrum Sensing Two different entities for spectrum sensing are identified in IEEE 802.22, namely the Spectrum Sensing Automation (SSA), and the Spectrum Sensing Function (SSF), that must be implemented both in BSs as well as in all CPEs. Basically, the CPEs should listen to the channel and report their measurements to the BS via the associated SSA. To perform sensing, the 802.22 protocol has to allocate quiet times, which are portions of time in which no data transmission could occur, and devices should only sense the spectrum to detect incumbent transmissions.

3.2.2.4.3 Self-Coexistence The self-coexistence between competing IEEE 802.22 networks is realized with three different mechanisms:

Neighboring network discovery/coordination IEEE 802.22 networks sense the spectrum, and try to understand whether other competing networks are present in the same geographical area. Any CPE that senses another IEEE 802.22 network must report the reading to its BS.

Coexistence Beacon Protocol (CBP) This translates into sending a periodic beacon to inform neighbors about the presence of an IEEE 802.22 network.

Resource sharing mechanism IEEE 802.22 networks cooperate, and if a network sense a channel as occupied by another IEEE 802.22 network, it goes to another free channel instead of interfering with the other network.

3.2.2.4.4 Channel Classification Based on the list of available channels to use, the BS decides on which one to transmit. This is done in two different steps: at first, the BS receives the list of available channels from the remote spectrum database, and classify them as:

- Protected: these are channels used either by primary users or IEEE 802.22 networks.

- Unclassified: these channels have not yet been sensed.

- Disallowed: channels excluded from the availability list due to regulatory constraints.

- Operating: this is the channel currently in use by the IEEE 802.22 network to transmit.

- Backup: channels that can become Operating if the current becomes unavailable.

- Candidate: channels candidate to become Backups.

Then, according to the policies, the BS selects one of the available channels to transmit data on.

3.2.2.5   Use cases

TVWS could also be used to enhance the current broadband service offered by Wireless Internet Providers (WISPs). In this case, the end device capabilities are usually higher than M2M communications, with users using laptops and higher end devices. Compared to M2M devices, the latter are less dense, but with significantly higher data rates requirements. Also in this case, mobility plays an important role, and it needs to be considered in allocating resources to users. In this kind of application, the MAC should also select the appropriate frequency and carrier aggregation to use based on the QoS requirements, which are higher than the previous list of applications. Example of these applications include:

- **Broadband Wi-Fi**, with TVWS a wi-fi service for more users could be deployed, having superior range than actual 802.11 a/b/g/n implementations. The 802.22 standard presented in section 3.2.2 will surely play an important role for these applications. Of course, Wi-Fi on these frequencies could cover a larger area, thus enabling municipal wi-fi and interconnection links between administrative buildings. Since the 2.4 GHz band is highly congested, and the additional 5 GHz will become so in the near future in dense areas, having additional bandwidth to offload these saturated bands will help in deploying new hotspots. In [101] the authors also show that the effective data rate of the wi-fi is primarily dependant on the used bandwidth instead on the frequency used. Still in [101], the author also noted that increasing the range has the drawback of bringing more interferences into play. Careful planning and adaptive algorithms are needed in order to mitigate the interferences while taking benefit of the increased coverage.

- **Backhaul for WiFi**, where traditional wi-fi is deployed, there is always the need to connect access point to the main router. This is typically done with cables, raising the cost and certainly not granting

much scalability. Using TVWS for wireless backhauls will improve scalability at a lower cost. With this solution, customers' equipment will continue to work as before, since the final connectivity will always be served with 802.11b/g/n access points, but the infrastructure is built using custom designed protocols for TVWS. Again, even in these situation TVWS are suitable due to their propagation characteristics and thus will save time, money and provide a better overall service. At the same time, guarantees about the spectrum availability are needed, to provide a stable service not disrupted by PUs.

- **Disaster recovery**, emergency temporary broadband infrastructure could be easily and rapidly deployed upon a disaster happened. When disaster happens, typically there is a lack of spectrum due to the heavy number of communications happening at the same time just after the fact. TVWS could be used in two different modes: they could offload the cellular network for some communications, thus making possible a higher number of communications between customer, or they could be used for emergency services in the area, to transmit data over a wide area with reliable communications. TVWS could also be used by small drones that are nowadays studied and developed to overcome the lack of connectivity after these disasters. Typically, these kind of equipment needs to transmit small chunks of data, like beacon messaging, at long ranges, and TVWS are the ideal candidate for this kind of transmissions for their good propagation characteristics.

3.2.3 IEEE 802.15.4m

In mid-2014, IEEE released the IEEE 802.15.4m standard, which covers TVWS operations for LR-WPAN. The standard defines the PHY and MAC layers to operate in TVWS. More specifically, there is one MAC definition, and three different PHYs, which are explained in the following.

3.2.3.1 Architecture

IEEE 802.15.4m foresees the presence of two different kind of devices: the Fully Functionality Device (FFD), built with a complete set of MAC instructions, and the Reduced Functionality Device (RFD), which instead contains only a subset of all the possible MAC instructions. The network is organized into a Personal Area Network (PAN), which must have a PAN Coordinator (PANC), and one or more devices that build the network, which can be either FFDs or RFDs. The logical connection between those is Master/Slave,

in which the PANC is the Master and all the other devices are the Slaves, like in a star topology. FFDs that are not PANC can become themselves PANC to extend the network to other devices.
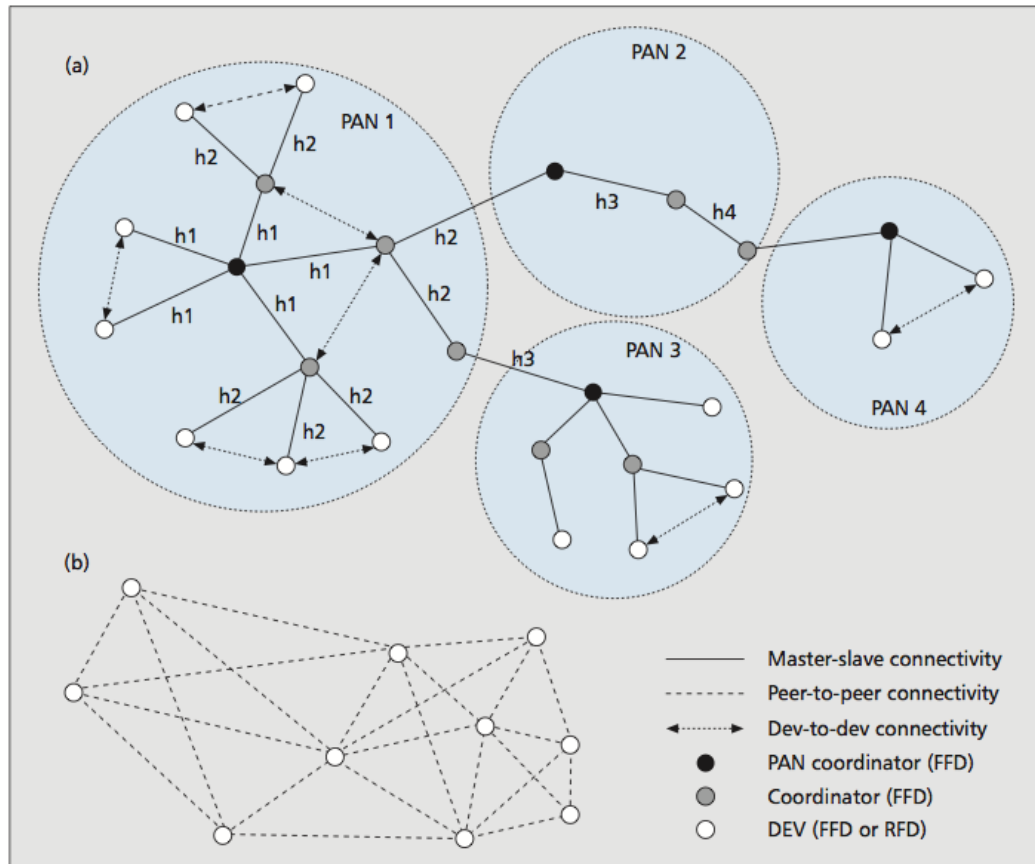
Figure 3.2: The IEEE 802.15.4m network architecture. Image credits to [106].

In Figure 3.2a it is shown the typical IEEE 802.15.4m network, in which are visible 4 different PANs with their coordinators, and all the other devices attached to them. IEEE 802.15.4m also foresees the possibility for devices to communicate between them, with a device-to-device (D2D) connectivity. Clearly, this kind of network is heavily centralized, in the sense that a PANC must exist, possibly with an energy supply, since its operations are energy consuming. Thus, the clustered topology of Figure 3.2a might not be suitable for all the use-case scenario in which IEEE 802.15.4m networks will be deployed.

To this end, IEEE 802.15.4m also offers the possibility to have a complete redundant, flat network architecture, shown in Figure 3.2b. Here, devices are

organized in a non-hierarchical architecture, where all nodes are equal and capable of performing the same communication tasks. This greatly enhance the redundancy of the network, and consequently its resilience to possible network malfunctions.

3.2.3.2 MAC

Regarding the management of the network, IEEE 802.15.4m defines the following primitives:

- MLME-BEACON-NOTIFY.indication

- MLME-START.request

- MLME-DBS.request

- MLME-DBS.indication

- MLME-DBS.response

- MLME-DBS.confirm

- MLME-DA.request

- MLME-DA.confirm

- MLME-DA.indication

Instead, concerning the data communication of the devices, the IEEE 802.15.4m MAC layer defines the following:

- MCPS-DATA.confirm

- MCPS-DATA.indication

The IEEE 802.15.4m MAC layer is also designed to offer Dynamic Band Switching (DBS). This means that IEEE 802.15.4m devices should be able to switch also to frequencies outside the TV Bands. This has been done in order to increase the industry confidence on the new standard, given its opportunistic nature. Due to the uncertainty on the availability of TV channels to use, it is important to also extend the possible frequencies to be used. IEEE 802.15.4m devices can thus switch to other frequencies if one becomes unavailable, like to the ones defined in IEEE 802.15.4g, where channel availability is known a priori.

3.2.3.3 PHY

IEEE 802.15.4m defines three different PHYs, to accommodate device diversity, and various use-cases. More in detail, IEEE 802.15.4m defines a FSK PHY, an OFDM PHY, and a NB-OFDM PHY.

3.2.3.3.1 802.15.4m FSK PHY The FSK PHY defines 5 different modulations, summarized in Table 3.3. It supports data rates ranging from 50 kb/s to 400 kb/s, with channels wide from 100 kHz to 600 kHz.

Table 3.3: IEEE 802.15.4m FSK Modulations

Mode	Data Rate (kb/s)	Modulation level	Modulation index h	Channel Spacing (kHz)
1	50	2-level	0.5	100
			1.0	200
2	100	2-level	0.5	200
			1.0	400
3	200	2-level	0.5	400
			1.0	600
4	300	2-level	0.5	600
5	400	4-level	0.33	600

The FEC support is optional, and three FEC schemes are included in the standard.

3.2.3.3.2 IEEE 802.15.4m OFDM PHY The OFDM PHY supports data rates ranging from 390.625 kb/s to 1562.5 kb/s, summarized in Table 3.4

Table 3.4: IEEE 802.15.4m OFDM Parameters

Parameter	Mandatory	Optional
Bandwidth (kHz)	1064.5	4258
BPSK Data Rate (kb/s)	390.625 (MCS0)	1562.5 (MCS3)
QPSK Data Rate (kb/s)	781.25 (MCS1)	3125 (MCS4)
16-QAM Data Rate (kb/s)	1562.5 (MCS2)	6250 (MCS5)

3.2.3.3.3 IEEE 802.15.4m NB-OFDM PHY The IEEE 802.15.4m NB-OFDM spans from 156 kb/s to 1638 kb/s, with a bandwidth of 380.95 kHz.

Table 3.5: IEEE 802.15.4m OFDM Sensitivity Requirements

MCS	Sensitivity	Link Budget
0	-97 dBm	16.72 dB
1	-94 dBm	19.72 dB
2	-88 dBm	25.72 dB
3	-91 dBm	15.04 dB
4	-88 dBm	18.04 dB
5	-82 dBm	24.04 dB

Table 3.6: IEEE 802.15.4m NB-OFDM Parameters

MCS	Modulation	CC coding rate	Data rate (kb/s)
MCS0	BPSK	1/2	156
MCS1	BPSK	3/4	234
MCS2	QPSK	1/2	312
MCS3	QPSK	3/4	468
MCS4	16-QAM	1/2	624
MCS5	16-QAM	3/4	936
MCS6	64-QAM	1/2	936
MCS7	64-QAM	3/4	1404
MCS8	64-QAM	7/8	1638

3.2.3.4 Use cases

Machine-to-machine (M2M) communications will be the backbone of the future Internet of things. Several studies report that there will be a huge increase in the number of devices simultaneously connected to the Internet, communicating to each other to offer new services to the end users. It has been reported that in 2020 there will be nearly 50 billions of devices simultaneously connected to the internet. Such a great number of connected devices demand a great availability of bandwidth and spectrum [27].

These kind of devices typically need lower bandwidth compared to other wifi-like devices, focusing more on the reliability and security of communications, and also might need to send messages at long ranges. M2M communication will exploit TVWS by taking advantage of the unique and superior propagation characteristics of this band, by enabling services like smart metering and environmental control in a way that without using low frequencies would not be possible. In fact, using lower frequencies can directly translate into less hops needed for the communication, with benefits on the energy consumption, and on the latency of the messages.

Table 3.7: IEEE 802.15.4m NB-OFDM Sensitivity Requirements

MCS	Sensitivity	Link Budget
0	-97 dBm	21.19 dB
1	-96 dBm	22.19 dB
2	-94 dBm	24.19 dB
3	-92 dBm	26.19 dB
4	-89 dBm	29.19 dB
5	-85 dBm	33.19 dB
6	-81 dBm	37.19 dB
7	-80 dBm	38.19 dB
8	-78 dBm	40.19 dB

Focusing on smart grid control and applications [8] [118], M2M communications will occur between devices that typically have low computational capabilities and low computational power, and have also energy constraints because usually are battery powered. Their typical message is like a beacon, carrying information read from various sensor these devices could have installed on them. Their communication thus need to be reliable and energy-efficient [98], also designing protocols that should deal with channel access by multiple devices.

Some devices could also be mobile, and mobility could play an important role in the type of infrastructure they could build. There will be the need to do Dynamic Spectrum Access (DSA) for managing the changing TVWS set, while ensuring about the routing of the messages through their final destination.

Security is an important part of M2M communications, and there are already some studies [25] [126] that highlight this fact. Communication should be secure, but since device are typically low-end as computational power, the computation required to make the communication reliable and secure should be aware of that. Cryptography [98] could be used by devices with enough computational capabilities, while for other there should be also energy efficiency and low computation, and thus cryptography could be used if it does not need too much resources.

M2M communication could be seen basically in three different fashion:

- **Home networks**: future homes will have a platoon of devices fully connected between each other and on the internet. While this is already possible with wi-fi, Bluetooth and zigbee, using TVWS will enable the use of low frequencies, with low transmission power, better obstacles and wall penetration. By using these frequencies, devices could have

a longer battery life and there will be less interferences in the ISMs bands, already heavy utilized.

- **Smart metering**: future utilities will need to query the home networks to gather data about water consumption, energy consumption and so on. These kind of communication should be regulated by a central base station managed by the utility provider, that will administer channel access and schedule access to smart meters. In these kind of communications, ranges are typically higher than in smart homes, while maintaining the same energy constraints. Base station have enough power to manage a big set of M2M devices, and since are main powered, energy-saving is not a main issue.

- **Monitoring**: another kind of M2M applications that could benefit from the TVWS introduction are about the monitoring of the environment or agricultural farms. Quickly recognizing possible changes in the weather could help workers to act in time and prevent disaster, saving peoples' life in the presence of tornadoes or hurricanes. As before, also in these kind of applications there are a lot of small, battery powered devices, that need to communicate with a central unit. In fact, typical requirements remain the same as before, with the need for energy-aware protocols and reliable communication of small messages.

3.2.4 Sigfox

Sigfox uses a technology named UNB, which stands for Ultra Narrow Band, to provide reliable and efficient communications.

The UNB technology uses license-free radio bands to transmit data, with narrow spectrum bands. The UNB technology is designed to achieve low throughput while being energy-efficient, and with a high level of sensitivity. Typical data rates for the SIGFOX technology spans from 10 b/s to 1 kb/s, and this data could be sent at very long distances, up to 40 km in the open field. UNB also passes well through obstacles, and this is also the reason for achieving such high distances, even when there is no LOS or the are obstacles between the sender and the receiver.

Since using narrow bands raises the sensitivity of SIGFOX's devices, less base stations are needed to cover even a large area. Every radio elements also performs energy-efficient communication, by using narrow bands at low power, thus widening the overall duration of batteries, a crucial requirement for M2M devices and the IoT communication in general.

SIGFOX network is hierarchical, and there are three main kind of devices:

UNB modems, Base Stations (BS) and Servers. The UNB modems are installed on the devices, and communicate with the base station to send and receive data. This allows covering large areas of hundreds square kilometers with a single base station and multiple UNB modems. What the BSs do is routing this messages to the server, limiting the computational complexity of the station and allowing a fast and reliable communication. Data check is performed by the servers, which are usually main powered and with high computational capabilities. Here, messages are checked for their integrity, and eventually routed to the final desired destination.

3.2.5   Weightless

Weightless[116] is a technology for M2M communications driven by a Special Interest Group (SIG) formed in early November 2012. Weightless has a MAC layer that is able to deliver a wide range of data rates, from 100 Kb/s to 16 Mb/s, serving over 100.000 devices per single base station. Due to the use of low frequencies, the Weightless vision is to keep the cost for a single device under 2 dollars, and a battery lifetime at least of 10 years.

The Weightless MAC could also adapt itself to use both licensed as well as unlicensed bands in the TVWS UHF band. As before, using this kind of frequencies can enlarge the global range achieved by devices that use this technology. The Weightless technology uses a TDD access scheme, in order to reduce collisions while preserving energy on the end devices.

Like UNB, also Weightless uses narrow band frequencies to limit the energy consumption and the interferences. This is usually done on the uplink, where devices typically have limited QoS requirements for data rates.

3.2.6   ECMA 392

The ECMA-392 [61] standard specifies PHY and MAC operation in the TVWS, and a set of techniques for protecting incumbent users from interferences.

An ECMA-392 network could be one of the two following topology: Peer-to-peer network or Master-slave network, as shown in figure 3.3. Based on network topologies, ECMA-392 defines three different kind of devices, a master device, a slave device and a peer device. In the typical Master-slave network formation, one device is the master, and all other devices could communicate with it. The master needs to coordinate channel access, and could also grant some slave devices to communicate with other slave devices without passing through the master. In the peer-to-peer network, devices
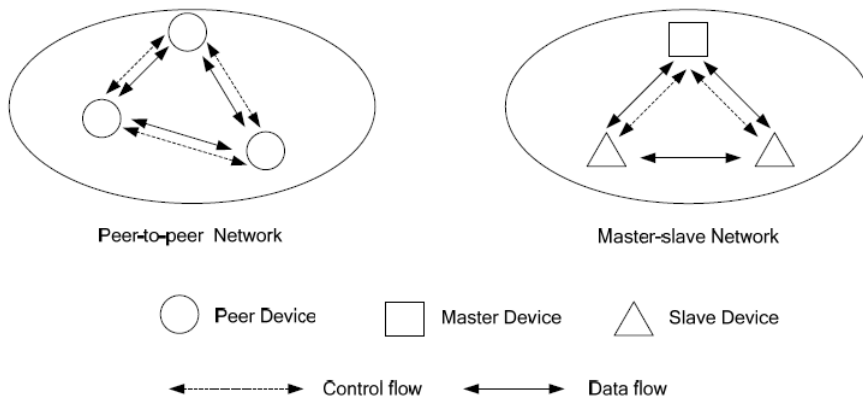
Figure 3.3: ECMA-392 networks

coordinate themselves to access channels, and each device can directly communicate with each other, as long as they are in range. For this reason, an ECMA-392 network can be ad-hoc, self-organizing and self-healing.

The ECMA-392 MAC layer is able to make devices communicate on a single channel thanks to the PHY layer, with two different channel access mechanisms: a reservation based channel access and a prioritized contention based channel access. Of course, the MAC layer is also responsible for the protection of incumbent users, as well as managing the network topologies even when the devices' mobility change the environment. The ECMA-392 MAC layer periodically exchanges beacon messages between devices to manage the network and inform other devices about scheduling information and reservations.

Part II

Contributions

Chapter 4

Spectrum Measurements for TVWS and TVGS

4.1 TV Gray Space scenario

Commonly, in literature it is possible to find a multitude of works on TV White Spaces, ranging from measurements campaign, to analytical modeling, to architectural proposals. The rationale is that:

- TV White Spaces are available in rural areas with several MHz of bandwidth, while it is harder to find free channels in dense populated areas.

- The propagation characteristics of the TV bands make them ideal to transmit at long range and through obstacles.

- The remote spectrum database can become an issue indoors, where it is difficult to obtain the position of the device.

Given the aforementioned issues, and the fact that most of the communication comes from indoor environments [27], much of the work have been focused on the opportunistic utilization of TV Gray Spaces (TVGS), or the spectrum underlay paradigm. TVGS are frequencies occupied at the rooftop, possibly free indoor due to high shadowing coming from walls, windows, and other obstacles. The first aspect to consider is that none of the current regulations allow this kind of behavior by the secondary network. Thus, the highest challenge is to provide the evidence that no harmful interference can be produced to disrupt the primary network.

In Figure 4.1 we show the scenario of opportunistic communication over TV Gray Spaces. We focus on indoor devices, and we evaluate the different wireless links that exist. Clearly, there is the primary signal coming from
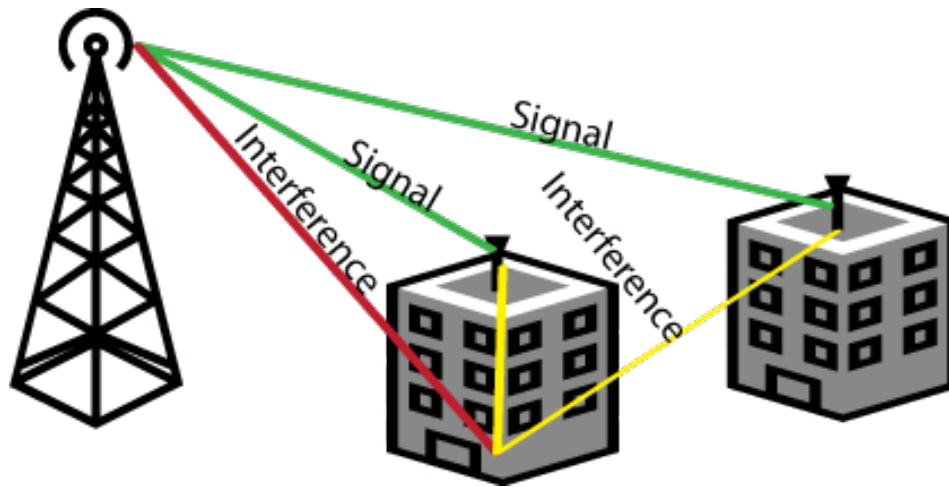
Figure 4.1: The TV Gray Spaces scenario. The red line is the interference from the primary transmitter, which is also the primary signal towards the DTV receiver, represented as green lines. Finally, the indoor devices might produce interference on the primary network, showed as yellow line.

the DTV transmitter, which should not be interfered by the secondary network. This exact same signal is also received, although with lower power due to shadowing effects, also by the indoor devices. Finally, there is the opportunistic communication of the secondary network, which might produce interference on the primary receiver. Before evaluating them in detail, we can make some first order consideration on their behavior:

- A stronger signal received by the DTV receiver allows a stronger interference from the secondary network. Thus, buildings at the coverage edge of the DTV cell radius are less tolerant and might be not suitable for this kind of communication, if too high interference is produced by the secondary network.

- A lower received signal indoor translates into a lower transmitting power needed in order to achieve a satisfactory SNR for the secondary network. Thus, not all gray spaces are equal between them, and the lower received ones are preferred.

- The transmitting power of the secondary network should be not more than the strict necessary, to alleviate possible interferences on the primary network.

Thus, studies to analyze the different communication links of Figure 4.1 have been performed.

4.2 Differences in received power

The first needed step is to assess the differences in received powers between different floors in the same building, to understand whether it might or might not be possible to operate a network on such conditions.

Thus, we performed a preliminary study in the city of Turin, Italy, to understand the differences in received powers at various heights in the building. Then, similar measurements have been performed in the city of Aachen, Germany.

4.2.1 Spectrum measurements in Turin, Italy

In this Section we describe how we carried out the spectrum measurements in the 470-798 MHz band. To perform the spectrum measurements we used a NARDA SRM-3006 spectrum analyzer, capable of detecting signals in the 9KHz-6GHz frequency range[1], equipped with a 3502/01 isotropic antenna which could span from 420 MHz to 6 GHz. All the relevant parameters are showed in Table 4.1.

Table 4.1: Measurements Parameters

Name	Value
Frequency Span	470 MHz - 798 MHz
RBW	100 KHz
DANL	-156 dBm/Hz

We performed extensive spectrum measurements in three different locations in Turin, Italy. The position of these buildings can be found on the map of Figure 4.2, along with the position of the strongest transmitter.

We then selected three different buildings in the city, and performed spectrum measurements at three levels: at the rooftop, at an intermediate floor, dependent on the height of the building, and in the basement.

The three scenarios examined are described as follows:

- **Via Reiss Romoli**: the first scenario is a 4 floor industry located on the northern part of Turin. The surrounding buildings have at maximum 2 floors, and there is partial visibility towards the DTV transmitter from the roof.

_____

[1]http://www.narda-sts.de/products/high-frequency/selective-radiation-meters/srm-3006.html
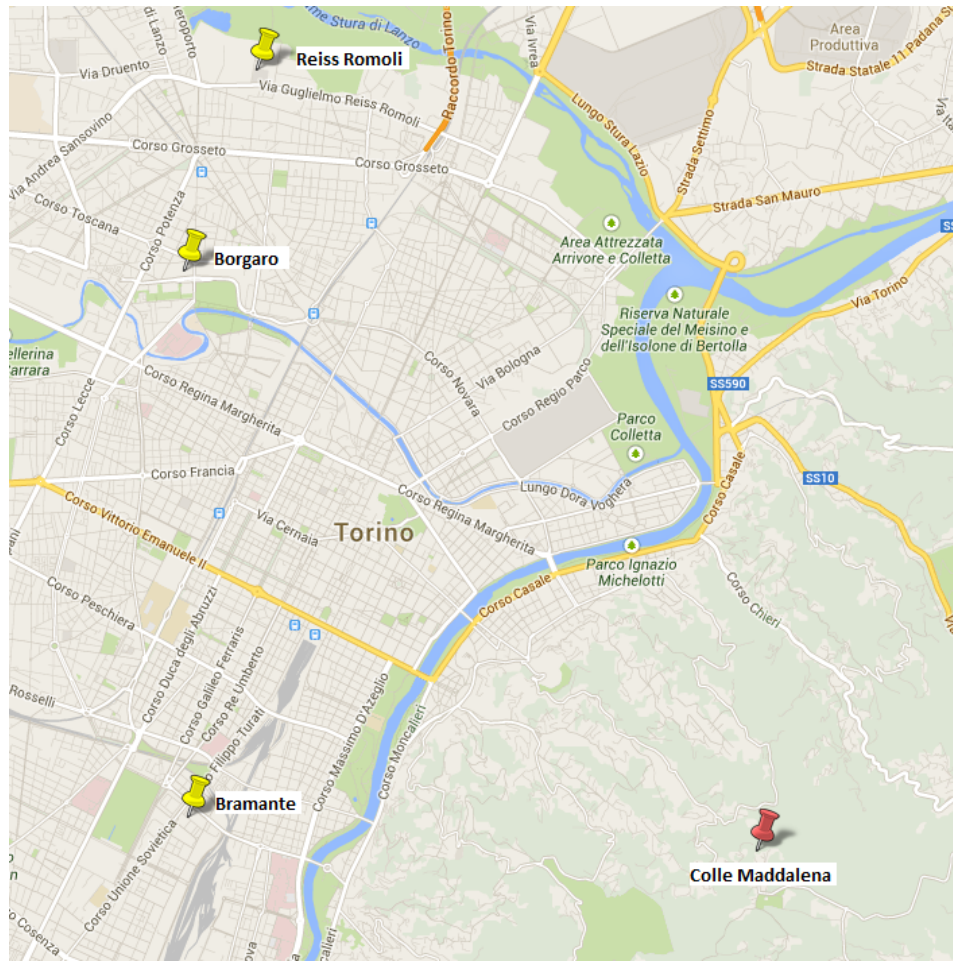
Figure 4.2: The map of Turin with the measured scenarios, along with the position of the strongest DTV transmitter.

- **Via Borgaro**: the second scenario is a 4 floor building located in the city center of Turin. It is surrounded by buildings, except on one side which is free and grants visibility to the DTV transmitter from the roof.

- **Corso Bramante**: the third scenario is a 5 floor building, in the hearth of the city. It is completely surrounded by tall buildings, and the roof gives a LOS access to the DTV transmitter.

The interference on the short range devices can be computed by analyzing the spectrum measurements at the same geo-point, but at different heights. We performed spectrum measurements in the three different scenarios, and
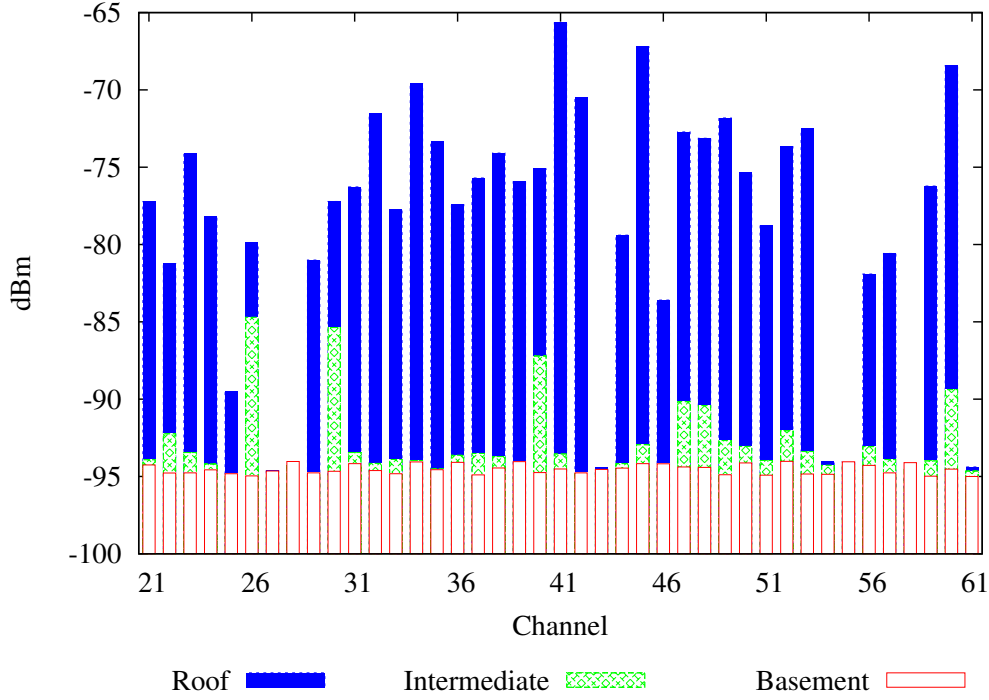
Figure 4.3: Received powers for the `Reiss Romoli` scenario.

we compute the total received power over a bandwidth T of $8\,\mathrm{MHz}$ centered in F as follows:

$$X_T^F = 10 \cdot log_{10} \left(\left(\frac{T}{RBW} \right) \cdot \left(\frac{1}{\frac{T}{RBW}} \cdot \sum_{i=1}^{N} 10^{\left(\frac{P_i}{10} \right)} \right) \right) \tag{4.1}$$

where P_i is the power received on the $100\,\mathrm{KHz}$ bin inside the T bandwidth. In Figure 4.3 we plot the received power at the same point, but at different heights, for the `Reiss Romoli` scenario. The `Borgaro` scenario and the `Bramante` are depicted in Figure 4.4 and 4.5, respectively. We performed measurements at the rooftop, in the basement, and in an intermediate floor. On the x-axis we show the UHF channels, while on the y axis we plot the received power in dBm. What is easy to see from the charts is that the channel occupancy is similar for all the three buildings, since they are not too far from each other, and the nearest transmitter is the same. Another aspect of the presented charts is the fact that the signals significantly drop in power as we move away from the roof, with a heavy difference even at the intermediate floor. What is important to catch from these figures is that occupied channels at the rooftop are almost always free in the basement. In
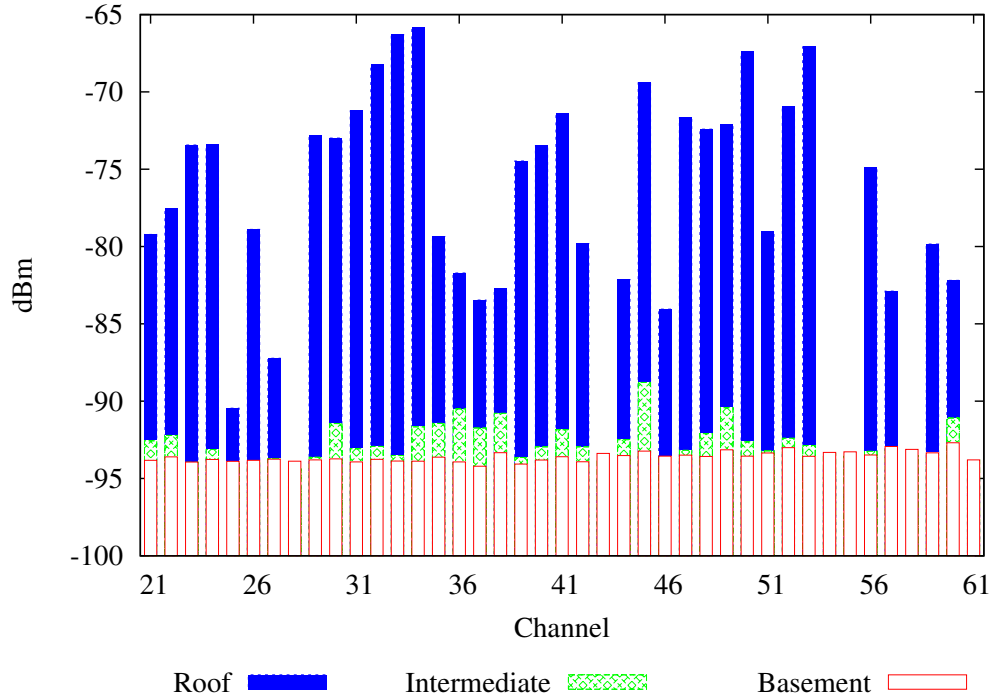
Figure 4.4: Received powers for the `Borgaro` scenario.

this paper we consider free each channel received below a threshold θ which we set to -90 dBm. We note that this value is even lower compared to similar works [122]. This is mainly due by two different aspects: at first, the DTV transmitters are placed to maximize rooftop coverage, and consequently it is obvious that the signal will be received at lower powers while diminishing the height. Second, the heavy shadowing caused by buildings in high population areas is an advantage in this scenario, since it helps in lowering even more the received signal. Out of the measurements we did, we can say that in Turin there are 6 unused channels outdoor (Channels 28, 43, 54, 55, 58 and 61), which corresponds to 48 MHz of available spectrum. At the intermediate floor indoor there is a wider availability of spectrum, since all the channels except channel 26, 40 and 45 for the `Reiss Romoli` scenario are sensed free. Finally, all the channel sensed are found free in the basement. The `Reiss Romoli` scenario present one further aspect to consider. It is possible to see that it is the only one which reports channels above the threshold θ even at the intermediate level. This is mainly due to the fact that it does not have tall buildings around that can shadow the signal, so from the walls of the intermediate floor it might be possible to have a LOS to the DTV trans-
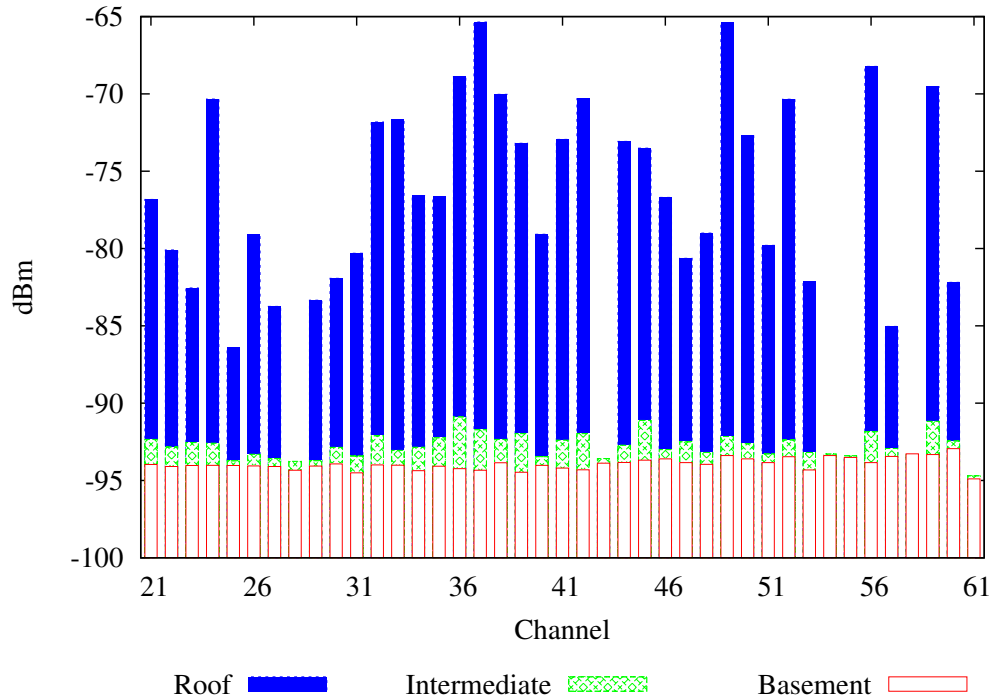
Figure 4.5: Received powers for the `Bramante` scenario.

mitter. In Figure 4.6 we plot the average sensed values at the rooftop, at the intermediate floor and in the basement, for the three different scenarios, along with the variance. Figure 4.6 shows that at the rooftop there could be a significant difference between the sensed values, while at lower levels the differences diminish, and we have more similar values in all the examined scenarios.

The whole spectrum band measured can be seen in Figure 4.7

4.2.1.1 Variation at the same floor

In Figure 4.8 we show the results from the measurements we performed at the ground floor in the Borgaro scenario, in which we moved from a central point by two meters in all the directions (i.e. N,S,W,E,NW,NE,SW,SE), and performed a total of 9 sensing operations. It is straightforward to note how different the received powers are, even at short distances, due to the complexity of the scenario and multipath effects. This fact should be taken into account when planning for indoor communications, mainly for two different aspects:

- **Interference to DTV receiver**. A low signal means that no DTV
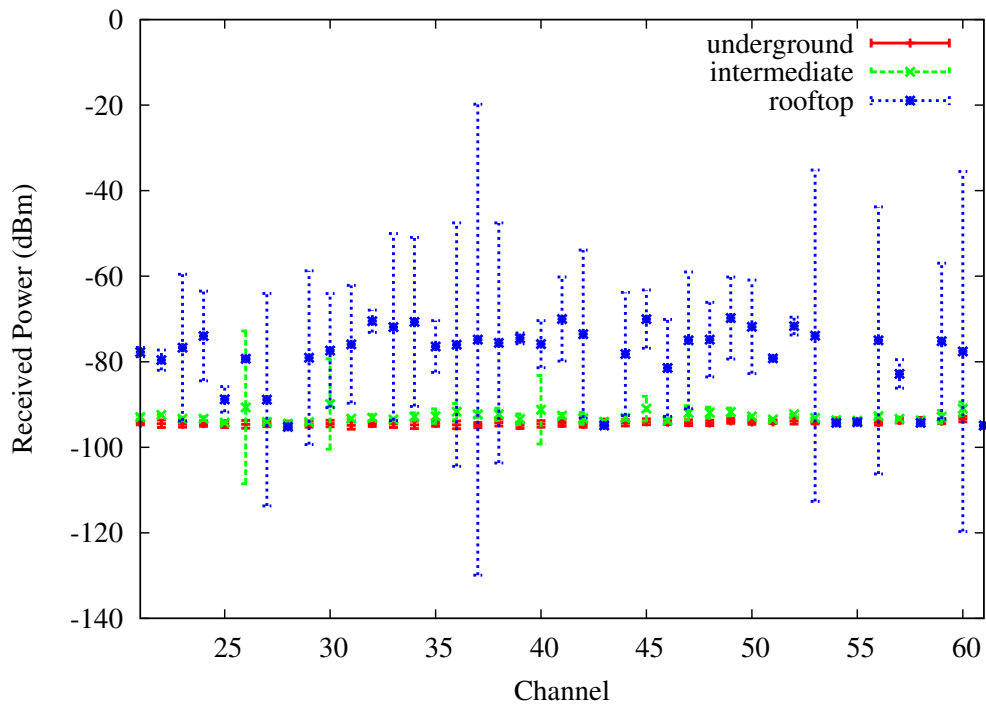
Figure 4.6: Average and variance of received powers for all the channels.

receiver can decode it, thus making that channel virtually free for other kind of communications. A high power means instead that the DTV broadcaster is actually using the channel, and the receiver might be receiving it, and thus, any communication should be avoided. For this purpose, extensive measurements should be taken prior to determine whether there are channels that could be utilized without causing harmful interference. These measurements could be in the form of static data, performed prior to the installation of the devices, with highly-precise instrumentation, or by devices, in the form of individual or collaborative spectrum sensing, like in IEEE 802.22.

- **High noise**. While on a channel received at a high power, devices need to raise their own transmission powers in order to win the noise interference perceived. This has two main drawbacks: at first, it can cause too much interference on the DTV receiver at the rooftop, thus making the channel not detectable. At second, it could rapidly deplete the battery of the devices, if battery powered. As for the previous point, this could only be assessed with spectrum measurements, in order to install the devices in the more favorable spots. As it was also stated
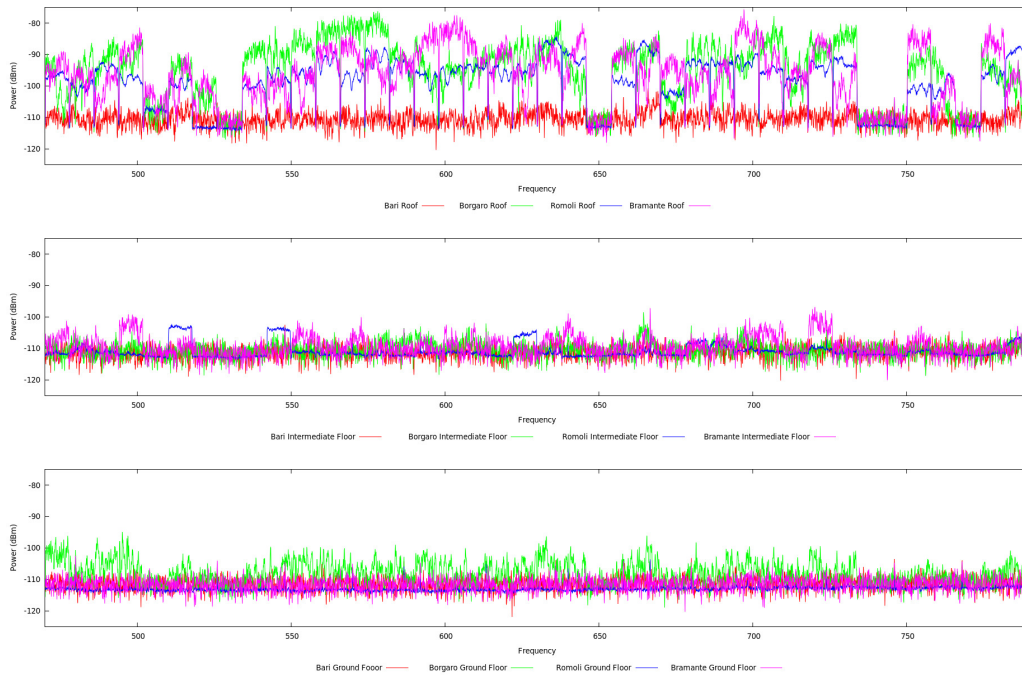
Figure 4.7: In Figure 4.7(a) we plot the frequency spectrum for the four measurement spots at the roof level. The same measurements for the intermediate floor and for the ground floor follow in Figure 4.7(b) and Figure 4.7(c), respectively.

> before, the antenna gain plays an important role, particularly at the cell edge. Far away from the transmitter, but still in its coverage radius, the signal can be correctly received only using directional antennas with high gain. Nevertheless, the same signal would be received indoor with levels close to the thermal noise, thus requiring less power for the indoor devices to achieve the desired SNR. However, when close to the cell edge, the DTV receiver could tolerate less interference, since the signal is received from the DTV transmitter with a lower power.

Several trade-off are found, thus selecting the best channel opportunity is not a straightforward operation, but requires further investigation and most probably dedicated algorithms.

4.2.1.2 Temporal Analysis

Since cognitive networks over TV White Spaces are opportunistic by nature, assessing the temporal availability is of paramount importance prior of deploying any real service on top of them. In other words, operators must
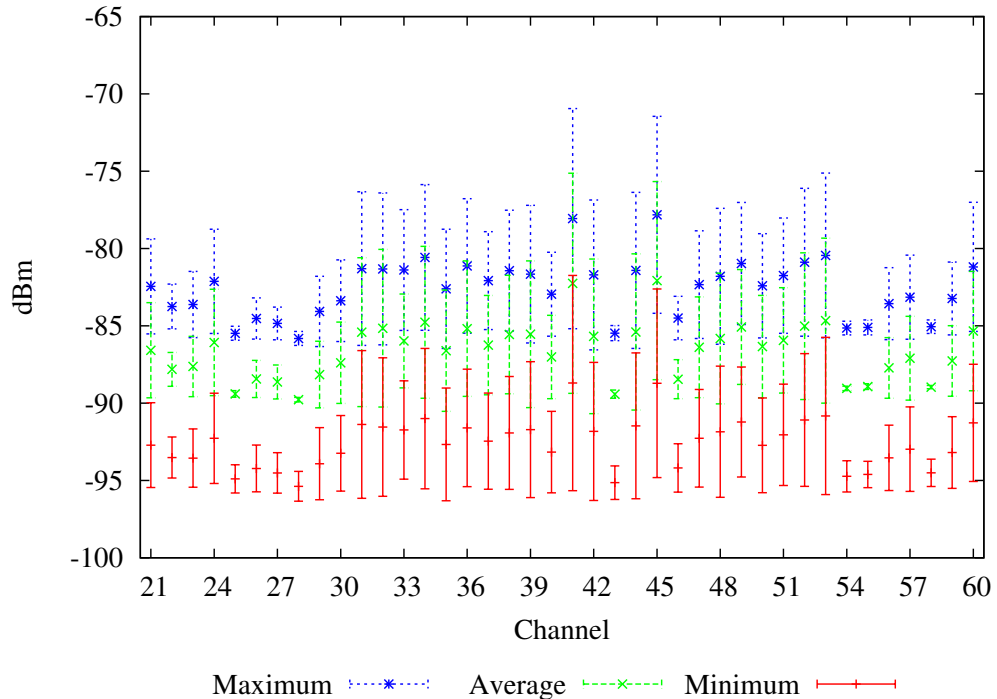
Figure 4.8: The spatial variance at the ground floor for the `Borgaro` scenario.

know in advance whether they can rely on channels for a sufficiently long time, or if the spectrum might change rapidly, thus disrupting the secondary service. In Figure 4.9 we present the temporal variation of three target channels in the `RR` scenario, which were found as occupied during the test. At each time of the x axis, we plot the relative dB difference between the power received at time t and the power received at midnight. From Figure 4.9 it is straightforward to note how little the differences are, always less than 0.5 dB at maximum. This results is helpful for those that want to invest in TVWS, since it provide the evidence that no significant variations in received power can be found through the day. The small differences are accountable for traffic and small changes in the scenario environment, and from interference of neighboring channels. This confirms the relatively static nature of TV channels.

4.2.2 Spectrum measurements in Aachen, Germany

Other measurements are presented in [10], where measurements in the city of Aachen, Germany, are performed, both indoors as well as outdoors. There, three different scenarios are investigated, in which measurements were per-
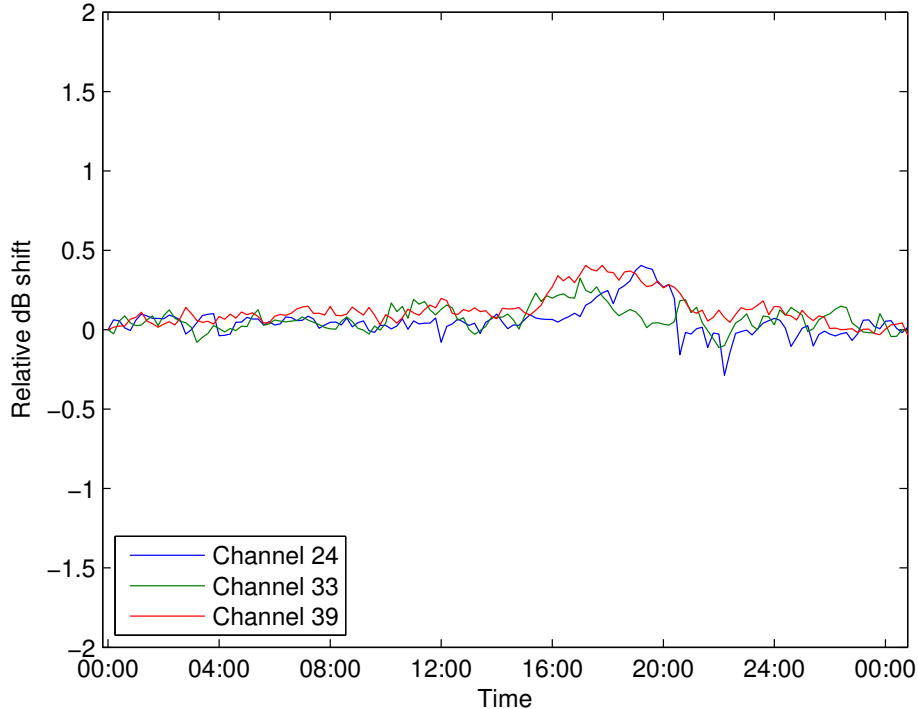
Figure 4.9: The temporal analysis for the `RR` scenario during a whole day of continuous measurements.

formed in two buildings for each one. The characteristics of the three different scenarios can be summarized as follows:

- Tuïme: in these student dormitories, both buildings are higher compared to the ground clutter height. Starting from the 3rd floor, there is direct LOS with the DTV transmitter.

- Uniklinik: two student dormitories located nearer to the transmitter compared with the others. There is no LOS with the DTV transmitter.

- Aachen downtown: these office buildings are located in Aachen downtown, and are surrounded by buildings of about the same height, which leads to NLOS conditions even at the top floor.

We have performed spectrum measurements on channels 26, 37, and 50, on which the same transmitter broadcasts with transmitting powers of 5 kW, 10 kW and 10 kW, respectively. The DTV transmitter is in Karlshöhe, placed at N 50 44.724', N 6 2.593'.

Table 4.2: Measurements locations and scenarios

Block	Building	Height	Near buildings clutter height
Türme	WEH	50 meters	0 meters
	TVK	50 meters	0 meters
Uniklinik	Kullen	25 meters	20 meters
	Kawo2	22 meters	15 meters
Aachen downtown	Super C	20 meters	15 meters
	Economics	15 meters	10 meters

In Table 4.2 the characteristics of the scenarios are reported, highlighting the differences between them. Then, Figures 4.10, 4.11, 4.12, 4.13, 4.14, and 4.15 report the measurements. Three channels were tested, more precisely channels 26, 37 and 50, which are transmitted from the near DTV transmitter at ERP power of 5 kW, 10 kW, and 10 kW, respectively. The most obvious thing that comes out from these measurement is the fact that the received powers do not closely follow the height from the terrain, as showed by other studies [82], but are more unpredictable. Buildings from Türme in Figures 4.10 and 4.11 report the higher received power at floor 4, then falls down, starts to rise up again starting from floor 7 in WEH, and from floor 10 in TVK. Channel 26 is always received at a lower power, since it is also transmitted at 5 kW less compared to the other two, equal to 67 dBm compared to 70 dBm. Multipath and fading effects clearly have an impact on the power received, and most probably this is the reason of the huge increase in the signal received at floor 4. Buildings in Aachen downtown have a more rigorous trend, with a natural increase in received power as the height from the terrain increase. The Super C building, which does not have tall buildings surrounding it, also experience higher powers, while the building of the Economics faculty does not report significant powers until floor 4. Finally, buildings near the Uniklinik experience different behaviors. The Kullen building, which measurements are shown in Figure 4.14, is mostly stable through the different floors. Surprisingly, at the ground floor it is possible to see an almost equal sensed value as at the rooftop, while on the intermediate floor the signal received is a bit reduced, with a reduction of around 10 dB on the average. Finally, the Kawo2 building, depicted in Figure 4.15, reports a trend similar to the already shown SuperC and Economics building, even though with different values. Out of the measurements did, reported both in [10] as well as in [11], it is possible to conclude that outdoor models fail to describe the pathloss experienced indoors, due to the complexity of the scenario and of the environment. Thus, as pointed out in [10], measurements have to be performed prior of deploying opportunistic
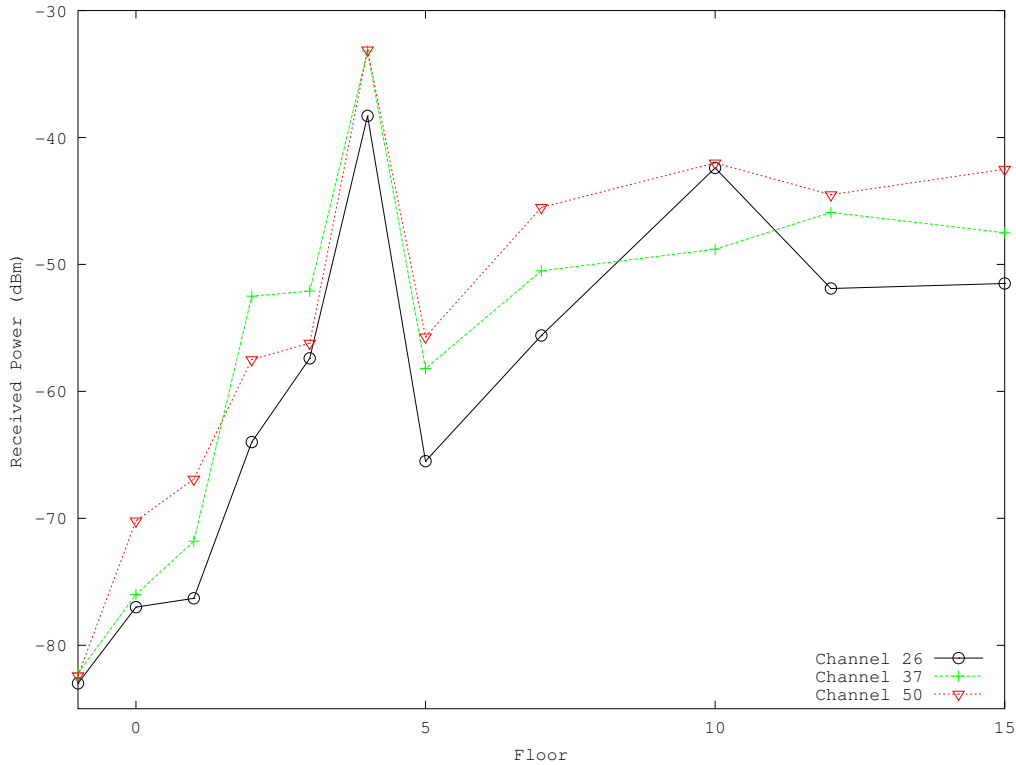
Figure 4.10: Spectrum measurements for the WEH Türme building.

networks that want to communicate over TV Gray Spaces rather than on TV White Spaces. This directly leads into higher costs for the network operator, which might eventually reduce the interests in such networks. Thus, the self configuring capabilities of devices should be exploited, in order to truly leverage the cognitive paradigm and better adapt to the environment.

4.3   Interference modeling

In this Section we evaluate the interference that indoor devices cause to the DTV receiver. We focus on two different kind of interferences: at first, we analyze the interference that the indoor device cause on the DTV receiver of its own building, which is discussed in Section 4.3.1. At second, we study the interference that indoor devices generate on the neighboring buildings, in Section 4.3.2. This behavior is depicted in Figure 4.1.
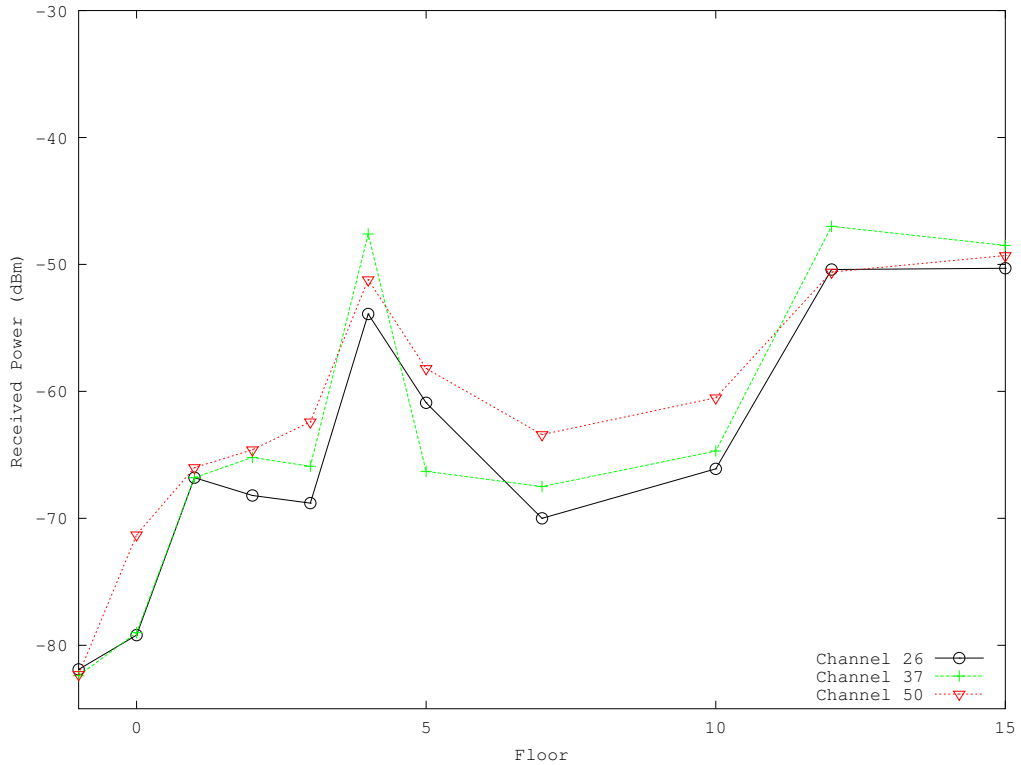
Figure 4.11: Spectrum measurements for the TVK Türme building.

4.3.1 Interference on the DTV antenna

In this Section we evaluate the interference that indoor devices cause on the DTV receiver of their own building. As it is not yet possible to transmit opportunistically in Italy on TVWS, we analyze the interference caused by indoor devices on the rooftop antenna with an analytical model which takes into account the path loss and the shadowing of the floors and the roof. We note that we perform a strictly conservative analysis on the transmitted powers. To be more precise, we assume that the neighboring indoor devices in the basement have to traverse just one wall and the roof of their building, and after that are in LOS with the antenna of the neighboring building. This of course is not true in most scenarios, but it is useful to give an insight on the potentials of this approach and analyze the worst case scenario which could occur. The interference device i causes on the antenna of its building can be computed using the following general equation:

$$\eta_i = P_{tx}^i - PL_i^I[d] - (n_f + 1) \cdot \alpha \qquad (4.2)$$
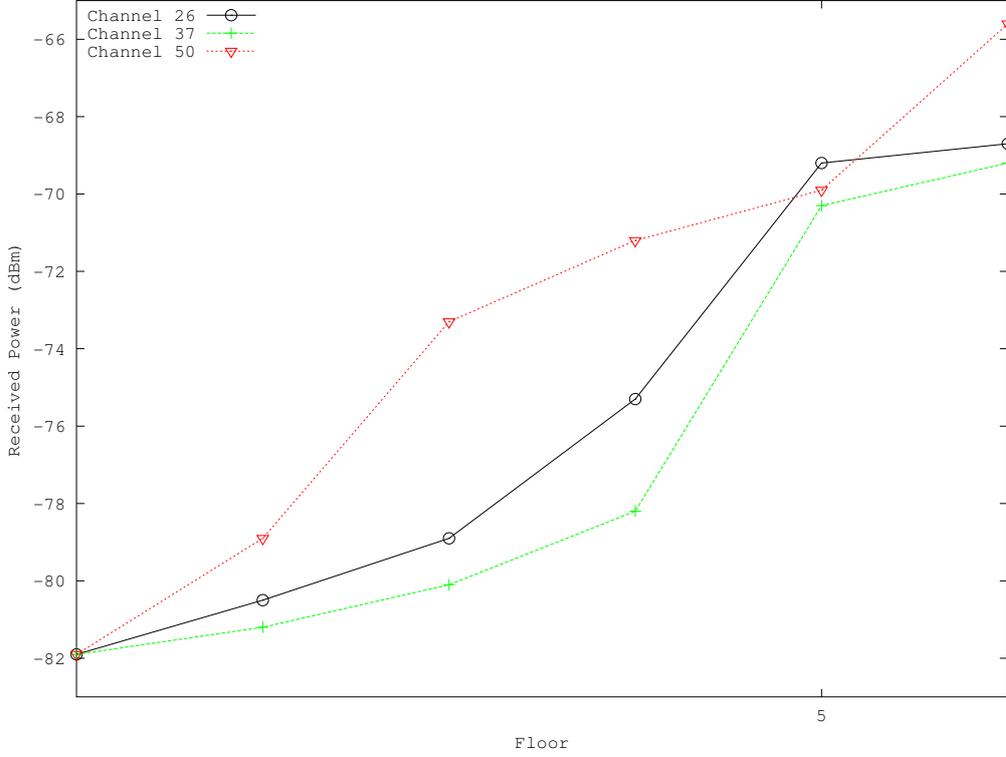
Figure 4.12: Spectrum measurements for the Super C downtown building.

where P_{tx}^i is the transmission power of device i, $PL_i^I[d]$ is the path loss from device i to the antenna of building I, n_f is the number of floors to traverse and α is the power loss due to shadowing for each floor. We set α to a conservative value of $20dB$ per floor [96]. The path loss term $PL_i^I[d]$ can be computed using the following Equation[94]:

$$PL[d_i^I] = 10\beta log_{10}(d_i^I) + 10\beta log_{10}(f) + X_g \qquad (4.3)$$

where d_i^I is the distance in meters, f is the transmission frequency and X_g is a zero-mean random gaussian variable with standard deviation σ. The terms β and σ have been studied for a plethora of different frequencies and scenario. In this work, we set them to $\sigma = 7$ and $\beta = 2$, which are quite conservative values regarding the pathloss experienced by experimental studies [96]. We assume that each floor is 3 meters high, so for instance at 6 meters the indoor device and the DTV receiver have 2 floors in between (1 floor and the roof). Basically, we want that the signal received by node j, transmitted from node i, is above a threshold SNR_j^{min} to make the signal detectable. The SNR is
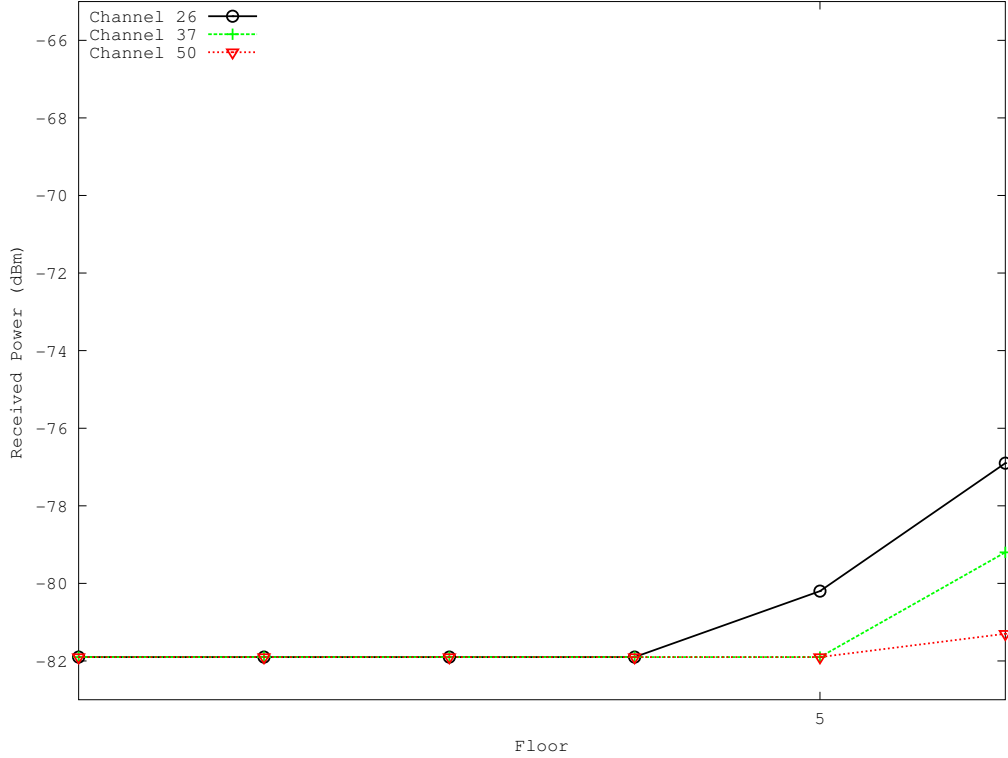
Figure 4.13: Spectrum measurements for the Economic downtown building.

defined as:

$$SNR = 10 \; log_{10} \left(\frac{S}{N} \right) \tag{4.4}$$

where S is the signal received, and N is the noise. Moreover, we also need to keep the interference on the DTV receiver below a threshold η_{max}^{DTV}. More formally:

$$Given: \; SNR_{\forall i}, \eta_{max}^{DTV} \tag{4.5}$$

$$To \; find: \; P_{tx}^i \tag{4.6}$$

$$Subject \; to: \; SNR_{i \rightarrow j} \geq SNR_j^{min} \tag{4.7}$$

$$\eta^i < \eta_{max}^{DTV} \tag{4.8}$$

To determine P_{tx}^i we act in two steps: first, we determine the minimum power needed to transmit one packet between the two farthest short range devices in the cluster. Second, we check if this power could cause harmful interference on the DTV antenna. In the remainder of this paper, we assume that all the short range devices in the cluster receive every channel with the same power.
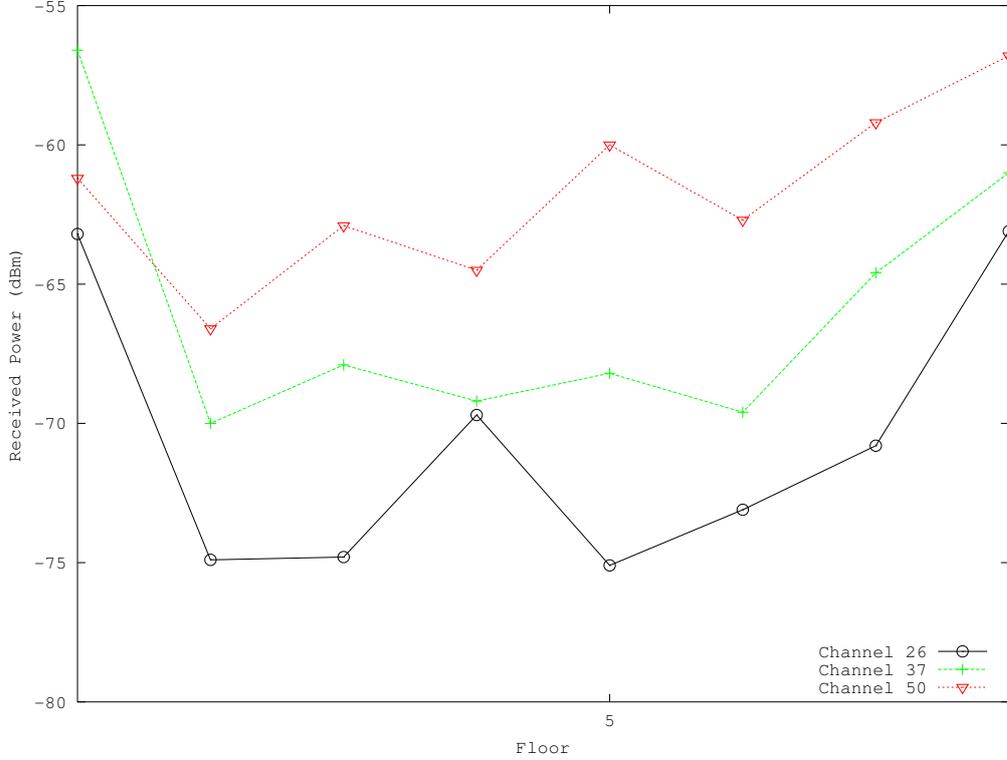
Figure 4.14: Spectrum measurements for the Uniklinik Kullen building.

Upon finding P_{tx}^i, we need to check if it can cause harmful interference on the DTV antenna, which should be below a threshold η_{max}^{DTV}, as Equation 4.8 states. Assuming that all the short range devices are placed underground and experience the same received powers, $P_{tx}^{i_k}$ is determined as follows:

$$P_{tx}^i \geq X_c + SNR_j^{min} + PL[_i^I] \qquad (4.9)$$

where X_c is the received power on channel c. At the same time, it should not exceed the threshold η_{max}^{DTV}. If the minimum required power P_{tx}^i would cause too much interference on the receiver, thus exceeding η_{max}^{DTV}, then no transmission is possible. Performance evaluation of the proposed study is given later in Section 8.4.

4.3.2 Interference on the neighbouring buildings

In this Section we evaluate the interference involved in neighboring buildings by indoor devices. Basically, the interference generated on the antenna of a building J by a cluster of transmitters $i_k \in I$ located on a near building I
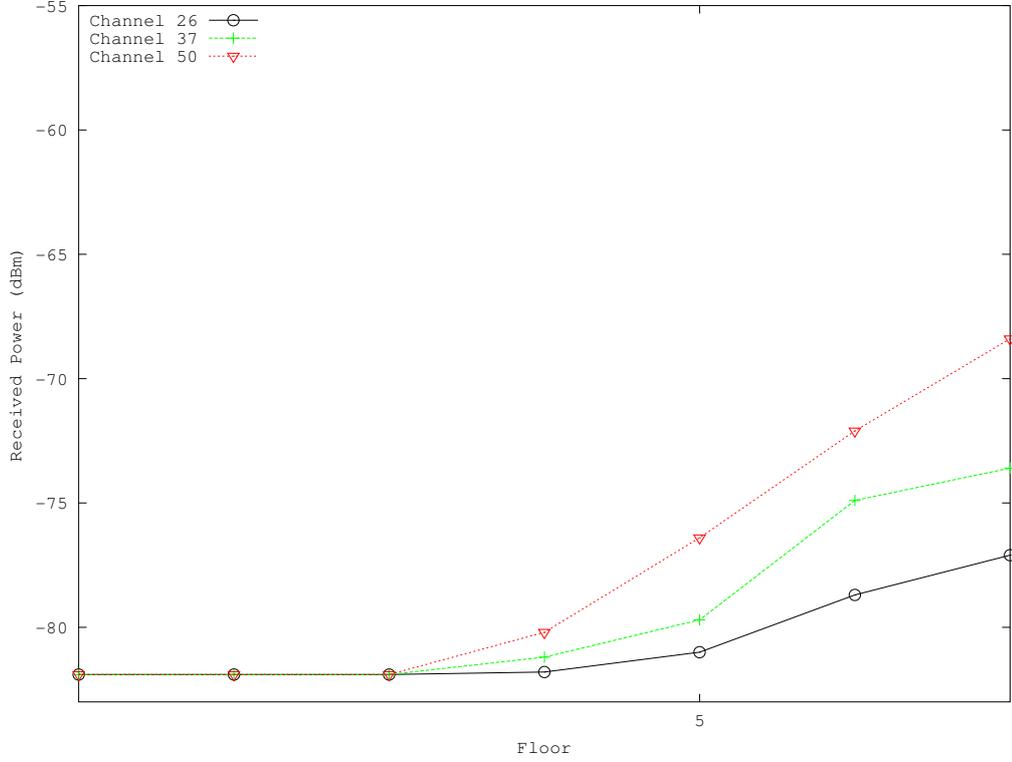
Figure 4.15: Spectrum measurements for the Uniklinik Kawo2 building.

can be computed as follows:

$$\eta_i^J = max_{\forall k \in J}(P_{tx}^{i_k} - PL[d_{i_k}^J] + \mu) \tag{4.10}$$

where $P_{tx}^{i_k}$ is the transmission power of device i_k, $PL[d_{i_k}^J]$ is the path loss between device i_k and the antenna located on building J. The term μ represent the loss of power due to the shadowing of the wall and the roof of building I, which we set to $\mu = 40dB$ [96]. The $P_{tx}^{i_k}$ term can be computed as before, regarding the transmission power device i_k needs to transmit intra cluster. The distance between device i_k and the antenna of building J is the Euclidean distance $d_{i_k}^J = \sqrt{s_J^I + H_J}$, where s_J^I is the distance between buildings I and J, and H_J is the height of building J. The term $PL[d_{i_k}^J]$ is the pathloss experienced by the signal transmitted by device i_k on the antenna located in building J, computed through Equation 4.3. We can compute now the total interference on the antenna of building K, which is equal to:

$$I_{tot}^K = max_{\forall i \in K}(\eta^i) + \sum_{J \in N} \sum_{k \in J}(\eta_K^I) \tag{4.11}$$
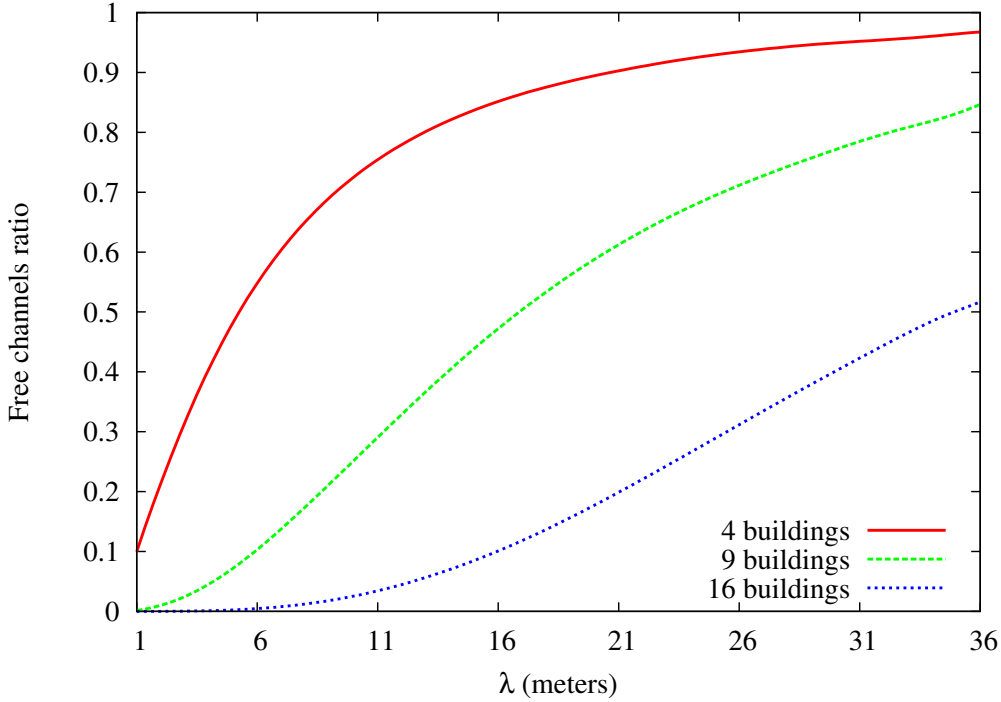
Figure 4.16: Ratio of interference-free buildings varying the height.

where N is the set containing all the neighbors of K.

4.4 Performance Evaluation

In this Section we evaluate the performance of the proposed framework while varying the scenario. Certainly, the most interesting aspect to study is about the ratio of free channels that it is possible to utilize without causing harmful interference to the DTV receiver. If not stated otherwise, in this Section we continue to perform strictly conservative analysis. That is, we assume that the channels are received at the low value of -75 dBm at the rooftop, so that the interference caused by indoor devices should be even lower to keep the desired SNR at the DTV receiver.

4.4.1 Analysis on buildings height

In this Section we evaluate the percentage of free channels, while varying the underlying scenario. More formally, we vary the buildings heights and the number of transmitting devices in the scenario. The heights H of the
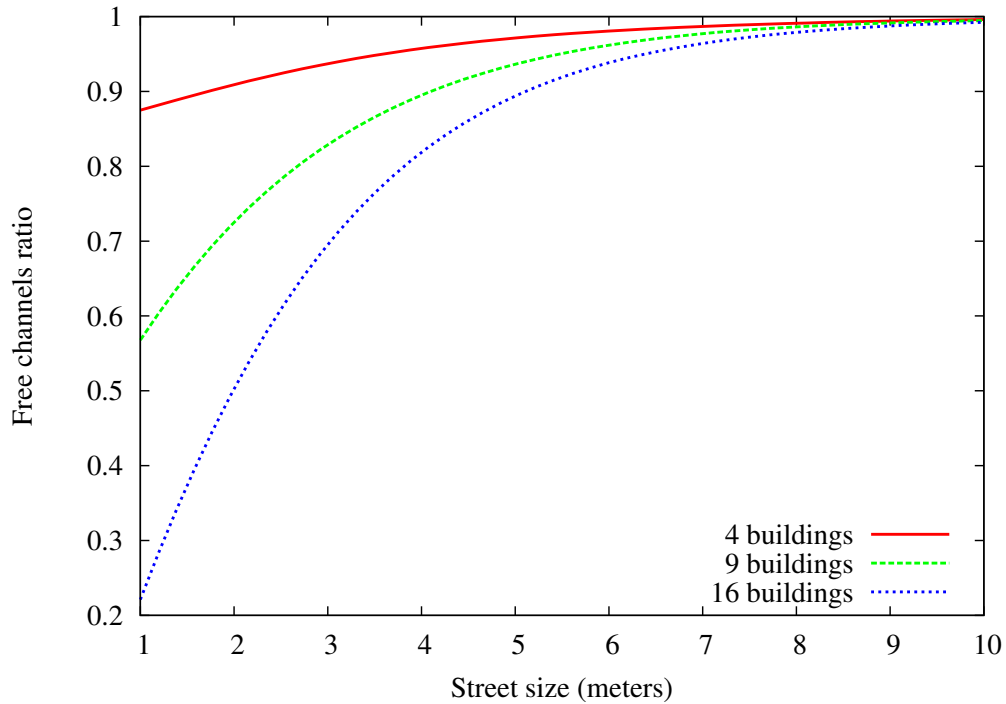
Figure 4.17: Ratio of interference free buildings varying the size of the streets.

buildings follow a Poisson distribution of parameter λ (i.e. $H \backsim P(\lambda)$).

In Figure 4.16 we plot the free channels ratio varying the parameter λ, that is, the height of the buildings. We also vary the scenario size, ranging from 4 to 16 buildings. We note that, again, we perform a conservative analysis. That is, we assume that all the indoor devices transmit exactly at the same time, so we sum them up in order to get the total noise on the DTV antenna. What arises from Figure 4.16 is that, as it may be intuitive, as the height of the building increase, also the ratio of free channels do so. In fact, taller buildings have a greater distance from the short range devices and the antennas.

4.4.2 Analysis on streets dimension

In this Section we analyze how the size of the streets s impacts on the interference on the DTV receiver. In Figure 4.17 we plot the ratio of buildings in which no harmful interference is perceived by communicating short range devices, while varying the size of the streets from 1 meter to 10 meters. The parameter λ is set to 15, and the transmitting power P_{tx}^i is set to $0\,\mathrm{dBm}$. The street size has a direct impact on the ratio of interference free buildings,
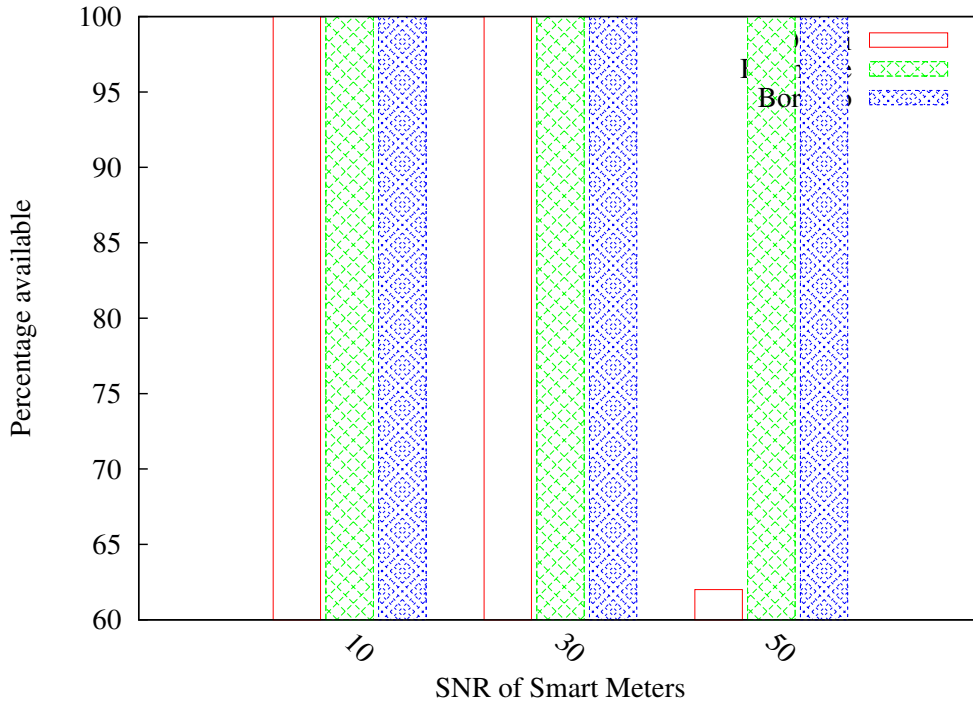
Figure 4.18: The percentage of available channels for the three scenarios, with SNR = 10.

since farther buildings interfere less within each other. It is possible to see that the size of the scenario has a direct impact only when the buildings are near to each other. As the distance from them increase, the ratio increases regardless of the number of interfering buildings.

4.4.3 Percentage of available channels

In this Section we study, based on the spectrum measurements, out of the occupied channels, how many channels can be used in the basement without causing harmful interference on the DTV antenna, for the three different scenarios. In Figure 4.18 we plot the percentage of available channels for the `Borgaro`, `Reiss Romoli`, and `Bramante` scenarios. In Figure 4.18 we can see the percentage of available channels when the SNR of the indoor devices is 10, while the SNR of the DTV receiver changes between 10, 30 and 50. It is clear that in the `Romoli` scenario there is a lower availability of gray spaces that can be used, since there is a slightly lower difference between the experienced powers, and because the building is not surrounded by tall buildings that can shadow the signal. This does not happen for the other

two scenarios, in which we experience a higher availability of gray spaces. We note that the fact that in the `Romoli` scenario there is a lower availability of gray spaces does not involve a scarcity of white spaces, since in the graph we present only the channels that are sensed as used at the rooftop (i.e. the signal received is $> \theta$). Moreover, we highlight the fact that gray spaces are more available in high populated areas is also a positive result, since this scenario is the one that experience the lowest availability of TV White Spaces.

4.5 Summary

In this section, we summarize on the results obtained and provide key factor to take into account for indoor communication over TVWS.

By looking at the results we provided, and to other similar found in literature [10] [111], it is possible to derive key factors for indoor communication over TV White Spaces and TV Gray Spaces.

- **Building height**. It is straightforward to note that the greater the distance from the DTV receiver, the higher the probability that no harmful interference is caused on the DTV antenna. On the other side, a lower building height might not be enough to shadow the signal coming from the building and from neighbors. Moreover, for instance in downtown, the height of the buildings may permit the usage of TV White Spaces indoor even at greater heights other than the basement, given the fact that the shadowing of the buildings contains the signal protecting the DTV antenna.

- **Building size**. Regardless of the height of the building, also the size have an impact on the protection of the DTV antenna. This is mainly due to the fact that smaller buildings have their antennas more exposed to the interference of neighboring buildings, while larger ones might help in creating additional protection thanks to a lower visibility of the antenna by neighbors.

- **Distance from the DTV transmitter**. Clearly, as the distance from the DTV transmitter increases, the received power drops. However, typically DTV transmitter are placed to maximize the coverage in highly populated areas, where it is also more common to find taller buildings. This fact is reflected in the received powers, and the SNR that should be maintained at the DTV antenna. Buildings at the edge of the DTV transmitter radius may experience low received powers, and

this implies that they can support only minimal noise from the indoor devices. On the inverse, when received powers are higher, DTV receiver may have a bigger budget in absorbing and discriminating noise.

- **Building materials**. The building material plays a paramount role in determining the availability of gray spaces. It has been shown how different materials impact the signal that goes through them [85] [96]. In general, it is difficult to find a general rule of thumb. In fact, there is a huge variance, dependent upon the frequency and the thickness of the material. Again, further measurements and results should be gathered prior to determine the effectiveness and possibility of indoor communications over gray spaces. The best option is to be as more conservative as possible. This means using the lowest attenuation values for the signal received from the DTV transmitter (so it is received at higher powers) and the highest for indoor communication (so more power is required to transmit).

- **Position on the floor**: in certain scenarios, the received power may change dramatically even few meters apart from two points. This means that, prior of any installation, it might be required to perform an on-site spectrum campaign, in order to locate the best spots to place the TVWS devices. This aspect would defintely raise the installation cost of secondary networks in TV Gray Spaces, reducing the attractivity of this kind of network deployments. Thus, the challenge is on how to minimize these installation cost to find the optimal spot in which to deploy the secondary network.

- **Temporal availability**: the DVB-T signal is quite static, and our measurements confirmed that. Moreover, also the refresh from the database is quite large compared to the time required to obtain a reply. Thus, no significant problem in temporal availability can be found. In other words, stakeholders can have the guarantee of a long availability in time of a TV channel, given the fact that sudden changes are unlikely.

Wireless communication is demanding a constantly increasing number of resources, either bandwidth to increase the network capacity, or new portion of spectrum to accomodate new services. In dense populated areas, it is challenging to find unused spectrum for a multitude of services, due to high utilization and the high number of services to allocate. Hence, TVWS can be considered as a good offload solution, but it is difficult to envision them as the unique wireless technology on a device.

Chapter 5

Comparison to other wireless technologies

Clearly, other bands and technologies exists, that might be capable to fulfill the user needs and provide the desired QoS. To this end, in this section we provide two different comparison, one between IEEE 802.11n and IEEE 802.11af, and the other one between IEEE 802.15.4m and other technologies in similar bands.

5.1 IEEE 802.11af and IEEE 802.11n

The TV bands have been considered, among the other use-cases, also for WiFi-like connectivity. Here, the propagation characteristics of the lower frequencies would help in reducing the probability of having a poor connection in complex environments or far from the AP. At the same time, an increased transmitting range also translates into an increased interference range [101]. IEEE standardized in the popular series of 802.11 standards the 802.11n amendment, for operations in the 2.4 GHz spectrum band, and the IEEE 802.11af amendment for operations in TVWS. While the former present much higher data rates, it struggles when obstacles obstruct the signal, while the latter present an opposite behavior. A full comparison of the two standards, along with a proposal of a new Modulation and Coding Scheme (MCS) adaptation has been presented in [11].

5.1.1 Pathloss and shadowing

Clearly, the pathloss model to be used, along with the penetration losses due to obstacles, is fundamental in order to correctly asses the performance of

both technologies. Even though specialized models for TVWS propagation exist, such as [10], to be consistent in this paper we use the same log-distance pathloss model, tuned with parameters gathered though studies which can be found in literature. The log-distance model is defined as in [96]:

$$P_l = 20 log_{10}(f) + 10\alpha log_{10}(d) \tag{5.1}$$

where f is the frequency in MHz, α is the distance power decay index, and d is the distance in meters. Moreover, we also apply a negative dB quantity based on the type and number of obstacles through which the signal passes. Here, TVWS experience a better obstacle penetration compared to ISM bands in the 2.4 GHz and 5 GHz [96]. The parameters we used in the rest of this work are detailed in Table 5.1. We note that these values are common in literature, and assumed as realistic by several works [66] [119], and the technical group on 802.11n [109], and show the better obstacle penetration lower frequencies have, compared to the upper bands.

Table 5.1: Path loss and shadowing parameters

Frequency	Parameter	Value
600 MHz (TVWS)	α	2.8
	External Wall	20 dB
	Interior Wall	3 dB
2.4 GHz (802.11n)	α	3.5
	External Wall	25 dB
	Interior Wall	4 dB

5.1.2 Capacity

The theoretical capacity is computed using Shannon's capacity equation:

$$C = B \cdot log \left(1 + \frac{S}{N} \right) \tag{5.2}$$

We plot this in Figure 5.1 and Figure 5.2. The difference between the two is only the size of the x axis: in Figure 5.1 we highlight the fact that, at long distances, 802.11af can maintain a higher capacity, thanks to a better propagation effect. However, since WLAN are used at shorter distances, and given the fact that improving the range does not directly translates into better throughput, as shown in [101], we plot in Figure 5.2 the focus on the capacity at short distances (i.e. less than 100 meters). Here, the benefits

of IEEE 802.11af become less evident, and worse compared to 802.11n on 2.4 GHz. Given this, one might conclude that for communications below a hundred meters 802.11n is still better compared to 802.11af. However, just looking at the capacity does not describe the propagation effects and the shadowing that the signal might incur into. We take into account these aspects in the following Section, when we consider the achievable data rates and the signal propagation aspects.
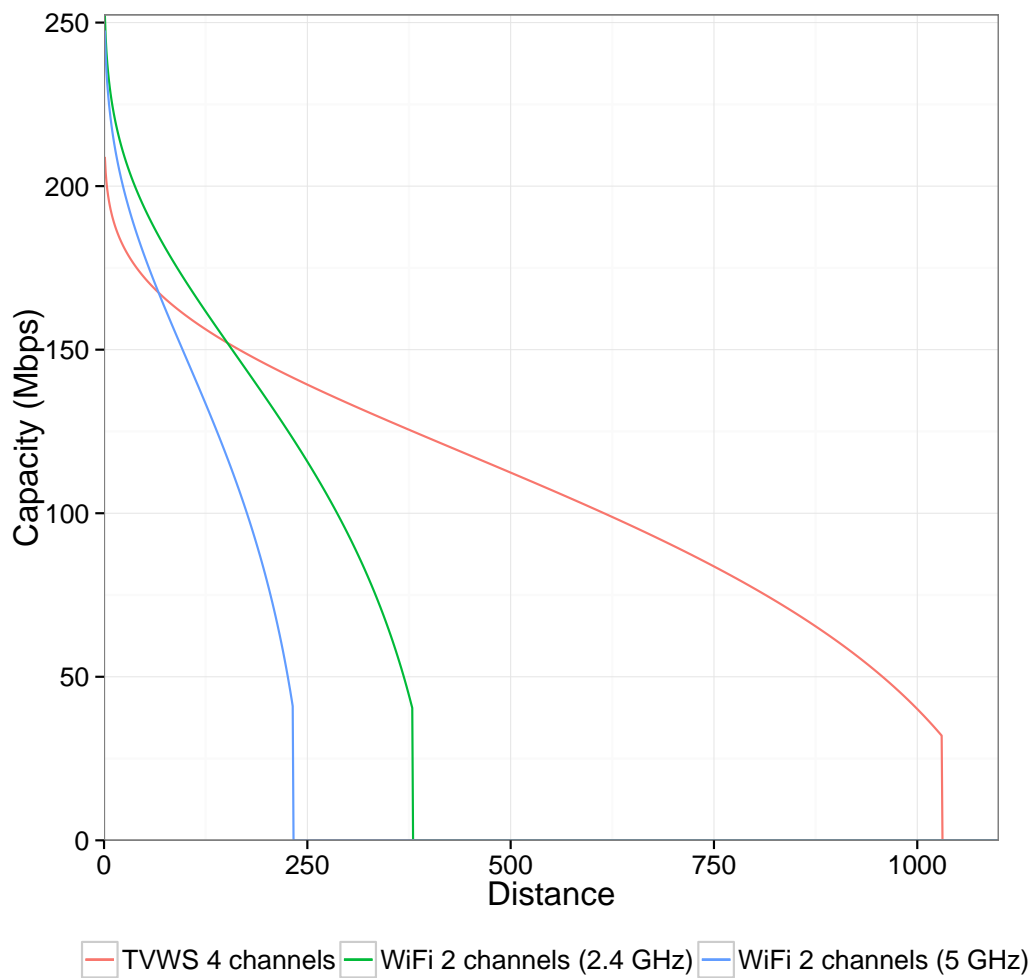
Figure 5.1: Capacity according to Equation 5.2.
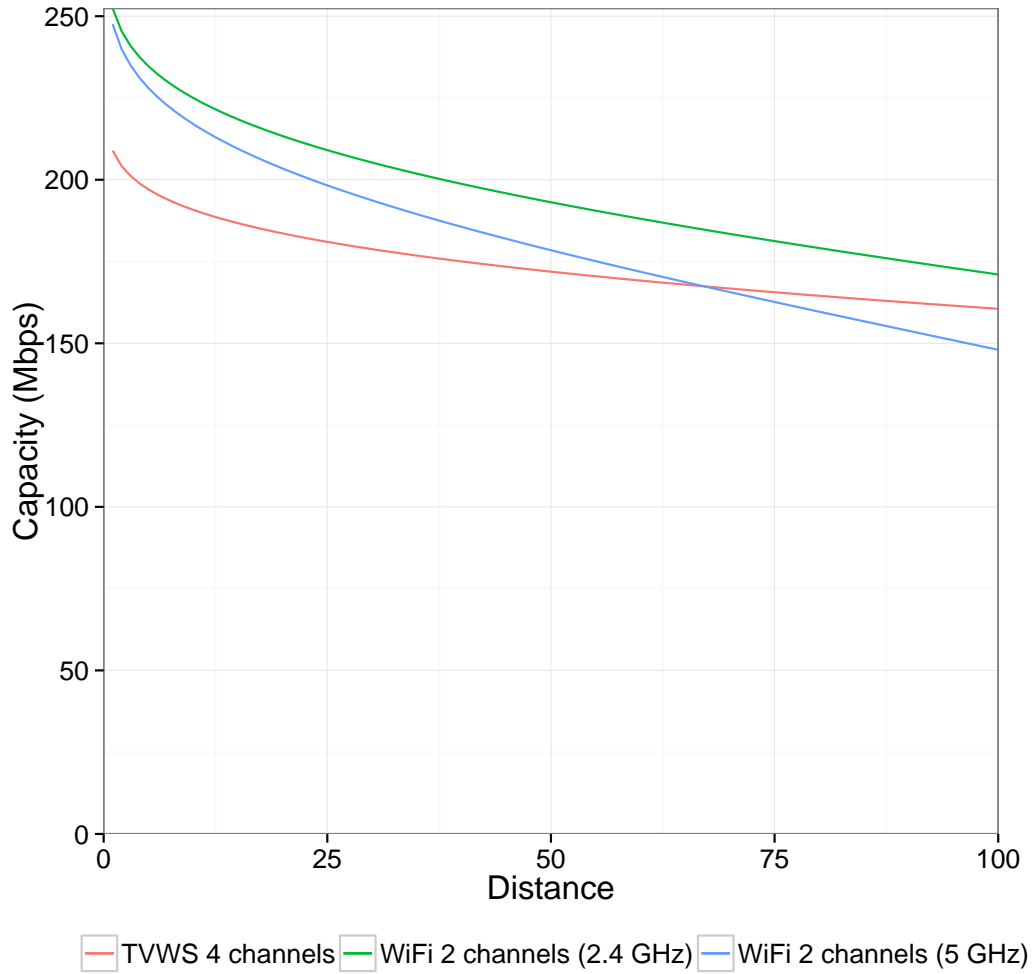
Figure 5.2: Capacity at short distance according to Equation 5.2.
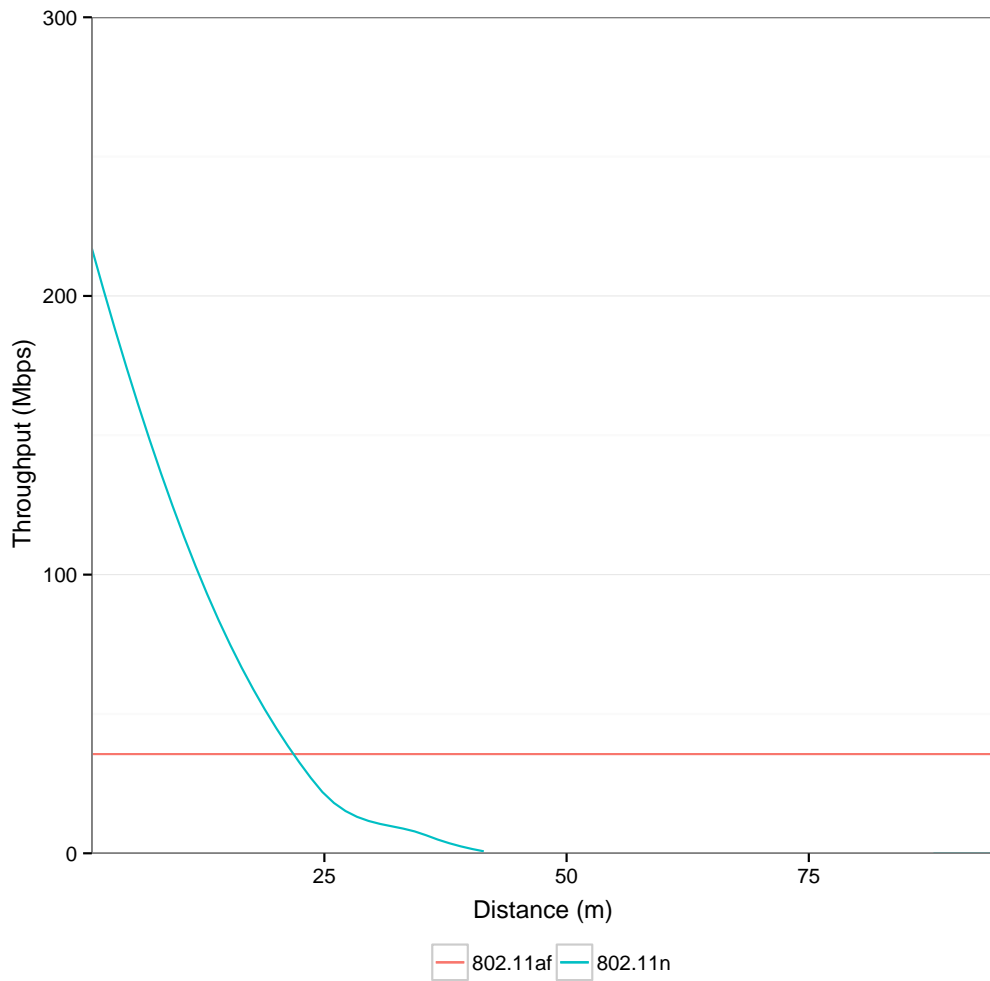
Figure 5.3: Throughput accounting propagation losses and shadowing effects.

5.1.3 Data Rate

Regarding the data rate, the two standards report very different achievable data rates, due to a greater bandwidth for the 802.11n compared to the TVWS amendment. The channel width of TV channels is 6 MHz in the US, and 8 MHz in Europe, against a wider 20 MHz or 40 MHz channels of the 802.11n. This leads to differences of more than 100 Mb/s for a single spatial stream, and nearly 450 Mb/s when bonding 4 channels together. We report this data in Table 5.2, along with the modulation used, for a single spatial stream. We note that, due to space constraints, we show only the data rate achievable with the highest coding scheme for each modulation. It is pos-

Table 5.2: Maximum data rates for a single channel

Technology	Modulation	Data Rate (Mbps)
802.11af	BPSK	2.7
	QPSK	8
	16-QAM	16
	64-QAM	26.7
	256-QAM	35.6
802.11n	BPSK	15
	QPSK	45
	16-QAM	90
	64-QAM	150

sible to see the much higher data rates achievable with 802.11n, due to the motivations already reported in this Section. However, an important aspect is the effective throughput achievable due to different environments, which shadow and reduce the received signal in Non-Line of sight (NLOS) conditions, such as indoors and urban areas. To study the effective throughput, we extended the Omnet++ discrete event simulator by adding the missing details for the studied protocols. Thus, in Figure 5.3 we plot the effective throughput, gathered through extensive simulations, in which we built a custom scenario and used a Constant Bit Rate application, always set to the maximum permissible data rate of each technology. Here, the benefits of IEEE 802.11af become evident. The increased shadowing losses due to the higher bands severely constrain the signal of IEEE 802.11n, while 802.11af remains basically constant at short distances, even though with a smaller data rate.

5.1.4 Algorithm

In this Section we detail our algorithm, in charge of selecting the best Modulation and Coding Scheme (MCS), based on the application layer constraints. Our channel is based on an Additive White Gaussian Noise (AWGN) model. Different environments have different propagation characteristics, thus we design the algorithm as self-adapting to the environment.

We define a vector $\Omega = \{\omega_1, \omega_2, \cdots, \omega_n\}$ containing the minimum SNRs for the n different MCS, ordered from the most robust one to the most performant, which means that $\omega_i \leq \omega_{i+1}$. If two MCS require the same SNR, then they are ordered according to the technology used, with 802.11af coming first. We also define a vector $\Psi = \{\psi_1, \psi_2, \cdots, \psi_n\}$, containing the data rates of the MCS according to the technology used, in the same order of Ω. Our algorithm is run by the Access Point, capable to switch between IEEE 802.11n and 802.11af. We assume that the access point can be on only one network technology at any given time, and we leave the synchronization between different access points as a future work. The purpose of the algorithm is to adapt to the current environment characteristics, and select the most suitable MCS given the received SNR. To this end, ε_{af} is computed according to the average SNRs of the packets received between two executions of the algorithm, every T_s seconds, if the last step was performed on 802.11af, and ε_n if the last step was on 802.11n. Given the fact that only one value can be computed, the other one is analytically derived according to the pathloss and shadowing models. We define ϕ as the bit-error-rate (BER) for a M-QAM modulation as:

$$\phi = \frac{4}{K} \cdot \left(1 - \frac{1}{\sqrt{M}}\right) \cdot Q\left(\sqrt{\frac{3K}{M-1} \cdot \frac{E_b}{N_0}}\right) \tag{5.3}$$

where M is the number of symbols of the current modulation, K are the bits per symbol, E_b represent the energy per bit, and N_0 is the noise. Q is defined as:

$$Q(x) = \frac{1}{\sqrt{2\pi}} \int_x^\infty e^{-\frac{1}{2}t^2} dt \tag{5.4}$$

We then compute the packet-error-rate (PER) λ as:

$$\lambda = 1 - (1 - \phi)^B \tag{5.5}$$

where B is the size in bits of the packet to be transmitted.

Finally, we derive Ψ' as follows:

$$\Psi' = \{\psi_1 \cdot (1 - \lambda_1), \psi_2 \cdot (1 - \lambda_2), \cdots, \psi_n \cdot (1 - \lambda_n)\} \tag{5.6}$$

where λ_i is the bit error rate of MCS i according to $\varepsilon_{\{af,n\}}$. As last step, we select $max(\Psi')$, which is the MCS that according to the current channel state gives the best performance, and update the clients about the technology and MCS which are going to be used in the next T_s seconds. We detail our proposal in Algorithm 1.

Algorithm 1: Adaptation

Every T_s seconds
if 802.11af **then**
  compute(ε_{af})
  $\varepsilon_n = af\_to\_n(\varepsilon_{af})$
else
  compute(ε_n)
  $\varepsilon_{af} = n\_to\_af(\varepsilon_n)$
end if
for i $= 1$ to n **do**
  compute($\phi_i(\varepsilon_{af,n})$)
  compute($\lambda_i(\phi_i)$)
end for
$\Psi' = \{\psi_1 \cdot (1 - \lambda_1), \psi_2 \cdot (1 - \lambda_2), \cdots, \psi_n \cdot (1 - \lambda_n)\}$
return $max(\Psi')$

5.1.5 Performance Evaluation

In this Section we evaluate the performance in terms of Packet Delivery Ratio (PDR) and achieved throughput. To this end, we built four custom scenarios to evaluate the performance in different conditions. More precisely, we built an `outdoor` scenario based on the buildings of the University of Bologna, in Italy, obtained through Openstreetmap[1], and imported into Omnet++, where we extended the Shadowing model [102] to account for different building materials, and different losses with respect to the frequency used to communicate [96]. Here, we place the Access Point in the center of the map. We also built an `indoor` scenario, in which we modeled a typical office building, in which devices can move inside the building boundaries, and in different rooms. Here, the Access Point is located in the middle of the building. We then extended the previous scenario, to model a `courtyard` in which the 802.11{n,af} Access Point is located in the center of the building, but devices can move also outside the building boundaries. Here, the outer walls severely degrade the received signal. Finally, we modeled a `rural` scenario,

---

[1]http://www.openstreetmap.org

in which devices move outside and inside buildings, but the building density is lower compared to the `urban` scenario, and consequently the probability to have a LOS communication is increased.

5.1.5.1 Packet delivery ratio

In this Section we evaluate the packet delivery ratio of the two different technologies in the four scenarios, varying the data rates and the number of hosts.
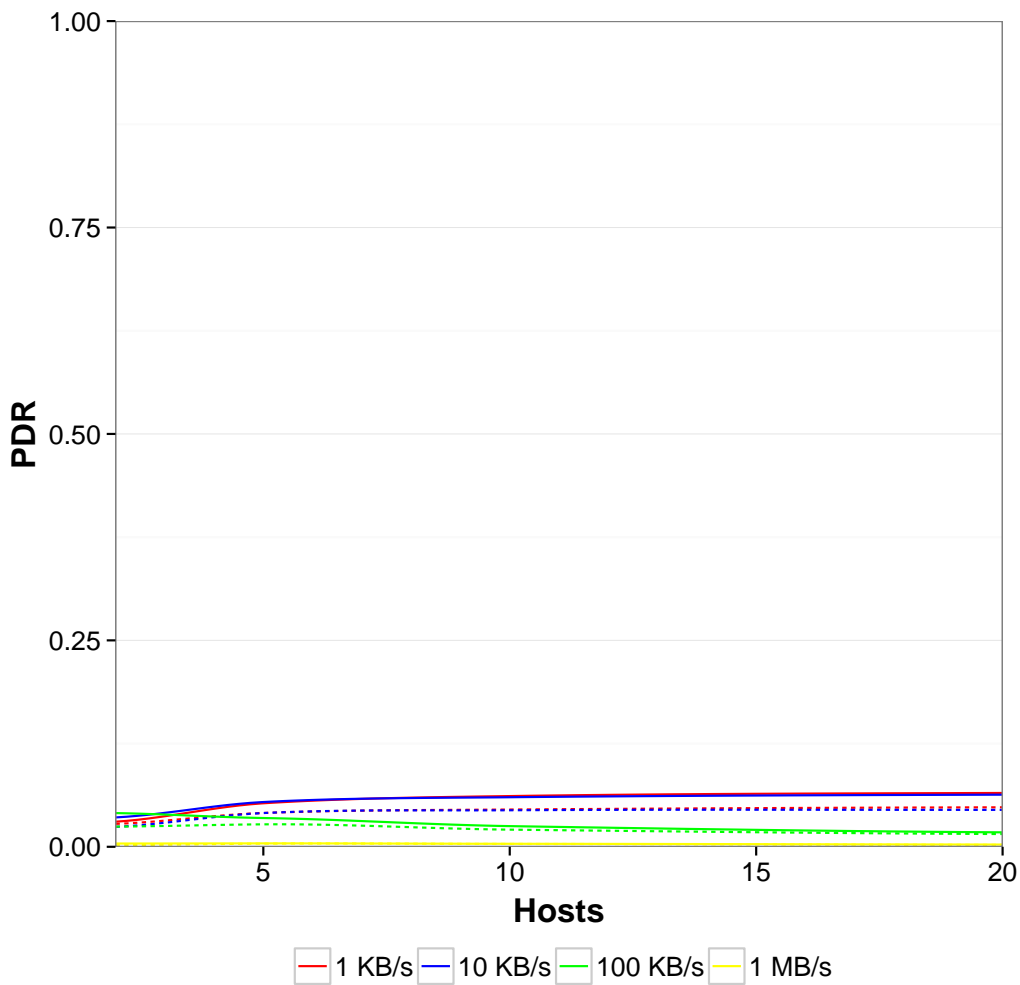

Figure 5.4: PDR for the `outdoor` scenario

In Figure 5.4 we plot the Packet Delivery Ratio (PDR) for the `urban` scenario. The `indoor`, the `courtyard`, and the `rural` scenarios are depicted in
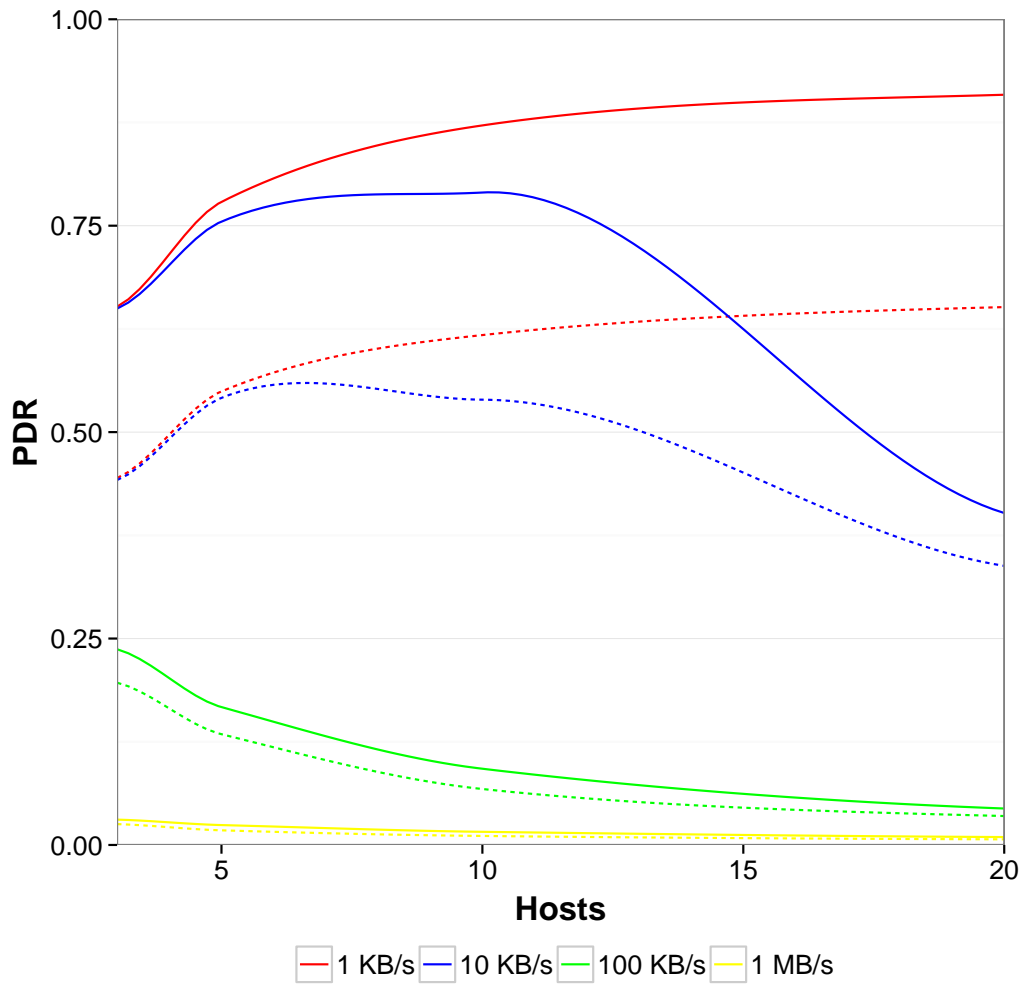
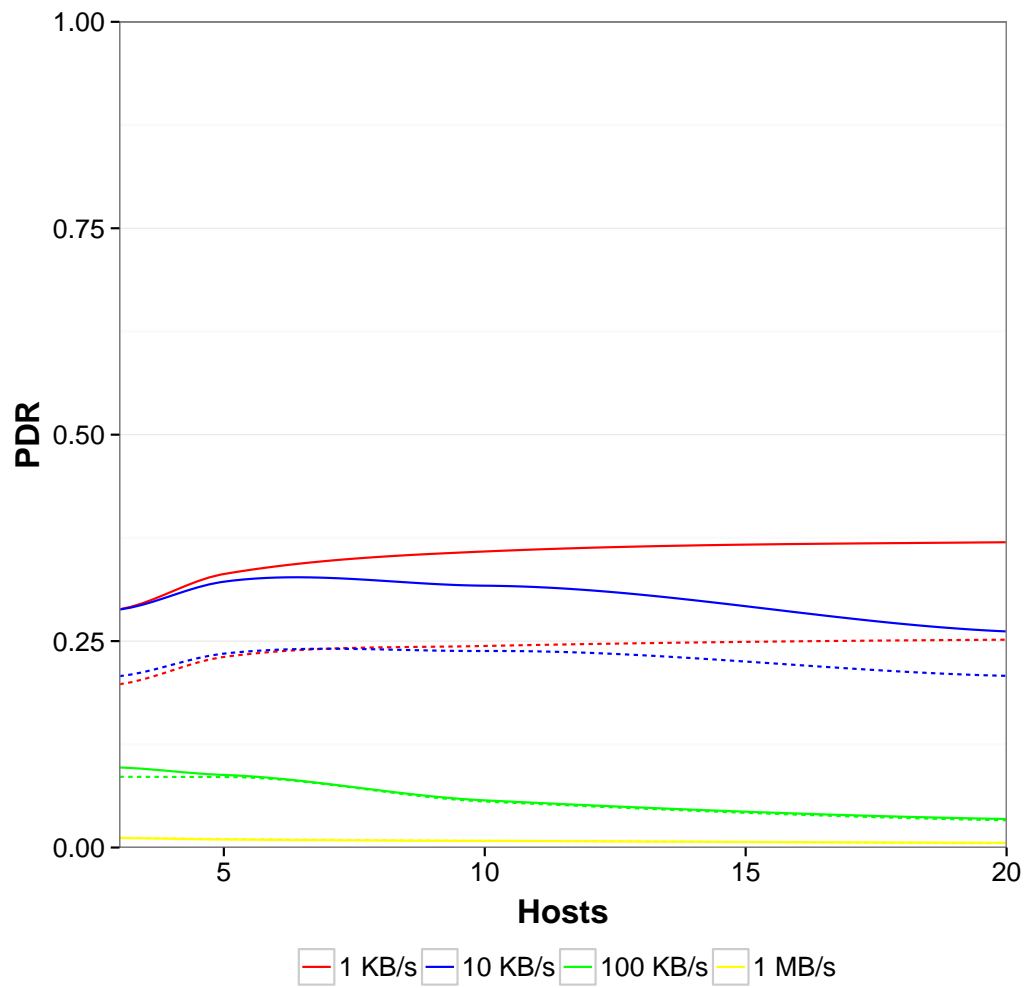Figure 5.5: PDR for the `indoor` scenario
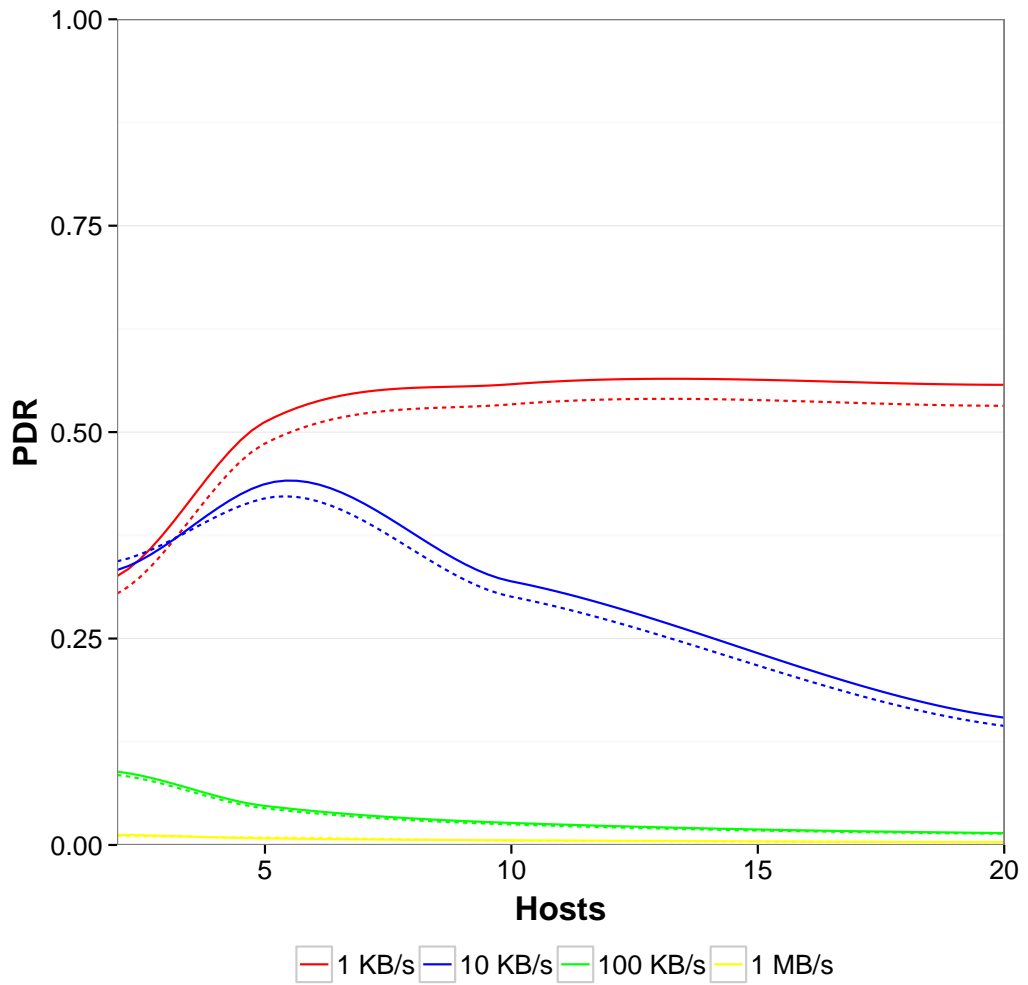
Figure 5.6: PDR for the `courtyard` scenario

Figure 5.7: PDR for the `rural` scenario

Figures 5.5-5.6-5.7. What it is possible to see in Figure 5.4 is that regardless of the technology used, only one access point is unable to serve the large urban area modeled. This is due to shadowing effects, which in dense areas degrade the signal which eventually reach levels at which it is not detectable anymore. This translates into a larger number of deployed access point, and shows that even though 802.11af can achieve a greater range, in urban areas it is still hard to perceive a benefits in terms of range. A different situation is depicted in Figures 5.5, 5.6, and 5.7. Here, the 802.11af Access Point is able to achieve better performance, and for large numbers of clients it can almost double the performance of the 802.11n Access Point. The PDR increases while increasing the number of clients, for small data rates, for the 802.11af because the scenarios are smaller, and thus a higher number of clients translates into a better probability of reaching the AP. On the inverse, the 802.11n Access Point fails to serve a larger number of clients, because of undelivered packets and re-transmission, which rapidly fill the wireless channel. To conclude, 802.11af networks might be interesting for shorter distances but in complex environments, contrarily to the common belief of using it to cover larger distances.

Although these results certainly not represent the whole set of possible scenarios, they are representatives of some specific use-case. In particular, the `indoor` scenario can have huge differences depending on the materials used, and the walls' thickness. However, the numbers could vary, but the general qualitative results will remain the same, regardless of these differences.

5.1.5.2 Algorithm Evaluation

In this Section we evaluate our algorithm, presented in Section 5.1.4, with the focus on the achievable throughput and on the packet error rate (PER). All the following evaluations have been performed on the `indoor` scenario. In Figure 5.8 we plot the achievable throughput by a IEEE 802.11n network, a IEEE 802.11af network, and with our algorithm deployed. We do this while varying the T_s parameter, which is the time step at which the algorithm is executed. What it is immediately evident to see is the fact that the IEEE 802.11n network is always better compared to its 802.11af counterpart, with an increase of nearly 3 Mb/s. However, increasing the T_s parameter decrease the performance, since the devices are not able to react fast to the mobility of the users. This less affects the 802.11af network, given the better obstacle penetration which does not change as fast as the user position. Another point is the fact that even though the 802.11n is always better compared to the 802.11af network, the data rate differences are much smaller compared to the theoretically achievable, due to shadowing which forces to use stronger
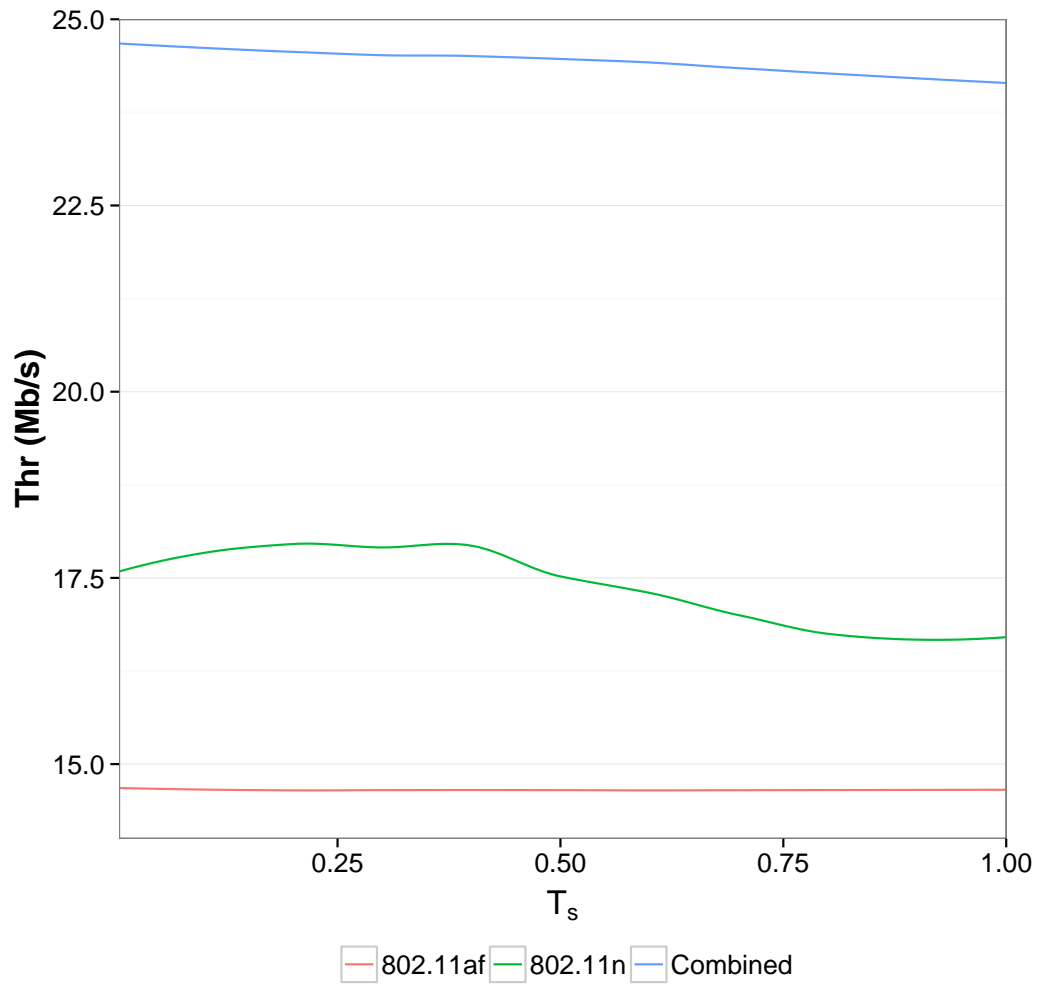
Figure 5.8: Throughput combining IEEE 802.11n and 802.11af networks.
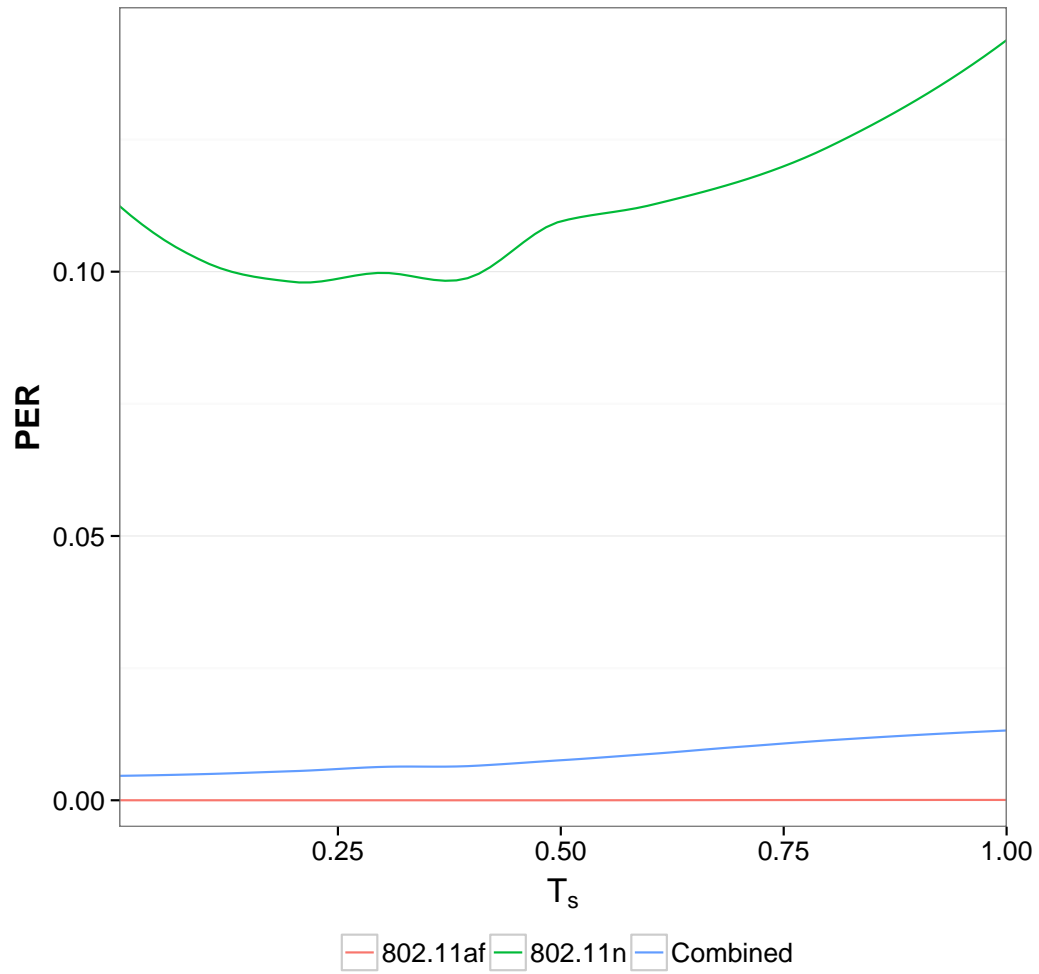
Figure 5.9: Probability of packet error (PER)

modulations on the 802.11n network. However, by combining both networks into one, using our algorithm to select the technology to be used and the most suitable MCS gives the best performance, with a gain of nearly 8 Mb/s over the 802.11n network. This is mainly due to a better PER while using the 802.11af network. However, here the problem of choosing a not too large T_s is still visible, although reduced. In Figure 5.9 we report the results with the same simulation setup, but focusing on the PER experienced. This closely follows the chart we shown in Figure 5.8. The 802.11n network achieves the worst performance, being stable at 0.10 until a T_s lower than 0.5 is chosen, and eventually increasing up to nearly 0.18. On the inverse, the 802.11af network achieves almost zero PER, thanks to the better signal propagation and obstacle penetration. Again, by combining the two technologies, our algorithm achieves better results, by switching to the slower network (i.e. the 802.11af) when experiencing difficult conditions on the channel, and switching to the faster one (i.e. the 802.11n) when closer to the Access Point. However, our algorithm achieves slightly worse performance, due to the fact that it can lose some packets before switching to 802.11af.

5.2   IEEE 802.15.4m and the 433 MHz and 868 MHz bands

5.2.1   433 MHz band

The 433 MHz band ranges from 433.05 MHz up to 434.79 MHz, and is divided into 69 channels spaced by 25 kHz. The 433 MHz band has some considerable advantages. First of all, the band is the same in almost all the countries worldwide, making it more cost-efficient for manufacturers to build devices that operate over this frequency range. Secondly, it has desirable propagation characteristics, which make the signal to travel better through walls and in buildings in general. For instance, in [110] the authors compare the propagation characteristics of signals in the 433 MHz band with 2.4 GHz. In general the frequency band is quite similar for TV-bands, and is even in the lower edge of those frequencies. Some small differences do exist between regulations worldwide. In Europe, ETSI states that this band can be used with a maximum output power of 10 mW (ERP) when the duty cycle is less than 10%. However, when used without duty cycle limitations, the maximum ERP is lowered to 1 mW [39]. This can be raised to 10 mW if smaller channel widths are utilized.

5.2.2 915 MHz band

The 915 MHz band ranges from 902 MHz up to 928 MHz, thus constituting a total of 26 MHz of bandwidth. The maximum effective isotropic radiated permitted power (EIRP) is -1.23 dBm. However, when using frequency hopping, this maximum power could be greatly increased. When hopping on less than 50 frequencies, the EIRP raises to +30 dBm, whilst when using more than 50 channels to hop on, the EIRP goes up to +36 dBm. Each single frequency should not be occupied for more than 0.4 seconds in a 20 seconds period, which corresponds to a 5% duty cycle. When using frequency hopping, each channels should be no more than 500 KHz wide [41].

5.2.3 868 MHz band

The 868 MHz band ranges from 863 MHz up to 870 MHz, thus constituting a total of 7 MHz of bandwidth. The maximum effective radiated permitted power (ERP) varies greatly depending on the effective portion of spectrum considered and on the duty cycle. It scales from as little as 7 dBm, when transmitting with a 100% duty cycle in the 869.7-870 MHz band, to 27 dBm when transmitting with a reduced duty cycle of 10% in the 869.4-869.65 MHz band. Larger bandwidths can be utilized when transmitting, for instance, in the 868-868.6 MHz and on the 869.7-870.2 MHz bands, even though the duty cycle should be reduced to 1% and 0.1%, respectively. The 868 MHz band is available only in ITU Region 1, while for ITU Region 2 the comparable band is in the 915 MHz range.

When using TVWS as a reference for the envisioned gray spaces operations, the strongest differences come from two aspects: maximum permitted power and available bandwidth. Regarding the maximum permitted power, in the 433 MHz band it is possible to transmit with 26 dB less than in TVWS and 9 dB less than in the 868 MHz bands, even when exhibiting a smaller duty cycle. Even though 433 MHz is a lower frequency, thus having better propagation characteristics, 26 dBm makes essential differences which can significantly reduce the transmitting range when compared with TVWS. Speaking about the bandwidth, in the 433 MHz band we can rely just on 25 kHz of channel bandwidth, compared to 600 kHz (at maximum) for 868 MHz, and a wider 8 MHz channel for TVWS. However, larger bandwidth in the 868 MHz range can be obtained only when drastically reducing the duty cycle. The relevant characteristics of each of the presented technology are summarized in Table 5.3, where C denotes the channel capacity at 1 meter distance, and D is the maximum permitted duty cycle. Note that for reasons of comparability, we neglect protocol overhead and conduct only a theoretical capacity

evaluation for a set of modulation schemes. Practical implementation will naturally achieve lower throughput.

Table 5.3: Comparison of different technologies.

Technology	Range (MHz)	B (MHz)	C (Mbps)	D (%)	P_{tx} (dBm)
433 MHz	433.05-434.79	1.74	11.49	10	10
433 MHz	433.05-434.79	1.74	11.22	100	0
433 MHz	433.05-434.79	0.025	0.17	100	10
868 MHz	863-870	0.05	0.33	0.1	14
868 MHz	863-870	0.3	2	0.1	14
868 MHz	868-868.6	0.6	3.98	1	14
868 MHz	868.7-869.2	0.5	3.32	0.1	14
868 MHz	869.4-869.65	0.25	1.71	10	27
868 MHz	869.7-870	0.3	1.97	100	7
868 MHz	869.7-870	0.3	2	1	14
TVWS	470-790	8	54.87	100	36

By using the α and β values derived from the indoor propagation measurements, we plot in Figures 5.10, 5.11 and 5.12, the achievable throughput that could be obtained indoors when using different modulation schemes and bandwidths. For each modulation taken into account (BPSK, 4-PSK, 8-PSK and 16-PSK) we consider the minimum required SINR to achieve a bit error rate of 10^{-6}, and plot the achievable throughput according to the Shannon-Hartley capacity,

$$C = B \cdot log_2 \left(1 + \frac{S}{N + I} \right) \tag{5.7}$$

, where B is the bandwidth, S is the received signal, N is the noise, and I is the interference signal.

We have selected the channel bandwidths to align with technologies in the other bands, e.g. 802.15.4 or ITU-T G.9959. Sudden drops in throughput are caused by the switching of the applied modulation scheme. We note the huge difference in achievable throughput between the three different setups, but find it also interesting to analyze the transmitting range. The higher transmitting power of TVWS (we assume this to be 36 dBm, but note that the regulations may differ) greatly enhances the range, compared to 10 dBm for the 433 MHz band and 27 dBm for the 868 MHz band, which also have severe limitations on the duty cycle. Regarding the range, we see a viable range of nearly 40 meters for the 8 MHz signal, compared to around 20 meters for the 300 kHz signal and less than 18 meters for the 25 kHz signal.
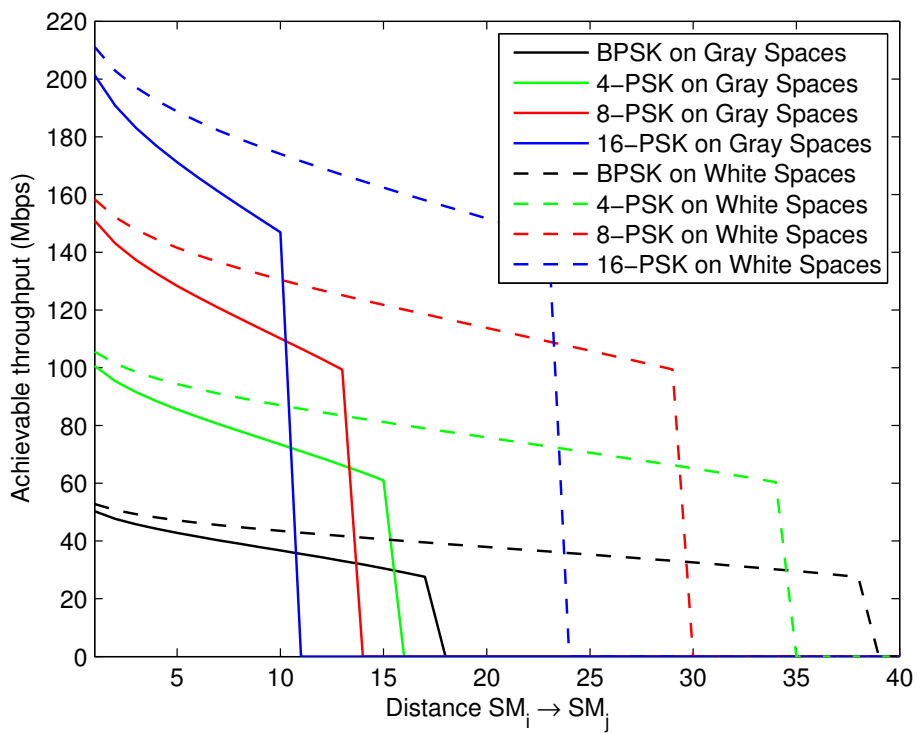
Figure 5.10: Differences in achievable throughput with a maximum BER of 10^{-6} for TV White Spaces.
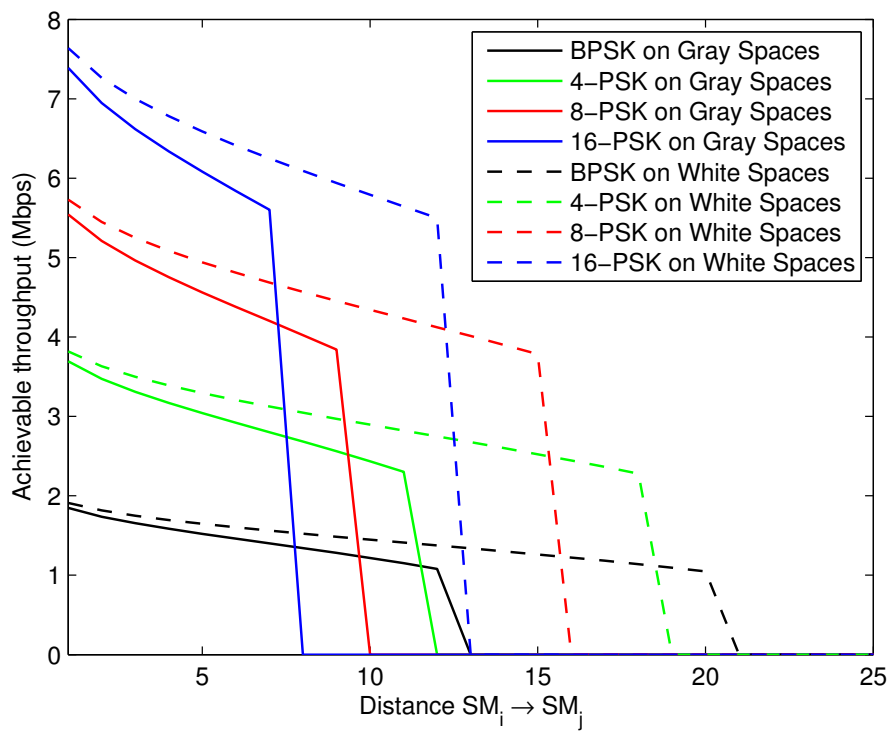
Figure 5.11: Differences in achievable throughput with a maximum BER of 10^{-6} for $300\,\mathrm{kHz}$ channels.
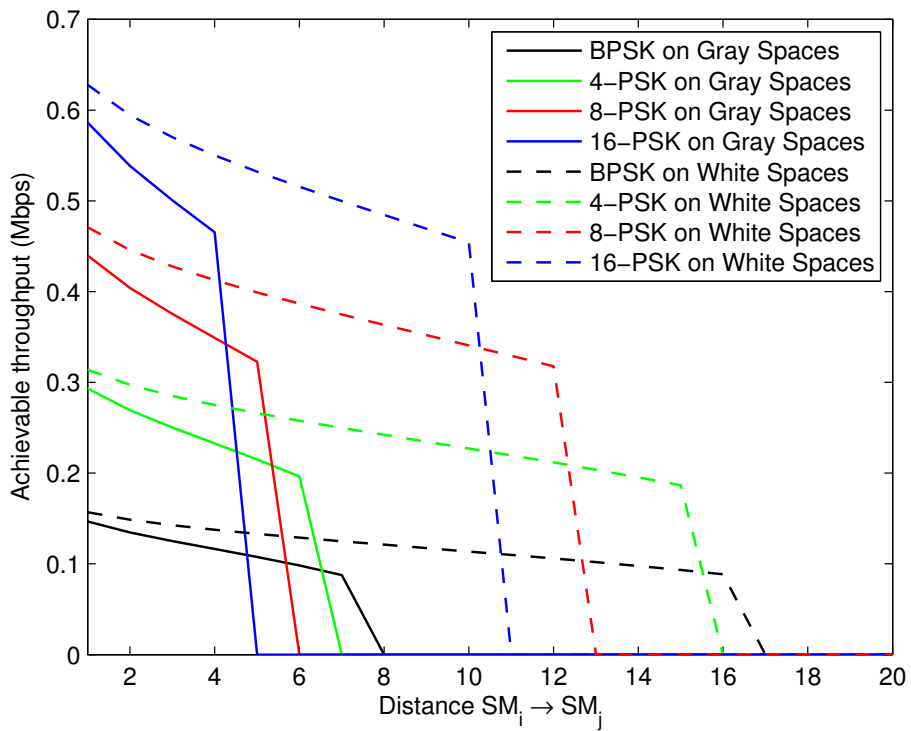
Figure 5.12: Differences in achievable throughput with a maximum BER of 10^{-6} for 25 kHz channels.

5.3   Summary

TVWS are certainly not the only technology that could be used to cut the digital divide, and bring additional spectrum to services that need it. In this section, we compared protocols using TVWS like the IEEE 802.11af and the IEEE 802.15.4m against other well knwon protocols and frequency bands, comparable for their specific use.

Regarding WiFi-like protocols, certainly the IEEE 802.11af protocol can bring a better transmitting range, at the cost of an increased interference. Section 5.1 has shown how they can be combined together, to leverage the benefits offered by both technologies. Section 5.2 focused instead on sensor-like networks, and analysed the benefits of TVWS operated networks against other similar bands like the 433 MHz and the 868-915 MHz band. The outcome is that TVWS can be useful for these service, due to their good propagation characteristics, and the considerably larger bandwidth they can offer. The picture is completed with a higher duty cycle, which is instead much reduced for the other spectrum bands if larger bandwidths are used.

Chapter 6

Per-Floor spectrum sharing

We are gradually moving from a licensed spectrum allocation, to a shared spectrum allocation, in which the spectrum is given based on the actual request by devices.

In this chapter we present and evaluate our proposed approach to spectrum sharing, showing how by allocating different channels at different floors it is possible both to protect the primary users, as well as serve the secondary users [13].

6.1 System Model

This section gives an overview of the system model that is used for the Per-Floors spectrum sharing paradigm.

We define a secondary network of N devices, deployed through the various floors of M buildings. More formally, we define the N devices as $\{n_0, n_1, \cdots, n_{N-1}\}$, and the M buildings as $\{m_0, m_1, \cdots, m_{M-1}\}$. Another assumption needed for this framework is the fact that each device has internet access.

Given $P_{rx}^{F,F'}$ the received power between two devices operating in floors F and F', with $1 \leq F \leq f_{m_i}$ and $1 \leq F' \leq f_{m_j}$ $(i \neq j)$, we define it as:

$$P_{rx}^{F,F'} = P_{tx} - PL[d_{F,F'}] \tag{6.1}$$

where $d_{F,F'}$ is the distance between floor F and floor F'. Clearly, obstacles can be present, and thus make NLOS links. Hence, $P_{rx}^{F,F'}$ can be considered as an upper bound on the effective received power.

The path loss model we use here comes from [10], and will be later described in Section 7.2.2. It is defined as:

$$PL[d] = 17.23 \times log_{10}(d) + 100.98 \tag{6.2}$$
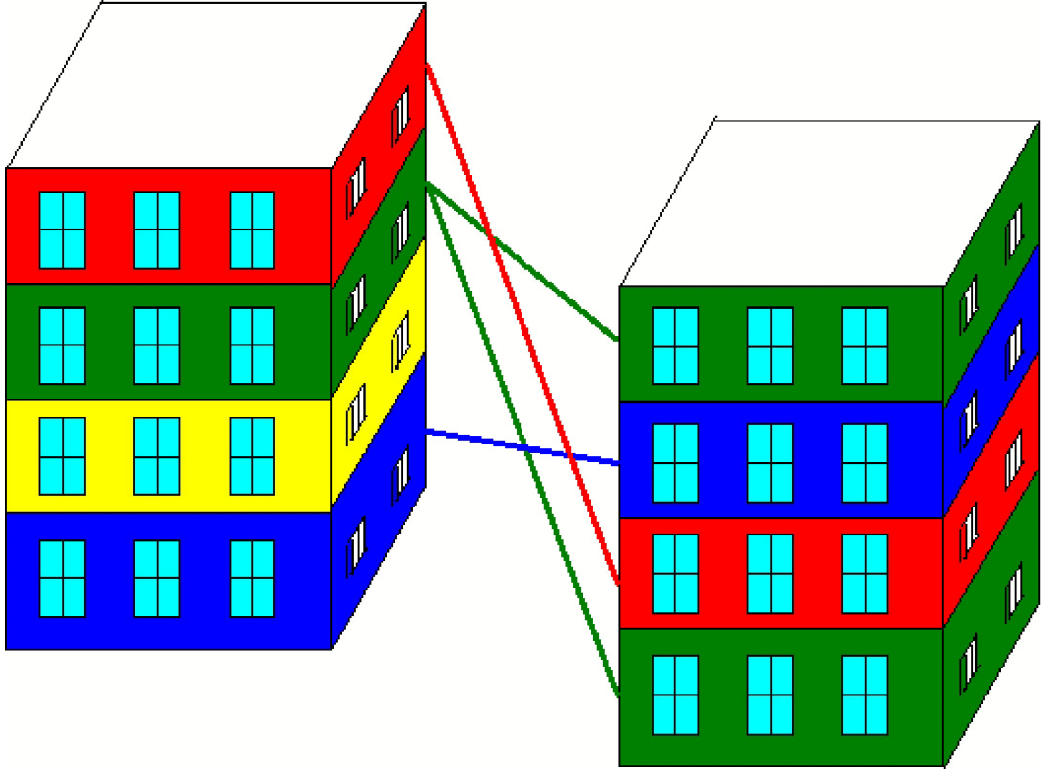
Figure 6.1: Per-Floor spectrum sharing. On the left building, 4 different channels are used, thus allowing to achieve no interference between them. On the right building, the same channel is used at the top and at the ground floor, thus achieving a separation distance of 3. Moreover, the co-building separation distance is 1, since the channel used at the 3rd floor in the left building is used also on the top floor of the right building.

To know whether to floors are interfering between each other, we simply check:

$$P_{rx}^{F,F'} > NF \tag{6.3}$$

where NF is the noise floor. For TVWS channel, the channel width can be 6 MHz, 7 MHz or 8 MHz, depending on the operating region.

We then define $I(F, F')$ as:

$$I(F, F') = \begin{cases} 1 & P_{rx}^{F,F'} > NF \\ 0 & \text{otherwise} \end{cases}$$

For sake of simplicity, we define that two buildings are interfering between each other if at least two of their floors interfere. We note that this assump-

tion can be relaxed in the future, but nevertheless represent a worst-case scenario analysis with respect to the effective interference. More formally, we define:

$$I(m_i, m_j) = max(I(F, F'), \forall F \in m_i, \forall F' \in m_j, i \neq j) \qquad (6.4)$$

$$I(m_i, m_i) = 0 \qquad (6.5)$$

which tells whether two buildings m_i and m_j have at least a pair of floors which interfere between each other. We note that in real deployments, the total number of interfering floors would be lower compared to our model, since especially for tall buildings, the shadowing added to the distance would reduce too much the signal.

Finally, we build a $M \times M$ matrix I as follows:

$$I = \begin{pmatrix} I(m_1, m_1) & I(m_1, m_2) & \cdots & I(m_1, m_M) \\ I(m_2, m_1) & I(m_2, m_2) & \cdots & I(m_2, m_M) \\ \vdots & \vdots & \ddots & \vdots \\ I(m_M, m_1) & I(m_M, m_2) & \cdots & I(m_M, m_M) \end{pmatrix}$$

which represents all the buildings of the scenario interfering with each other.

To make the analysis more realistic, and to add dynamicity in our system model, we define two parameters s and S, which represent the number of floors to consider as potential interferers in the same building and in other possibly interfering buildings, respectively. Thus, for a floor F, we consider as interfering the floors in the interval $F \pm s$ on the same building, and floors $F \pm S$ on neighboring interfering buildings.

In the following, we define two possibilities in which our model can be utilized, namely the Primary User Protection, and the Secondary Network Coexistence.

6.1.1 Primary User Protection

The first scenario in which we study our system model is about the PU protection. We then consider a deployed primary network, and DVB-T decoders can receive the signal from either a rooftop or a settop box antenna. In the following, we assume that all the devices at each floor receive the signal with set-top boxes, which certainly represent the worst-case for SU operation in TVGS. We note that our previous results indicate that indoor there is poor reception of this signal, and typically the signal is received through rooftop antennas. Thus, real deployments would certainly have better protection compared to our results, since rooftop antennas are farther to low floors, and

thus more protection is granted. Moreover, high gain antennas, typically used for DVB-T reception, would also benefit from additional protection due to the directionality of the antenna gain [63].

DVB-T receivers report the channel they are actually receiving to a central entity, via an internet connection. Thus, gathering all the information together, the central entity defines a vector $\omega_{m_i} = \{c_1, c_2, \cdots, c_{f_{m_i}}\}$ for each building m_i, where each c_i represent the channel which the DVB-T receiver of floor i is receiving.

In the context of PU protection, the parameters s and S define the acceptable interference that the secondary network might induce on the primary network. In this scenario, a SU transmitting in floor F must not use any of the channels seen by PUs in floors $F \pm s$ in its building, and $F \pm S$ in all its interfering buildings. More formally, the total set of available channels C_F at floor F of building m_i is defined as:

$$C_F = C \setminus \omega_{m_i}[F - s, F + s] \setminus \bigcup_{I(m_i, m_j)=1} \omega_{m_j}[F - S, F + S] \qquad (6.6)$$

where C is the set containing all the possible channels, $\omega_{m_i}[F-s, F+s]$ defines all the channels seen in floors $F \pm s$ of building m_i, and $\bigcup_{I(m_i, m_j)=1} \omega_{m_j}[F - S, F + S]$ defines all the channels seen in floors $F \pm S$ of all the buildings m_j interfering with m_i.

6.1.2 Secondary Networks Coexistence

The second scenario taken into account is about secondary networks coexistence. Here, each SU has a list of possible channels $C' \leq C$ available to communicate, and the model is used to find the separation that can be granted between two devices transmitting on the same channel. To be more precise, C' represents the TVWS available for the SU to use. Clearly, here we do not define the s and S parameter, but we instantiate our model to find the separations between SU using the same TVWS, which primarly depends on the cardinality of C'. More in detail, for a floor F of building m_i, transmitting on channel c'_F, we define

$$s_F = min_{c'_{F \in m_i} = c'_{F' \in m_i}} \left(|F - F'|\right) \qquad (6.7)$$

$$S_F = min_{c'_{F \in m_i} = c'_{F'' \in m_j}} \left(|F - F''|\right), \forall m_j \text{ such that } I(m_i, m_j) = 1 \qquad (6.8)$$

where s_F represent the maximum separation between two devices which use the same channel in the same building, and S_F represent the maximum separation between two devices which use the same channel in two interfering

buildings. So the maximum separation at floor F can be easily calculated as $min(s_F, S_F)$.

6.2 Analytical Model

This section details the analytical model defined using the system model hereby described. The main goal of the analytical model is to compute the average number of free channels given the building density, and the two parameters s and S.

The first step is to determine for each floor the average number of interfering floors. Thus, we need to estimate the average number of interfering buildings for each building in the scenario. We assume that buildings are distributed according to a Poisson density distribution of mean λ, were $\lambda = \lambda_{B(km^2)}$ is the number of buildings per km^2. By taking into account the transmitting power of each device, along with the path loss model, we can compute the maximum distance of interference d_{max}. Again, to perform a worst-case scenario analysis, we assume that devices always transmit at the maximum allowed power, which is $20\,\text{dBm}$ for mobile devices. Thus, to know the maximum distance at which a device can interfere to another one, we substitute the relevant values in the equations we already presented, and we get $d \simeq 25$.

It is then possible to formulate the value of $\lambda_{B(d_{max})}$ of the Poisson distribution for the number of buildings inside an area of radius d_{max}. More formally we define:

$$\lambda_{B(d_{max})} = \lambda_{B(km^2)} \cdot \pi d_{max}^2 \tag{6.9}$$

To find the number of interfering buildings n_B in a radius d_{max} centered in a generic building b_i, i.e. the number of buildings within the radius d_{max} not including the building b_i, we compute:

$$n_B = (\lambda_{B(km^2)} - 1) \cdot \pi d_{max}^2 \tag{6.10}$$

Given n_B, knowing the number of interfering floors is simply a matter of using the s and S paramters. We do this defining f_{int}, which calculates the number of interfering floors in the same building requesting a minimum of s_{int} floors of separation in a building of n_F number of floors.

$$f_{int}(s_{int}, n_F) = \begin{cases} n_F & \text{if } s_{int} \geq n_F \\ \frac{(n_F - s_{int})(2s_{int}+1) + s_{int}^2}{n_F} & \text{if } s_{int} < n_F \end{cases} \tag{6.11}$$

where n_F is the case in which there are less floors than s_{int}, and where the second case in Equation 6.11 can be derived summing up all the interfering
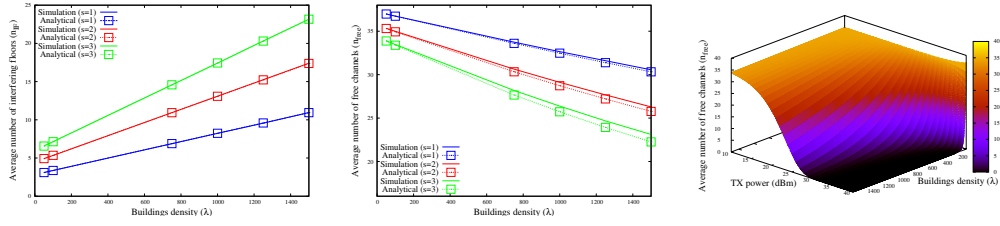
Figure 6.2: Average number of interfering floors varying the building density and the degree of separation (Fig. 6.2(a)). Average number of free channels over the building density and the degree of separation (Fig. 6.2(b). Average number of free channels over the building density (λ) and the transmitting power (Fig. 6.2(c)

floors at each floor of the building and then averaging it over the number of the floors.

Therefore the number of interfering floors into an area of radius d_{max} is defined as follows:

$$n_{IF} = f_{int}(s, n_F) + f_{int}(S, n_F) \cdot n_B \tag{6.12}$$

In Equation 6.12 we assume n_F to be constant, but of course it can be defined for each building of the scenario, and computed accordingly.

Given the set of possible channels C with cardinality $|C| = n_C$ that are used by the primary users, the probability that the cardinality of the set of free channel $C_{free} \subseteq C$ is equal to k, identified as n_{free}, is defined as:

$$P(n_{free} = k) = \binom{n_C}{k} \cdot (p_{free})^k \cdot (1 - p_{free})^{n_C - k} \tag{6.13}$$

It is straightforward to note that $P(n_{free} = k)$ follows the binomial distribution, where the probability p_{free} is the probability that a channel is free, i.e. the channel is not chosen among all the interfering floors, and is defined as:

$$p_{free} = \left(1 - \frac{1}{n_C}\right)^{n_{IF}} \tag{6.14}$$

Finally, we compute n_{free} as the expected value of a binomial distribution:

$$n_{free}(n_{IF}) = n_C \cdot p_{free} \tag{6.15}$$

which represent the average number of free channels.

In the following, we instantiate our analytical model to test its effectiveness. To compare it, we also built a simulation model, which follows the same concepts already presented in this chapter.

In Figure 6.2(a) and 6.2(b) it is shown a comparison between the analytical model and a simulated scenario. To obtain these figures, we set $n_F = 8$, and an equal value of degree of separation for intra-building and inter-building protection, i.e. $s = S$.

Figure 6.2(a) shows that the number of interfering floors increase, as expected, with the requested level of separation and according to the building density. Like in the previous results, in Figure 6.2(b) the number of free channel decreases with the degree of separation and with the building density, i.e. increasing the number of interfering floors. In Figures 6.2(a) and 6.2(b) we see that the analytical model accurately follows the simulated results. However, it is possible to notice a small error, accountable to the non-linearity of Equation 6.15, more precisely because:

$$\frac{\sum_{b \in B} \sum_{f \in F_b} n_{free}(n_{IF}(b, f))}{\sum_{b \in B} F_b} \neq n_{free}\left(\frac{\sum_{b \in B} \sum_{f \in F_b} n_{IF}(b, f)}{\sum_{b \in B} F_b}\right) \quad (6.16)$$

where B is the set of all the building into the scenario, F_b is the set of the floor of building b and $n_{IF}(b, f)$ is the actual number of interfering floors at floor f of the building b. The first term of Equation 6.16 is the simulated one, i.e. the number of free channels is calculated for each floor of every building and then averaged, while the second term is the analytical one computed with Equation 6.15, where at first we take the average of the number of interfering floors and then we calculate the number of free channels. Anyhow, the error is small, and thus n_{free} can be considered a good approximation of the real value.

Finlly, Figure 6.2(c) shows the impact of the transmitting power over the number of free channels. For this particular case, we vary the transmission power, and it is straightforward to note that when the transmitting power is small, the value of n_{free} is not affected by the building density; on the inverse, increasing the transmitting power decrease the n_{free} curve towards zero, still according to the building density.

6.3 Numerical Results

This section gives numerical results of our model when instantiated in real cities. The evaluation is done for two different use-case: gray space communication, which is studied in Section 6.3.2, and network coexistence, which

follows in Section 6.3.3. The cities we take into account are Bologna (Italy), Toronto (Canada), Boston (MA, USA), New York City (NY, USA), Muenchen (Germany), and London (UK). But first, we validate our simulation model against the analytical one present earlier.

6.3.1   Validation

This section validates our analytical model presented in Section 6.2 against real city scenarios.
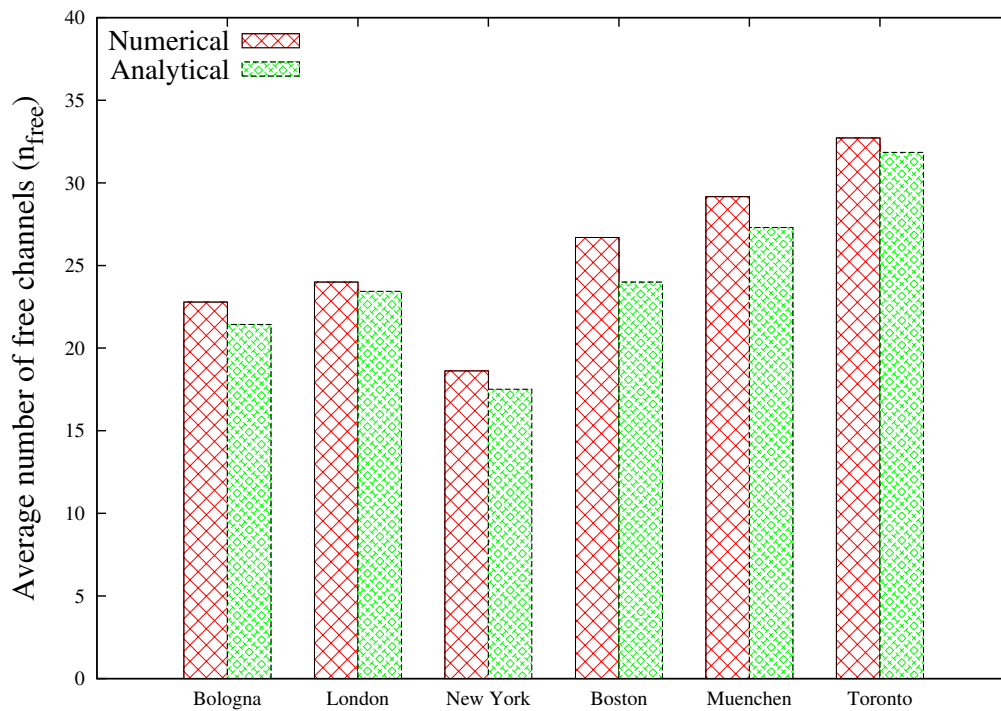
Figure 6.3: Analytical model validation.

Figure 6.3 shows the average number of free channels for the six cities taken into account in our analysis. The value of each bar can be found in Table 6.1. Both the figure as well as the table clearly shows how small the errors are, and that our analytical model always understimate the number of free channels. This aspect has been already explained in Section 6.2, and shown in Figure 6.2(b).
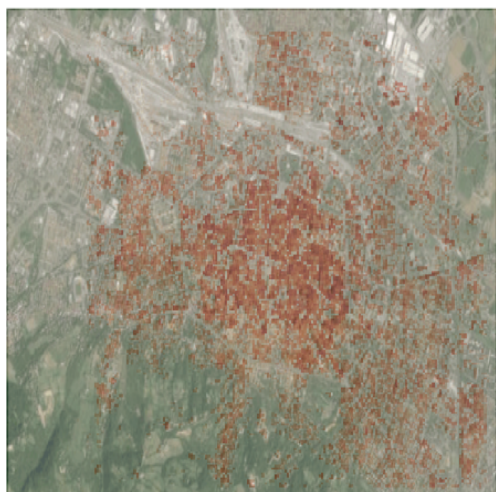
(a) Bologna, Italy
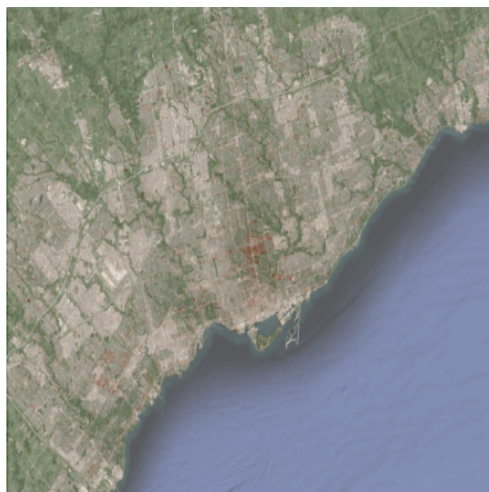
(b) Toronto, Canada
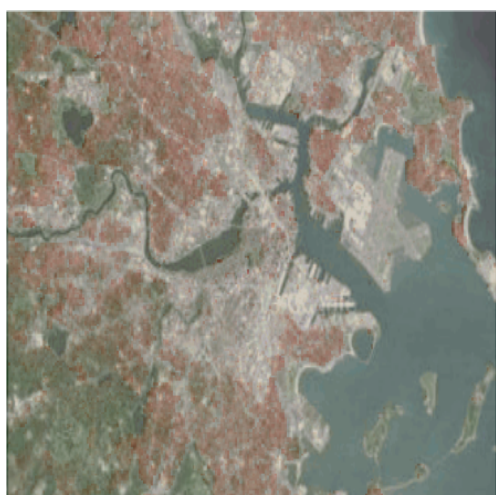
(c) Boston, MA, USA
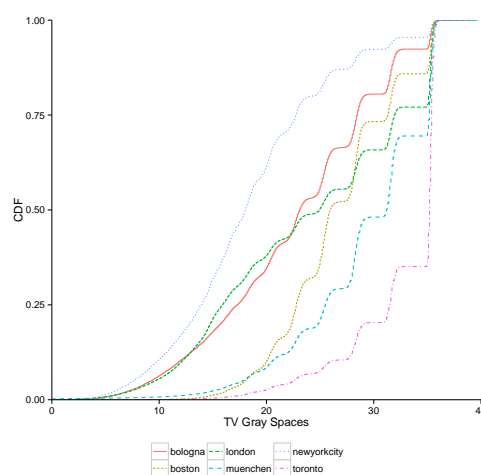
(d) CDF

Figure 6.4: Visual results about gray space communication in three candidate cities: Bologna, Toronto, and Boston. Figures 6.4(a), 6.4(b), and 6.4(c) are computed with $s = S = 3$. Figure 6.4(d) shows a comparison on the CDF between 6 different cities: Bologna, London, New York City, Boston, Muenchen, and Toronto.

Table 6.1: Validation on real scenarios

City	n_{free} (Simulations)	n_{free} (Analytical)	Error
New York City	18.61	17.5	1.11
Bologna	22.78	21.42	1.36
Boston	26.69	24	2.69
Muenchen	29.16	27.3	1.86
Toronto	32.71	31.85	0.86
London	23.99	23.44	0.55

6.3.2   Gray Space Communication

This section studies the first use-case, in which secondary users communicate on TVGS, possibly interfering with Primary Users. We note that this behavior is currently not envisioned by regulators, but these results can be exploited as possible spectrum utilization opportunities, by providing a sufficient degree of protection to the primary users. This means that by setting highly enough values for s and S, it is possible to achieve the requested level of protection to the primary network.

As it is possible to note from other works [10] [12], 2 floors of separation in the same building end up in providing enough shielding between the primary and the secondary user. Clearly, more protection is possible, at the cost of a reduced availability of channels for secondary access.

In Figure 6.4 we plot the PU protection results for three candidate cities: Bologna (Italy), Toronto (Canada), and Boston, MA (USA). The color chart ranges from white to red, where a white color means that all the channels can be used without causing interference to the primary users, and red means that no channel can be used. Colors in between repesent different availabilities. As it is straightforward to note, downtowns experience scarcity of TVGS, since buildings are denser and thus each floor typically have more neighboring buildings and eventually less channels available for transmissions. On the inverse in the outskirts a lot more communication opportunities can be found. The architecture of the city plays a fundamental role in determining the availability of channels for secondary operations. As we can see in Figure 6.4(a), where we plot the results for the city of Bologna, just outside the city center a lot of channels can be utilized. In the core of the city less opportunities are found, because buildings are clustered together. Toronto, which is instead a more modern city compared to Bologna, experience a different behavior. Hence, buildings are farther from each other, and thus even in downtown a lot of channels can be exploited for secondary access without interfering with the PU. Finally, in Boston, where a lot of buildings

(a) $s = S = 1$ (b) $s = S = 2$
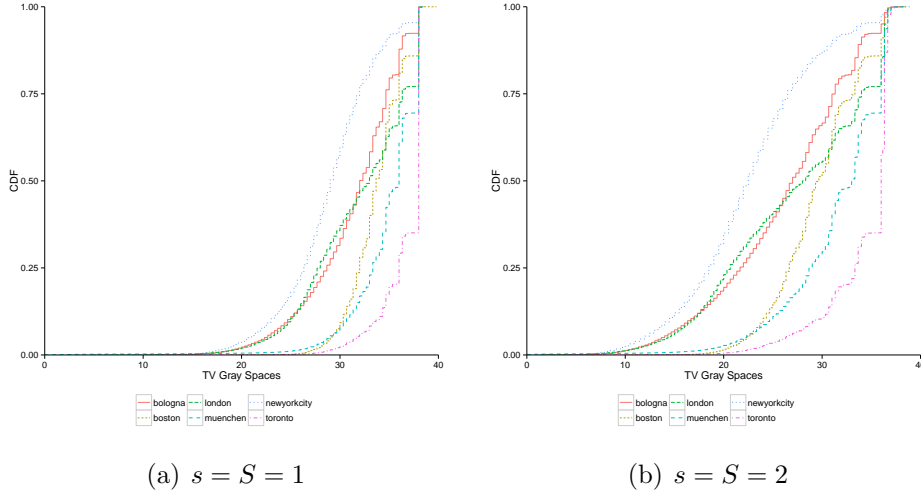
Figure 6.5: CDF Comparison for different s and S parameters.

are to be found both in downtown as well as in the outskirts, we can see that a sufficiently high degree of protection to the Primary Users translates into a reduced number of available channels for secondary operations.

Figure 6.4(d) shows a comparison with a wider set of cities. We plot the Cumulative Distributive Function (CDF) also for New York City (NY, USA), London (UK), and Muenchen (DE). What emerges from these charts reflects the structure of the city taken into account. With $s = S = 3$, depicted in Figure 6.4(d), we see that denser cities like New York City, Bologna and Boston, experience steeper slopes compared to other cities. This is due to the structure of the city, where a higher number of buildings that might interfere between each other eventually reduce the number of available channels.

Different figures can be obtained by reducing the degree of protection to the PU, which translates into a higher availability for secondary operations. Figure 6.5 shows the CDF comparison while varying the s and S parameters. It is straightforward to note how the desired level of protection have a huge impact on the channels availability for SU. However, we already shown that even with a high level of protection setting $s = S = 3$ in Figure 6.4(d), TVGS could still be found and available for secondary use.

6.3.3 Coexistence

This section provides results about the evaluation of our framework for the coexistence scenario. Here, secondary devices have to compete to access the spectrum, and thus can produce interference within each other. We perform the study on the same cities of Section 6.3.2, and we consider different
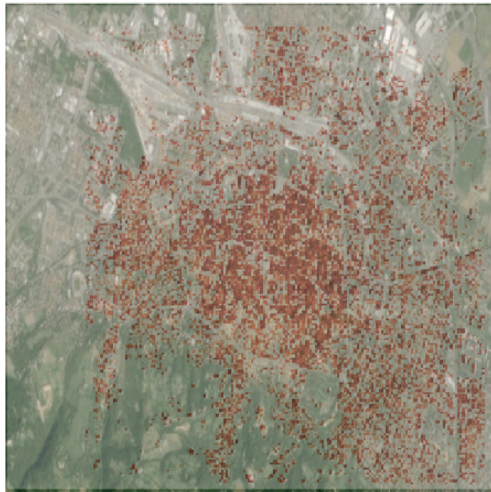
(a) Bologna, Italy

(b) Toronto, Canada

(c) Boston, MA, USA

(d) CDF

Figure 6.6: Visual results about secondary network coexistence in three candidate cities: Bologna, Toronto, and Boston, along with the CDF comparison.

amounts of TVWS for each city, according to candidate remote spectrum databases. We selected 6 channels from Bologna [58], 31 channels for London [90], 1 channel for New York Ci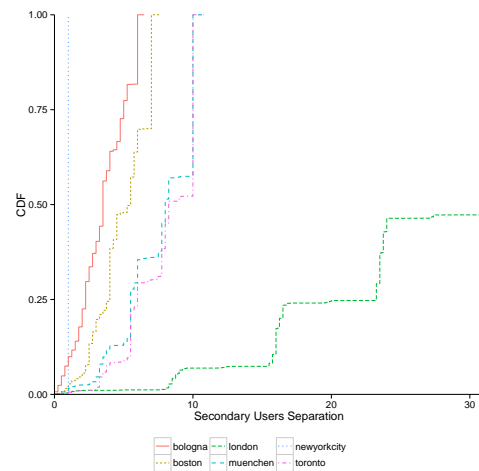ty [53], 7 channels for Boston [53], 10 channels for Muenchen [17], and 10 channels for Toronto [20]. These numbers are dynamic, and thus might be different from the time of writing.

In Figure 6.6 we depict the results of our framework for the coexistence scenario for three candidate cities: Bologna, Toronto, and Boston. Again, like already seen in Figure 6.4, denser cities like Bologna and Boston show more challenges for secondary network operations. We note that each chart is normalized over the number of TVWS, so a red square in Bologna means 0 separation out of 6 TVWS, while in Toronto means 0 separation out of 10 TVWS and so on. These results follow the one presented in Section 6.3.2, since also in this context what matters the most is the structure of the city and the position of the buildings. Thus, denser cities present less separation for secondary networks, and possibly an increased interference between them, while more open cities can grant a better protection, regardless of the number of TVWS.

This same behavior is also shown in Figure 6.6(d), where we plot the CDF for the same cities of Figure 6.4(d) considering the coexistence use-case. Contrarly to Figure 6.4(d) where the structure of the city was the most prominent difference between the different results, in Figure 6.6(d) we see that the curves are mostly affected by the number of available TVWS. These suggests that both the structure of the city, as well as the number of TVWS, clearly defines the viability of secondary operations.

6.4 Summary

Clearly, 6 cities can not be representative of the whole world. Nevertheless, some general considerations can be extracted from the results provided in this analysis.

- **Buildings height**: taller buildings do not present less availability of TVGS, compared to smaller buildings. Only the protection constraints matter, and thus downtowns, where skyscrapers are present, can be compared to other areas in which lower buildings can be found.

- **Street size**: this aspect is certainly more important. As also shown in Figure 4.17. where the street dimension impact has been taken into account, smaller streets translate into a higher interference to the neighboring buildings. This happens because buildings are denser, and thus

more of them are considered as neighbors assuming a fixed interference range of 50 meters.

- **Number of TVWS**: for protection to the PU, the number of TVWS in the area has a small impact. In fact, all the presented charts were produced assuming no TVWS in the area of interest. This makes some buildings to have no available TVGS at all, because either the channels watched in the building, or by the neighbors, severely limits them. If n TVWS are instead available, that would mean that at least n channels are available in every building. TVGS might be more difficult to find, because having less channels used increase the probability that a user is watching a specific channel. However, since TVWS are certainly preferable compared to TVGS, this does not constitute a problem.

- **World Area**: looking at the presented results, it is also possible to note that Canada and U.S., with the notable exception of New York, typically present a wider availability of TVGS. This is due to the different architecture of the cities, with the American ones that are typically larger, with more space between each building. On the inverse, in Europe cities are typically denser, and this translates into a reduced portion of available TVGS.

Chapter 7

Machine-to-Machine

Machine-to-Machine communication on TV White Spaces and TV Gray Spaces can be beneficial for a multitude of services, ranging from Wireless Sensor Networks to Smart metering communication for the smart grid. The benefits of using the TV bands come from a greater coverage range, crucial to deploy services with devices detached in every house, and from a higher energy efficiency due to a lower power needed to transmit. Moreover, the superior obstacle penetration characteristics of the TV bands make them the ideal choice to build networks in hard-to-reach places like cellars, basements, and to deploy environmental monitoring networks.

Thus, in the following we study mainly the smart grid scenario, focusing both on the energy efficiency, and on the communication on TVGS.

7.1 Smart metering Scenario

7.1.1 System Models

In this section the two system models used in the following are presented. Smart meters gather measurements and consumption information about the household in which they are installed, and report these readings to a central coordinator. By aggregating all the data together, the utility operator is then able to perform load balancing, and perform operations that can balance the network and eventually provide a more stable service to the customers. In Figure 7.1 a typical smart metering scenario is depicted. Here, multiple smart meters need to report their sensor readings to a central aggregator once per day, that is in charge of merging data and transmitting them to the utility servers. Here, we focus on the last part of this communication architecture, where the smart meters need to perform the first hop of the communication.
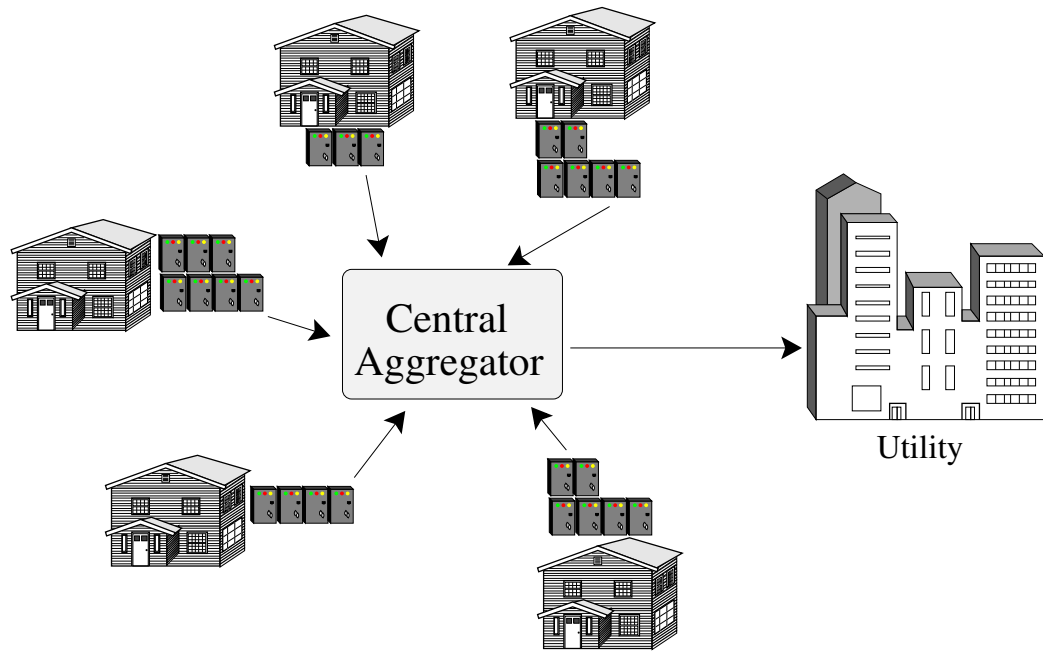
Figure 7.1: The Smart metering scenario.

Two architectures arise, the first one is a mesh like deployment, which is presented in Section 7.1.1.1. The second one is centralized, and closely follows in Section 7.1.1.2.

7.1.1.1 Mesh like Indoor Network Deployment

In this section we present the first network topology. Here, smart meters are interconnected together, and exchange data via a wireless connection. This network deployment might be challenging to be realized if high separation distances between devices are in place. At least one of the smart meters in the cluster must have a connection to relay the data to the central aggregator. This can be a wired ADSL, a cellular connection, or even a WiFi connection to the building's AP. We note that due to shadowing effects, not all smart meters can be in range of each other, and consequently routing should be implemented. We also note that we do not model carefully the indoor relay, since we assume that every node in the building can perform this role. We also note that using lower frequencies, in the TVWS range, can significantly improve the range and thus the possibility for smart meters to be connected together, if compared with higher bands.
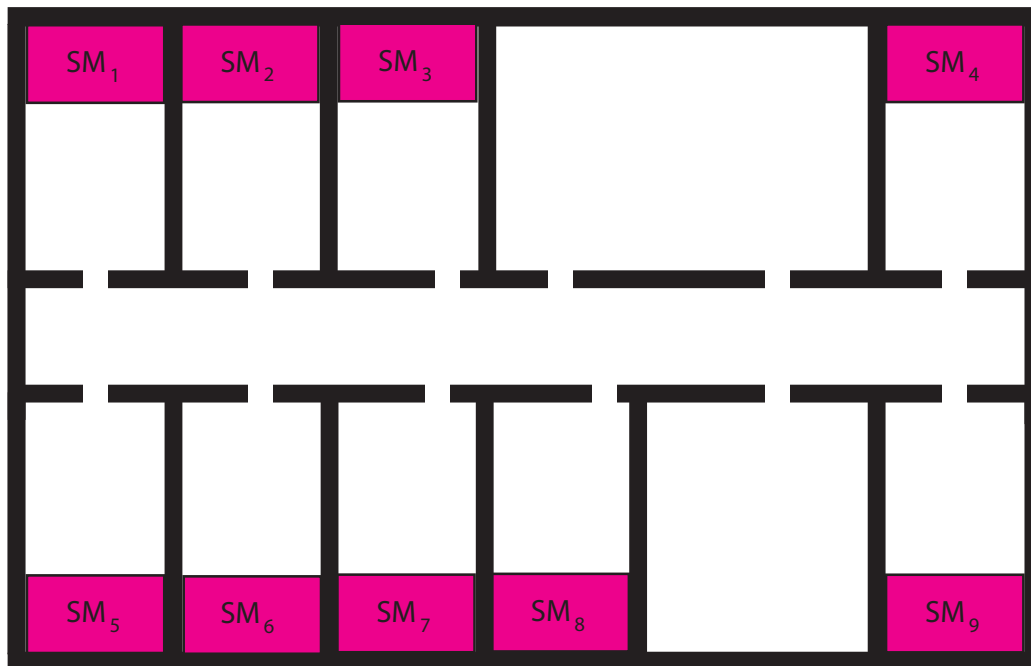
Figure 7.2: The mesh like network deployment for the smart metering scenario, in which each Smart meter SM_i communicates with the other smart meters SM_j, and one of them will eventually report the readings to a central aggregator.

7.1.1.2 Centralized Offloading for Outdoor Scenarios

In this network deployment, each smart meter has to report its own readings to the neighborhood coordinator, located outside and near to the buildings to be served. This coordinator is then connected to the internet via either a cabled connection, or through a cellular connection, and is then able to relay the message to the central aggregator. Being located outside, the received signal strength perceived by the coordinator from the primary network is certainly higher compared to indoors, where shadowing effects degrade the transmission, and thus this network deployment is more challenging compared to the mesh network [10].
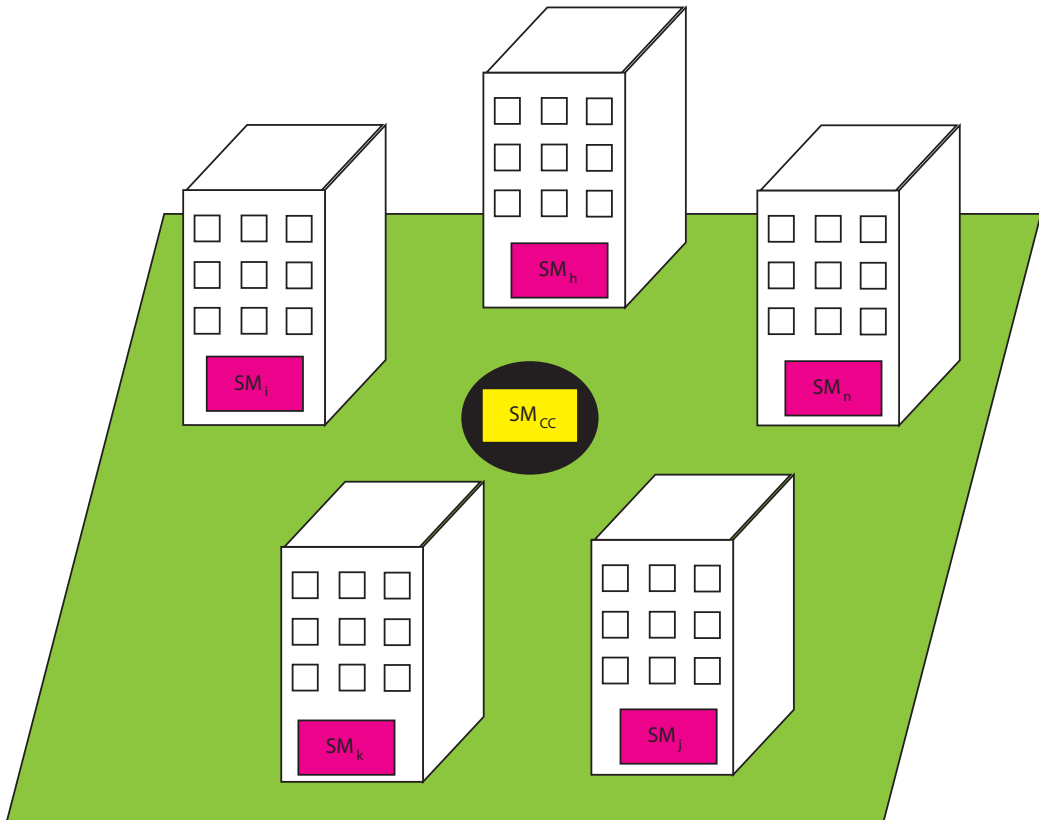
Figure 7.3: The centralized network deployment for the smart metering scenario, in which each block of smart meters inside every neighbor building reports their readings to a neighborhood coordinator, which will eventually relay the data to the central aggregator.

7.1.2 Permissible transmit power of indoor smart meters

Smart meters interference will necessarily lead to a reduction of DTV signal quality due to the increased noise floor. If the interference becomes too high, DTV receivers will not be able to decode the signal and a reduction in coverage of the DTV transmitter will occur. In the following, we calculate the relative reduction in coverage if a certain level of interference at the DTV receiver is permitted. This will allow us also to derive the necessary trade-off the regulator would need to make between permissible secondary transmit power and coverage reduction in gray spaces scenarios. As noted earlier, current TVWS regulations do not envision gray space operations, however, we argue that if the emissions are small/short, smart meters may be exempted from this rule. In order to see how much coverage the DTV broadcasting network would lose when allowing interference from the smart meters on the DTV receiver, we plot in Figure 7.5 the coverage difference by the same DTV transmitter when the DTV receiver is interfered with increasing powers by the smart meters. We employ the Okumura-Hata model for outdoor propagation modeling and assume circular-symmetric propagation characteristics. The horizontal line represent the minimum SNR required for successful decoding by the DTV receiver, which we assume to be 16.5 dB [31]. The same behavior is also depicted in Figure 7.4, where we plot the reduction relative to the total coverage area while increasing the received power from the smart meters. A value close to 1 means that the reduction of coverage due to the interference is almost equal to the maximum possible coverage, i.e. no DTV reception at all will be possible. The most challenging situation naturally arises at the coverage edge, where the DTV signal is received with the lowest power, and even a small interference can disrupt the received signal and the successful reception, thus reducing the coverage area. In general, we can say that even small interferences can cause big coverage reduction (the left part of Figure 7.4), which mainly constitutes the zone far away from the DTV transmitter. Consequently, TV gray spaces operations need to be sufficiently shielded, particularly at the edge of the coverage region.

7.1.3 Smart meters interference towards a rooftop antenna

Since smart meters inside buildings will cause interference primarily to the same building's rooftop antenna, it is necessary to discuss this particular link. To this respect, the greater the number of floors between the smart meters and the rooftop antenna, the greater protection from the interference
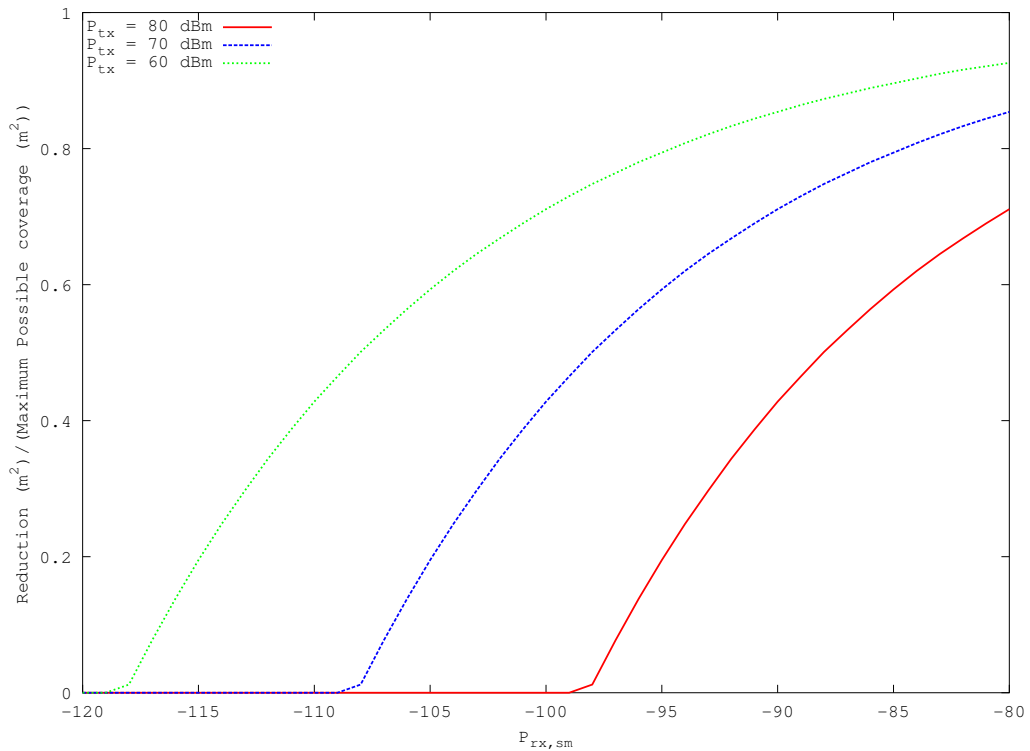
Figure 7.4: Coverage reduction ratio while receiving the signal from the SM at increasing power.

can be provided. From the measurements presented in Section 4, we know that increasing the number of floors significantly attenuates the original signal, and even at short distances beyond 10 meters the received signal power falls below the noise floor. With a narrower bandwidth, however, the signal might still be detectable for smart meters up to the second floor of the same building. However, we note that according to the current regulations, the transmit power of the TVWS device has to be spread evenly over the full range of the DTV channel (i.e. 8 MHz), but due to forward error correction, the DTV receiver may actually be able to compensate narrowband short-term interference.

No rules of thumb exist on the expected shielding towards the antenna, since the propagation characteristics greatly vary with the building materials and thickness of the floor. All our discussion refers to the construction materials of the building in which we performed the experiment, which can be deemed to be quite typical modern office building in Germany. It is obvious that the attenuation will be different for different building materials. Several
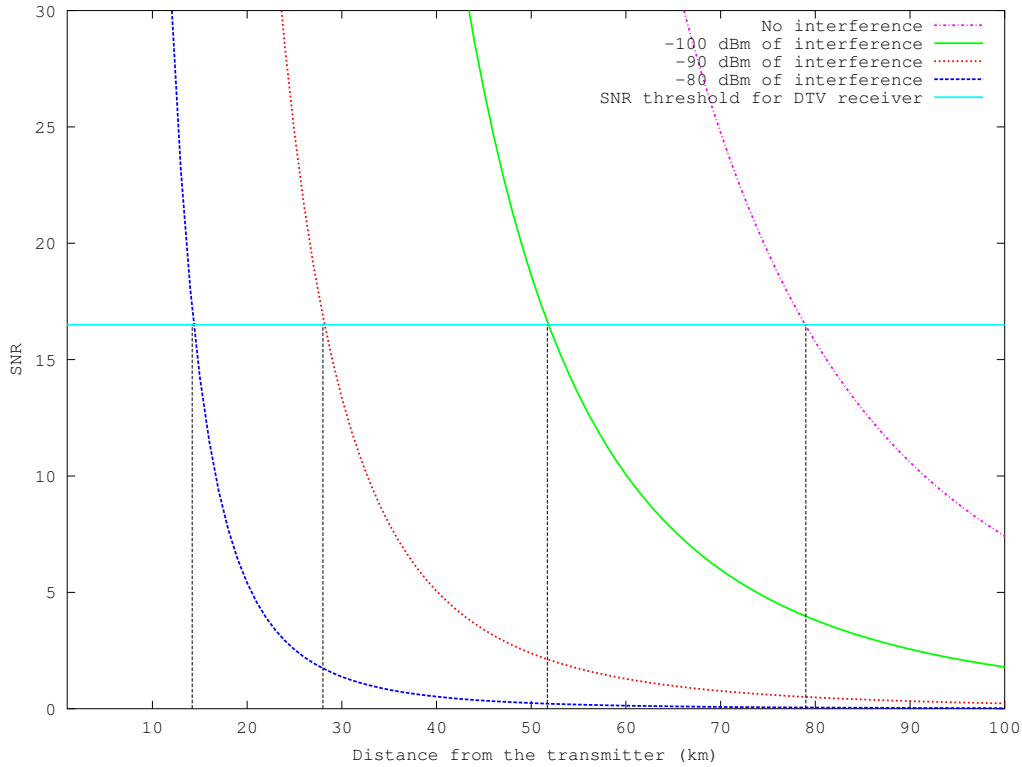
Figure 7.5: Coverage reduction regarding the SNR using the Okumura-Hata pathloss model. The power of the DTV transmitter is set to 70 dBm.

studies estimate the attenuation that floors and walls of different materials might introduce. We refer the reader to [85] and [96] for further reading.

It is important to note that the gain of DTV antennas may allow for high secondary transmit powers. The high vertical angular directionality discriminates differently between the wanted signal (i.e. the one that comes from the DTV broadcaster transmitter) and the interfering signal (i.e. the one that comes from the smart meters). In [63], the ITU provides a recommendation on the losses due to imperfect alignment of the DTV receiver, which are usually accounted for in DTV planning. We consider this when studying the interference between the smart meters and the DTV antennas and find that the relative angle between the DTV signal and the smart meter interference may end up in the $75° - 90°$ range, which according to [63] provides more than 15 dB of additional discrimination. For neighboring buildings, angles might be smaller, and thus the discrimination would be less. However, the additional shielding by the outside walls will likely reduce the interference at those antennas below the interference measured at A_{lb}. For high build-

ings, the discrimination would still be quite high, thanks to the high relative angle, while for lower buildings we might experience a lower discrimination and thus protection from interference. The worst case scenario is, in fact, a low neighboring antenna, since it would perceive a signal similar to the one received from the DTV broadcaster transmitter, and at the same time it could experience less shadowing by walls and its own roof. Thus regulations on permissible transmit powers may be relaxed, if shielding and antenna directionality are taken into account.

7.2   Gray Spaces communication

Smart metering communication require more reliability rather than data rate, and low latency. Thus, it is of paramount importance that the communication medium, either cable or wireless, provides the necessary guarantees on this. Clearly, cable communication are reliable, fast, and have low latency, but harder to deploy in cellars and basements, where typically smart meters are installed. Thus, wireless communication have to be investigated for these network paradigms, and the TV bands promise to be one ideal candidate, thanks to their good propagation characteristics, that could bring connectivity also for indoor smart meters behind walls and windows. So TV White Spaces can be utilized to deploy smart metering networks, and bring connectivity in both rural areas as well as in metropolises. Unfortunately, as already stated, it is challenging to find white spaces in dense populated areas, and consequently deploying the metering networks on an opportunistic technology, which is not guaranteed to properly work where most of the customer live, seems unpractical. TV Gray Spaces can also be used for this network paradigm, given the fact that the transmission time is quite short since the packets to transmit are small in size.

7.2.1   Indoor-to-indoor propagation

TV bands are generally used for outdoor to outdoor communications, or for outdoor to indoor for cable-top antennas. It is then hard to find appropriate pathloss models for indoor-to-indoor and indoor-to-outdoor communication in the TV bands. Thus, we built a testbed to assess and evaluate the wireless characteristics of an indoor device transmitting on TV bands.

We present experimental results from a setup we built in order to estimate the pathloss that indoor communication on TVWS or TVGS would experience. We placed an Agilent E4438C vector signal generator inside an office on the ground floor of a typical office building in Aachen, Germany.

The building comprises four floors with office rooms on each floor, separated mostly by dry walls. Each floor has a similar layout. We set the transmission power of the signal generator to -6 dBm, amplified by a power amplifier to 32 dBm. We account for 0.5 dB of cable loss, and 2.5 dBi for the antenna gain. We then transmitted a sinusoidal signal with center frequency of 472 MHz. We moved inside the building, and performed power measurements with a Rohde & Schwarz FSH3 hand-held spectrum analyzer attached to a 2.5 dBi gain antenna.
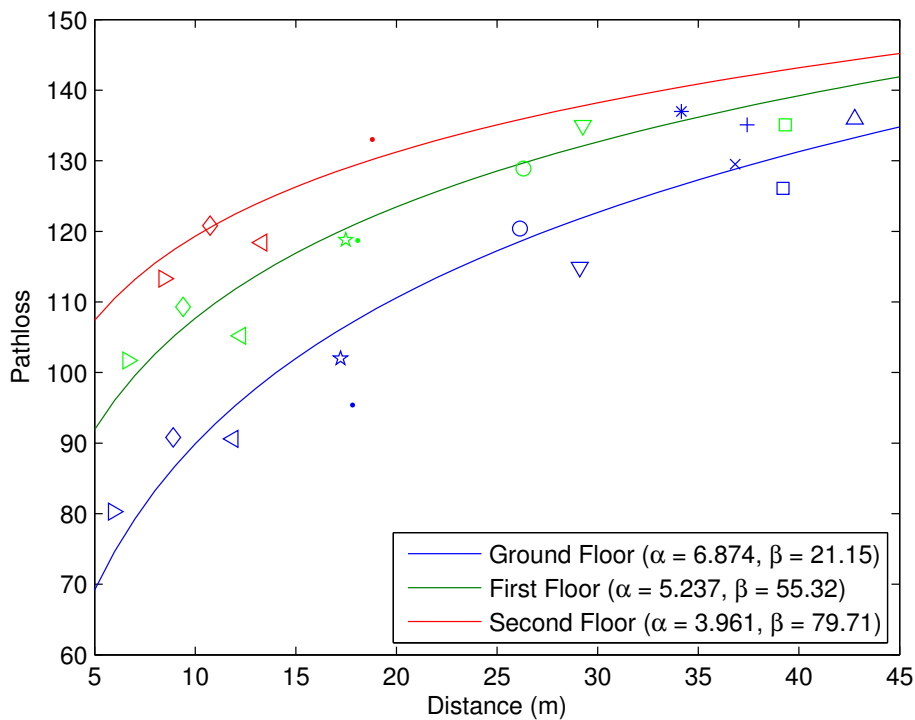
Figure 7.6: Indoor pathloss.

In Figure 7.6 we plot the pathloss measured in the different measurements spots, as well as the regression line according to the log-linear trend

$$PL = 10 \cdot \alpha \cdot log_{10}(d) + \beta, \tag{7.1}$$

where d is the distance between the transmitter and the receiver in meters. The heavy attenuation that walls and floors cause on the signal becomes immediately visible as we lose up to 80 dB even few meters apart from the transmitter on the same floor. When considering different floors, the pathloss increase beyond 100 dB even for short distances.
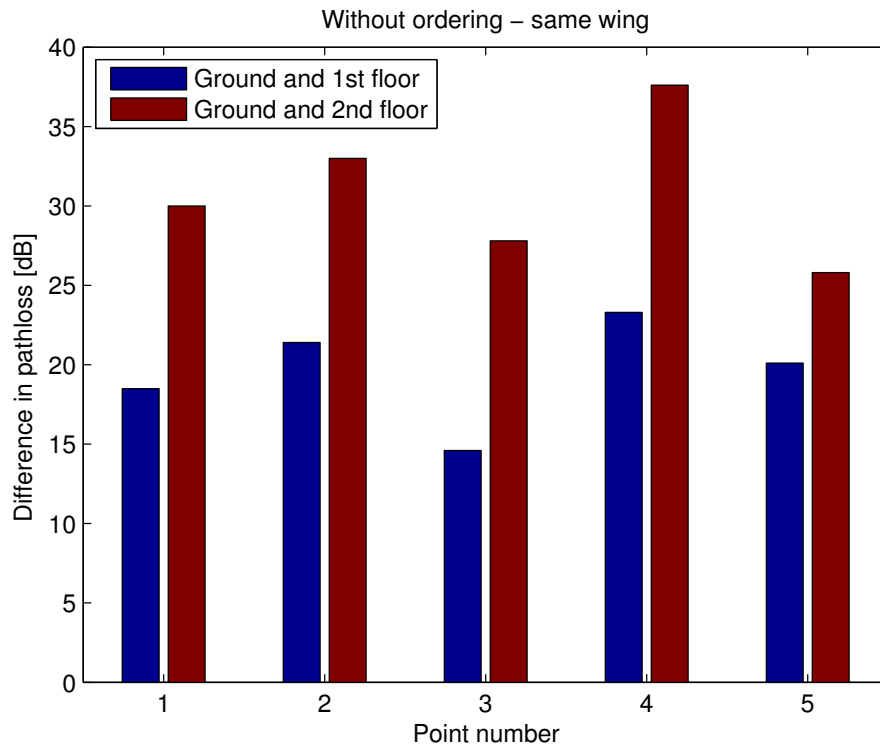
Figure 7.7: Differences of the received power in dB on the same point but a different floors, compared with the ground floor.

Figure 7.7 shows the differences in received powers in the same setup points, but at different floors, compared to the ground level received powers, i.e loss due to floors without considering the effective distance from the transmitter. In our scenario, the penetration losses by floors account for around 20 dB for the second floor, and 30 dB for the third floor.

At the fourth floor, having the transmitter placed at the ground floor, we were unable to detect the signal, even when measuring on the same relative position of the signal source. This said, we can conclude that for direct communication, smart meters need to be placed on the same floor, not too far from each other in order to benefit from a reduced pathloss, and thus requiring less power to transmit. If links span multiple floors, it may be required to use relaying.

7.2.2 Indoor-to-outdoor propagation

With the same setup presented in the last section, we also performed outdoor measurements to assess the feasibility of the second network topology, towards a neighborhood coordinator.
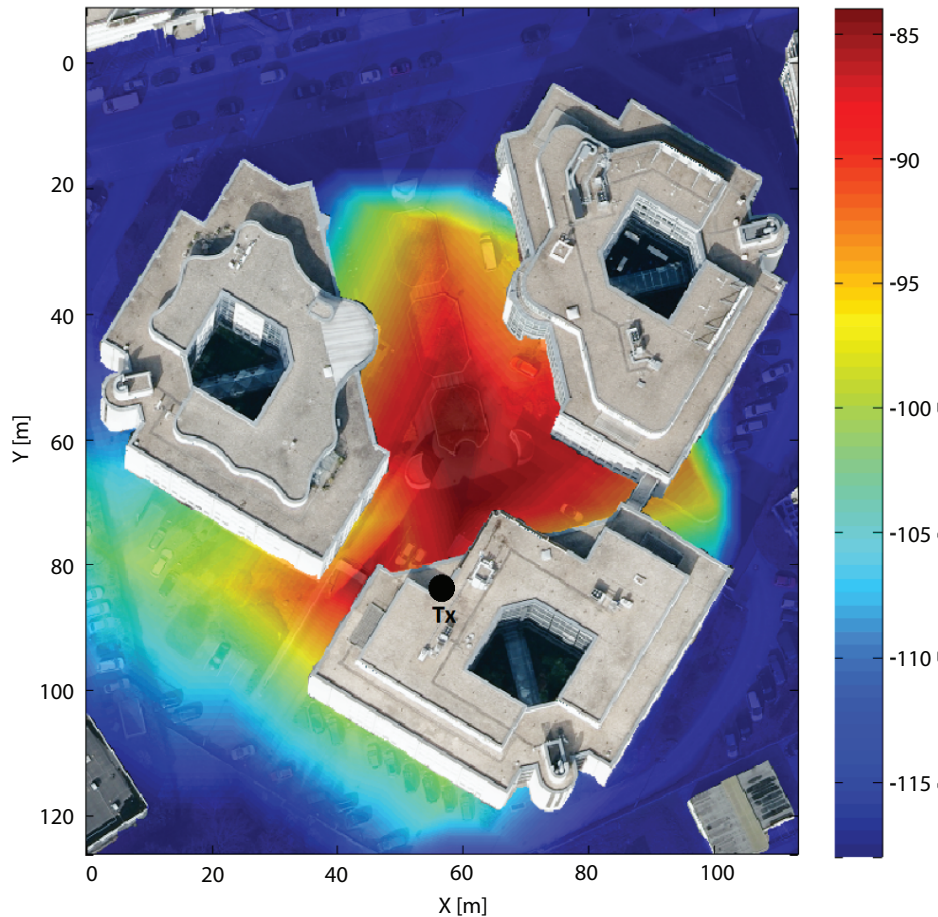
Figure 7.8: Measured outdoor signal strength for indoor transmitter for the reference office building studied in this paper.

In Figure 7.8 we show a heatmap derived from our measurements outside the building. The signal generator was placed on the northwest end of the south building. The heavy attenuation is caused by the concrete walls and the thermal-coated windows, with pathlosses as high as 100 dB already in front of the room the signal generator was placed in. High data rates may thus be difficult to obtain, while for low data rates we can make the following argument: in [38] the authors examine the minimum required SNR in order

to achieve a determined data rate. We can assume that in our system, given
the fact that throughput requirements are low, one might not require a large
SNR. According to [32] and [38], nearly 2 Mbps can be obtained using a
QPSK coding, with a SNR as little as 3.5 dB. In [32], the authors also study
the BER while varying the SNR, and their results show that lower data rates
can be obtained even with lower SNR, which is the case of major interest
for our target scenario. In Figure 7.9 we show the pathloss with respect of
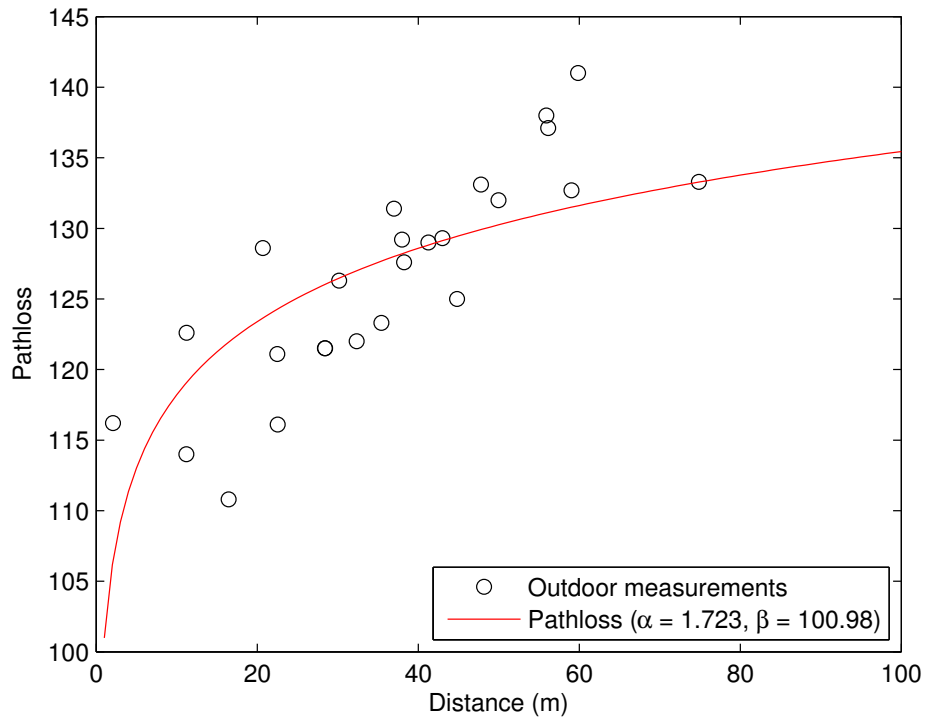
Figure 7.9: Estimated distance-dependent pathloss for indoor-to-outdoor
communications in reference office building scenario.

the distance to the transmitter. On the achievable throughput, Figures 7.10,
7.11, and 7.12 show the maximum capacity the network could offer for the
three studied technologies.   The difference between the straight and the
dotted line comes from a higher noise level for gray spaces, which we set to
-81 dBm/8 MHz, and for white spaces to the thermal noise. Note that in
practical gray space scenarios, the noise floor is likely to exceed this value.

The setup considered in Figures 7.10, 7.11, and 7.12 consists of a indoor
transmitter, and an outdoor receiver. When using a free channel, thus with
noise level equivalent to thermal noise, all the three technologies can achieve
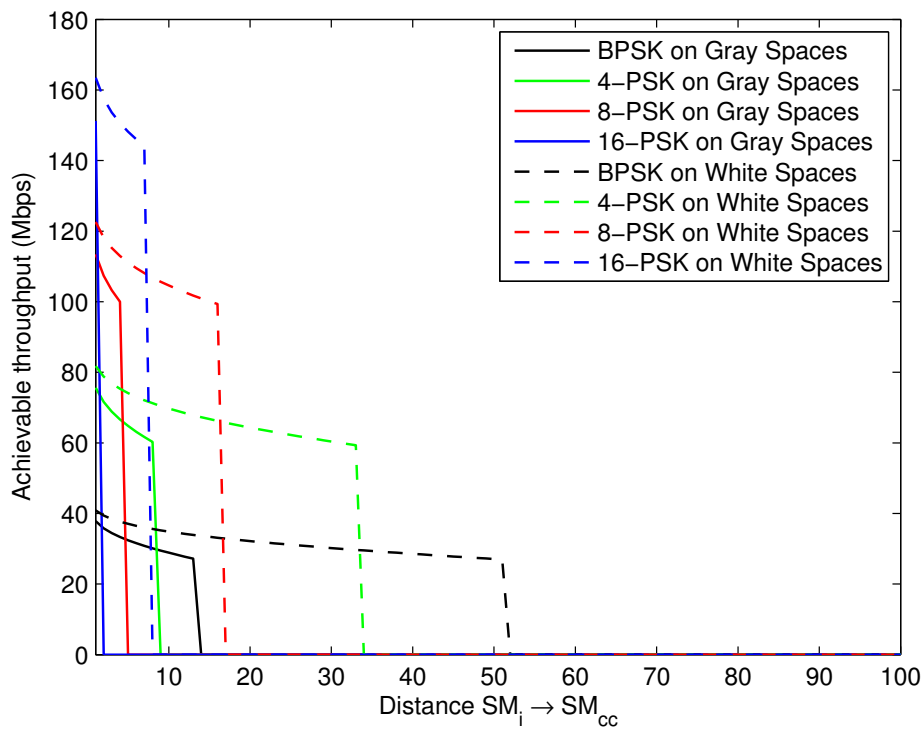
Figure 7.10: Differences in achievable throughput with a maximum BER of 10^{-6} for TVWS. The noise floor is -81 dBm.
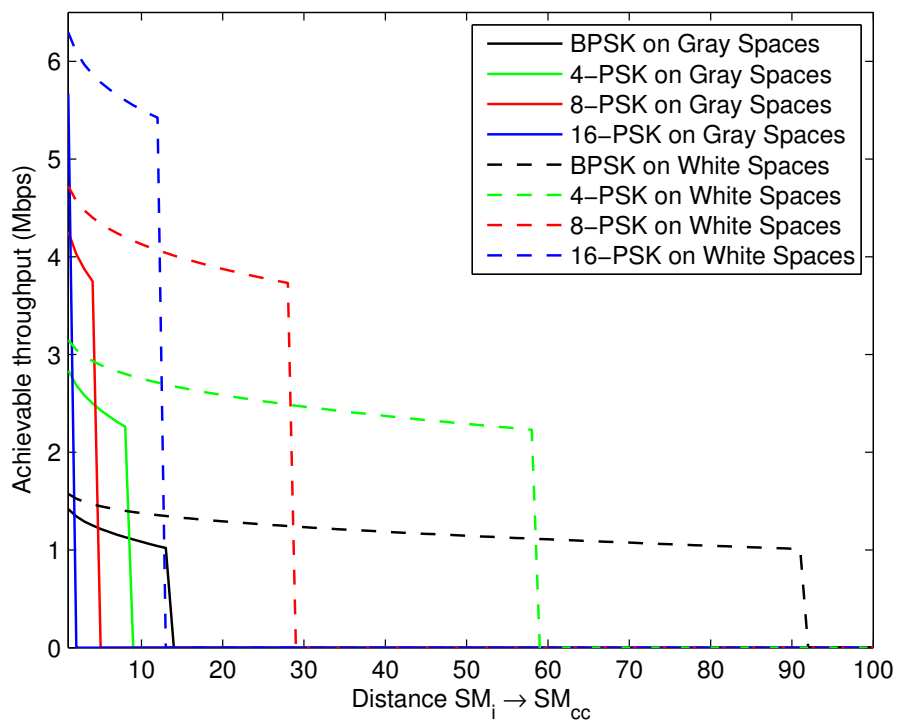
Figure 7.11: Differences in achievable throughput with a maximum BER of 10^{-6} for the 868 MHz band. The noise floor is -95.26 dBm.
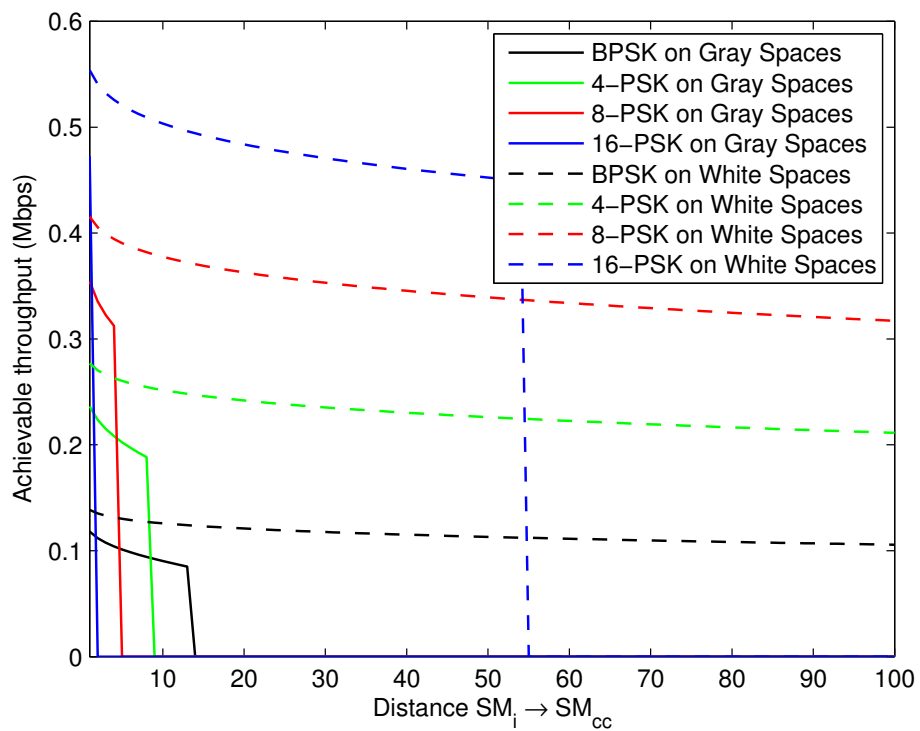
Figure 7.12: Differences in achievable throughput with a maximum BER of 10^{-6} for the 433 MHz band. The noise floor is -106.05 dBm.

a range greater than 50 meters, which is seemingly enough for this kind of communication. However, the achievable throughput is greatly increased when transmitting on TVWS, reaching 40 Mbps with a BPSK signal, compared to around 1.5 Mbps for the 868 MHz band, and around 0.1 Mbps for the 433 MHz band. Finally, if the SM_{CC} needs to feedback to the SM_i inside the buildings, we are skeptical that this may be achieved while providing enough protection from the interference to the DTV receiver, due to the reduced spatial distance and with generally lower attenuation by the buildings.

7.2.3   Discussion

Given the results from the setup we built, we can derive some first order characteristics of smart metering communication in TV Gray Spaces.

The first mesh like network topology appears to be technically feasible. The low frequency in which the TV bands are enhance the obstacle penetration properties of the signal, and are consequently beneficial for NLOS scenario like indoors. However, each building present some unique characteristics, according to the material used and to the interior architecture. Moreover, the DTV signal is received at very low powers indoor, and this requires a smaller transmitting power to achieve the desired SINR for the secondary network. Thus, deriving a general rule of thumb is still hard, but it is possible to give a positive outlook on this network topology.

On the inverse, in the second centralized network topology, it is harder to give a positive feedback. Problems comes from the fact that outer walls are generally thicker compared to interior walls, and thus the dB losses increase. Figure 7.8 clearly shows how the signal is heavily constrained between buildings, and how its power drops significantly even few meters apart from the transmitting point. Here, gray spaces are even worse, in the sense that outside the signal coming from the DTV transmitter, treated as interference by the secondary network, is certainly higher compared to indoors, thus requiring a higher transmitting power, which could interfere with the primary networks in the neighborhood.

7.3   Bursty Interference to the PU

In this section we evaluate the interference to the PU by the secondary devices, when bursty and short transmission are experienced. More in detail, we apply the operational characteristics of the recently published IEEE 802.15.4m standard for low-rate wireless personal area networks (WPANs), and derive performance metrics on the feasibility of gray space networks

under bursty interference estimation. At first, we derive the maximum permissible packet length, and consequently the maximum over-the air duration of an IEEE 802.15.4m packet. Along with the maximum transmit power, and realistic SNR requirements for DVB-T receiver [68], we study protection boundaries for the primary network. If a minimum separation distance is maintained, it is possible to mitigate and erase the effects of interferences to the PU by adopting appropriate FEC mechanisms. At the same time, there is a tradeoff between the connectivity experienced by the secondary network, and the maximum possible interference levels on the primary network. To study the technical and economical viability of such deployments, we perform a large scale simulation study in Germany. The rationale is that national regulators might allow secondary underlay operations, if satisfactory operational constraints are found, and the PU is protected. These include the transmission power, the frequency, and the periodicity of the messages to be sent.

7.3.1 IEEE 802.15.4m Indoor Performance Evaluation

Here performance metrics for IEEE 802.15.4m networks in TVWS and TVGS are evaluated. The focus is on the interference that the primary system impose on the secondary network, and consequently the achievable performance for IEEE 802.15.4m networks if operated in TVGS. We also evaluate the effect of bursty transmission, or shot noise. Here, small interfering packets may be compensated at the DVB-T receiver, with FEC techniques. We assume, in the rest of this section, that secondary devices always operate at the maximum permissible power, if they are deployed indoors.

7.3.1.1 Secondary Throughput with Primary Interference

Here we evaluate the achievable throughput for secondary networks, if operated in TVWS or TVGS, for indoor deployments. As indoor path loss model, we use the one presented in [10], which is defined as:

$$\gamma(d) = 10 \times \alpha \times log_{10}(d) + \beta \tag{7.2}$$

where $\alpha = 6.874$, and $\beta = 21.15$. We also assume that any smart meter device always use the highest MCS given the sensed SINR .

We show in Figure 7.13 the achievable throughput versus the distance between the sender and the receiver, for the indoor network deployment presented in Section 7.1.1.1. Is it possible to see how much communication in TVGS suffer from the interference on the channel, which basically reduce the distance and the throughput at which communication is technically possible.
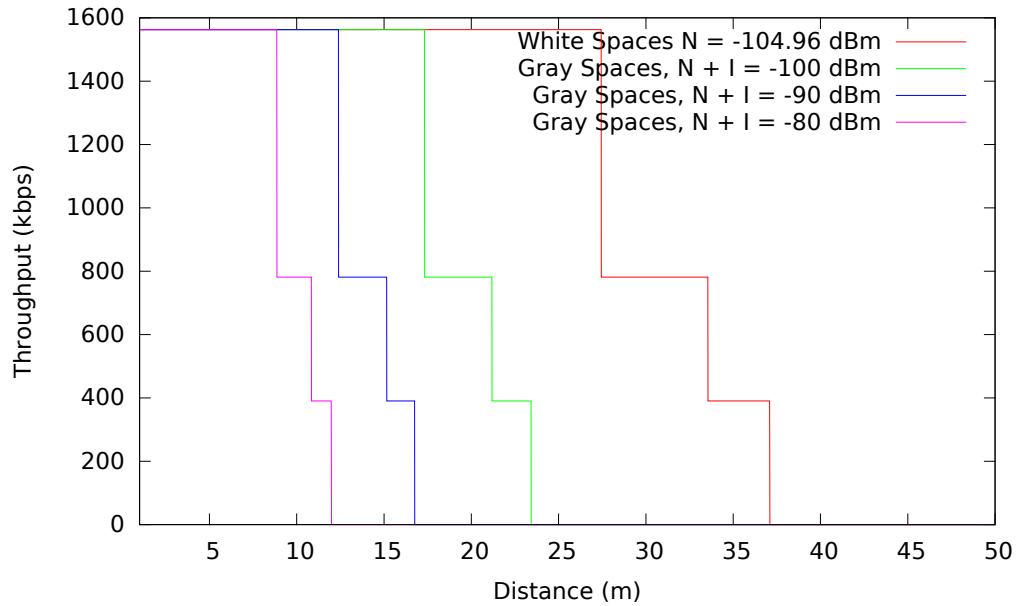
Figure 7.13: Achievable throughput in indoor scenario.

When allowing as little as -100 dBm of interference, communication is not possible beyond 25 meters, and with significantly less throughput compared to the TVWS case.

7.3.2   Secondary Interference to Primary Users in Indoor Environments

In this section, we evaluate the impact that bursty interference, or shot noise, generate on the primary network. We assume that the DTV receiver is located indoor, with a set-top box antenna. We firstly derive the operational constraints that IEEE 802.15.4m must adhere to, and then we show how this might be compensated by FEC mechanism at the DVB-T receiver. Finally, we also study the minimum separation distance between IEEE 802.15.4m networks and the primary users, if operated simultaneously.

7.3.2.1   IEEE 802.15.4m OFDM Frame Duration

At first, we compute the maximum frame duration for IEEE 802.15.4m operated networks. We note that, depending on the application type, the effective over-the-air time might be smaller. The maximum number of symbols per

frame defined in the standard is:

$$phyMaxFrameDuration = STF + 2 + 1 +$$
$$\lceil (aMaxPhyPacketSize + 1) \cdot phySymbolsPerOctet \rceil \quad (7.3)$$

where STF can be 1, 2, 3 or 4, depending on the length. In order to derive the maximum length, we choose $STF = 4$ in our analysis. The maximum packet size $aMaxPhyPacketSize$ defined by the standard is 2047 octets. By replacing all the variables with their respective highest numbers defined in the IEEE 802.15.4m standard, Equation 7.3 for the three mandatory MCS modes becomes:

$$phyMaxFrameDuration_{MCS0} = 7 + \lceil 256 \cdot 0.16 \rceil = 48 \quad (7.4)$$

$$phyMaxFrameDuration_{MCS1} = 7 + \lceil 256 \cdot 0.08 \rceil = 28 \quad (7.5)$$

$$phyMaxFrameDuration_{MCS2} = 7 + \lceil 256 \cdot 0.04 \rceil = 18 \quad (7.6)$$

For every MCS defined in the standard, the symbol duration is $128\,\mu s$, so the maximum over-the-air times for the three modulations T_{MCS0}, T_{MCS1}, T_{MCS2} can be computed as:

$$T_{MCS0} = 48 \cdot 128 = 6,144ms \quad (7.7)$$

$$T_{MCS1} = 28 \cdot 128 = 3,584ms \quad (7.8)$$

$$T_{MCS2} = 18 \cdot 128 = 2,304ms \quad (7.9)$$

Considering the numbers just computed, according to [68], TV receivers would not be able to treat interference as bursty, and thus gain additional protection margins in terms of dB of interference being able to support. Bursty transmission are sporadic transmissions, considerably shorter compared to other normal transmissions. [68] defines bursty transmission as long as 0.5 ms, with a maximum duty cycle of 20 ms. Thus, a Quasi-Error-Free (QEF) transmission is possible when the ration between the desired and undesired signal is at maximum 16 dB. In this time, it possible to transmit approximately 25 bytes with MCS0, 49 with MCS1, and 98 with MCS2. Although small, they might be enough for smart meter operations. Finally, we note that is also possible to split longer messages in shorter ones, and transmit them while respecting the maximum duty cycle for bursty transmission.

When longer transmissions are experienced, [68] show that the limits are comparable to the continuous case. Thus, to obtain a QEF transmission, the D/U ratio must be at least 22 dB [68].

7.3.2.2   Simultaneous Transmission

In this section, we evaluate a special case of bursty interference, which although short, can be multiple at the same time. This effect increase the total interference perceived by the PU. Here, we study the probability that such case would happen. We assume no synchronization between the secondary users, which directly access the channel.
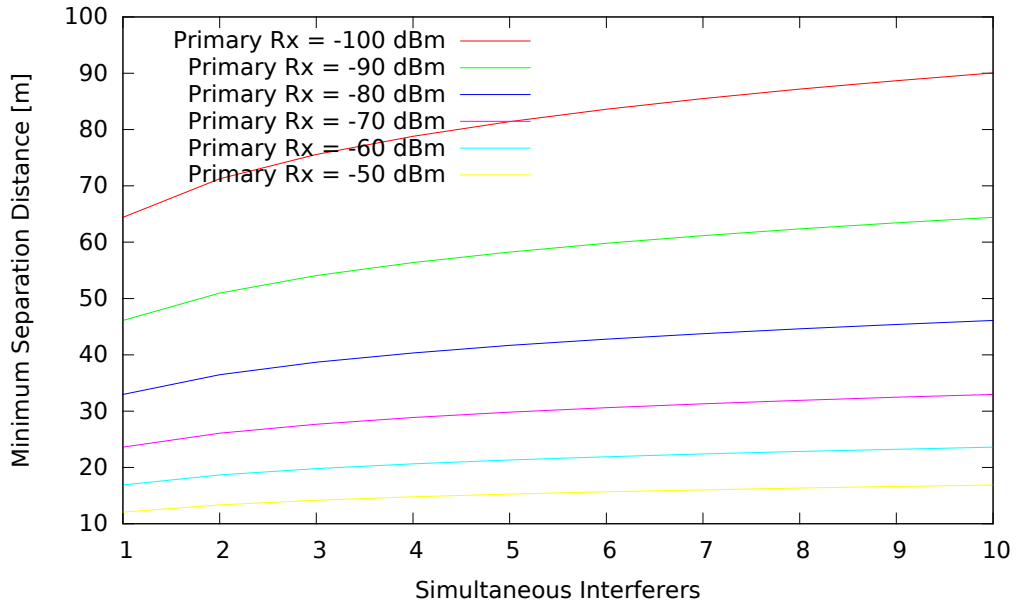
Figure 7.14: Minimum PU-SU Separation under simultaneous interferers.

In Figure 7.14, we show the minimum primary-secondary separation distance versus the number of simultaneous interferers. For this analysis we assumed full message overlapping at the primary receiver. Thus, the total interference is the sum of all the received packets. Basically, Figure 7.14 shows that if the PU is near the DVB-T transmitter, it can allow a much grater number of simultaneous interferers. Instead, at the cell edge, where the received power is considerably less, increasing the number of simultaneous interferers increase the separation distance by tenths of meters. However, although potentially harmful, the event of having simultaneous transmissions is unlikely to occur. The probability that t smart meters communicate in the

same slot is given by the following Bernoulli probability:

$$P = N\left(\binom{N-1}{t-1}\left(\frac{1}{T}\right)^{t-1}\left(\frac{T-1}{T}\right)^{N-t}\right) \tag{7.10}$$

where N is the total number of smart meters, t is the number of smart meters that communicate in the same slot, and T is the number of slots during a time cycle [15] [95], which we set to $T = 15$ minutes in our experiment.
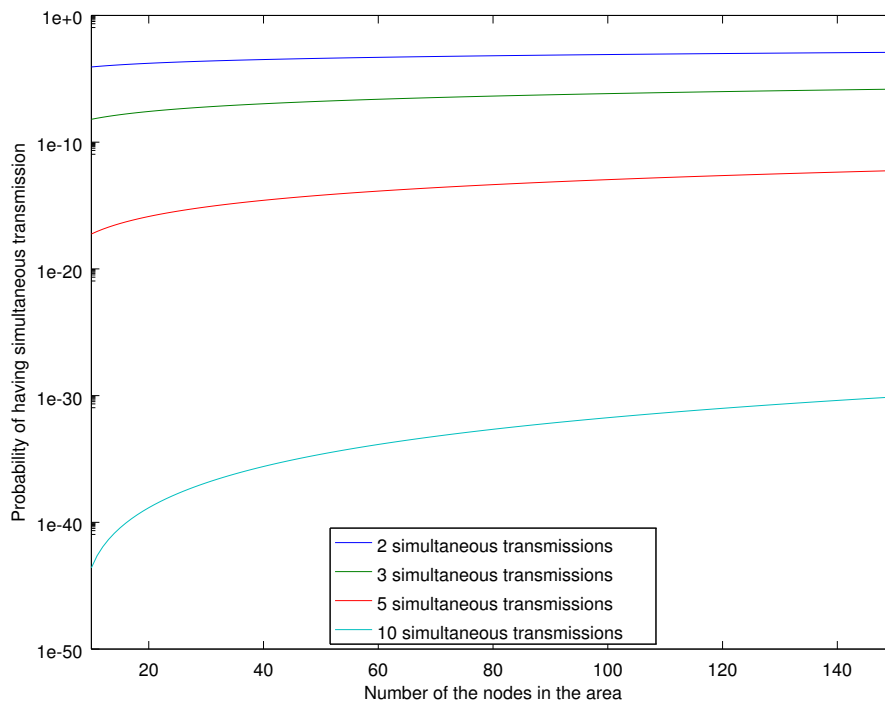
Figure 7.15: Probability of simultaneous transmissions.

Figure 7.15 shows the probability of having simultaneous transmissions according to Equation 7.10. The event of having simultaneous transmissions is unlikely to happen, even when a huge number of nodes is operating in the area of interest. Typically, interference levels are studied assuming only one interferer at the same time. We show here that generally speaking, for the smart metering scenario and for bursty transmission, this assumption can be further relaxed. This translates into the possibility to study only the interference coming from a single secondary device, which however is comparable to multiple interfering nodes, as shown in Figure 7.14.

7.3.2.3   Separation Distance

In this section we study the minimum separation distance that must be granted between the primary and secondary network, in order to respect the interference level constraints. We highlight the fact that the results provided here are a worst case approximation, and that regulators might allow more relaxed constraints if bursty transmissions are taken into account, as discussed in Section 7.3.2.1.

In Figure 7.16, we show the maximum supported distance between two secondary devices, versus the transmission power of the smart meters. Studying operations in TVGS, we perform the same analysis for three different primary received powers, -60 dBm,-75 dBm, and -80 dBm. Again, the indoor pathloss between the smart meters is computed like [10]. Clearly, a lower reception of the DTV signal translates in an increased minimum separation distance between the secondary transmitter and the primary receiver. Bursty interference can alleviate this behavior, thanks to the higher transmitting power at which bursty transmission can be operated. The gains are in the range between 3 meters and 8 meters, when the transmission power of the smart meters is increased.
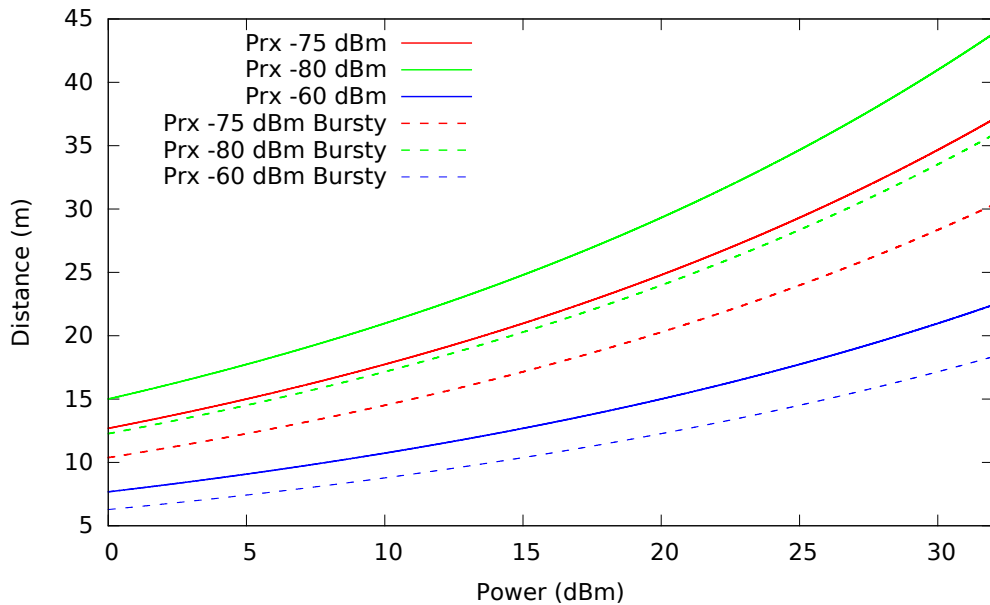
Figure 7.16: Minimum separation distance between primary receiver and secondary transmitter, for bursty and continuous interference.

Finally, Figure 7.17 shows the PU-SU and SU-SU separation distances, versus the SINR sensed by the primary network. Clearly, the SU-SU distance

has to be considered as a maximum, while the PU-SU distance has to be considered as a minimum value. As it can be easily seen, the SINR has a major impact on the separation distance. Devices at the cell edge experience a lower received power, and thus a higher protection separation must be granted. On the inverse, near the DVB-T transmitter, less separation can be allowed, given the higher received power of the primary system. TVGS are mostly needed in areas where no TVWS are available, such as metropolises and dense populated areas, typically near the DVB-T transmitter. There, TVGS operated networks are technically feasible, and can rely on a shorter separation distance which translates into a possibly higher throughput.
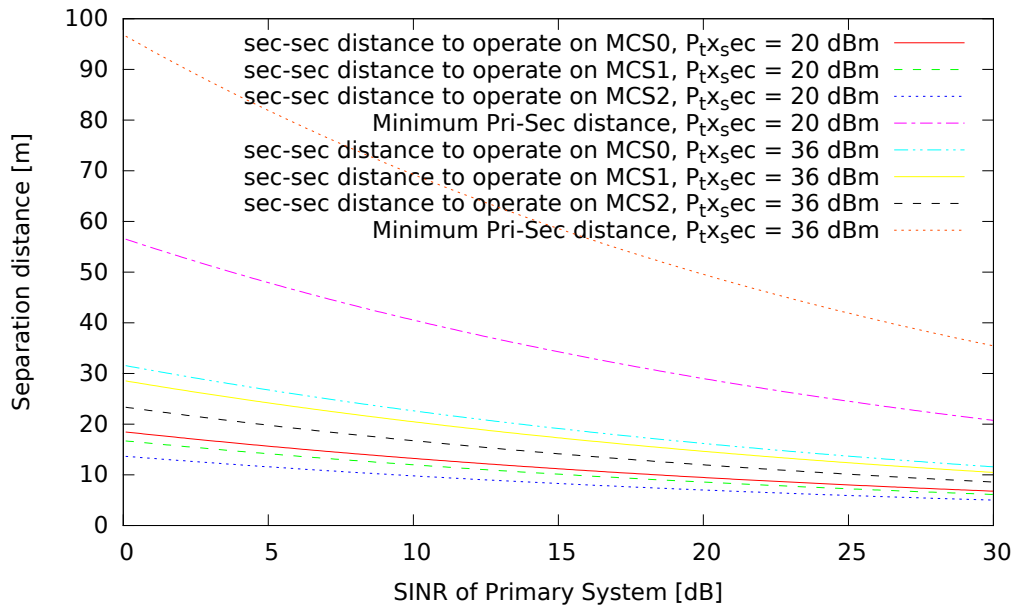
Figure 7.17: PU-SU and SU-SU distances at which a given MCS can be used, versus the primary SINR.

7.4 Germany TVGS Performance Evaluation

Here, we study the performance levels of IEEE 802.15.4m networks in a large scale scenario. In particular, the results are presented for Germany. We focus on the scenario in which the data is collected by a neighborhood aggregator, to which all the smart meters of the area of interest send their readings. Technically speaking, this scenario is highly challenging, since outdoor the signal coming from the DVB-T transmitter is received at a higher power compared

to indoors, and this translated into an increase in transmitting power by the smart meters to meet the SINR constraints to obtain communication. The methodology to model the system is described in [3]. The study area covers around $354.000\,\text{km}^2$. It is taken into account the propagation characteristics of the signal coming from the DTV transmitter, and the indoor devices are model to account for propagation losses and possible interference to the primary receiver. More details on the methodology, and the tools used, can be found in [111].

As path loss model to evaluate secondary outdoor network deployments, we have used the COST-231 Walfisch-Ikegami model [29], to be able to determine the pathloss under LOS conditions between smart grid devices. It is defined as:

$$\gamma(d) = 42.6 + 26 \times \log_{10}(d) + 20 \times \log_{10}(f), \qquad (7.11)$$

where d is the distance in kilometres, and f is the operating frequency. To make the analysis tractable, and without loss of generality, we set f to $800\,\text{MHz}$, which is the highest frequency within the TV broadcasting range. So our analysis can be considered as a worst case scenario.
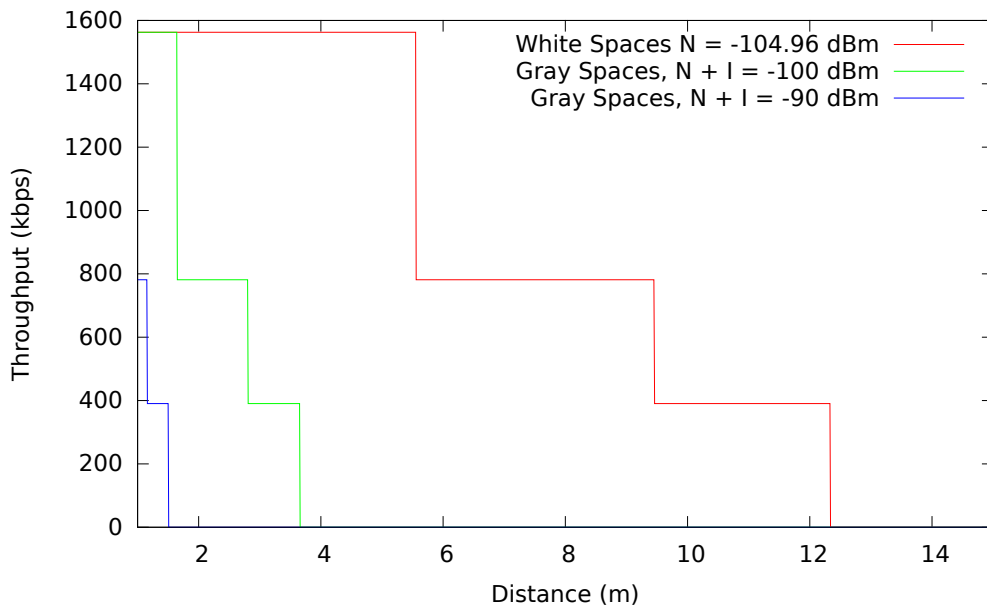
Figure 7.18: Throughput using the Walfisch-Ikegami model.

By using the well known open-source propagation modelling tool Splat! [72], we computed the expected primary signal strength at each pixel, which

is approximately 50×80 meters, applying the Longley-Rice Irregular Terrain Model (ITM) [70] for the average location and time probability case, F(50,50)[1]. Other small variations, which contribute to modify the received signal strength, are taken into account. To this end, an additional Gaussian shadowing term ξ with zero mean and standard deviation $\sigma = 5.5$ is added.

For the rest of this analysis, we assume that both the smart meters and the coordinator have antennas placed on the rooftop of buildings. This makes the modeling less prone to error coming from the parameters used. There is also no protection from wall shielding, and thus the link is LOS with the DVB-T transmitter. This scenario can be realized if smart meters reuse antenna deployments of the buildings in which they are installed.

7.4.1   Connectivity in Outdoor TVGS Scenarios

The first analysis we carried out is about the connectivity performance of secondary networks operated in TVGS. We assume that smart grid devices always operate on a strongly received DVB-T channel. The motivation behind this choice is the fact that, if allowed, TVGS operations should be operated on channels with good reception, otherwise the PU communication might be easily disrupted. It is worth to note that DVB-T transmissions are fixed-rate, which means that a reduction in SNR does not directly mean a reduction in service quality, if the SNR stays above the minimum threshold.

We show in Figure 7.19 the fraction of the surface area of Germany for which it is feasible to achieve connectivity between smart meters, considering the interference coming from the primary system. Channels pictured in black, which are the ones received at the strongest power in the area of interest, severely limits the feasibility of TVGS network. Here, short separation distances must be maintained, in order to keep the communication between the secondary devices. Clearly, focusing on weaker channel, it is possible to keep the connectivity in a higher fraction of area. Nevertheless, when considering weaker channels, a very dense network architecture should be deployed, since the separation distances between secondary devices remain under 100 meters when considering at least 50% of the area object of the study.

A similar analysis, with more realistic numbers, is presented in Figure 7.20, where we also take into account the population densities. On the y axis of Figure 7.20 we plot the ratio of people in Germany that can benefit from smart metering deployments operated in TVGS. Here it is more evident that

---

[1]F(x,y) means that the expected signal strength is exceeded in x% of locations during y% of time.
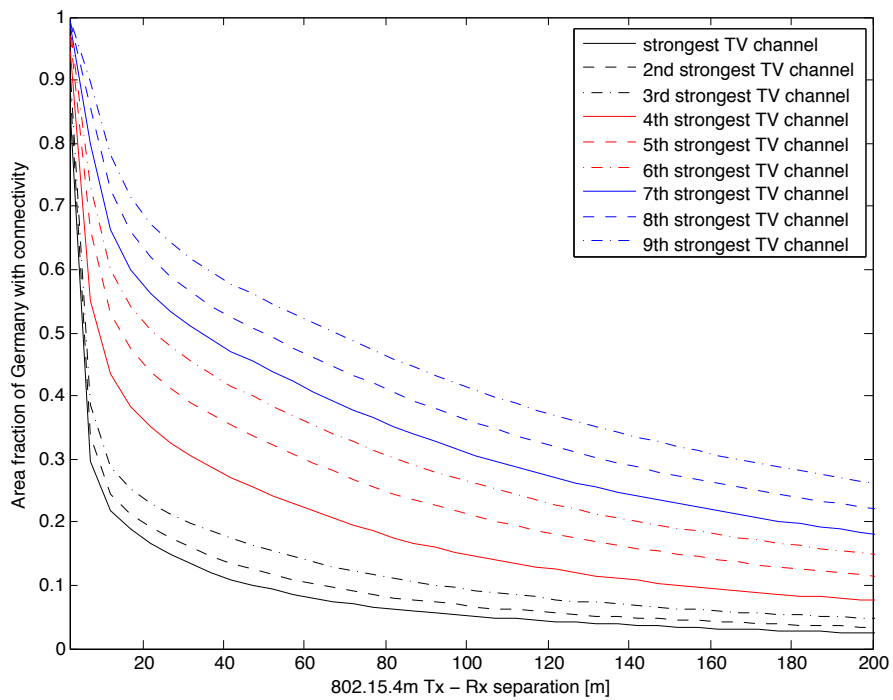
Figure 7.19: Fraction of the surface area of Germany in which smart-grid connectivity is feasible given a specific transmitter-receiver separation. Each curve shows the connectivity for a different local channel. The channels are sorted according to their received signal strength (figure courtesy of Andreas Achtzehn, RWTH Aachen University).

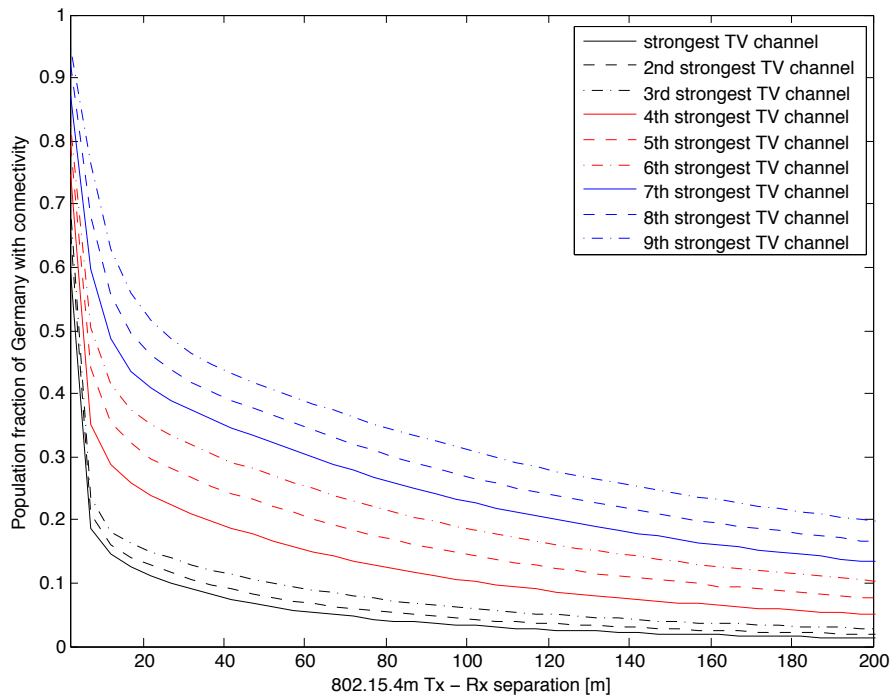Figure 7.20: Fraction of the German population for which smart-grid connectivity is feasible at their location of residency given a specific transmitter-receiver separation. Each curve shows the connectivity for a different local channel, whereby the channels are sorted according to their received signal strength (figure courtesy of Andreas Achtzehn, RWTH Aachen University).

the communication is more constrained by distance. However, this results should not be a surprise, given the nature of the DVB-T system, which is deployed to maximize the coverage in urban areas, where most of the people live. If we consider the urban areas of Berlin, Cologne, or Munich, there is a single high-power transmitter which serves the whole metropolitan region. To graphically show this, we plot the connectivity distribution for Germany considering connection distances of 50 m and 100 m, in Figure 7.22 and Figure 7.23, respectively. We assume to communicate in each area on the tenth strongest channel, which is generally not the one used to deliver content in the region, and thus the received signal is typically coming from other transmitters. If we compare these figures with Figure 7.21, we can see that the denser populated areas in Germany are not well covered. Thus, we can conclude that generally speaking, TVGS connectivity can be considered quite low.

To conclude this part of the analysis, we can make a short discussion on the results provided. All our analysis considered a worst case scenario, with no shadowing from walls, and LOS conditions. If higher shielding is experienced, then the performance figures certainly improve for TVGS. However, at this stage of development, no regulators discriminate between indoor and outdoor communication. Clearly, if this will be taken into account, higher transmitting power might be granted indoors, given the fact that they would not interfere with the primary system.

A second remark is about the antenna gain. In our study, we considered only omnidirectional antennas. It is straightforward to understand that if directional antennas for static deployments are taken into account, the separation distance can be decreased and thus the connectivity will improve.

7.4.2   Throughput in Outdoor TVGS

Focusing on the areas in which TVGS secondary operations are technically feasible, it is certainly important to understand the performance metrics regarding the throughput of such networks. Even though generally high data rates are not required by smart grid operations, achieving a high throughput translates into shorter over-the-air times, and thus less interference to the primary system, which at the same time finds easier to recognize shot noise interference and discriminate it against the signal.

As first step, we have calculated the maximum generally achievable MCS in each location, with a distance varying from 2 up to 200 m. Clearly, increasing the distance eventually result in a switch into a lower MCS, which will generate a lower throughput for the network, to cope with the reduced SNR. In Figures 7.24, 7.25, 7.26, and 7.27, we show the ratio of area of Germany in
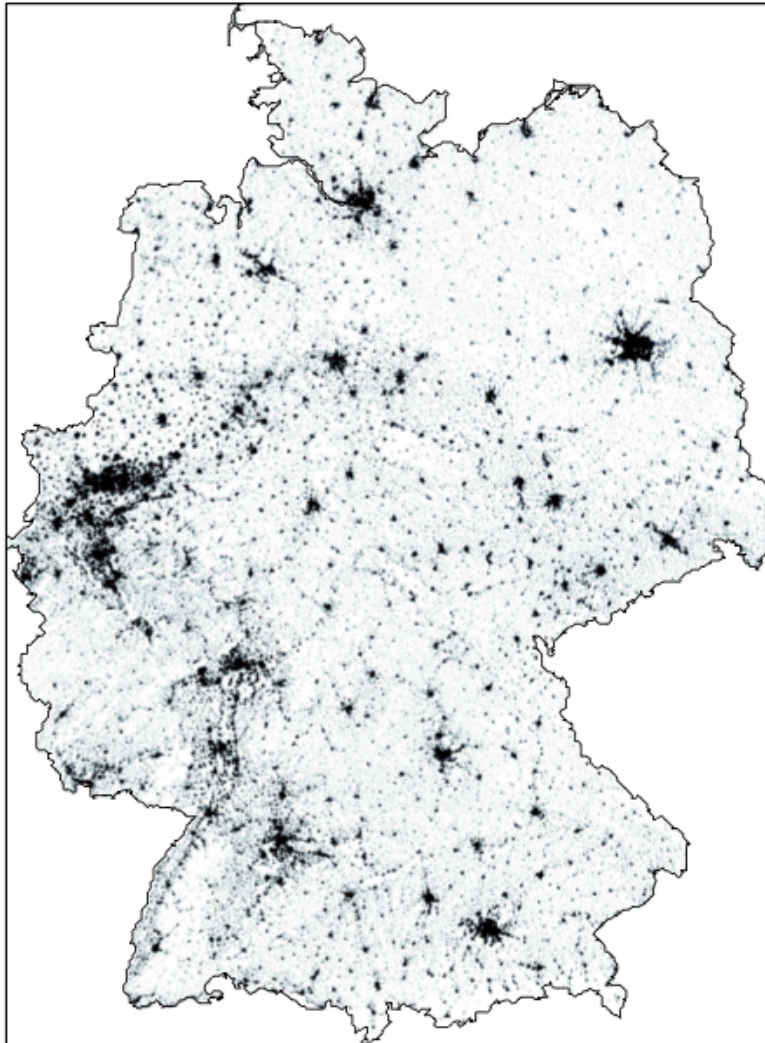
Figure 7.21: Population distribution of Germany (figure courtesy of Andreas Achtzehn, RWTH Aachen University).
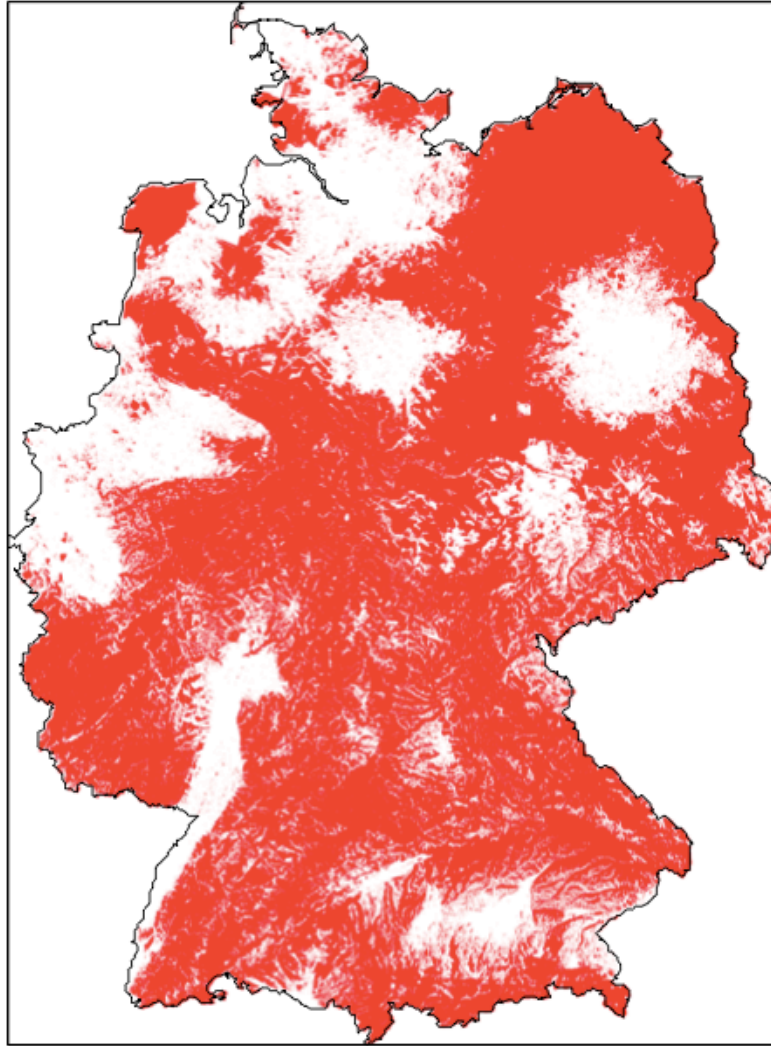
Figure 7.22: Connectivity for $d = 50m$ (figure courtesy of Andreas Achtzehn, RWTH Aachen University).

Figure 7.23: Connectivity for $d = 100m$ (figure courtesy of Andreas Achtzehn, RWTH Aachen University).

Figure 7.24: Strongest channel, conditioned on area (figure courtesy of Andreas Achtzehn, RWTH Aachen University).

Figure 7.25: Tenth strongest channel, conditioned on area (figure courtesy of Andreas Achtzehn, RWTH Aachen University).

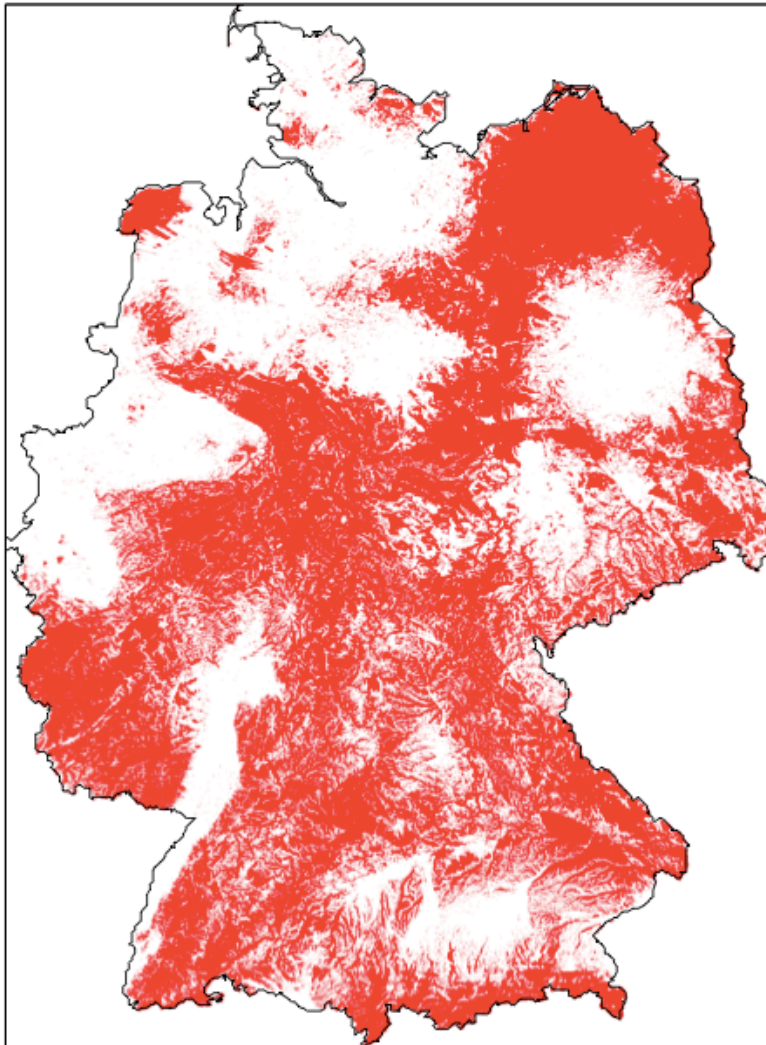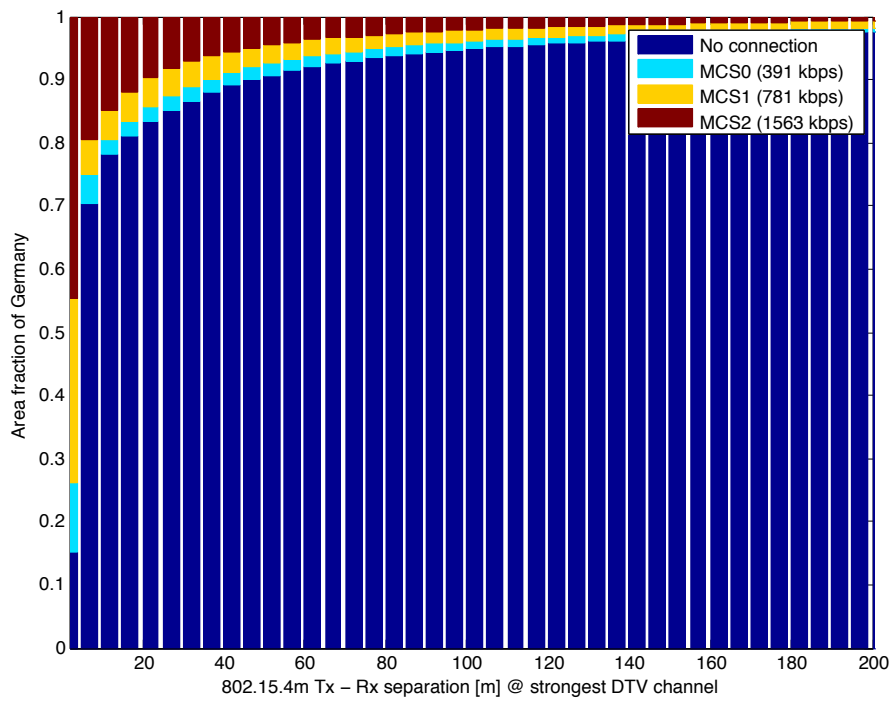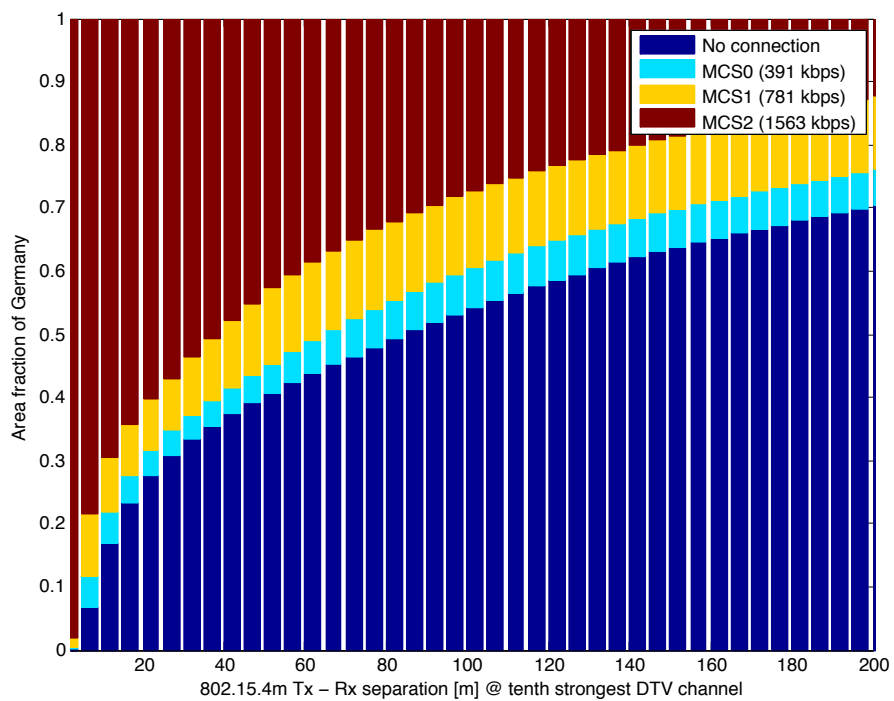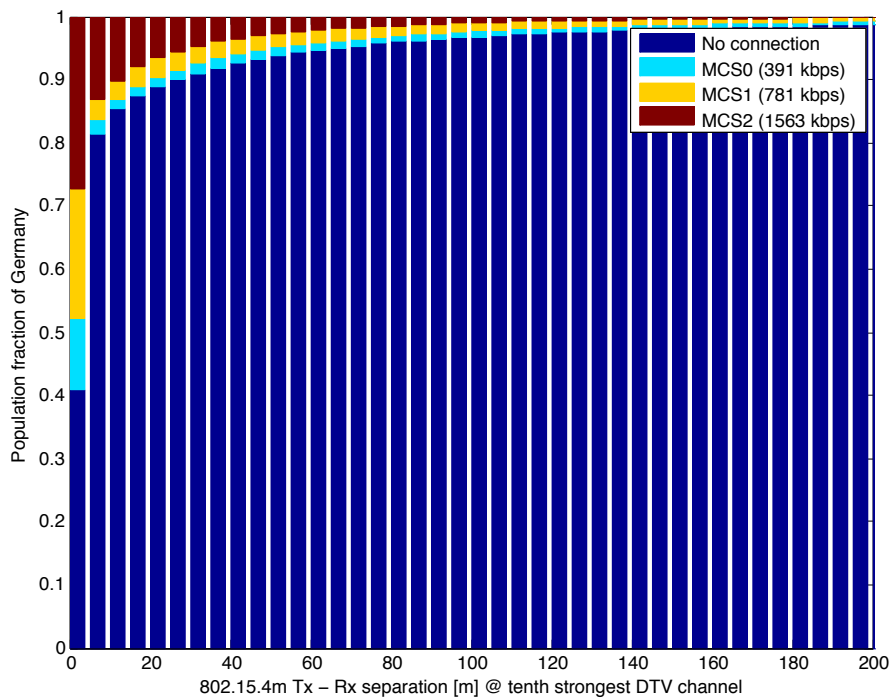Figure 7.26: Strongest channel, conditioned on population (figure courtesy of Andreas Achtzehn, RWTH Aachen University).
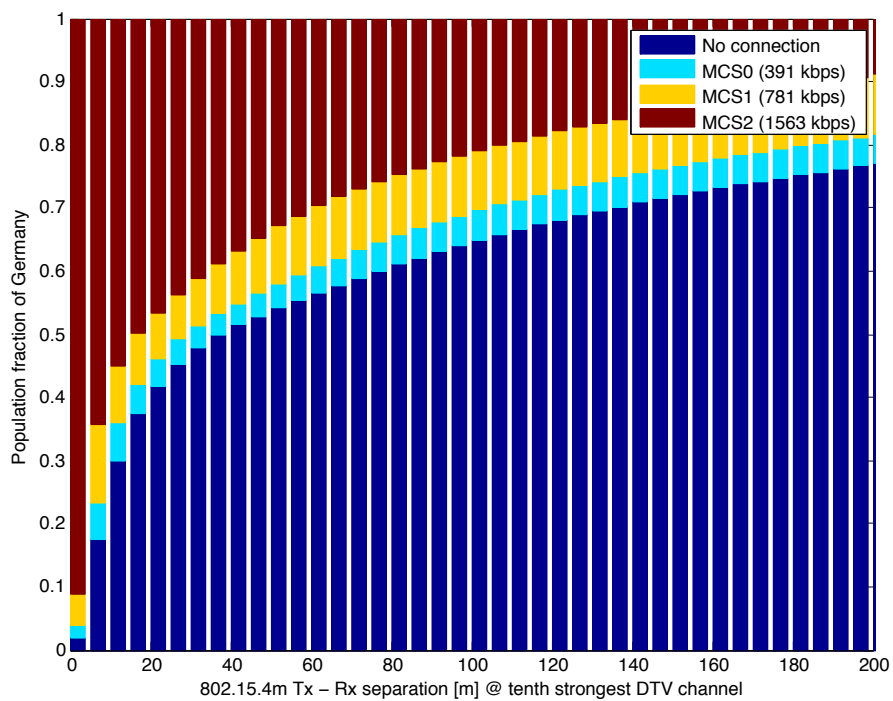
Figure 7.27: Tenth strongest channel, conditioned on population (figure courtesy of Andreas Achtzehn, RWTH Aachen University).

which a certain MCS can be used. The analysis is performed considering the strongest channel, in Figure 7.24, and the tenth strongest channel, in Figure 7.25. The same analysis is also taken into account the ratio of population that can use a given MCS, and the relevant Figures are Figure 7.26 for the strongest channel, and Figure 7.27 for the tenth strongest channel. Focusing on the area, it is evident that gray space communication on the strongest channel are technically challenging. As it can be seen from Figure 7.24, most of the areas in Germany can not achieve connection even by using the strongest MCS. Another interesting aspect is that the strongest MCS (MCS0 and MCS1) are in fact less used compared to MCS2. This means that where TVGS operation are technically feasible, they can be generally performed by using the highest MCS. This fact would suggest to implement stronger MCS for IEEE 802.15.4m, to allow operations where the signal coming from the primary network severely interferes with the secondary deployment. Another option would be to implement stronger FEC mechanism at the receiver.

Looking instead at Figure 7.25, is it possible to see that connection is possible almost in every area of Germany, although with short separation distances. However, the fact that MCS2 is the most used one, as already stated, can be seen also for the tenth strongest channel. If we consider a separation distance of up to 40 m, nearly half of the surface of Germany can be served with MCS2, which supports a throughput of 1563 kbps. For distances up to 80 m, the same percentage of covered area can be maintained by allowing transmission on MCS1. Finally, MCS0 can bring connectivity to the same area of Germany for distances up to 120 m. Similar remarks can also be drawn considering the ratio of population that can use a given MCS. The relevant Figures are Figure 7.26 for the strongest channel, and Figure 7.27 for the tenth strongest channel.

Performing a similar analysis, by fixing the MCS to be used, it is possible to derive the maximum separation distances between IEEE 802.15.4m devices. This analysis is performed in Figures 7.28, 7.29, and 7.30, for the strongest channel and for MCS0, MCS1, and MCS2, respectively. Gray space operations on the tenth strongest channel is analyzed in Figures 7.31, 7.32, and 7.33. For all the 6 figures, areas in which connection is not possible are depicted in white. Is it possible to see that the southern regions experience a better possibility for gray space operations, while in the northern regions there are several areas which remain out of connectivity, even with the strongest MCS. Considering the tenth strongest channel, the separation distances are much increased. However, some dense urban areas such as Berling, Hamburg, and Frankfurt, remain excluded from gray space operations. This can be seen by looking at the big white areas of the map, which represent the urban areas. Moreover, in southern Germany the Alps shield

the country by other neighboring transmitter, which translates into a better exploitation of TVGS operations.

Our results, although derived for the Germany scenario, can also be generalized to other similar European countries, as showed in [111].

In Figures 7.34 and 7.35 we plot the cumulative distributive function (CDF) for the maximum separation distance, considering all the three MCS, for the strongest channel and the tenth strongest channel, respectively. Figure 7.34, which takes into account transmissions on the strongest channel, show that basically no significant variation can be found on the three different MCS. This is in line to what we already found, and severely limits the economical viability of such operations, given the fact that secondary networks should be dense, to cope with the reduced maximum separation distances.

On the inverse, Figure 7.35 present a different behavior. Here, transmissions on the tenth strongest channel are foreseen, and is it possible to see that by choosing a stronger MCS like MCS0, the maximum separation distance greatly increase compared to other MCS. For instance, the maximum separation distance possible with MCS0 is 300 m, while MCS reach up to 500 m, and MCS2 nearly 650 m. To conclude, we can say that Gray Space operations are technically feasible for short to medium separation deployments, and where the interference of the primary network is too high. We showed that operations on the strongest channel are highly challenging, while communication on the tenth strongest channel seems more feasible.

7.5   Energy efficiency

Another beneficial aspect of M2M communication in the TV bands is related to the energy consumption of the devices. Transmitting in lower frequencies compared to the 2.4 GHz band or the 868 MHz band require less energy to cover the same distance, and eventually guarantee a longer battery life. This is not needed for main powered devices, such as smart meters for the energy monitoring, but for gas smart meters, which cannot be main powered, is crucial.

Following the regulations imposed by national regulators such as the FCC and Ofcom, devices need to query the remote spectrum database in order to get the list of available channels at their position. For the smart metering scenario, and for being energy efficient, this has two main drawbacks:

- Obtaining the position of the device indoors is technically challenging, since the GPS struggles to work, and other technologies cannot guarantee a sufficient degree of precision.

Figure 7.28: Maximum permitted local transmitter-receiver separation to maintain connectivity using given modulation scheme on the strongest channel for MCS0 (figure courtesy of Andreas Achtzehn, RWTH Aachen University).
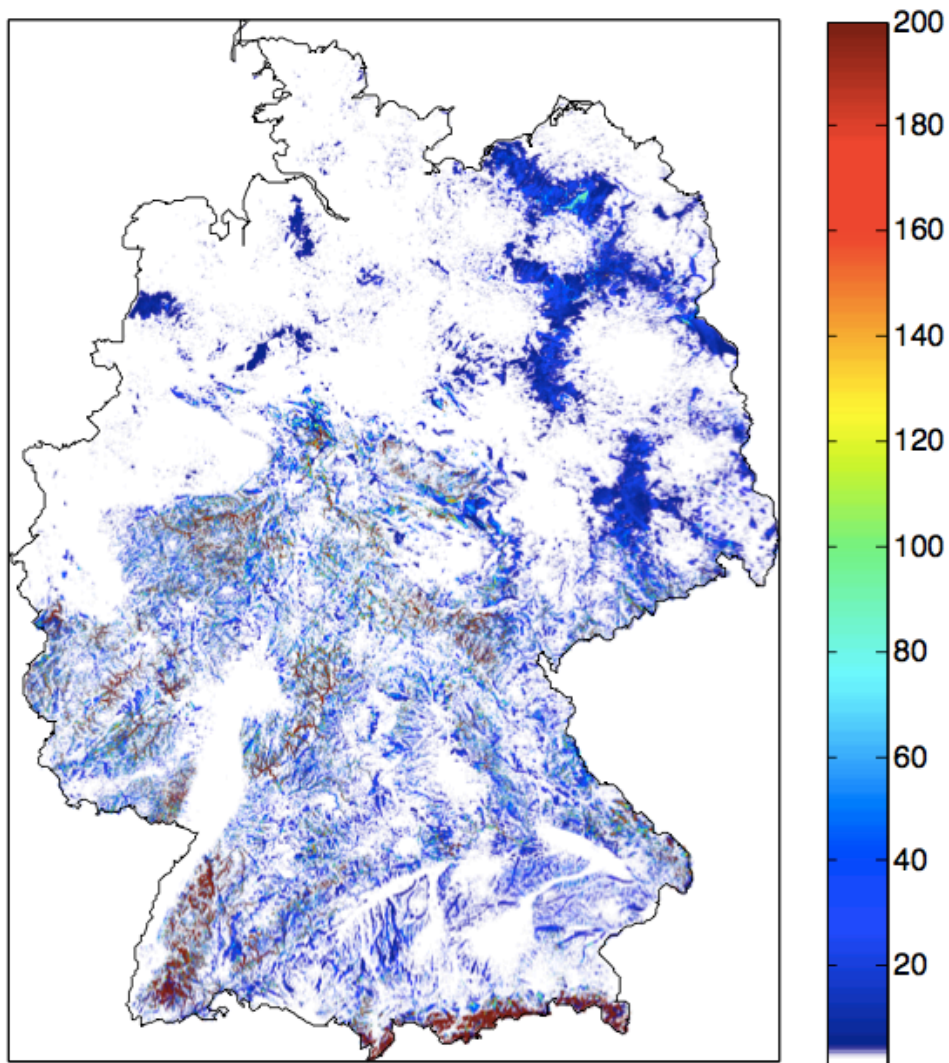
Figure 7.29: Maximum permitted local transmitter-receiver separation to maintain connectivity using given modulation scheme on the strongest channel for MCS1 (figure courtesy of Andreas Achtzehn, RWTH Aachen University).
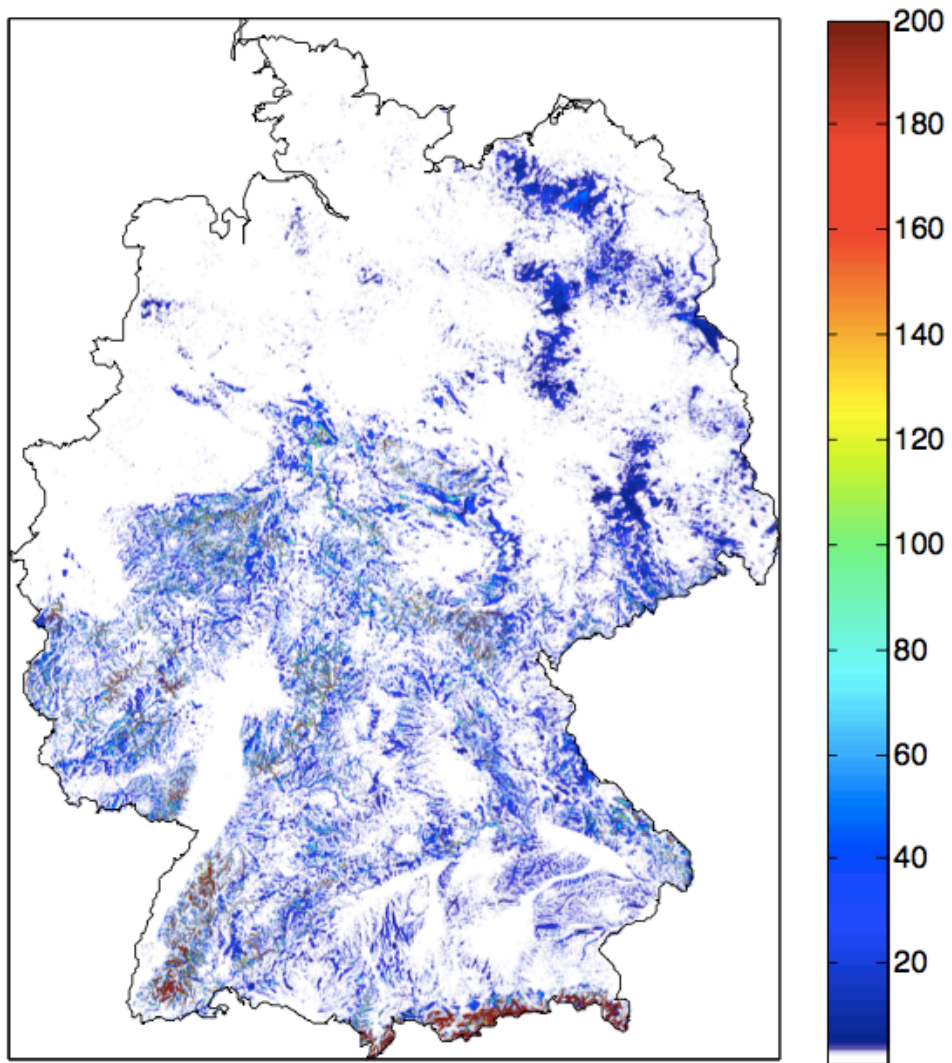
Figure 7.30: Maximum permitted local transmitter-receiver separation to maintain connectivity using given modulation scheme on the strongest channel for MCS2 (figure courtesy of Andreas Achtzehn, RWTH Aachen University).
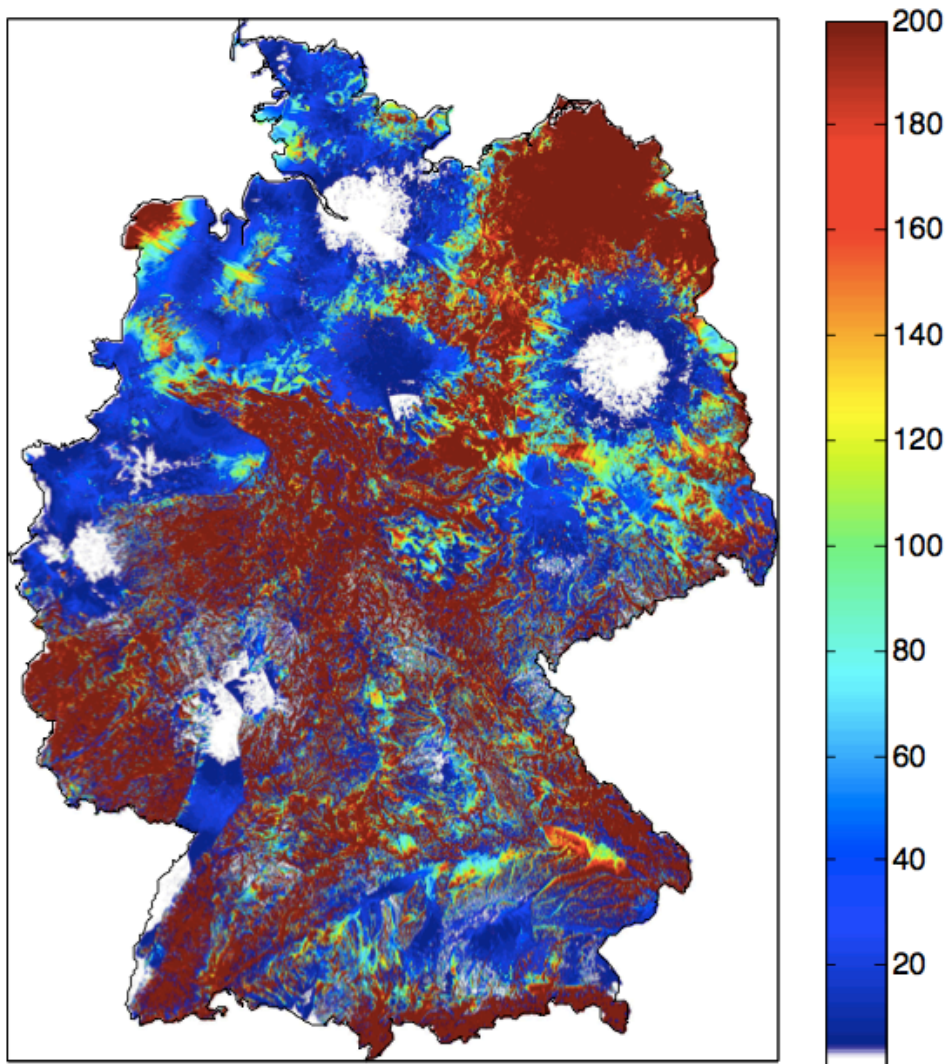
Figure 7.31: Maximum permitted local transmitter-receiver separation to maintain connectivity using given modulation scheme on the tenth strongest channel for MCS0 (figure courtesy of Andreas Achtzehn, RWTH Aachen University).
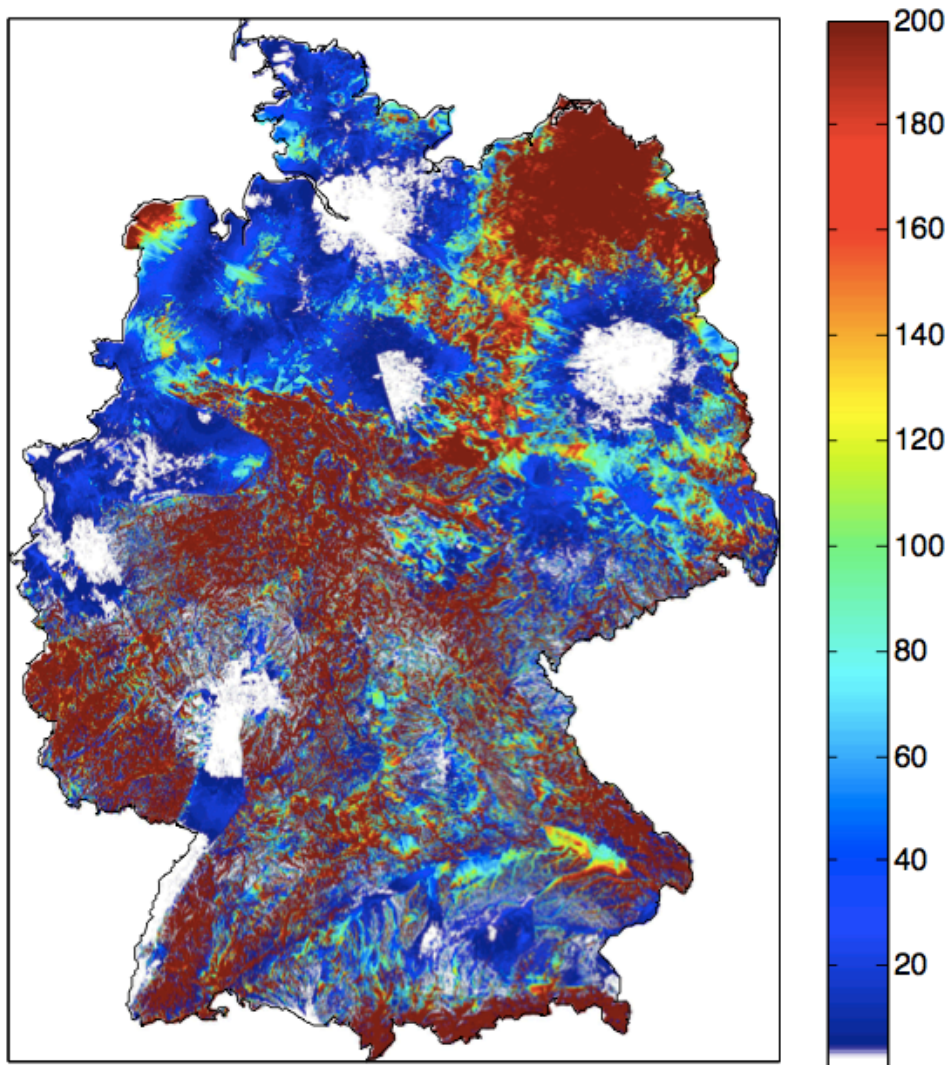
Figure 7.32: Maximum permitted local transmitter-receiver separation to maintain connectivity using given modulation scheme on the tenth strongest channel for MCS1 (figure courtesy of Andreas Achtzehn, RWTH Aachen University).
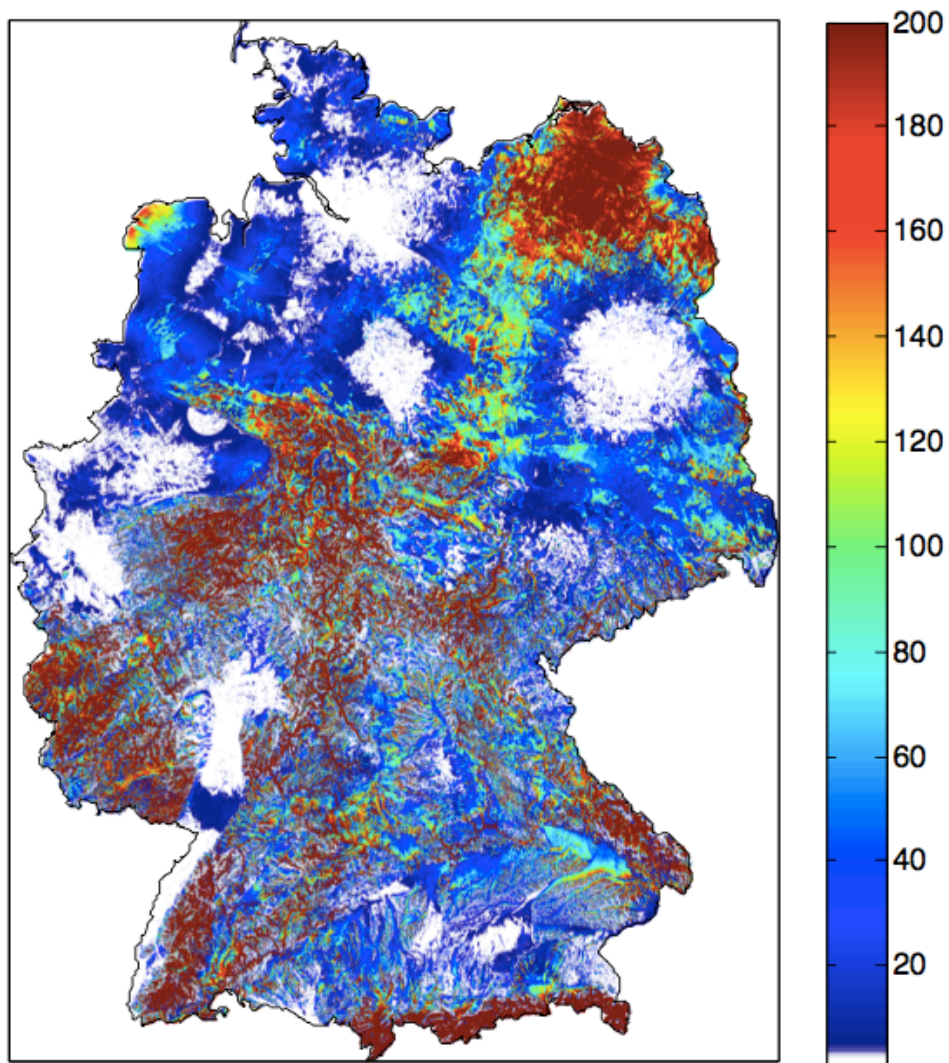
Figure 7.33: Maximum permitted local transmitter-receiver separation to maintain connectivity using given modulation scheme on the tenth strongest channel for MCS2 (figure courtesy of Andreas Achtzehn, RWTH Aachen University).
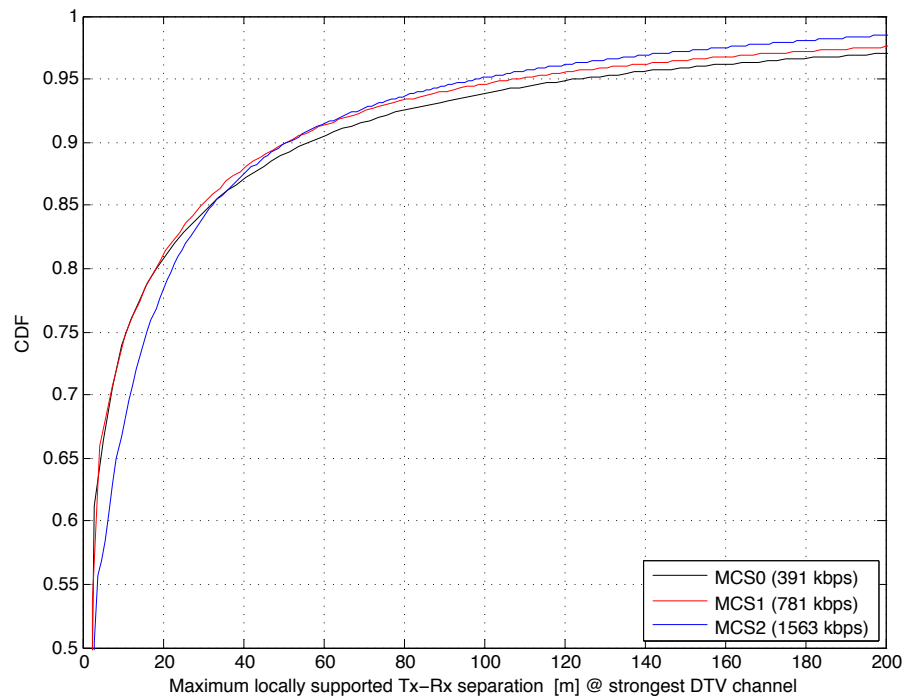
Figure 7.34: Cumulative distribution function of the maximum permitted local transmitter-receiver separation to maintain connectivity using a given modulation scheme on the strongest TV channel (figure courtesy of Andreas Achtzehn, RWTH Aachen University).
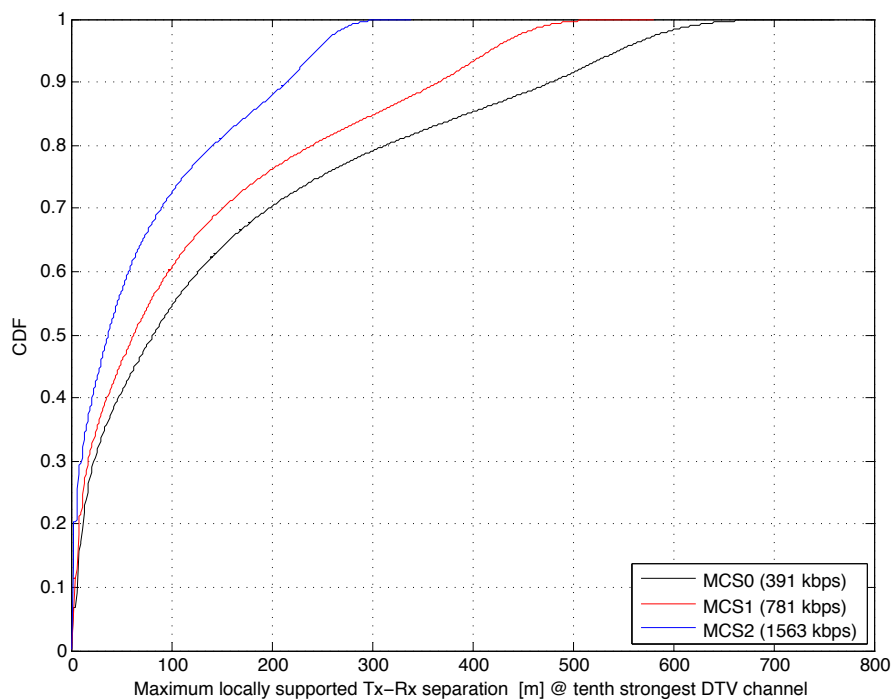
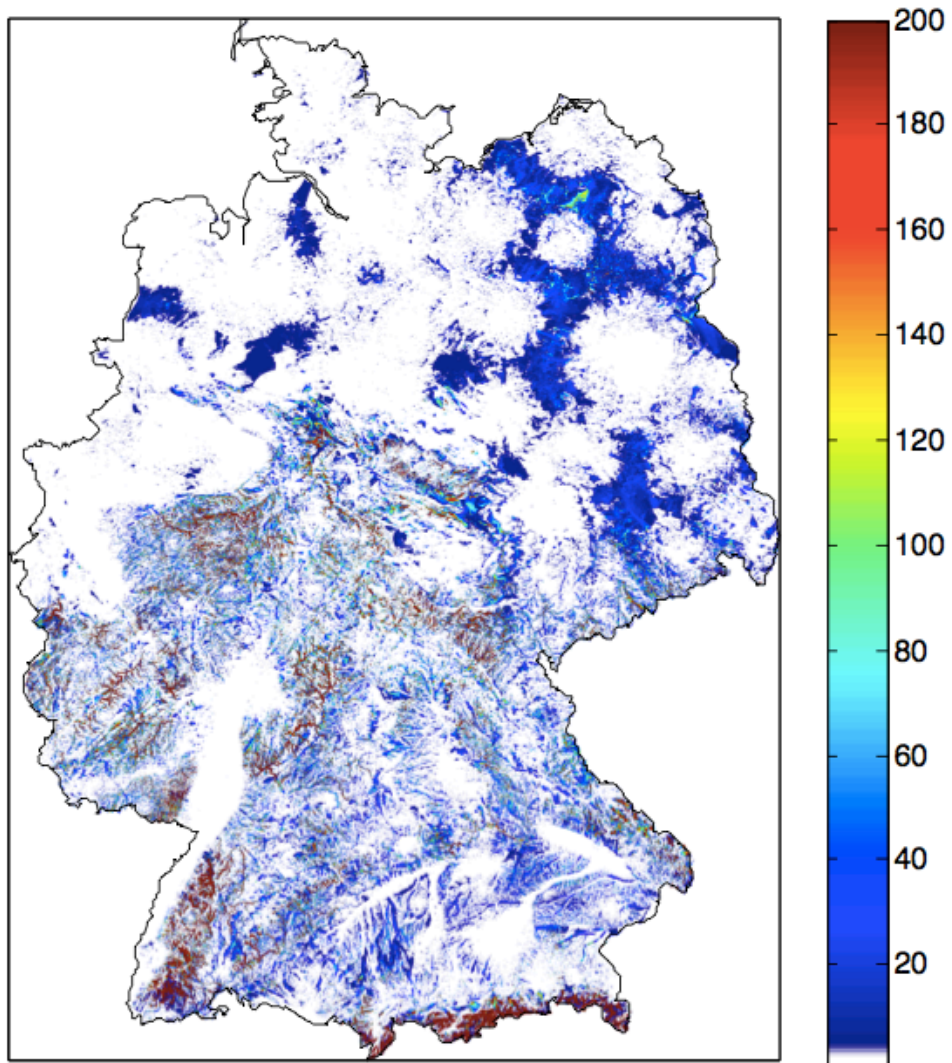Figure 7.35: Cumulative distribution function of the maximum permitted local transmitter-receiver separation to maintain connectivity using a given modulation scheme on the tenth strongest TV channel (figure courtesy of Andreas Achtzehn, RWTH Aachen University).

- Transmitting and receiving are two of the most energy consuming tasks for a device, and thus should be kept at minimum. Querying the database each time the device wants to transmit would severely degrade the total battery life of the devices.

Thus, we investigated whether it is possible to reduce the amount of communication involved, while respecting the constraints imposed by regulators. Each set of rules foresee the presence of two classes of devices, namely Master and Slave (following Ofcom naming) [89], or Mode I and Mode II (according to FCC) [43]. The Master or Mode II devices can directly query the remote spectrum database, while the Slave or Mode I devices need to ask a Master or Mode II device to make the query on their behalf. Without loss of generality, in the following we name MD the Master devices, and SD the Slaves.

We seek to cluster smart meters together, and elect one of them to be the relay of the message to the central aggregator. This can be seen as a clustering problem, which has been extensively studied in literature [2] [19] [67] [69]. Examples of battery-aware clustering algorithms include the EEHC protocol [7], which is based on nodes annoucing their willingness of becoming cluster head to other nodes. Depending on their distance, and according to a certain probability, the cluster head is elected, and nodes are informed. The HEED protocol introduces the concept of creating clusters distant from each other, to distribute them better through the network [123]. Interestingly, they also do not consider the energy consumption to be equal among all the devices, which we take into account too in our proposal. Later, HEED has been extended to better manage nodes that are not part of any cluster [59]. A similar approach, although with more aggressive goals, and with a complexity of *O(1)*, is proposed with the DWEHC algorithm in [36]. Finally, MOCA introduces the concept of overlapping clusters. The rationale is that nodes should be a cluster heads, or at a maximum distance from any cluster head [124].

7.5.1   Daily schedule

The proposal is to opportunistically switch the role of MD and SD in order to save energy and prolong the lifetime of the system. The higher cost for these deployments come from the maintenance that operators should do on the devices, such as changing the batteries. Thus, reducing the need to physically go on site and fix what is needed, would increase the attractiveness of these network architectures, and their economic viability.

The tasks that each smart meter needs to perform each day can be summarized as in Figure 7.36.
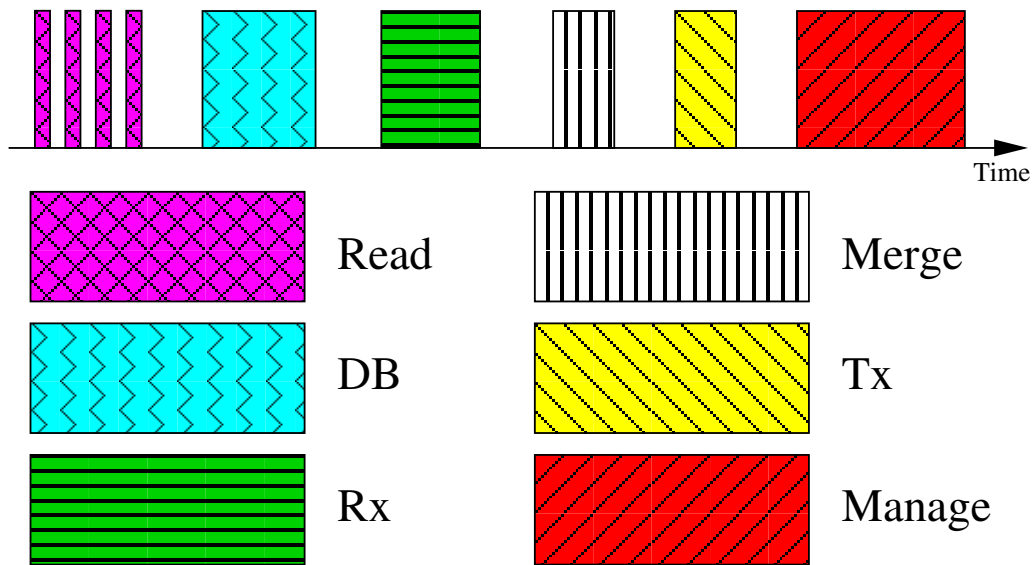
Figure 7.36: The actions a MD perform every day. SDs perform only the read operation and send the value to the MD at minimum required power.

Here, six different time slots are identified: the Read slot, in which each smart meter performs the reading; the DB slot, in which the MD queries the spectrum database and communicates to SDs the available TVWS and the selected channel to be used in the cluster; the RX slot during which the MD receives the SDs readings on the selected channel; the Merge slot in which the MD puts together the readings in a single packet; the TX slot in which the MD transmits this packet to the central aggregator; finally the Manage slot in which the MD decides whether to start an election process to decide the next MD of the cluster, according to the scheduling policy.

Reducing the Read slots it is not viable, since they are defined by operators and national regulators. Thus, we focus on the optimization of the communication part, from the DB query to the actual transmission of the readings.

Smart meters are naturally clustered together, since the installation are typically done in the same rooms in the basements or in the cellar. Thus, they can transmit using low power and narrow bandwidth between each other, saving several energy compared to the case in which they would have to communicate with the remote DB or with the central aggregator. We elect a cluster head, the MD, in charge of gathering the list of available channels from the remote spectrum database, inform the SD of the channel selected for the communication, gather all the readings, and eventually send everything to the central aggregator. Finally, the MD also need to perform the cluster

election, in which it is decided the next cluster head. Even though the `Read` part is performed several times per day, the communication to the central aggregator is usually once per day, and so also our cluster head selection.

We firstly study this problem with an analytical model, which will derive upper and lower bounds to the energy consumption, in Section 7.5.2.

7.5.2   Analytical model

In this Section we present our analytical model to estimate the lifetime of the cluster of smart meters considering both the consumption due to data communications and to the overhead for TVWS detection. We assume smart meters are grouped into clusters. Each cluster is composed by a single Master Device (MD) and a number of Slave Devices (SD). Each smart meter is capable of working both as MD or as SD, depending on the scheduling policy.

Although batteries are highly non linear device, we assume here, for sake of simplicity, that they follow a linear discharge. We note that, however, the behavior is different [44] [45]. Even though the behavior between the full charge and the completely discharge might change, we are interested in the total energy that the battery can provide, and thus our assumption can be done withouth loss of generality.

In case, the election process works as follows: the MD sends a message to all the SDs. Each SD replies with its availability (given by the specific scheduling algorithm in use) on being the MD for the next day. At this point, the MD examines all the replies and decides which device will be the next MD, sending a direct message to it. For each election, a total of 2 messages are sent by the MD, while each SD sends 1 message only. For ease of modeling, we assume in this study that elections will be performed at each `Manage` slot, which constitutes a lower bound in terms of energy efficiency of the cluster. We will relax this assumption in Section 7.5.5. SDs are responsible only to send their smart readings to the MD, thus limiting their transmission power as stated before.

Both the MD and SDs enter in a power saving mode to save battery life while not performing any of the activities stated above.

In the following, we derive the energy consumed each day by a MD as the sum of the actions depicted in Figure 7.36. This is given by Equation 7.12:

$$E_{MD} = E_{re} + E_{DB\_MD} + E_{rx} + E_{ag} + E_{tx} + E_{ma\_MD} + E_{id\_MD} \qquad (7.12)$$

where E_{re} is the energy consumed to read the house consumption, E_{DB_MD} is the energy needed to query the remote database in order to receive the list of available channels, E_{rx} is the energy consumed with the radio in receiving

Table 7.1: The symbols used in the analytical model

Symbol	Description
t_r	Time needed to perform a single sensor read
r	Number of sensor readings per day
c_r	Computational cost to pay for a single sensor read
t_{q_db}	Time needed to transmit a query to the database
γ	Energy needed to transmit a packet at full power
δ	Energy needed to transmit a packet at reduced power
t_{db}	Duration of the DB time slot
α	Energy consumed while in sleeping mode
β	Energy consumed while in Rx mode
n	Number of nodes
t_s	Time needed to transmit a message to the central aggregator
t_{ag}	Time needed to merge a message from a Slave device into the final packet to be sent to the aggregator
t_{a_SD}	Time needed to send a packet to the Master device to get the list of available channels
c_a	Energy consumed by the active CPU
t_{el}	Duration of the election packet
t_{SD}	Duration of the packet containing the readings to the MD
t_{DB}	Duration of the DB slot
t_{MA}	Duration of the Manage slot
t_{idle_MD}	Time a Master device passes in idle mode
t_{idle_SD}	Time a Slave device passes in idle mode
E_{id_MD}	Energy consumed in power saving mode by a Master device
E_{id_SD}	Energy consumed in power saving mode by a Slave device
s_{day}	Seconds in a day, i.e. 86.400
E^{start}	Initial amount of energy
t_{rx}	Time during which the device is in receiving state

mode, E_{ag} is the energy needed to merge together neighbor's packet into the final message sent, E_{tx} is the energy consumed for sending the aggregated packet to the aggregator, and E_{ma} is the energy a MD must spend in order to manage the switching process, determining if it still need to be the MD or an election must occur. Finally E_{id_ch} is the time consumed while in power saving mode. By referring to Table 7.1, we derive all the single terms of Equation 7.12:

$$E_{re} = r \cdot t_r \cdot c_r \tag{7.13}$$

$$E_{DB\_MD} = 2 \cdot (t_{q\_db} \cdot \gamma) + (t_{DB} - 2 \cdot t_{q\_db} - (n-1) \cdot *t_{a\_SD}) \tag{7.14}$$

$$E_{rx} = t_{rx} \cdot \beta \tag{7.15}$$

$$E_{ag} = (n-1) \cdot t_{ag} \cdot c_a \tag{7.16}$$

$$E_{tx} = \gamma \cdot t_s \tag{7.17}$$

$$E_{ma\_MD} = 2 \cdot t_{el} \cdot \gamma + n \cdot c_a + (t_{MA} - 2 \cdot t_{el}) \cdot \beta \tag{7.18}$$

$$t_{idle\_MD} = s_{day} - (n-1) \cdot t_{ag} - r * t_r - t_{DB} - t_{RX} - t_s - t_{MA} \tag{7.19}$$

$$E_{id\_MD} = \alpha * t_{idle\_MD} \tag{7.20}$$

The energy consumed by any SD is defined instead as:

$$E_{SD} = E_{re} + E_{DB\_SD} + E_{tx\_SD} + E_{ma\_SD} + E_{id\_SD} \tag{7.21}$$

where E_{re} is the same as before, E_{DB_SD} is the energy for asking the MD the list of available channels, E_{tx_SD} is the energy needed to send a message to the neighbor by using the minimal transmission power, E_{ma_SD} is the energy consumed during the `Manage` slot by any SD, and E_{id_SD} is the energy needed to spend the rest of the time in power saving mode.

As before, we derive all the terms in Equation 7.21:

$$E_{db\_SD} = 2 \cdot t_{a\_SD} \cdot \delta \tag{7.22}$$

$$E_{tx\_SD} = \delta * t_{SD} \tag{7.23}$$

$$E_{ma\_SD} = t_{el} \cdot \delta + (t_{MA} - t_{el}) \cdot \beta \tag{7.24}$$

$$t_{idle\_SD} = s_{day} - t_{SD} - r \cdot t_r - 2 \cdot t_{a\_SD} - t_{MA} \tag{7.25}$$

$$E_{id\_SD} = \alpha * t_{idle\_SD} \tag{7.26}$$

Let j be SD or MD, and $E_j[d]$ be the amount of energy consumed by any device of the cluster while being in mode j until day d. This can be written as:

$$E_j[d] = E_j * d \tag{7.27}$$

Analogously we derive the energy remaining at day d for device i being in mode j as:

$$E_{i,j}^{left}[d] = E_i^{start} - E_j[d] \tag{7.28}$$

where E_i^{start} is the initial amount of energy of device i. As depicted in Figure 7.37 for a configuration with E_i^{start} equal to 16000, $E_{i,MD}^{left}[d]$ and $E_{i,SD}^{left}[d]$ describe two lines, and all possible energy consumptions fall in between the two lines. Let θ_j be the time in which the device reaches out of energy with the current energy E while always being in mode j:

$$\theta_j[E] = \frac{E}{E_j} \tag{7.29}$$

It is easy to see that the lifetime of device i will fall between $\theta_{SD}[E_i^{start}]$ and $\theta_{MD}[E_i^{start}]$, because a device cannot consume more energy than always being a MD, and inversely, a device could not consume less energy than always being a SD. Therefore, the following inequality holds:

$$\theta_{MD}[E_i^{start}] \leq \theta_\lambda[E_i^{start}] \leq \theta_{SD}[E_i^{start}] \tag{7.30}$$

7.5.3   Satisfying a goal

Based on the analytical model described so far, we introduce the notion of cluster goal, expressed in terms of battery life of the cluster. The cluster lifetime is defined as the time passed from the initial deployment till the first death of any smart meter. This is a common assumption found in literature, and is also practical from our point of view: when a battery expires, human intervention is required, and the costs to change a battery to a device or to a couple of devices near to each other are almost the same. More specifically, we define the goal as follow:

Definition 1 (goal). *a goal is a minimal duration ψ expressed in days every device in the cluster should guarantee.*

We also define the notion of no return point as follows:

Definition 2 (nrp). *given a day d, a no return point (nrp) χ_d is the lowest energy value for which, $\theta_{SD}[\chi_d] + d \geq \psi$.*

The χ_d of any device at day d simply indicates whether the device could become a MD, or if it needs to remain a SD in order to guarantee the goal. In Figure 7.37 we depicted a configuration of devices with the notion of goal and nrp. Since devices may have different residual energy, and the nrp could be passed with a single day as a MD, we now define the notion of soft no return point.
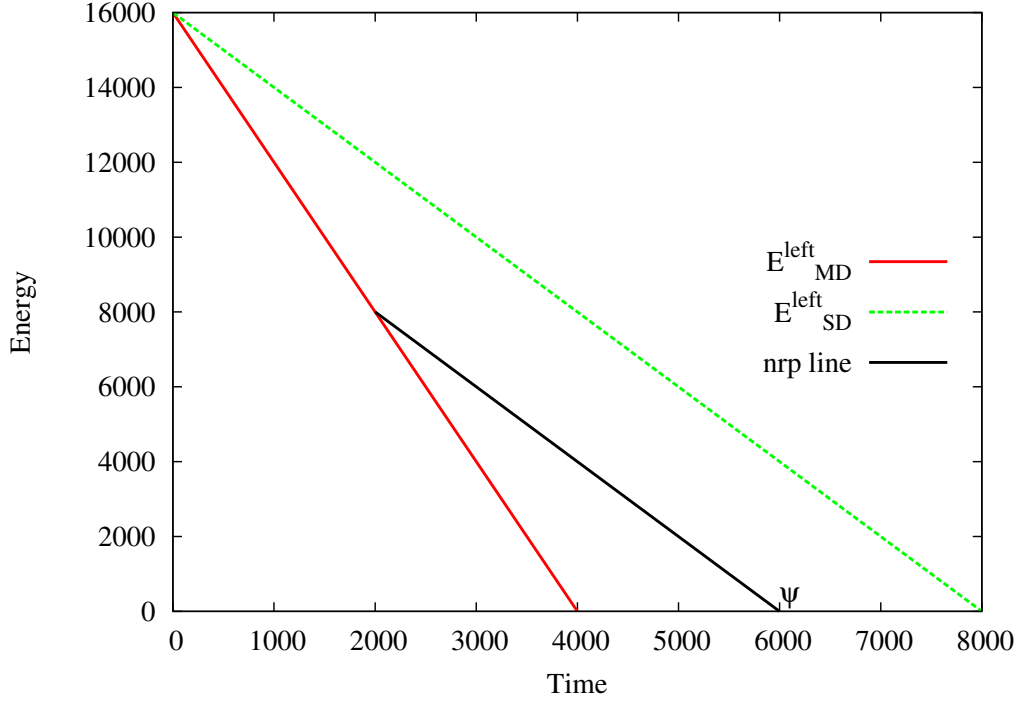
Figure 7.37: The goal ψ and the nrp line for $E_i^{start} = 16000$.

Definition 3 (soft nrp). *Suppose $E^i[d]$ is the energy left for device i at day d. A soft nrp is the greatest point z_i for which the inequality $E^i[z_i] - E_{MD} \geq \chi_{z+1}$ holds.*

Intuitively, the soft nrp z_i indicates the total number of days device i could serve as MD, considering that the switching operations are performed once per day. We now define ρ as the sum of the soft nrp points of the devices (i.e. $\rho = \sum_{i=0}^{n} z_i$). This indicates the total number of days the cluster of smart meters could be served by a MD. We can now derive the notion of satisfiability as follows.

Definition 4 (satisfiability). *Assuming all smart meters can reach the goal if they are always in SD mode, a system is satisfiable when the cluster can reach the goal. This happens iff $\rho \geq \psi$.*

Definition 4 claims that the system can reach the goal if there is a device that can serve as MD in every day till the goal ψ.

If at a certain time all the devices reach their own soft nrp, then no MD can be elected, and therefore the system is not satisfiable.

7.5.4 Centralized framework

In this Section we use the analytical model presented in Section 7.5.2 to derive an optimization framework that determines the Master/Slave scheduling assignments among the devices. We formulate the scheduling as an optimization problem, in which the inputs are the number of nodes in the cluster N, the amount of time each device i can be Master MD_i, and the global goal ψ. The output of the centralized framework is a vector D where D_i is the total amount of days node i has to be the Master device of the cluster. More formally:

$$Given:\ n, MD_i, \psi \tag{7.31}$$
$$To\ find:\ D \rightarrow \{D_0, D_1, \ldots D_{n-1}\} \tag{7.32}$$
$$Subject\ to:\ D_i \leq MD_i \tag{7.33}$$
$$\sum D_i \geq \psi \tag{7.34}$$
$$minimize\left(max_{i \in [0,n[}\left(\frac{D_i}{MD_i}\right) - min_{i \in [0,n[}\left(\frac{D_i}{MD_i}\right)\right) \tag{7.35}$$

Here, Constraint 7.33 ensures that any device will not be requested to schedule more days as Master than what it can afford (given by MD_i). Constraint 7.34 guarantees that the vector D satisfies the goal, according to Definition 4. Finally, Constraint 7.35 is the fairness condition, since we attempt to balance the effort of coordinating the cluster among all the devices.

The MD_i is exactly the soft nrp point of device i, and can be computed through geometrical reasoning as:

$$MD_i = \left\lfloor \frac{E_i^{start} - E_{SD} \cdot \psi}{E_{MD} - E_{SD}} \right\rfloor \tag{7.36}$$

Given this problem, we can show that the optimum can be reached when each smart meter i contributes as MD to the goal in a proportional way, based on its own MD_i value. More formally, the term D_i for smart meter i is computed as follows:

$$D_i = \left\lceil \psi \cdot \frac{MD_i}{\sum_{j=0}^{n-1} MD_j} \right\rceil \tag{7.37}$$

We show now that this assignment is fair given Condition 7.35 and determines a feasible assignment guaranteeing the goal ψ if the system is satisfiable according to Definition 4.

Theorem 1 (Fairness)**.** *The proposed system is fair, i.e the difference in energy consumed between any two nodes is minimal.*

Proof 1 (Fairness)**.** *The fairness of the system is bounded in the* $\left[0, \frac{1}{min(D_i)}\right[$ *interval. This is straightforward following algebraic transformations in Equation 7.35 by substituting the D_i term with the one given in Equation 7.37. The proof of fairness is straightforward, since according to Equation 7.37 it is easy to see that in Equation 7.35 the maximum and minimum term are equal to* $\frac{\psi}{\sum_{j=0}^{N-1} MD_j}$*, therefore the difference between those is zero.*

We prove now the satisfiability of the goal with the Master/Slave scheduling using Equation 7.37.

Theorem 2 (Satisfiability)**.** *The proposed system always finds a solution if there is one.*

Proof 2 (Satisfiability)**.** *According to Definition 4, a system is satisfiable if* $\sum_{j=0}^{n-1} MD_j \geq \psi$*, then* $\frac{\psi}{\sum_{j=0}^{n-1} MD_j} \leq 1$*, so* $D_i \leq MD_i$*, therefore Constraint 7.33 is satisfied. At the same time, it is easy to see that Constraint 7.34 is satisfied since* $\sum_{i=0}^{n-1} D_i \geq \psi$*.*

7.5.5   Distributed Scheduling protocols

Solving the optimization problem presented in Section 7.5.4 requires central coordination, either by the aggregator or by another entity and might involve considerable computation effort. For this reason, we propose here and evaluate different distributed scheduling algorithms to approximate the optimum given by Equation 7.32. The first three algorithms follows straightforward approaches, but are tested here to provide lower and upper bounds on the metrics evaluated in Section 7.5.6. The last algorithm (i.e. the Cost Aware) is proposed to prolong cluster lifetime while addressing the fairness issues.

7.5.5.1   No election protocol

This algorithm does not take into account the optimization framework. Basically, every device acts as there is no cluster, and thus makes its own queries to the spectrum database, serving as a Master device. In this case, the final goal is satisfied iff all devices have $E_{MD}[z] \geq \psi$. This protocol minimizes the overhead for the cluster management since no elections are performed.

7.5.5.2   Highest first protocol

In this algorithm, the device with the highest residual energy serves as the Master. As a result, an election is issued at the end of every day. This algorithm provides an upper bound on the overhead for the cluster management.

7.5.5.3 Greedy protocol

In this algorithm, each smart meter i acts as Master for MD_i days, i.e. the maximum number of days it can serve as Master device before passing the soft nrp threshold. It is easy to see that this method reduces the number of elections but does not provide the fairness of the system, since some smart meters might serve for MD_i days while others may not become a Master device at all.

7.5.5.4 Cost Aware Protocol

This algorithm provides a distributed implementation of the centralized schedule given by Equation 7.37, while relaxing the worst case assumption taken in the analytical model. To this aim, each device i maintains two values $\overline{E_{i,SD}}$ and $\overline{E_{i,MD}}$ representing the average energy consumption for being in SD or MD mode. We highlight that $\overline{E_{i,SD}}$ and $\overline{E_{i,MD}}$ may not be constant due to the fact that elections might be issued or not at each `Manage` slot, thus impacting the energy consumption per day of each device. At network setup, $\overline{E_{i,SD}} = E_{SD}$ and $\overline{E_{i,MD}} = E_{MD}$, i.e. the worst case scenario configuration is utilized, and an election is issued at the first day. At each election, smart meter i updates its MD_i value with Equation 7.36 (using $E_{SD} = \overline{E_{i,SD}}$ and $E_{MD} = \overline{E_{i,MD}}$), thus accounting for its actual battery consumptions and network capabilities, and sends it to the MD. Based on these values, the current MD populates the vector D by using Equation 7.37 and chooses the smart meter j with maximum value of D_j. At this point, the smart meter j will be in MD mode for exactly D_j days, till issuing another election with the same mode described above.

7.5.6 Performance evaluation

In this Section, we evaluate the distributed protocols proposed so far, by considering the following metrics for the comparison:

- **Cluster lifetime**: this is defined as the time elapsed from the network setup till the instant of the first death, i.e. when the first smart meter runs out of battery.

- **Goal satisfaction**: fixing a goal and a number of simulation runs for a specific network configuration, this is the percentage of runs in which the goal is satisfied by the cluster.

- **Fairness**: this is a measure of the workload balance among the devices and it is defined through Equation 7.38.

- **Elections**: this is defined as the total number of elections issued in the network till the goal is reached. Practically, it measures the overhead involved by each scheduling algorithm for cluster management operations.

For the evaluation, we model a smart metering scenario within the Omnet++ tool, and we vary the number of devices in the network. Each smart meter communicates at full transmitting power γ (to reach the central aggregator) and δ (to reach its neighbors). Nodes are heterogeneous and are provided with different initial energies (E_i^{start}) and energy consumption values (i.e. E_{SD} and E_{MD}) while being a Slave or Master device. In each simulation run, these values are randomly generated in the interval given by Table 7.2.

Table 7.2: Simulation parameters

Name	Value
Initial energy	8.000 Ah → 12.000 Ah
n	2 → 200
E_{SD}	1
E_{MD}	$(1 \rightarrow 3) + N \cdot c_a$

7.5.6.1   Cluster lifetime

Figure 7.38 shows the total cluster lifetime using the different scheduling algorithms as a function of the number of smart meters in the network. It is immediately evident that using no elections at all gives the worst results in term of cluster lifetime. Inversely, the battery lifetime is greatly improved by using the Cost aware and Greedy algorithms, which show a similar trend in terms of trade-off between the number of devices and the battery lifetime. In fact, for a number of devices lower than 10, the lifetime of the cluster increases with the number of devices since the MD overhead is shared among more devices. At the same time, this benefit is reduced as the number of devices is greater than 10, since the E_{MD} cost is proportional to the cardinality of the cluster. Although the aggregated performance of the Cost aware and Greedy algorithms are similar, we will show the benefits provided by the first solution in terms of fairness in Section 7.5.6. Having more neighbors to manage increase the energy spent as Master device, but also more devices could become Master thus prolonging the total cluster lifetime. The probabilistic algorithm and the distributed gives the best result in terms of maximum lifetime of the cluster, while the others decrease the performance over time due

Lifetime of the cluster
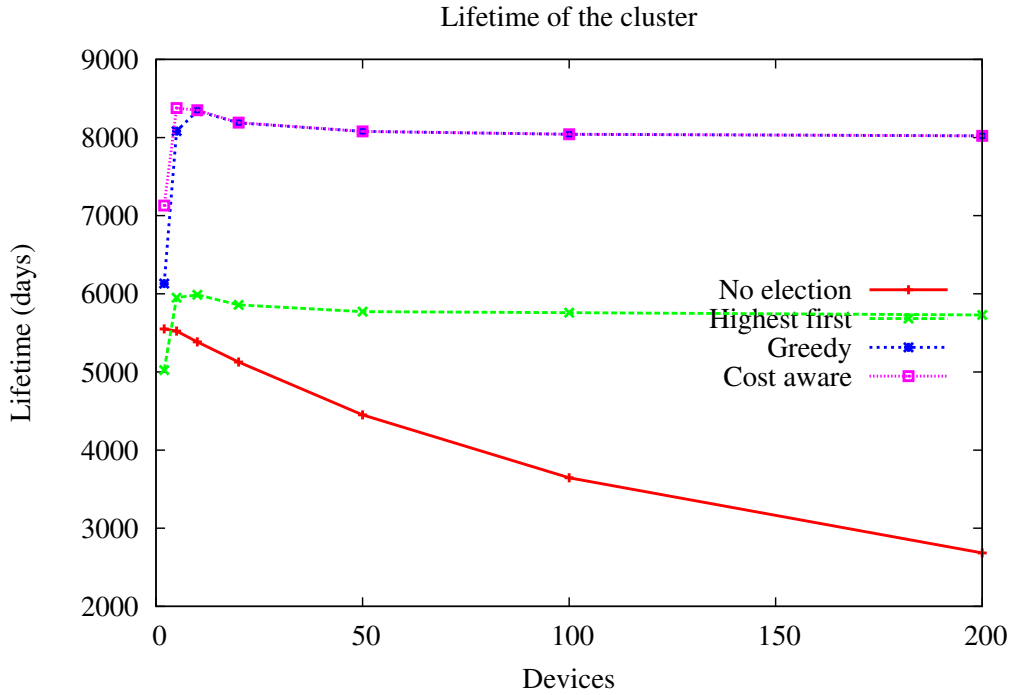
Figure 7.38: Cluster lifetime using different algorithms.

to excessive cost of the management operations. Since we assumed all M2M devices to be equal, with the same amount of energy at the beginning, it is clear that always selecting the device with more energy left gives the best results. The randomic algorithm gives slightly worse results, since it could happen that sometimes the next cluster head is not the one with the highest energy left. The probabilistic algorithm gives somewhat worse results, since the election is not called at the end of every day, but it is called probabilistically. This could also be seen in figure 7.42, where the total number of elections is shown. It is clear that the highest algorithm and the randomic algorithm have the same results, since they call for an election at the end of every day. What is interesting to see is the probabilistic algorithm, which decreases the number of elections over time. This happens because having more devices will divide the burden to be the Master device among more M2M devices, thus prolonging global lifetime.

7.5.6.2 Goal satisfaction

In this Section we keep constant the number of devices and we evaluate the ability of the proposed algorithms to satisfy a pre defined goal. Figure
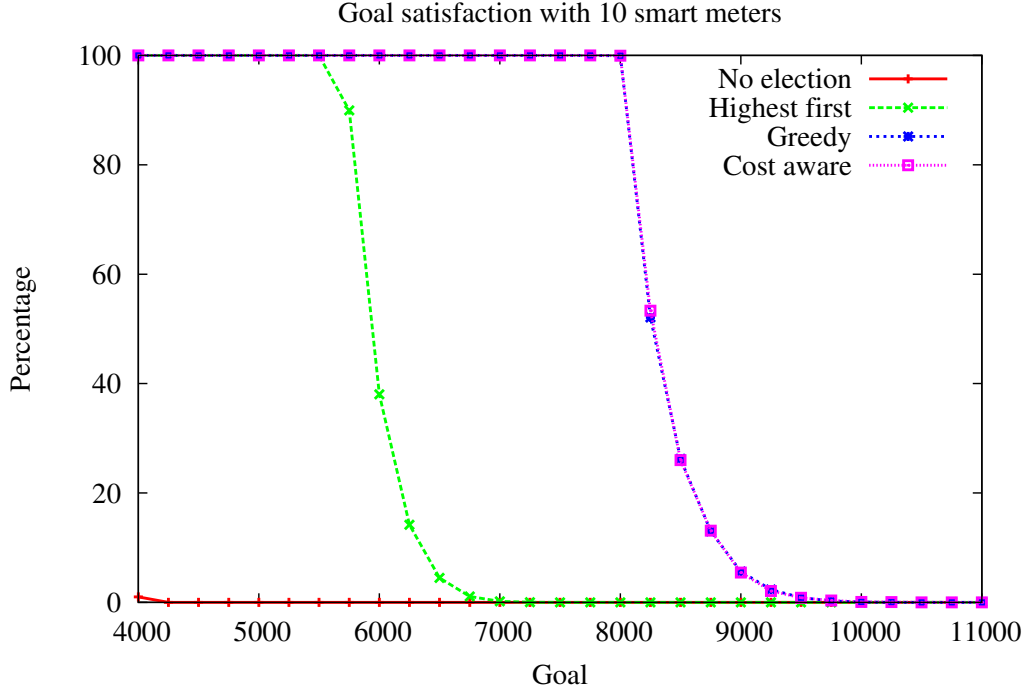
Figure 7.39: Percentage of goals satisfied with 10 devices.

7.39 and Figure 7.40 depicts the percentage of simulations runs in which the goal (on the x-axis) is satisfied, for a configuration with 10 and 500 devices respectively. We considered 1000 runs for the evaluation with the parameters of Table 7.2. As for the previous analysis, the Cost aware and the Greedy algorithms provide better performance, achieving a higher percentage of satisfied goal compared to the other two algorithms. Both figures show the same trend, although with different slopes due to the impact of the number of devices on the power consumption of the cluster.

7.5.6.3 Fairness

In this Section we evaluate the work balance between the smart meters of the scenario by considering the fairness index F computed as follows:

$$F = 1 - \left(max_{i\in[0,n[} \left(\frac{D_i}{MD_i} \right) - min_{i\in[0,n[} \left(\frac{D_i}{MD_i} \right) \right) \qquad (7.38)$$

Here, D_i is the amount of time a device has been the master, and MD_i expresses its MD capacity according to Equation 7.36. An F value close to

Goal satisfaction with 500 smart meters
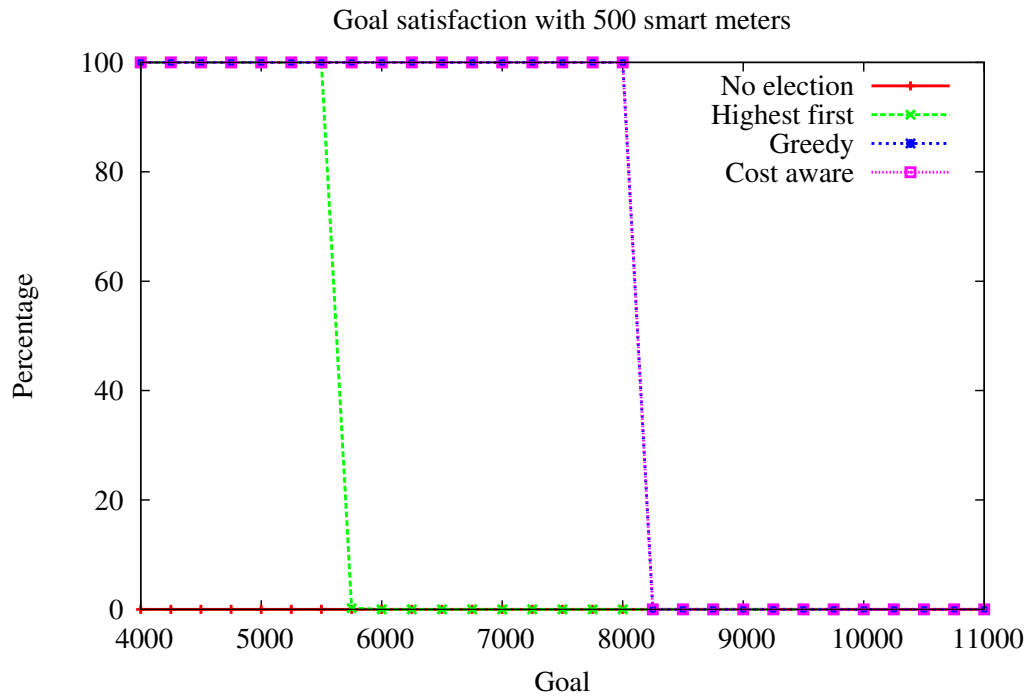
Figure 7.40: Percentage of goals satisfied with 500 devices.

1 indicates a higher fairness in balancing the Master/Slave scheduling operations, while a value close to 0 has to be intended as a greater diversity between work loads of the devices, and thus a low fairness. In Figure 7.43 we show the F metric as a function of the number of devices, for three scheduling algorithms (we omit the No election protocol since each device acts as MD, and thus no switching operations occurs). Here, the Greedy algorithm experiences the worst performance, due to the fact that in some configurations devices with low MD values are excluded from the cluster management. Similarly, the same behavior is shown with the Highest first algorithm, where however devices with higher battery life contribute more than others to the cluster management, particularly after network deployment. Inversely, the Cost aware algorithm guarantees an F value close to 1, as the workload is maximally balanced among the devices, according to their MD values. All the other algorithms fail in balancing the load between the devices, even while achieving a high percentage of goal satisfied. This happens since in the distributed algorithm, the fairness is maintained day by day until reaching the goal, while the other algorithms act firstly in reaching the final goal, and then on the fairness. After a certain limit, all the algorithms fail to balance
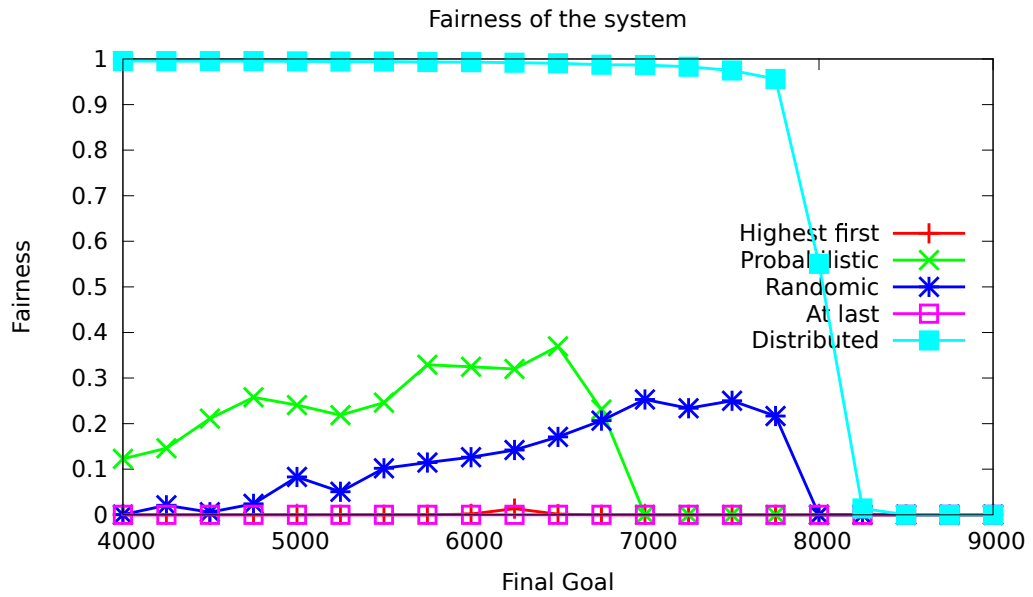
Figure 7.41: Fairness metric computed with Equation 7.38.
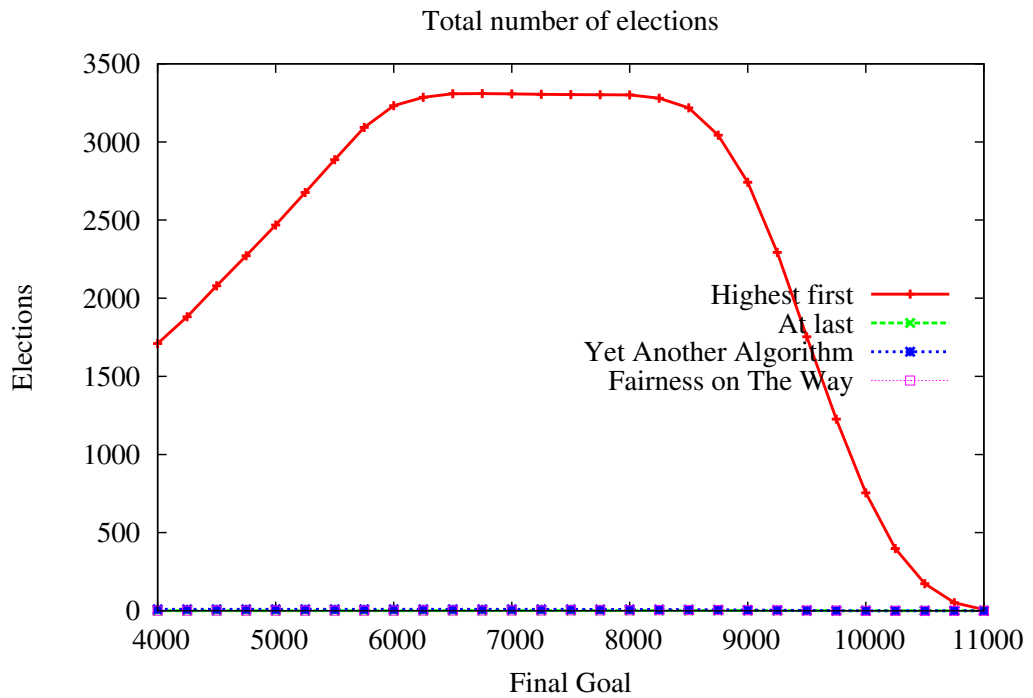
Figure 7.42: Total number of elections performed using different algorithms.

the load, since in this case the goal is not satisfiable anymore, as we could also see in figure 7.39.

7.5.6.4 Elections

In this Section, we evaluate the total number of elections performed by smart meters to decide the current MD during the cluster lifetime. The number of elections provides an indication of the stability of the system in terms of switching operations between Master and Slave devices. The frequency of elections impacts on the lifetime of each device i through $\overline{E_{i,SD}}$ and $\overline{E_{i,MD}}$ values close to the worst case scenario, modeled by E_{SD} and E_{MD}, respectively. Nonetheless, it gives also an idea of algorithms performance if the cost of the election changes and depletes more energy. In Figure 7.44 we plot the average number of elections (occurring from network setup till the goal is reached or the instant of the first death), while varying the number of devices in the scenario. We consider a fixed goal, equal to 10000. As before, we do not depict the No election algorithm, since in this case no elections occur at all. It is easy to see that the Highest first algorithm involves the highest number of elections, since they occur every day, unless a smart meter runs out of battery before the goal (in this case, the number of elections is equal to the lifetime of the cluster, otherwise it is equal to the goal). For the Greedy algorithm, the number of elections is at maximum the number of devices, if the system is satisfiable. Otherwise, after all the devices $i = 0, ..., n - 1$ have performed MD_i days as MD, elections are issued once per day, and this explains the decreasing trend of the curve as the number of devices increases. Finally, Figure 7.44 shows that for the Cost aware algorithm the number of elections is below the number of devices, since when the system is not satisfiable each MD tries to maximize its lifetime. All the algorithms have a similar behavior, reaching a maximum of elections when the system is close to the maximum capacity. This means that smart meters need to spend a high percentage of their energy to be the MD, and a high number of elections is needed to balance the workload. The distributed proposal has instead no elections at all since the clients know when they need to take the relay thanks to the initial discovery phase.
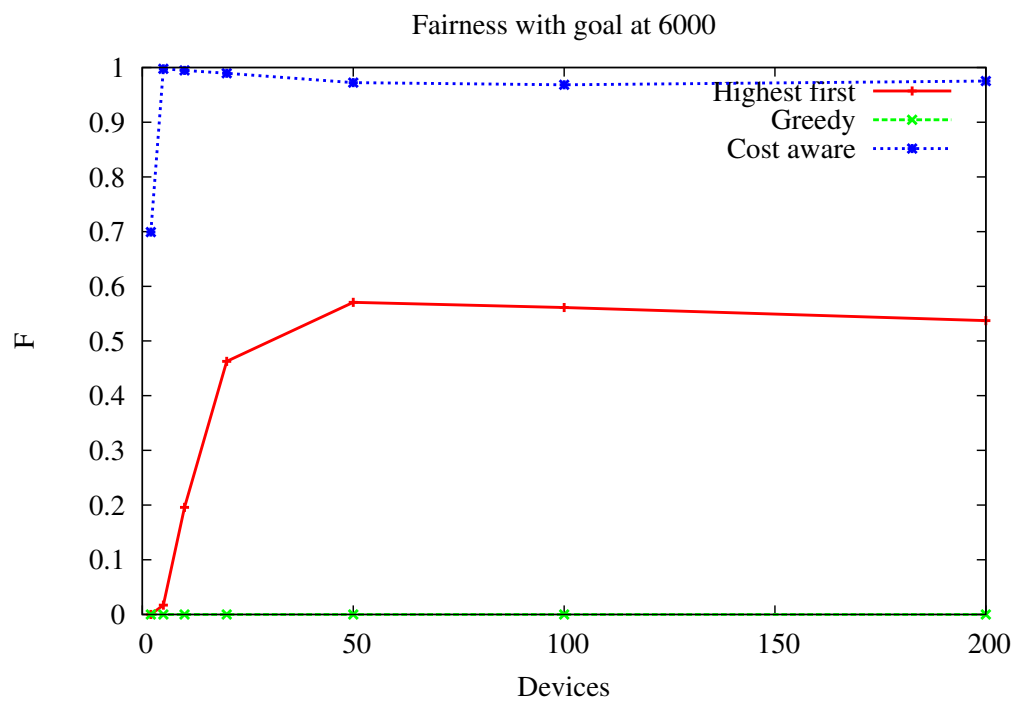
Figure 7.43: Fairness of the system with a fixed goal and varying the number of smart meters
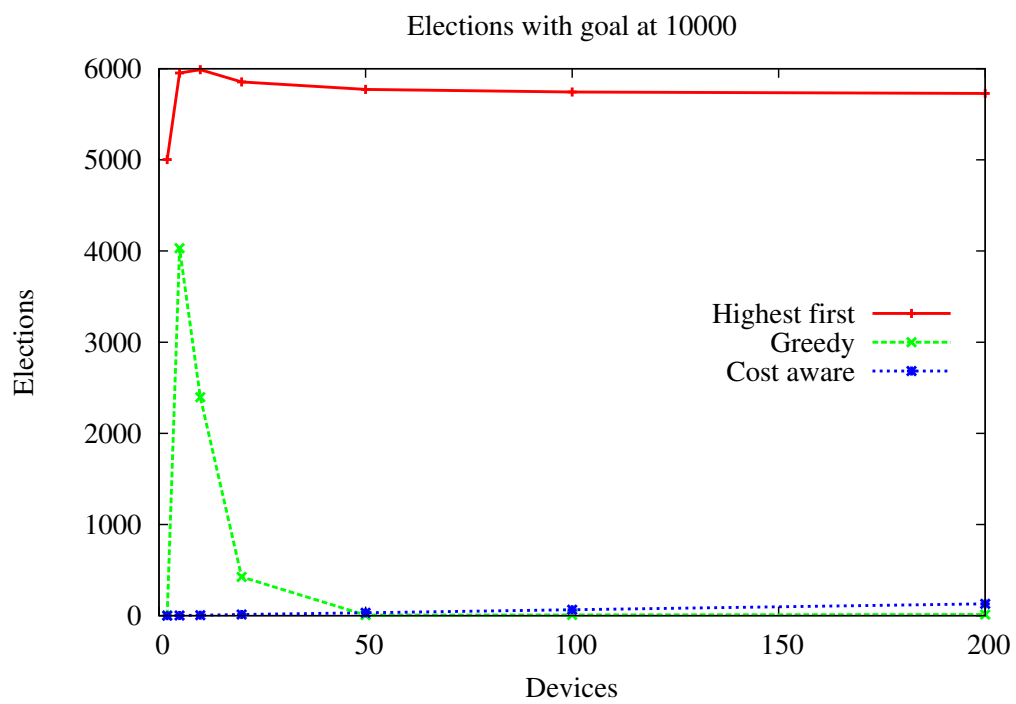
Figure 7.44: Number of elections as a function of the number of devices.

Chapter 8

Distributed Femto-Databases

Not all devices can use the TV bands by themselves, if not provided with a direct connection to the remote spectrum database, and able to provide the required information for the query. Thus, the availability of the channel occupation information is of paramount importance for each device.

We hereby study how to increase the spatial and temporal availability of this information, by caching valid queries and replies of the database in the devices. Thus, they can be seen as small spectrum database, which we call Femto-Databases. The benefits are a reduced latency for the Slave devices to have the information, and an increased availability due to a multihop mechanism, able to reach Master devices even if not in direct contact with the Slave.

8.1   The PAWS protocol

In this Section we briefly present PAWS, highlighting the part of the query from the devices to the remote spectrum database. We note that a deep discussion of the protocol is outside the scope of this work, and we refer the interested reader to [60], and to RFC 6953.

All the messages exchanged in the PAWS protocol are in the JSON format. Particularly, we focus on two of them:

- `AVAILABLE_SPECTRUM_REQ`: with this message a Master device asks for the channel list given its location. Otherwise, the message is sent from a Slave device to a Master, to relay it to the remote spectrum database.

- `AVAILABLE_SPECTRUM_RESP`: with this message, the database replies to the Master device with the list of available channels. If the original

query was made on behalf of a Slave device, the Master will eventually forward it.

In complex environments, in which there might be several different schedules for the spectrum band, the `AVAILABLE_SPECTRUM_RESP` message might grow in size, up to several KBs.

Actual regulations do not say how the `AVAILABLE_SPECTRUM_RESP` message should be treated by the Master device, and thus the information is destroyed after the successful transmission to the Slave device.

8.2   Proposal

In this Section we detail our proposal to store the `AVAILABLE_SPECTRUM_RESP` messages by Master devices, and the benefits of multihop to provide a higher probability for Slave devices to successfully reach a Master.

8.2.1   Caching

The first part of our proposal is the `AVAILABLE_SPECTRUM_RESP` messages caching mechanism, to make Master devices able to act as small local database, named Femto-Databases. Based on each message residual time for each spectrum schedule, any Master device i can choose whether to store the `AVAILABLE_SPECTRUM_RESP` or not. The main difference between using the caching mechanism or not arises when a `AVAILABLE_SPECTRUM_REQ` message arrives to a Master device from a Slave device. Upon arrival, if the Master device is using the caching mechanism, it checks for an already valid `AVAILABLE_SPECTRUM_RESP` in its internal database. If it has a valid reply that satisfies the Slave device, then it builds a `AVAILABLE_SPECTRUM_RESP` with the stored information in it, and answers to the Slave device. If the Master device does not have a valid reply, or if it does not use the caching mechanism, then it should query the remote spectrum database with a `AVAILABLE_SPECTRUM_REQ` message. According to the actual regulations, the device that receives a `AVAILABLE_SPECTRUM_REQ` can only drop the message if it is a Slave device, or forward it to query the remote spectrum database if it is a Master device. It is important to note that our solutions is completely transparent with respect to the PAWS protocol and to the following regulations, since no additional messages are involved in the process.

It is evident that using our approach less `AVAILABLE_SPECTRUM_REQ` messages are exchanged, and thus the cellular network is less used, while also the latency of Slaves' queries is improved. Detailed performance evaluation of the proposed framework are presented in Section 8.4.

Since it might be possible that the Master device does not have a previously cached query for the exact same position of the current Slave device, we discuss here how to choose the answer to give back.

As we already stated before, each query has a temporal validity and a spatial validity. Clearly, a longer remaining validity of the message means a higher probability to use it in the future. Looking instead at the spatial validity, there is a tradeoff. If a Master device already has a query made in a position really near to the actual Slave position, then clearly that is a good reply. However, it might not always be possible for Master devices to have queries made in the past near to the actual one. To evaluate this behaviour, any Master device would reply to the Slave if it has a cached query made within a distance of maximum α from the actual position of the Slave device.

8.2.2 Multihop

In this Section we detail how the multihop mechanism is performed, and the issues related to it. Multihop message relaying is performed while taking into account a maximum number of hop at which the message can travel, to reduce unnecessary relaying. This is a classical solution in literature, however in ad hoc networks it could generate a lot of collisions, due to the problem of the Broadcast Storm [84]. The Broadcast Storm is known as the impossibility for devices to communicate due to the excessive relay of broadcast messages. This problem happens when a huge number of devices transmit broadcast packets, with the result of a high number of collisions and thus poor communication [84]. In literature it is possible to find a plethora of proposals that tackle the problem, particularly for vehicular ad hoc networks [34] [92], and we direct the interested reader to them.

For the proposed Femto-Databases approach we estimate the best relay i for a `AVAILABLE_SPECTRUM_REQ` message received by device j with the following Equation:

$$LB_i^j = \frac{|dB_i^{max}| - |dB_i^j|}{|dB_i^{max}|} \tag{8.1}$$

where dB_i^j is the power at which the message is received, and dB_i^{max} is the maximum sensitivity of the radio of device i. Basically $LB_i^j \in [0, 1]$, where a value close to 1 means a signal received at a high power, while a value close to 0 correspond to a poorly received message. Based on that, each device is then able to modify its content window, to favor far devices opposed to near devices, to push the message farther. To do that, each device i modifies its contention window CW_i used to send the message as follows:

$$CW_i^j = \lceil CW_{min} + (CW_{max} - CW_{min}) \cdot LB_i^j \rceil \tag{8.2}$$

where CW_{max} and CW_{min} are respectively the maximum contention window and the minimum contention window of device i. Using Equation 8.2, CW_i is bounded in the $[CW_{min}, CW_{max}]$ interval, making devices that received the message at a lower power able to react faster than devices that received the message at a higher power. We note that this does not always mean that the farthest node will be selected, due to fading and shadowing effects, but it gives a simple estimation that is sufficient for our purposes. Finally, if a device hears the same message that is re-transmitted by someone else, or if it receives a message that it already sent in the past, it drops the message and does not transmit it anymore. In that way, we limit the number of re-transmissions and mitigate the broadcast storm effect. Again, we note that this solution does not guarantee that only one message will be re-transmitted, but it limits the number of re-transmissions.

8.3   Analytical model

We want to study the number of queries done to the database as a function of the number and the speed of the nodes. We define $P_r(r)$ similarly to [80].

Given x and y with Gaussian distribution with 0 mean, and given σ_1 and σ_2 the two standard deviations, we define $d_x = x_2 - x_1$ and $d_y = y_2 - y_1$, characterized by standard deviation $\sigma_1\sqrt{2}$ and $\sigma_2\sqrt{2}$.

We now define the probability density function (pdf) on $r = \sqrt{d_x^2 + d_y^2}$ as follows:

$$P_r(r) = \frac{r}{2 \cdot \sigma_1 \cdot \sigma_2} exp\left(-\frac{r^2}{8} \cdot (\sigma_1^{-2} + \sigma_2^{-2}) \right) \cdot I_0 \cdot \left[\frac{r^2}{8} \cdot (\sigma_1^2 - \sigma_2^2) \right] \quad (8.3)$$

where I_0 is the modified Bessel function. For $\sigma_1 = \sigma_2 = \sigma$, we have

$$P_r(r) = \frac{r}{2 \cdot \sigma^2} \cdot e^{-\frac{r^2}{4 \cdot \sigma^2}} \quad (8.4)$$

We now define P_1 as the probability of having a 1 hop connection, defined as:

$$P_1 = P_r(1 - hop) = P_r\{r \le R\} = \int_0^R P_r(r)dr = 1 - e^{-\frac{R^2}{4 \cdot \sigma^2}} \quad (8.5)$$

We can now define the probability P_m that a Slave device has a Master device at 1 hop, which is defined as:

$$P_m = \alpha \cdot P_1 \quad (8.6)$$

where alpha is the rate of Master devices over Slave devices.
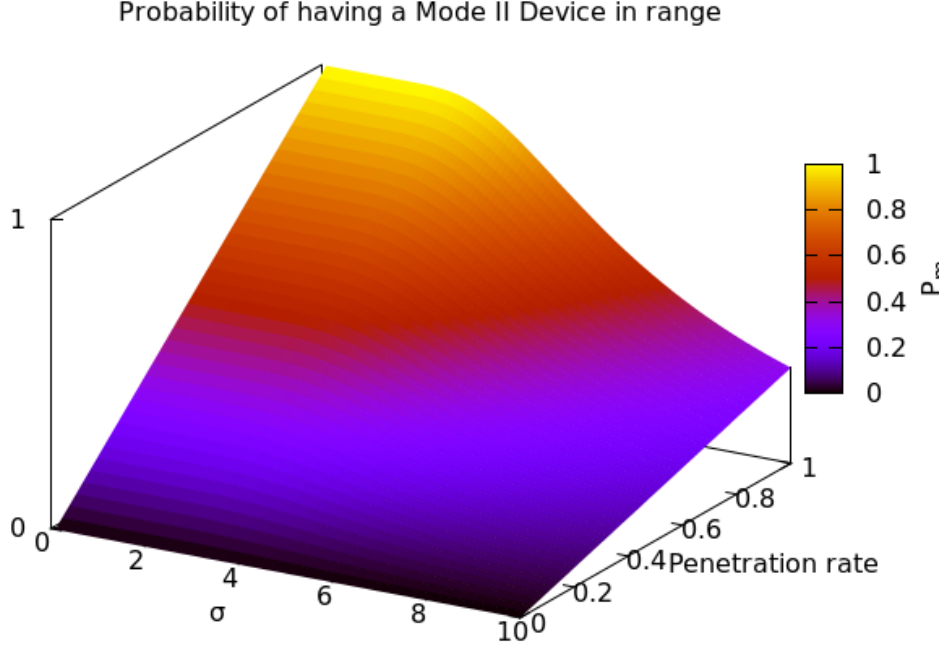
Figure 8.1: Probability of having a Mode II Device in range, P_m, for a range R equal to 150 meters.

Figure 8.1 shows the probability of having a Mode II device in range at 1 hop, which is proportional to the penetration rate α, and to the parameter σ of the Gaussian distribution.

8.3.1 Speed

Given P_m, we now derive the total number of query during a second, which gives a metric of the network load.

Given the speed v, we now want to define the probability of making a query in a second. Obviously, if $v = 0$, the device will make only a query till the end of the validity. Otherwise, its number of queries will increase as its speed v increases. We define d_{MAX} as the maximum distance between two different queries, and x_q and y_q as the coordinates of the last query. Thus, $dx = x + x_q$ and $dy = y + y_q$, and $d = \sqrt{dx^2 + dy^2}$. We define the speed of vehicle i as v_i, and we derive the probability P_q^i, which is the binary probability of making a query, given the speed v_i. Intuitively, $P_q^i = 1$ if

$v + d > d_{MAX}$, and is 0 otherwise. For ease of notation, we define $P_q^i = 1$ as P_{q1}^i, and $P_q^i = 0$ as P_{q0}^i. We are now ready to define P_q as the probability of making a query, which is defined as:

$$P_q = P_{q0} = \{d \geq d_{MAX} \ OR \ v + d < d_{MAX}\} = 0 \tag{8.7}$$

$$P_q = P_{q1} = \{d \geq d_{MAX} \ OR \ v + d > d_{MAX}\} = 1 \tag{8.8}$$

This only states that if, during a second, vehicle i does not exceed d_{MAX}, it does not make any query, which is P_{q0}^i. Inversely, P_{q1}^i is when we exceed d_{MAX} in the next second at the current speed. We now derive the number of queries made by vehicle i during a second, which is given by:

$$N_q^i = \frac{v_i}{d_{MAX}} \tag{8.9}$$

$$p_i = \frac{P_{q1}^i}{P_{q0}^i} = \begin{cases} 1, & \text{if } v \geq d_{MAX} \\ \frac{v}{d_{MAX}}, & \text{otherwise} \end{cases} \tag{8.10}$$

The probability p_i indicates the probability for vehicle i of making a query during a second, given its speed v_i. To estimate the overhead, which is the load on the existing infrastructure to allow Mode II devices to make query to the database, we define N_q as:

$$N_q = P_m \cdot \sum_{i=0}^{N-1} N_q^i \tag{8.11}$$

If we suppose all speeds equal, $v_i = v$, then all the terms N_q^i are equal, and N_q could be written as:

$$N_q = N \cdot (P_m \cdot N_q^i) \tag{8.12}$$

The throughput T is then easily derived as:

$$T = N_q \cdot s \tag{8.13}$$

where s is the size of a query to the database. In Figure 8.3.1 we show the communication overhead as the number and the speed of the vehicles increase. It is clear that if the speed increase, also the communication overhead increase, because N_q^i becomes bigger.

8.4   Performance Evaluation

In this Section we evaluate our proposed approach, based on different metrics. We extended the Omnet++ discrete event simulator, by implementing the
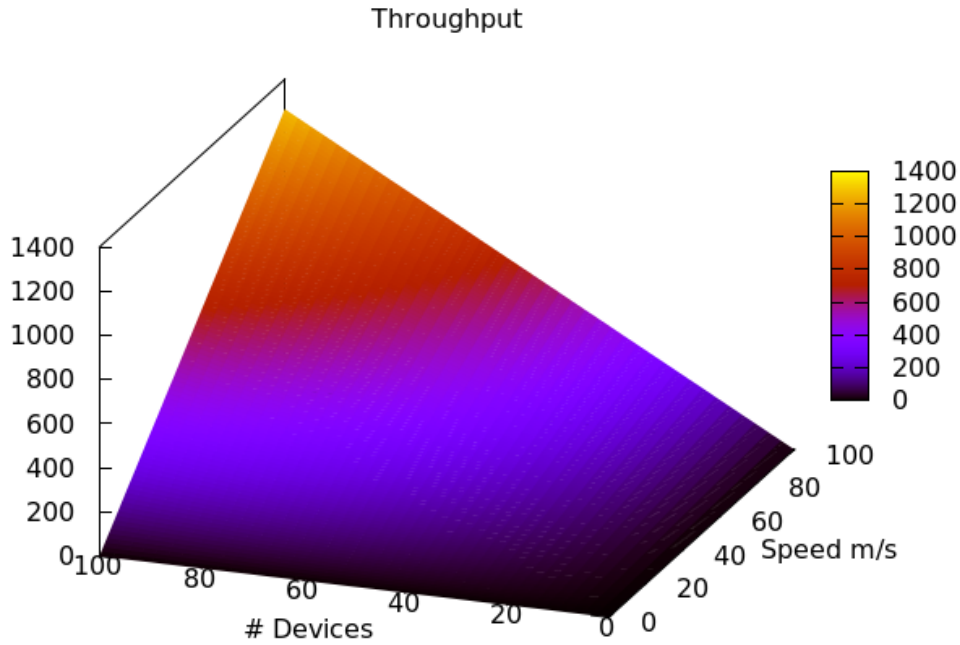
Figure 8.2: Overhead

PAWS protocol and the remote spectrum database. We then built a custom scenario of 800x800 meters with a varying number of nodes.

To make the analysis deeper, we evaluate four different algorithms, which we describe as follows:

- **Basic**: no caching and no multihop mechanism are involved. Practically speaking, it is the current algorithm envisioned by regulators, without Femto-Databases.

- **FD-M**: no caching is performed by Master devices, but the multihop mechanism is active to enlarge the Masters availability to Slaves.

- **FD-C**: no multihop is performed by Master devices, but the caching mechanism is active.

- **FD**: both the caching as well as the multihop mechanism are active, and devices can benefit from the full potential of our proposal.

To evaluate the aforementioned algorithms, we study three different metrics:

- **Overhead**: defined as the amount of communication involved to send the `AVAILABLE_SPECTRUM_REQ` and the `AVAILABLE_SPECTRUM_RESP` messages.

- **Stimulus Satisfaction**: defined as the ability for the algorithm to satisfy the stimulus of the Slave devices, defined in Section 8.4.2.

- **Round Trip Latency**: defined as the average time needed for a Slave device to get a `AVAILABLE_SPECTRUM_RESP` from a queried Master device.

8.4.1 Overhead
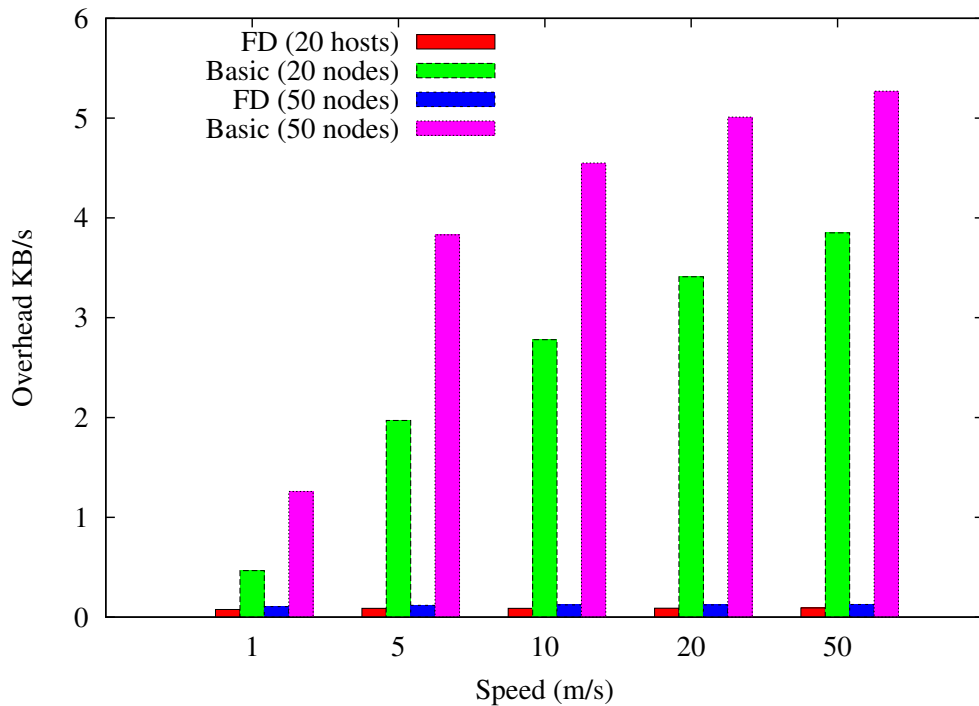
Figure 8.3: The overhead per single device on the cellular connection while varying the speed of the devices.

In Figure 8.3 and Figure 8.4 we plot the overhead on the cellular connection to make queries to the spectrum database by Master devices, while
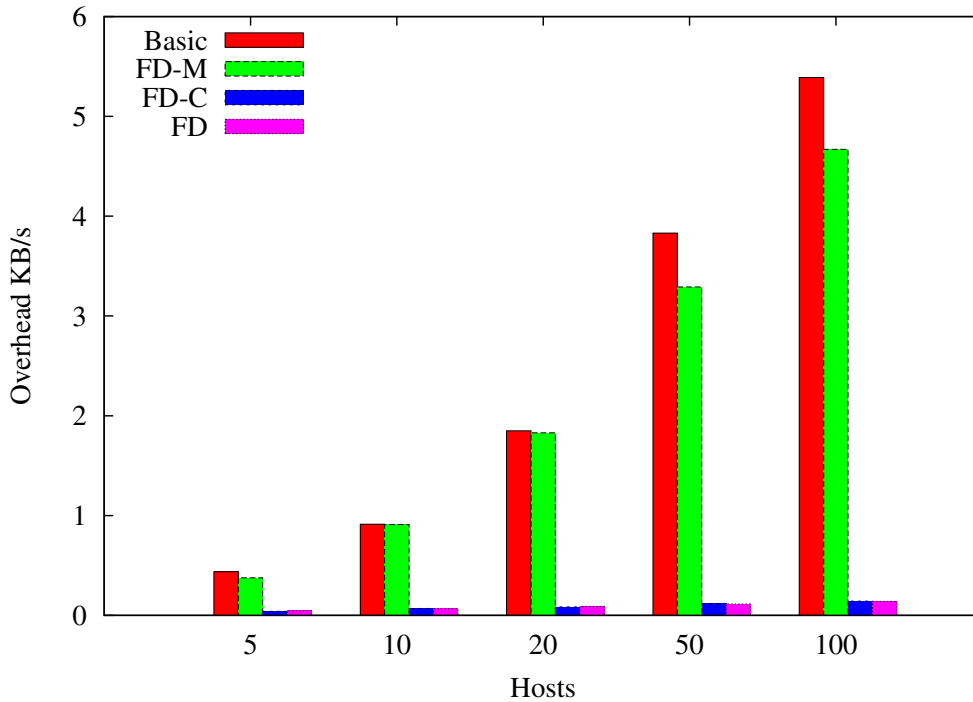
Figure 8.4: The overhead per single device on the cellular connection while varying the number of the devices.

varying the movement speed and the number of devices. What is immediately straightforward to note is that the FD approach provides a much lower number of queries compared to the case when no caching is performed, which results in a lower overhead on the cellular network. This is due to the fact that Master devices act as database themselves, answering to Slave devices if they already have a reply from the remote database suitable for the Slave needs, without using the cellular connection. Clearly, increasing the number of devices also increase the overhead, since a higher number of queries are made which eventually results in collisions and thus re-transmissions.

A similar trend is experienced with a variation in the number of devices in Figure 8.4, where we plot the overhead on the cellular connection used to communicate with the database, for two different speeds. As before, also in this scenario the FD approach provides a lower number of queries to the database, thus resulting in a better spectrum utilization and a lower load on the remote database.

Finally, in Figure 8.5 we vary the α parameter, with a fixed number of host set to 20. Here, it is possible to see the great enhancement that both
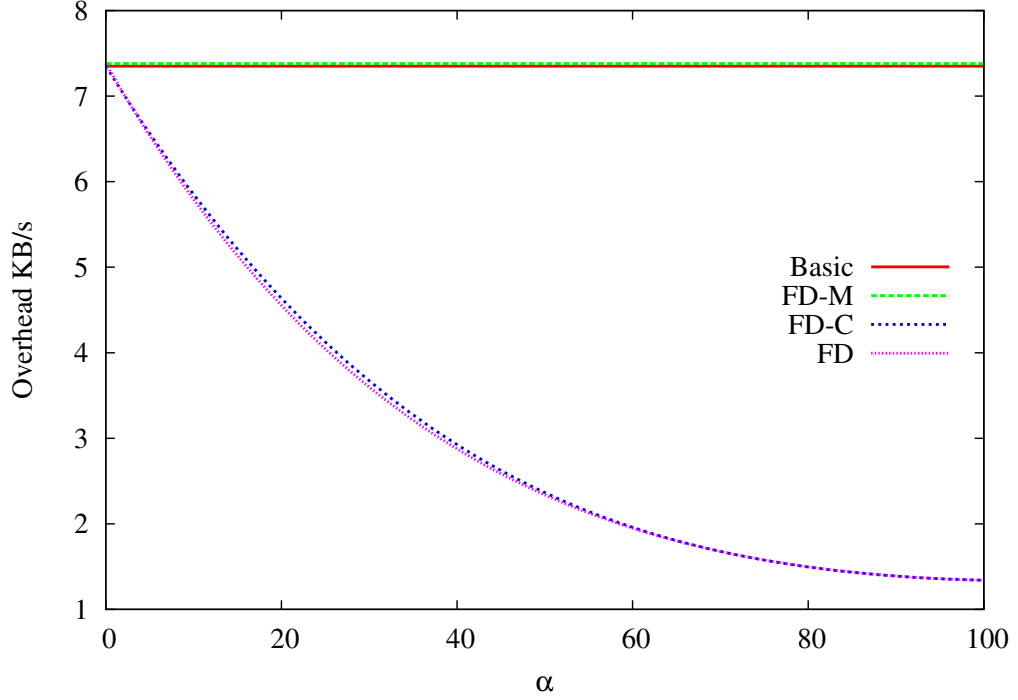
Figure 8.5: The overhead per single device on the cellular connection while varying the α parameter.

FD and FD-C introduce. By increasing the α parameter, we are implicitly increasing the probability that a Master device has a valid reply for the Slave device, and thus avoid to query the remote spectrum database. It is worth to note that the FD-C and FD algorithms performs almost the same, which means that the biggest benefit for the overhead metric comes from the caching rather than the multihop.

8.4.2   Stimulus satisfaction

In this Section we evaluate the satisfaction of stimuli of Slave devices. We define the stimulus SS as the ratio between the satisfied query over the total number of needed Master queries, that is, $SS = \frac{S_i}{N_i}$, where S_i is the total number of queries for which the Slave device got a response from a Master device, over N_i, which is the total number of queries made by Slave device i.

As we can see from Figure 8.6, the Basic algorithm produces the lowest performance, achieving a lower SS value as the number of devices increase. This is partially mitigated by FD-C, which is able to reply faster to the Slave device, and thus achieve a higher probability of delivering the message to

the Slave device. `FD-M` achieves better performances, leveraging the spatial proximity of devices in order to eventually reach a Master device. As before, `FD` is the algorithm that performs best compared to others, as it combines lower latency thanks to the caching mechanism, as well as a wider availability of Master devices thanks to the multihop. It can be seen that all the algorithms perform more or less the same when the number of devices is high (i.e. > 70). This happens because as the number of devices increase, also the probability of having a Master device at one hop is raised, and thus the benefits offered by the multihop mechanism are not tangible. However, `FD` can provide a higher availability of Master devices to Slaves, thanks to the multihop mechanism, which results in a higher Slaves satisfaction even on sparse scenarios.
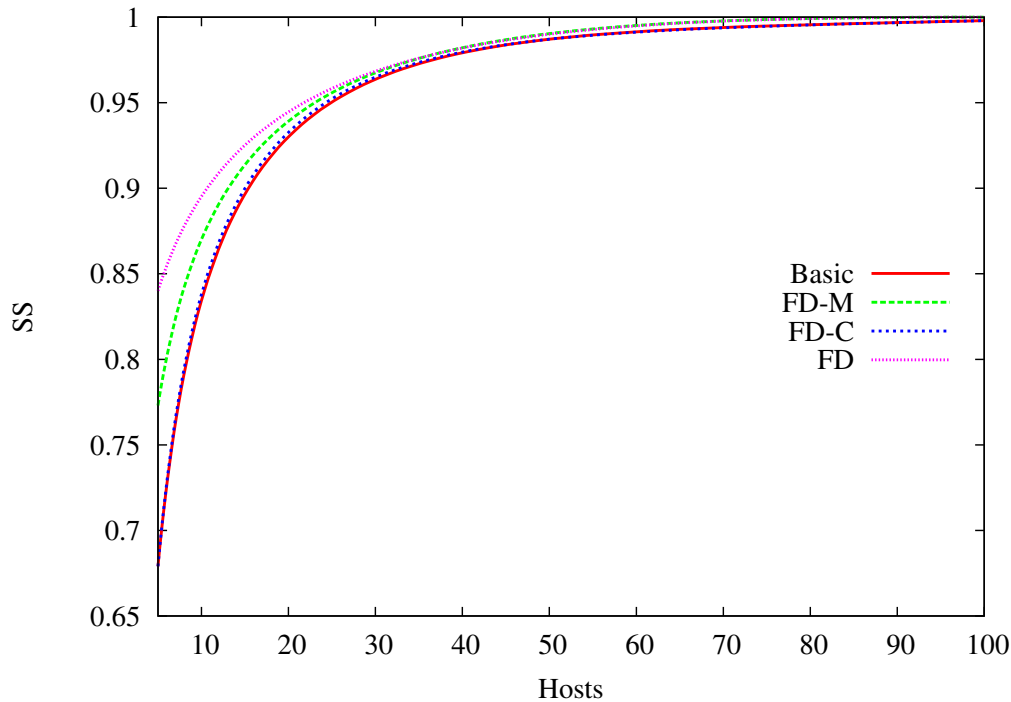
Figure 8.6: The Stimulus Satisfaction while varying the number of devices.

8.4.3 Round Trip Latency

Another aspect related to the Master/Slave queries to the DB is about the round trip latency. When a Slave device makes a query, it needs the answer from the DB as fast as possible, in order to maximize the utilization of the
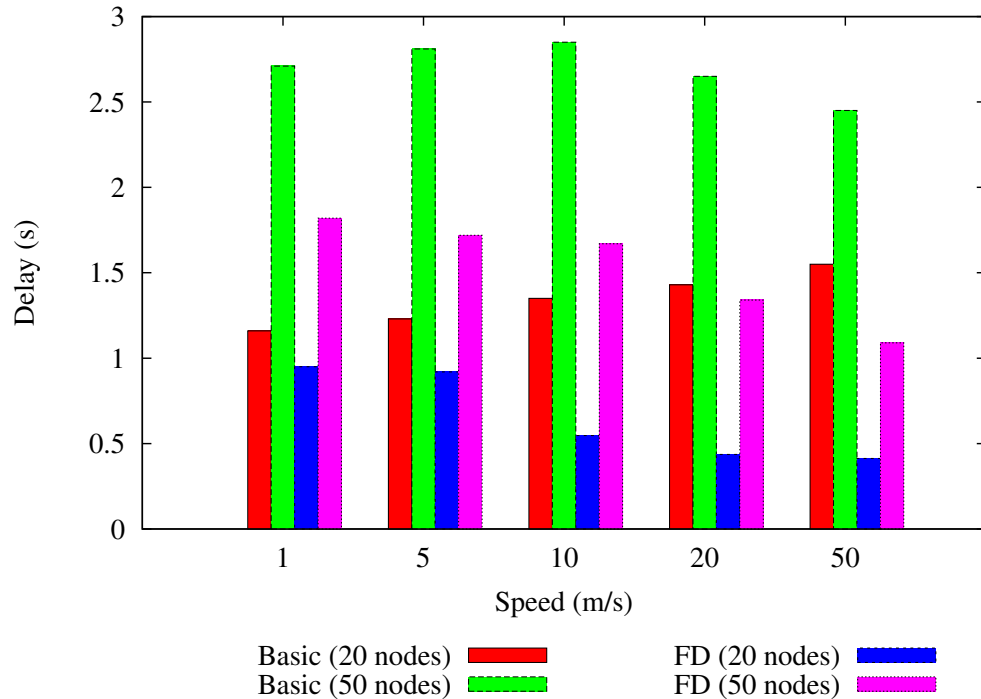
Figure 8.7: The latency while varying the α parameter.

available channel list. Using `FD`, the answer may come directly from the Master device, thus reducing the delay involved in cellular communications and possible bottlenecks formed at the remote database. In Figure 8.7 we plot the average latency to a Slave device after issuing the `AVAILABLE_SPECTRUM_REQ` message. Using a low number of nodes (i.e. 20 nodes), the benefits of the `FD` algorithm are not tangible, even if it improves the overall result. What is instead evident is the behavior with 50 nodes, where the `Basic` algorithm experiences a higher latency as the average speed increases, while `FD` is able to reduce it. This happens because with a higher speed, Master devices are able to build a larger local database, and thus it is more probable that they can serve a Slave device without asking the remote spectrum database. For the `Basic` algorithm, instead, a higher speed only means a higher number of queries to the database, and consequently a higher probability of collisions, which results in larger latencies due to increased overhead on the cellular network. We note that the high delays on sparse scenarios are due to the fact that there are few Master devices, and thus it is harder for Slaves to find one which can relay the query.

In Figure 8.8 we show the latency while varying the α parameter, with
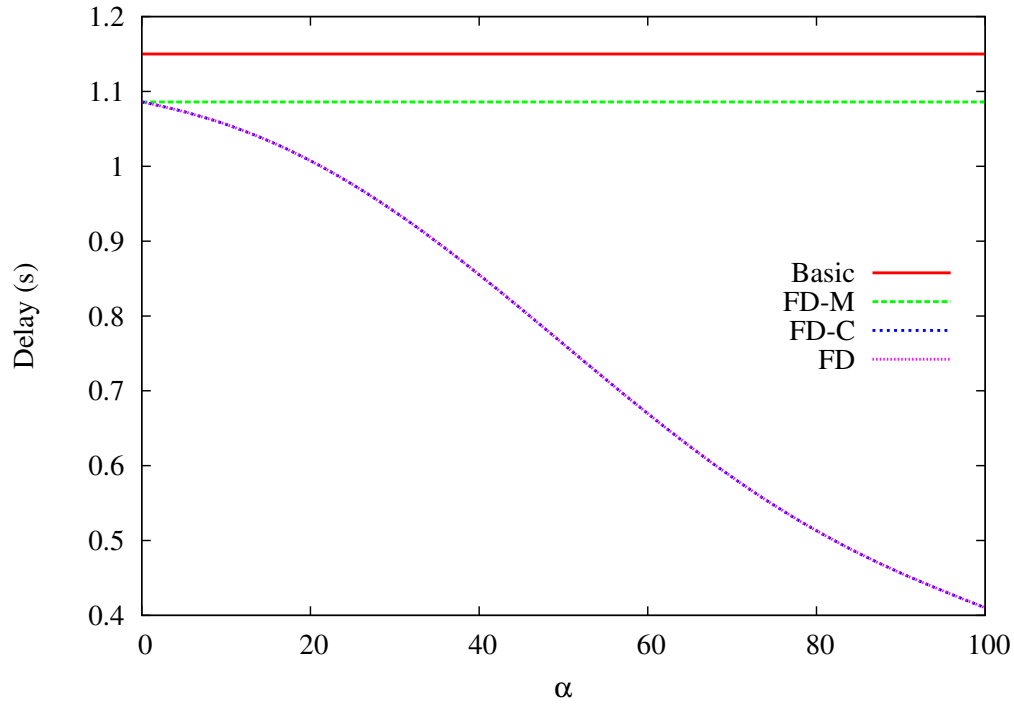
Figure 8.8: The average latency time by a Master device to a Slave query.

a fixed number of host of 20. Clearly, the `Basic` and the `FD-M` algorithms perform the worst, since they don't perform any caching and thus always have to query the remote spectrum database. It is important to note that the `FD-M` is slightly better than the `Basic` algorithm, since a greater number of Slave devices could be served by a single Master device, and thus the Slave device might find a Master device that is able to relay their query to the remote spectrum database earlier.

Chapter 9

Cognitive Vehicular Communications

A particular case in which cognitive networks have been studied is the context of Vehicular Ad Hoc Networks (VANETs) [76]. Here, vehicles exchange information to know in advance particular road conditions from other vehicles, or infotainment packets. The IEEE standardized the IEEE 802.11p standard, along with the IEEE 1609.4 which enables multi-channel operations. In [33], we have taken into account safety messages that are sent between cars, according to the IEEE 802.11p and IEEE 1609.4 protocols.

The IEEE 802.11p and IEEE 1609.4 protocols define that vehicles have to switch between a common control channel (CCH) and one of the available service channels (SCH) every 50 ms. This severely limits the time guarantees to deliver safety messages, which might be delayed up to 50 ms when generated at the end of the CCH period. To be more precise, two problems arise [33]:

- **Synchronous Collisions Problem**: since vehicles continuously switch between CCH and one of the SCH, it might happen that at the beginning of the CCH more than one client has to send a safety messages, thus generating multiple collisions.

- **Bandwidth Shortage Problem**: by switching between CCH and SCH, every 50 ms part of the spectrum remains not used.

Since most of the work tackle only one problem at a time, we developed a framework to leverage the cognitive capabilities of the devices, and address both issues at the same time. In addition, both problems are correlated between each other, as a better spectrum utilization would lead to less collisions, and less collision would reduce the need of additional spectrum. To this end,

in [33] we proposed a Dynamic Spectrum and Contention Control Framework (DySCO). DySCO proceeds in two steps: at first, it determines the optimal size of the contention window (CW), to keep the collision probability under a threshold. At second, it determines the minimum PHY bandwidth to deliver all the messages on time (i.e. before the end of the CCH interval).

9.1   Model

9.1.1   Network Architecture

The network architecture we consider is depicted in Figure 9.1. It can be seen that two different kind of nodes are present: moving vehicles, and road side units (RSU) . Each vehicle is capable to communicate with any other vehicles in its transmitting range, and possibly with near RSU, which form a fixed infrastructure that covers the entire scenario taken into account.
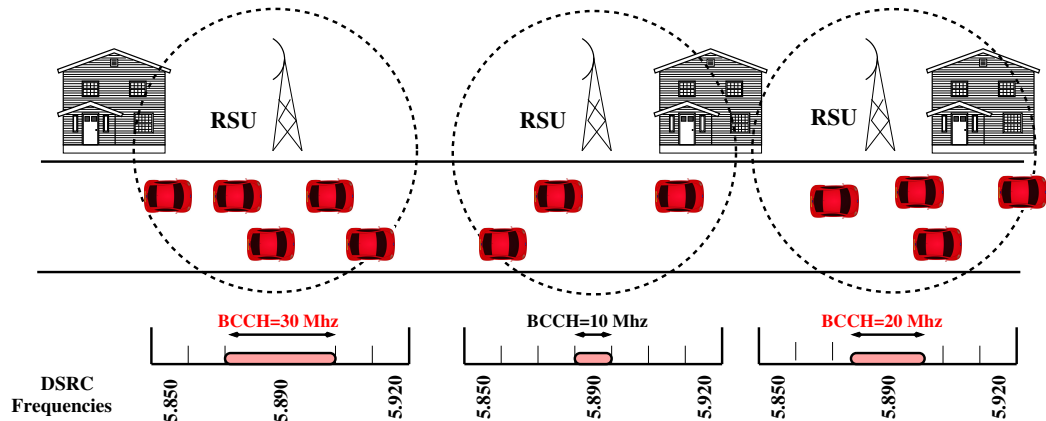
Figure 9.1: The network architecture and channel model in use.

9.1.2   Network Traffic Model

We focus on safety messages, and we consider, without loss of generality, that each vehicle of the scenario will produce λ packets to be transmitted during each CCH interval. The content of each `SAFETY` message can be of any kind, and can include periodic information like the vehicle position, its speed, and anything required for the implementation of safety-related services. We also assume that no queuing mechanism is implemented at each client, and thus each message should be delivered in the CCH slot in which it is produced, or in the next CCH interval if produced during a SCH interval.

This assumption is reasonable, since it limits the sending of possibly outdated information. Moreover, we assume that each safety application has its own QoS requirements, defined as the minimum Packet Delivery Ratio (PDR) that must be offered by the network. We then define the ϵ parameter as:

$$\epsilon = 1 - \frac{\lambda_r}{\lambda} \tag{9.1}$$

which defines the maximum packet loss probability tolerated by the vehicular application. Both λ and λ_r are assumed fixed and known to the vehicles and to the RSUs of the scenario.

9.1.3 Channel Model

We assume that each device in the scenario has a Software Defined Radio (SDR), able to communicate according to the IEEE 802.11p network stack. Moreover, it also provides CR functionalities, that permits to tune the communication parameters depending on the scenario. As already stated, we assume that each device is able to reconfigure its CW, and the channel bandwidth.

In this Section, we investigate the performance of safety broadcast applications in VANETs through analytical and simulation results. To this aim, we use the system model described in Section 9.1, and we introduce new assumptions (detailed in Section 9.2) to make the analysis tractable Through the analytical model described below, we then characterize the impact of MAC/PHY parameters on the performance of safety-related broadcast applications (Section 9.2.1), and we derive important considerations that are used in the proposal of our DySCO framework (Section 9.3).

9.2 Analytical Model

We consider a system like the one depicted in Figure 9.1. To make our analysis more tractable, and without loss of generality, we consider a subsystem with 1 RSU and N vehicles. We also assume that all the vehicle in our simulated scenario are in the same transmitting range, and thus we abstract from the hidden node problem. Another assumption is that all the SAFETY messages are generated during the SCH interval, to be transmitted in the next CCH interval. Finally, every SAFETY message that fails to be delivered by the end of the CCH interval is discarded at the end, so no re-transmissions occur.

We model our framework using Markov Chains, following a similar analysis like [15]. The MAC backoff procedure using Markov Chains is shown

Table 9.1: Model Variables

N	Number of vehicles
B_i	i-th state of the Backoff process
W	Maximum MAC Contention Window (CW) Size
τ	Probability of transmission in a slot
p_i	Probability of having an idle slot
p_b	Probability of having a busy slot
p_s	Per-slot probability of successful transmission
p_c	Per-slot probability of MAC collision
p_{ps}	Per-packet probability of successful transmission
σ	PHY duration of an 802.11p slot
S	`SAFETY` packet payload
R_{CCH}	PHY Transmitting rate on CCH
B_{CCH}	PHY Bandwdith of the CCH
T_s	Average time of a successful transmission
T_c	Average time of a collision
T_{CCH}	Duration of the CCH interval

in Figure 9.2. Table 9.1 contains instead the list of symbols that are used through the analysis.

We define B_i as the i-th state of the Markov chain [1], and $P(B_i)$ as the stationary probability of being in the state B_i. When $i = 0$, B_0 corresponds to the case when the vehicle has completed the backoff, and is now allowed to use the wireless control channel. $\tau = P(B_0)$ represents similarly the probability for the current vehicle to transmit a `SAFETY` message on a given slot of the CCH time interval. It is then possible to derive τ as follows [15]:

$$\tau = P(B_0) = \frac{2}{W + 1} \tag{9.2}$$

Clearly Equation 9.2 models a saturated network scenario, but we can also derive our special case study, since we assume that all `SAFETY` packets are generated during the SCH interval, and then continuously transmitted during the following CCH interval. In addition, we neglect the problem of "consecutive freeze process" that might occur once a wireless node keeps accessing the channel without deferring because of a zero-backoff procedure.

We now introduce the concept of virtual slot, defined as a step unit of the Markov chain, as proposed in [15]. Each virtual slot has a time duration that

---

[1]B_i corresponds to the backoff state with Contention Window (CW) size equal to i.
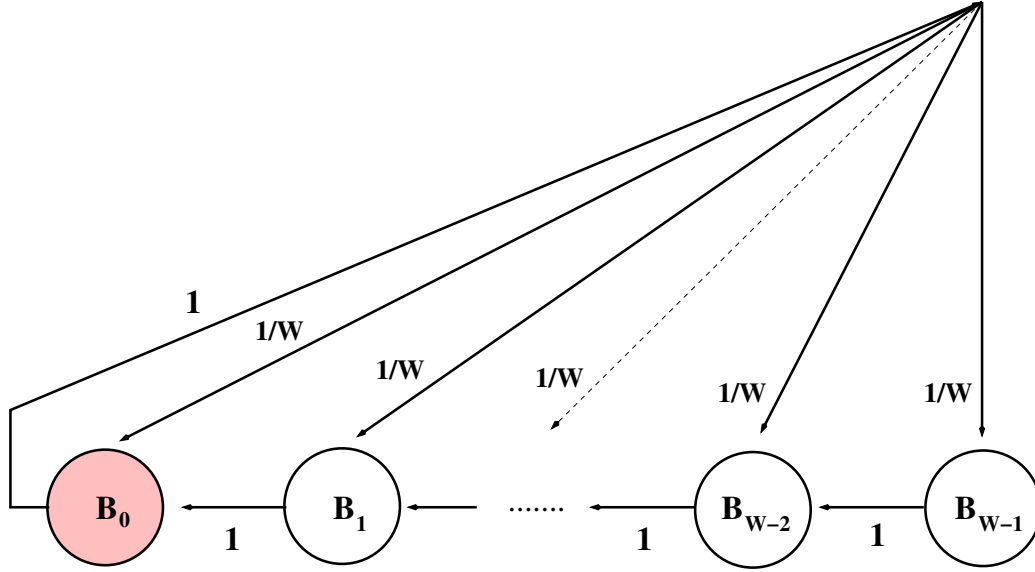
Figure 9.2: The Markov chain used to model the broadcast communication performed by each vehicle of the scenario.

depends on the result of the sensing of the channel, if it is idle or busy. We then define p_i, which denotes the probability of having an idle slot, and also p_b, which is instead the probability of having a busy slot. For the latter, p_s is defined as the probability to have a slot occupied by a successful transmission, and p_c is the probability that a collision happened. It is straightforward to note that all the probabilities just defined can be easily derived from τ as follows:

$$p_i = (1 - \tau)^N \tag{9.3}$$
$$p_b = 1 - p_i \tag{9.4}$$
$$p_s = N \cdot \tau \cdot (1 - \tau)^{N-1} \tag{9.5}$$
$$p_c = 1 - p_i - p_s \tag{9.6}$$

Since we want to investigate the performance of safety-related broadcast communication, we analyze our framework in terms of Packet Delivery Ratio (PDR). From the model just described, it is easy to compute the per-vehicle PDR as follows:

$$PDR = \frac{\text{Num\_Pkts\_Successfully\_Transmitted}}{\text{Num\_Pkts\_Transmitted}} = \frac{\kappa \cdot p_{sp}}{\lambda} \tag{9.7}$$

A `SAFETY` packet is considered as successfully transmitted if and only if all the neighboring vehicles are able to receive it without interference. Basically,

the packet is received if and only if no collisions happened. In Equation 9.7, p_{ps} denotes the probability of successfully transmitting a `SAFETY` message. By assuming the independence among consecutive transmission attempts, the probability p_{ps} is derived from the probability of having a successful transmission in a virtual slot, knowing that the given slot is busy:

$$p_{ps} = \frac{p_s}{p_b} = \frac{N \cdot \tau \cdot (1 - \tau)^{N-1}}{1 - ((1 - \tau)^N)} \qquad (9.8)$$

The term κ in Equation 9.7 represents the average number of `SAFETY` packets that are transmitted during the CCH slot, accounting for the average MAC access delay required to transmit each packet (which we define as $E[T_{access}]$ in the following), and the length of the CCH interval (T_{CCH}), defined by the IEEE 1609.4 standard. Assuming again independence among consecutive transmissions, it is possible to reasonably estimate κ as follows:

$$\kappa = min\left(\lambda, \frac{E[T_{access}]}{T_{cch}}\right) \qquad (9.9)$$

Equation 9.9 models the fact that the maximum number of CCH accesses for each vehicle depends primarily on the time duration of each access compared to T_{CCH}, and certainly it cannot be greater than the traffic request λ.

The equation for $E[T_{access}]$ is derived as follows. We note that we do not account for propagation losses in our analysis. $E[T_{access}]$ is expressed as a function of the average duration of the backoff delay (i.e. $E[BF]$), of the duration of each transmission (T_s) and of the average duration of a virtual slot (i.e. $E[T_{slot}]$):

$$E[T_{access}] = E[BF] \cdot E[T_{slot}] + T_s = \frac{W}{2} \cdot E[T_{slot}] + T_s \qquad (9.10)$$

The average duration of the virtual slot depends on whether the slot is idle or not. Basically, if it is occupied by a transmission or by a collision:

$$E[T_{slot}] = p_i \cdot \sigma + T_s \cdot p_s + T_c \cdot p_c \qquad (9.11)$$

where σ is the duration of an empty slot. $T_{success}$ is instead the time required for a successful transmission, and correspondingly T_{coll} is the average time of a collision event. Based on the packet size S, the transmission time of the preamble (T_{PRE}) and the data-rate used (R_{CCH}) on the control channel, and excluding the cases of consecutive transmissions in the same logic slot due to the assumption of a single (synchronous) collision domain, the exact values

of T_s and T_c can be derived as:

$$T_s \;\; = \;\; DIFS + \sigma + \frac{S}{R_{CCH}} + T_{PRE} \qquad (9.12)$$

$$T_c \;\; = \;\; EIFS + \sigma + \frac{S}{R_{CCH}} + T_{PRE} \qquad (9.13)$$
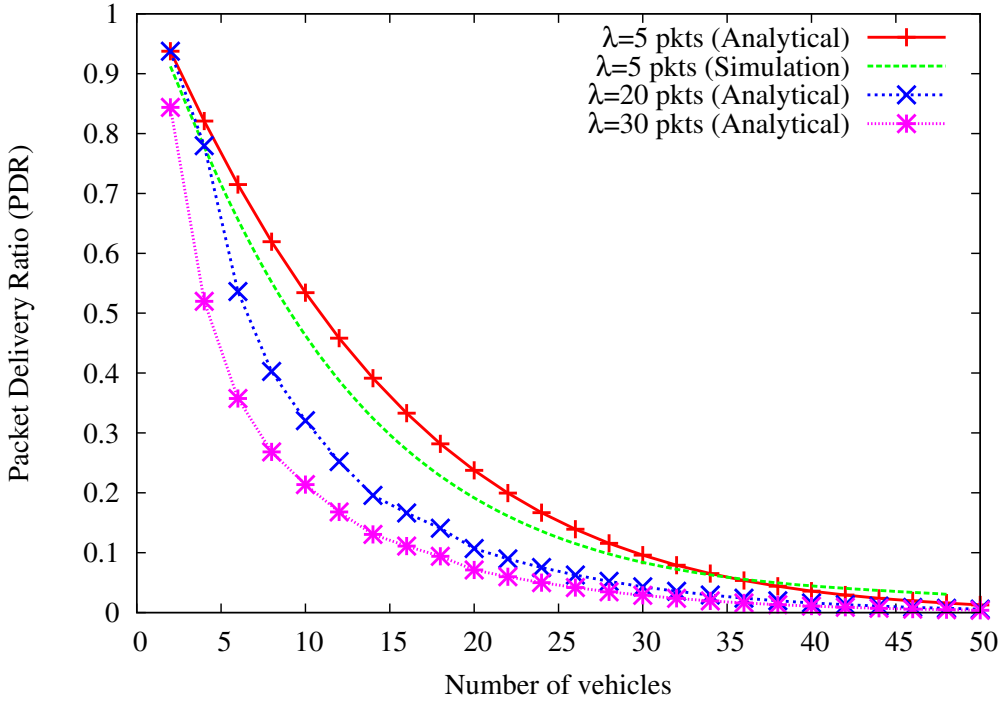
Figure 9.3: The PDR index as a function of the number of vehicles, and for different values of λ.

In Figure 9.3 we show the PDR computed through Equation 9.7, as a function of the total number of vehicles on the scenario. Here, we also take into account different traffic loads by varying the λ parameter. For $\lambda = 5$, we also compare the analytical and simulation results, obtained by configuring the NS-2 model of the IEEE 1609.4 protocol [49]. We consider a configuration with $S = 200 bytes$, $R = 3$ Mb/s, $W = 16$. Figure 9.3 shows that the PDR metric decreases significantly when increasing the number of vehicles and the traffic load λ. As demonstrated in the analysis of Section 9.2, packet losses are produced by (i) MAC collisions and by (ii) un-transmitted packets events (i.e. $\kappa < \lambda$) caused by the end of the CCH interval. Moreover, Figure 9.3 confirms the effectiveness of our analysis, since the simulation results closely match closely the analytical results.
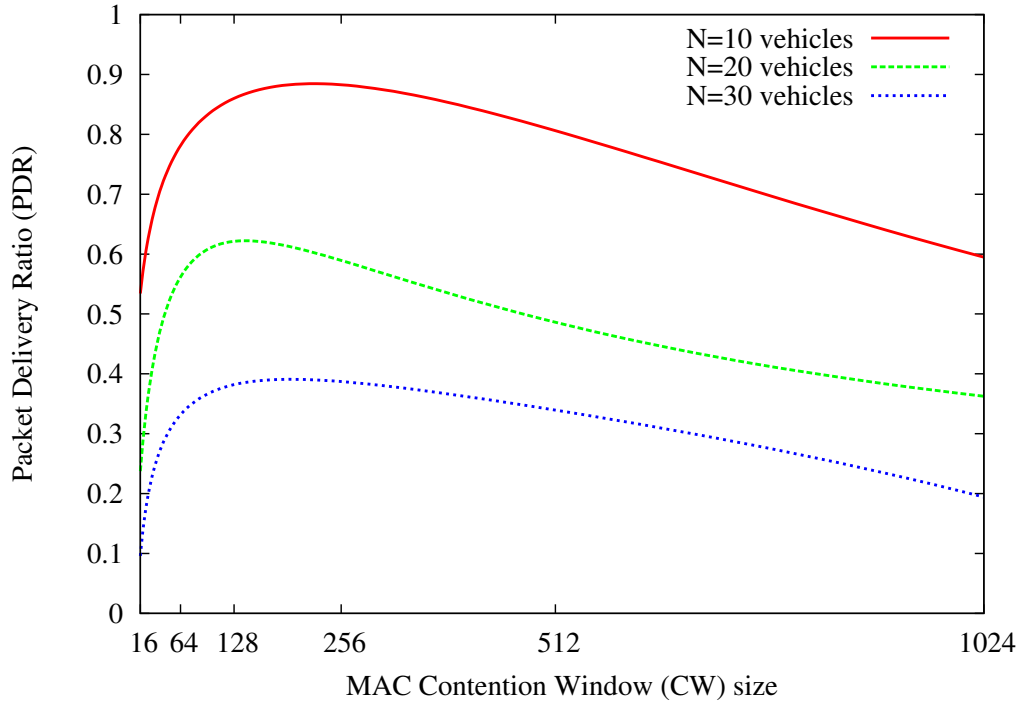
Figure 9.4: The PDR as a function of MAC Contention Window (CW).

9.2.1   Parameter Characterization

In Figure 9.4, we show the PDR for different values of the MAC Contention Window (CW), comprised between a minimum (equal to 16), and a maximum value (equal to 1024). Moreover, in the same Figure we show three curves for different configurations of N, i.e. the number of vehicles in the network. For each value of N, Figure 9.4 confirms the existence of an optimal value of CW maximizing the per-vehicle PDR metric. This is in accordance with previous results on the performance of MAC 802.11 protocol. However, Figure 9.4 reveals also the existence of a performance trade-off that is intrinsically related to the operations of IEEE 1609.4-based multi-channel VANETs. If the CW size is below the optimal value, then synchronous MAC collisions might occur among vehicles selecting the same slot, thus causing a performance loss in terms of per-vehicle PDR. On the opposite, if the CW size exceeds the optimal value, then packet losses might occur at the end of the CCH interval, since some of the λ packets might not have chance to be transmitted before the expiration of the CCH interval. This intuition is confirmed by Figure 9.5, where we depict the MAC Collision risk on the x1y1 axes (computed through Equation 9.3), as a function of the CW size, while
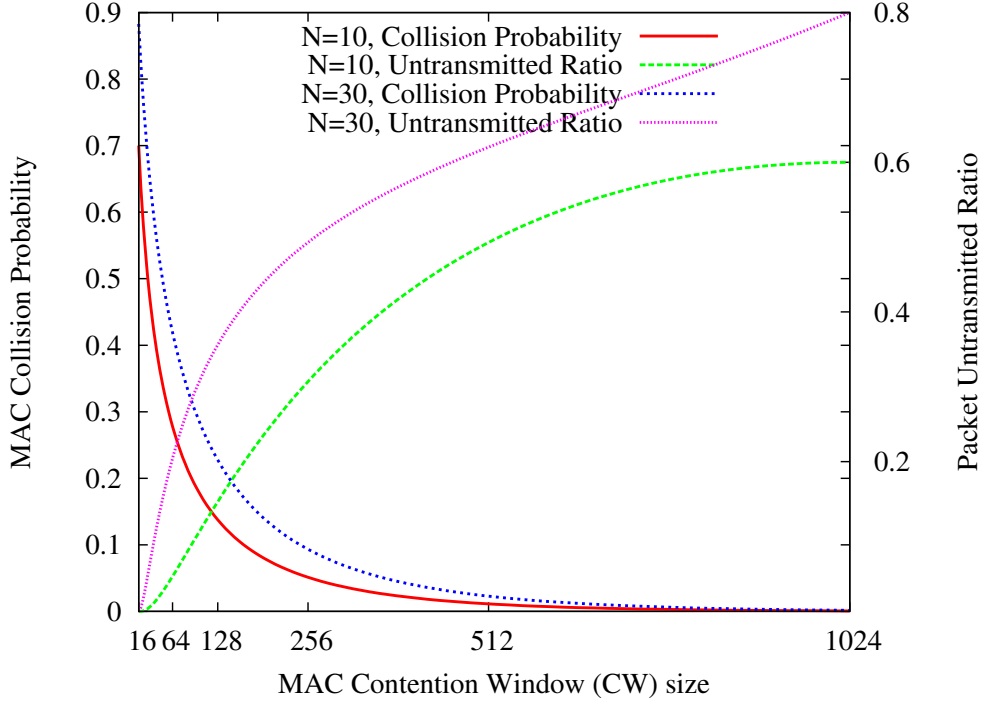
Figure 9.5: The p_c probability and the PUR index.

in the x1y2 axis we show the Packet Untransmitted Ratio (PUR), defined as the ratio of packet discarded at the end of the CCH interval as follows:

$$PUR = 1 - \frac{\kappa}{\lambda} \tag{9.14}$$

We consider two configurations of N, for the same traffic load $\lambda = 5$. As expected, the MAC Collision Risk decreases when increasing the CW size. However, this in turn increases the average MAC access delay (defined by Equation 9.10), thus producing higher values of the PUR index. Finally, Figure 9.6 shows the PDR as a function of the CW size, for different configurations of the PHY transmitting rate, i.e. R_{CCH}. Again, we consider a configuration with $N = 10$ and $\lambda = 5$. Figure 9.6 shows that increasing the PHY transmitting rate can mitigate the performance loss caused by the untransmitted packets at end of the CCH slot, since each vehicle experiences a lower average MAC access delay (e.g. $E[T_{access}]$) to transmit each SAFETY packet. To summarize, two important considerations can be drawn from previous results: (i) the PDR of broadcast applications is mainly determined by an appropriate selection of the CW size at the MAC layer, and of the transmitting rate at the PHY layer and (i) given the joint impact of these
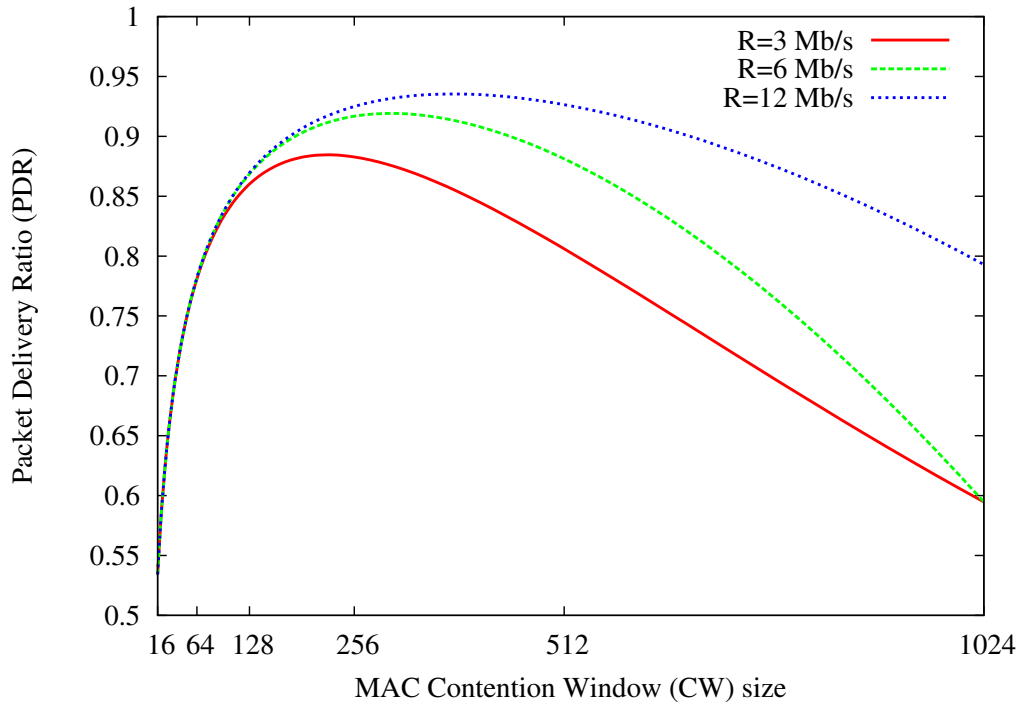
Figure 9.6: The impact of different PHY transmitting rate.

parameters on the delivery rate, cross-layer design should be considered for performance optimization.

Based on the analysis carried out so far, we now propose a DYnamic Spectrum and Contention COntrol (DYSCO) framework to decide the optimal configurations of MAC/PHY transmitting parameters in order to enhance the performance of safety-related broadcast applications. Using cognitive techniques in the design of the framework, it is possible to significantly improve the results of all the presented metrics. We consider the network architecture of Figure 9.1, and we assume that the DYSCO framework is implemented at each RSU, that in turns propagates the result of the decision process to the vehicles in its transmitting range. We are aware of the drawbacks of a centralized architecture (e.g. single point of failure, low scalability, etc), but we rely on the presence of a centralized node to be able to exploit the memory effects of the RSU, and to ensure that all vehicles of the scenario will use the same radio settings during the CCH interval. We will consider the extension to a distributed architecture as future work. We now provide an overview of the DYSCO framework implemented by each RSU. The details of the parameter decision algorithm are described in Section 9.3.1, while

the implementation aspects are discussed in Section 9.3.2.

Algorithm 2: RSU operations

    At each CCH interval:
    Sense the CCH channel and compute p_b through Equation 9.23.
    Update the estimation of N through Equation 9.25.

    At each T_f interval:
    Determine W with Equation 9.18.
    Determine R_{CCH} with Equation 9.21 and B_{CCH} with Equation 5.2.
    Bound W value to the range $[W_{DEF} : W_{MAX}]$
    Bound B_{CCH} value to the range $[B_{DEF} : B_{MAX}]$
    Compute $PDR^{new}(W, B_{CCH})$ through Equation 9.7
    if $(PDR^{new}(W, B_{CCH}) > PDR^{old})$ **then**
        Create a `NETCONF`=$< W, B_{CCH}, T_f >$ packet
        Transmit it on next SCH interval
    end if

9.3   Proposal

In every CCH interval, each RSU senses the CCH, and determines what is the current channel contention conditions through the approach which we later describe in Section 9.3.2. Then, every T_f time units, the RSU executes Algorithm 2 to determine the most suitable values of the MAC Contention Window (CW) size and of the PHY channel bandwidth to be used by each vehicle of the scenario. These values are computed taking into account the behavior according to what is described in Section 9.2. Through these values, the RSU computes the current PDR metric (i.e. PDR^{new}) with Equation 9.7 and compares it with the previous stored value of the PDR, i.e. PDR^{old}. This check is required to avoid the case in which the CW increases too much, which would determine an intolerable number of untransmitted packets, so that the performance of the application decreases. In case $PDR^{new} < PDR^{old}$, no parameter optimization is performed by the DySCO framework. In case $PDR^{new} > PDR^{old}$, then the information about the new MAC/PHY configuration to be used by each vehicle of the scenario are encapsulated on a `NETCONF` packet, that is periodically transmitted by the RSU on each service channels during the SCH interval. The `NETCONF` is composed like:

$$< W, B_{CCH}, T_{stamp} > \tag{9.15}$$

Here, W and B_{CCH} represent respectively the values of the MAC CW size and of the PHY bandwidth of the CCH (computed through the method detailed in Section 9.3.1), while T_{stamp} is the temporal validity of the parameters' setting (equal to T_f in our experiments). On receiving the `SAFETY` message, each vehicle: (i) adjusts the value of its MAC CW size to W, and (ii) computes R_{CCH}, and re-configures its radio accordingly.

9.3.1   Decision Algorithm

Here, we detail how the W and B_{CCH} values are determined by the RSU in order to meet the QoS requirements of safety-related vehicular applications. The ϵ threshold and the traffic request λ are assumed to be fixed and known by the RSU. This is a reasonable assumption, which takes into account that the application requirements are known in advance. A straightforward approach to solve the problem would be to determine the combination of $< W, R_{CCH} >$ parameters that maximizes Equation 9.7. However, this might involve high computation efforts from the RSU, and might also lead to excessive spectrum resource utilization from the vehicular network. For this reason, we propose a two-step decision process that has the main advantage to be practically implementable by RSUs, although at the cost of potentially incurring in suboptimal solutions. The solution works as follows:

- **Step 1**. Each RSU determines the optimal MAC CW size (W) in order to mitigate the risk of packet losses caused by synchronous channel access by vehicles that have selected the same MAC slot for their transmission attempts.

- **Step 2**. Based on the value of W, the RSU computes the minimum rate R_{CCH} required in order to ensure that each vehicle is able to transmit all its λ packets during the CCH interval.

For Step1, we impose that the probability of successful MAC transmission must be higher that the QoS threshold $1 - \epsilon$, i.e.:

$$p_{ps} > 1 - \epsilon \tag{9.16}$$

where p_{ps} is given by Equation 9.8. Since we know that $(1-\tau)^N \sim (1-\tau \cdot N)$ if $\tau << 1$, we get:

$$(N - 1) \cdot \tau > \epsilon \tag{9.17}$$

from which we can derive, by substituting τ with Equation 9.2, the following upper bound on W:

$$W > \frac{2 \cdot (N - 1)}{\epsilon} \tag{9.18}$$

After completing Step 1, in Step 2 we attempt to determine the minimum value of rate R_{CCH} such that each vehicle is able to transmit all its λ packets during the CCH slot, i.e.:

$$\frac{T_{CCH}}{E[T_{access}]} \geq \lambda \tag{9.19}$$

where $E[T_{access}]$ represents the average access time according to Equation 9.10, and T_{CCH} is the default CCH interval duration (fixed to 50 ms). If we consider that $T_c \sim T_s$, and that $p_b = 1 - p_i = p_s + p_c$, we can rewrite Equation 9.10 as follows:

$$E[T_{access}] = \frac{W}{2} \cdot \sigma \cdot (1 - p_b) + T_s \cdot \left(1 + p_b \cdot \frac{W}{2}\right) \tag{9.20}$$

Using Equation 9.20 in 9.19, and considering that T_s is mainly dominated by the transmitting delay (i.e. $T_s \sim S/R_{CCH}$), we can derive R_{CCH} as follows:

$$R_{CCH} \geq \frac{S \cdot \lambda \cdot \beta}{T_{CCH} - \alpha \cdot \lambda} \tag{9.21}$$

where $\alpha = \frac{W}{2} \cdot \sigma \cdot (1 - p_b)$ and $\beta = 1 + p_b \cdot \frac{W}{2}$. The term α represents the average idle time associated to each transmission. Thus, a suitable assignment of R_{CCH} exists only if the total number of empty slots does not exceed the T_{CCH} interval. Otherwise, we set R to the maximum transmitting rate R_{MAX}. From the transmitting rate R_{CCH}, the RSU can then determine the value of the B_{CCH}.

In Algorithm 2, we replaced Equations 9.18 and 9.21 with equalities, so that the minimum value of R_{CCH} that satisfies Equation 9.21 is selected in order to minimize the overall spectrum resources utilization. Thus, the final W and R_{CCH} transmitted in the NETCONF packet are as follows:

$$\begin{cases} W & = \frac{2 \cdot (N-1)}{\xi} \\ R_{CCH} & = \frac{S \cdot \lambda \cdot \beta}{T_{CCH} - \alpha \cdot \lambda} \end{cases} \tag{9.22}$$

Moreover, in Algorithm 2, we introduced upper and lower bounds for the values of W and B_{CCH}, i.e. we adjust the value of W to be in range $[W_{REF} : W_{MAX}]$ and B_{CCH} in the range $[B_{REF} : B_{MAX}]$. The upper bound is used to limit the utilization of spectrum resources, and to avoid undetermined backoff process durations.

From the description provided so far, it is easy to verify that the DySCO framework is highly adaptive to the current CCH contention conditions. In fact, in a scenario with heavy CCH load utilization produced by a high

number of N (e.g. peak hours of traffic), the W value is increased to avoid MAC collisions, and consequently the B_{CCH} value is expanded to reduce the MAC access delay of each transmission attempt. Conversely, as soon as N decreases (e.g. vehicular traffic density is reduced), the W value is reduced accordingly, and thus less DSRC bandwidth is requested.

9.3.2   Channel Load Estimation

In order to be able to determine the current value of W and B_{CCH} using Equation 9.22, the RSU must know the current value of N and p_b. Generally speaking, these values are hard to be determined in practice, also considering that the RSU does not maintain a list of authorized stations in the vehicular network. However, assuming smooth variations of vehicular traffic conditions, the load conditions of the control channel can be derived by means of the Slot Utilization (SU) metric proposed in [16]. At the start of each CCH, the RSU counts the number of transmission attempts it observes on the channel (Num_Busy_Slots) and then divides this number by the total duration of the observation window, i.e. W. The result is a lower bound on the contention level of CCH:

$$SU = \frac{Num\_Busy\_Slots}{W} \tag{9.23}$$

It is easy to see that SU provides a punctual approximation of the channel load that will converge to p_b for an enough long period of observations. For this reason, at each CCH interval the RSU updates the current estimation of SU as follows:

$$SU = SU_{new} \cdot \alpha + SU_{old} \cdot (1 - \alpha) \tag{9.24}$$

Here, SU_{new} is the value computed through Equation 9.23 during the current CCH interval, SU_{old} is the previous stored value of the SU metric, and α is a parameter that decides the relevance of history in the current decision. Using Equation 5 with $SU = p_b$, and the approximation $(1 - \tau)^N \sim (1 - \tau \cdot N)$, the RSU can estimate the value of N as follows:

$$N = SU \cdot \frac{W + 1}{2} \tag{9.25}$$

In the section below, we show that this approximation works reasonably well also under varying traffic conditions.

In this Section, we evaluate the performance of the DYSCO framework under different network and load conditions. To this aim, we consider an highway scenario with 4 lanes, and vehicles uniformly distributed over them. Following the same approach used in Sections 9.1.3 and 9.2.1, we consider

Table 9.2: Model Variables

Number of lanes	4
Number of vehicles	[4:48]
Default CW size (W_{REF})	16
Max CW size (W_{MAX})	1024
Default CCH rate (R_{REF})	3 Mb/s
T_{CCH} duration	50 ms
Traffic Request λ	$\{1, 2, 5, 10\}$
SU-α value	0.7
Number of runs	20

a subset of the network architecture with N vehicle and 1 RSU in the same scenario. We use the Ns-2 tool for the simulation analysis, with the extension described in [49] to model IEEE 1609.4-based vehicular networks. Unless specified otherwise, we use the simulation parameters of Table 9.2 in the evaluation. In the following, we compare the performance of:

- *MAC 802.11p.* This is the reference IEEE MAC 802.11p, with the default configurations of MAC/PHY parameters as foreseen by the standard. Each vehicle transmits `SAFETY` packets with a default CW size W equal to 16 [2] and a constant rate R_{DEF} equal to 3 Mb/s.

- *DySCO-CW.* This is a sub-configuration of the DySCO framework, in which only the CW size optimization is performed at the MAC layer through Equation 9.18. As before, each vehicle transmits `SAFETY` packets at a default rate R_{DEF} equal to 3 Mb/s, by following the MAC 802.11p backoff scheme for channel access.

- *DySCO.* This is the full configuration of the DySCO framework, in which both CW size optimization (through Equation 9.18) and PHY rate optimization (through Equation 9.21) are performed by the RSU.

In Section 9.4.1 we analyze the impact of vehicular traffic density (reflected by the value of N) on the system performance. In Section 9.4.2, we perform the same analysis varying the application load. In Section 9.4.3 we consider a dynamic scenario where we vary the vehicular traffic conditions during the simulation time.

---

[2]We assume all packets belong to the same TC. We will model EDCA traffic differentiation as future work.

9.4   Performance Evaluation

9.4.1   Analysis I: Vehicular density impact

In Figure 9.7, we show the PDR of the three schemes for different number of vehicles (N) transmitting in the same collision domain. Each vehicle transmits $\lambda = 5$ packets at each CCH. Figure 9.7 demonstrates that the MAC 802.11p suffers of high packet losses under moderate and high vehicular density conditions. This is caused by the fact that broadcast packets are not acknowledged, and are transmitted using the minimum CW size (i.e. 16). As a result, the performance of vehicular applications with delivery rate requirements might be seriously compromised. On the other hand, the DySCO-CW framework provides an effective enhancements of the PDR for $N < 16$, while it incurs in severe packet losses under high density vehicular scenarios, due to the increased number of un-transmitted packets caused by the additional backoff delay introduced by Equation 9.18. The complete DySCO framework accounts for this problem by increasing the CCH rate accordingly. As a result, Figure 9.7 shows that the DYSCO framework is able to improve the delivery rate significantly even for $N=40$ vehicles. This analysis is also confirmed by Figures 9.8 and 9.9. In Figure 9.8, we depict the MAC collision risk as defined in Section 9.2.1. As expected, the collision risk of the MAC 802.11p increases significantly with N, while it is kept constant by the DySCO framework configurations through the adjustment of the MAC Contention Window (CW) provided by Equation 9.18. Moreover, Figure 9.8 confirms the effectiveness of this approach, since the MAC collision risk is always below the application threshold ϵ (set equal to 0.1) for all values of N. Figure 9.9 completes the analysis by showing the PUR metric for the DySCO framework configurations. The PUR index is higher for the DySCO-CW framework, while it is greatly mitigated in the DySCO configuration by the rate adaptation scheme.

9.4.2   Analysis II: Application load impact

In this Section, we consider a scenario with 20 vehicles (i.e. $N=20$), and we vary the number of packets (λ) transmitted by each vehicle at each CCH interval. Figure 9.10 shows the PDR of the three schemes, for different values of λ. Figure 9.10 demonstrates that both DySCO configurations enhance the delivery rate of the MAC 802.11p for all the values of λ. However, the PDR of DySCO-CW decreases significantly under high traffic loads since the CW optimization (Equation 9.18) does not account for the traffic request. On the opposite, the rate adaptation algorithm of Equation 9.21 is based on
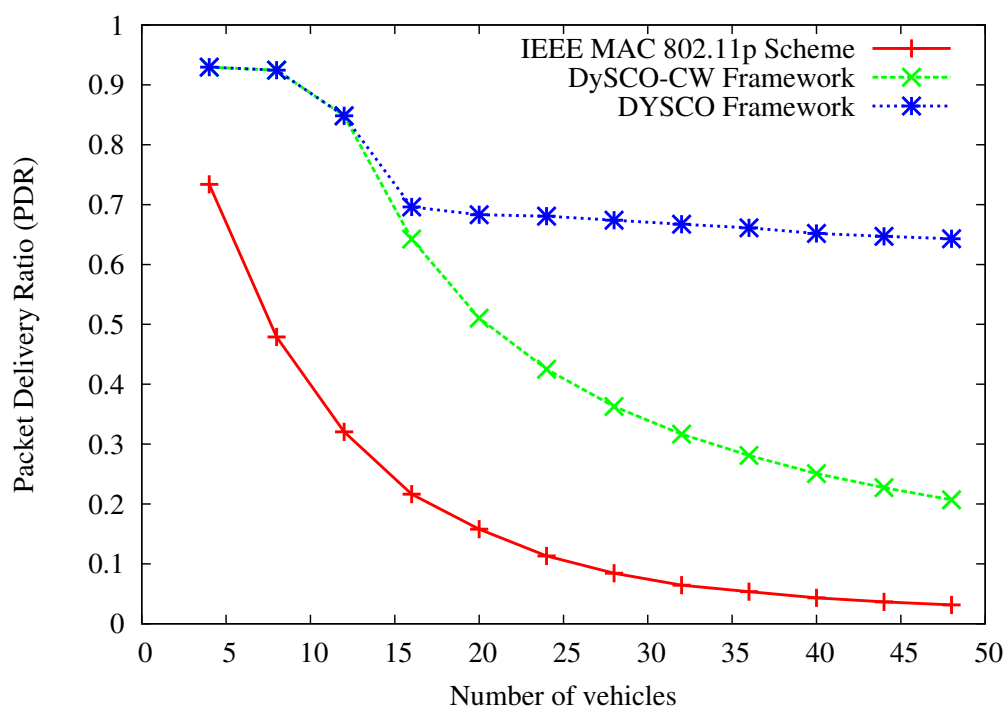
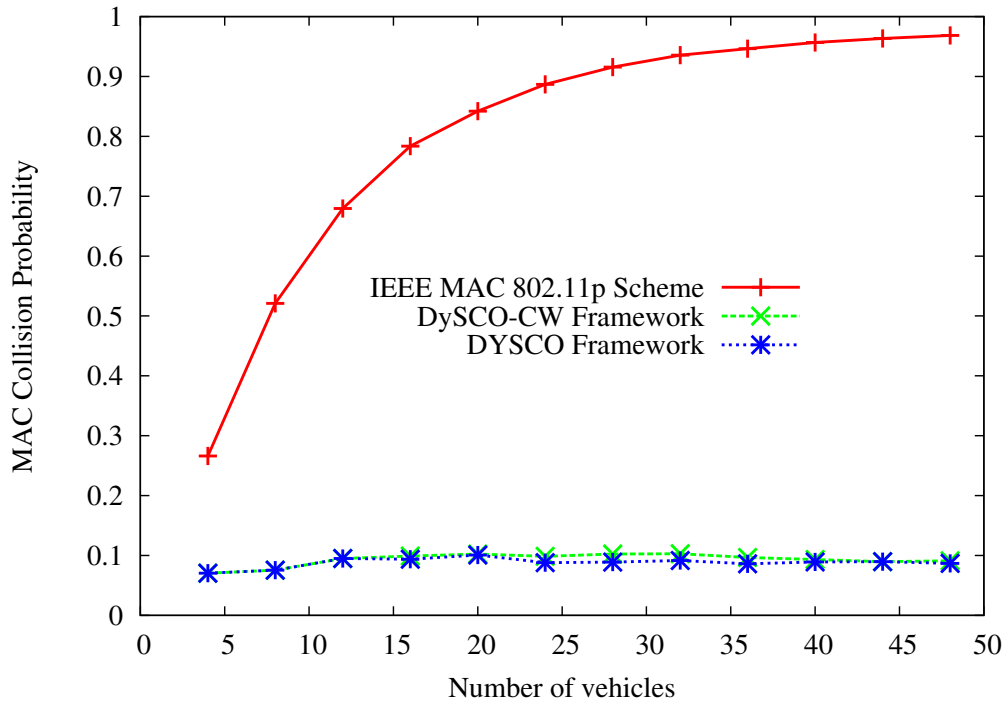Figure 9.7: The PDR as a function of N (Analysis I).

Figure 9.8: The MAC Collision Risk for the Analysis I.

the value of λ, and this explains the enhancement provided by the DySCO framework. This is also confirmed by Figure 9.11 that depicts the PUR metric as a function of λ.

9.4.3   Analysis III: Dynamic Scenario

In the previous Section, we evaluated the system performance in vehicular environments with fixed number of vehicles during the simulation length. Conversely, in this Section, we consider a vehicular scenario in which the number of vehicles can dynamically vary during the simulation, in order to investigate the ability of our framework to adapt to varying traffic conditions. In both Figures 9.12 and 9.13, we consider a scenario with 4 vehicles transmitting 5 packets at each CCH. From the time instant $t=10$ sec, a new vehicle is added to the network every 2 seconds, till $N=40$. From the time instant $t=100$ sec, one vehicle is removed from the network every 2 seconds, till the initial configuration with $N=4$ vehicles is reached. This scenario can model realistic urban scenarios, where traffic jams can dynamically occur at intersections with traffic lights. Figure 9.12 shows the PDR for the three evaluated scheme, as a function of the simulation time. Again, Figure 9.12
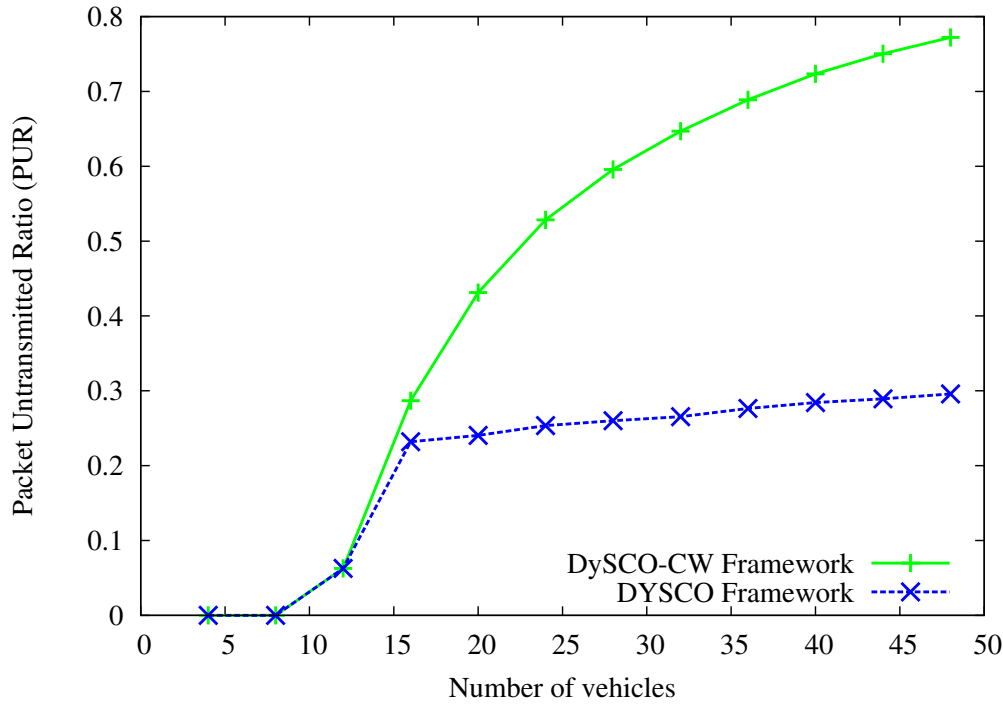
Figure 9.9: The PUR metric for the Analysis I.

confirms that the DySCO framework is able to mitigate the impact of packet losses also in highly congested scenarios, with reduced fluctuations of the PDR. Figure 9.13 provides more insights of system behaviour. On the x1-y1 axis, we depict the SU metric as computed by the RSU, for the MAC 802.11p scheme and the DySCO framework. In the first case, the SU increases when we add more vehicles in the network, and decreases after $t=100$ seconds. In the DySCO framework, the SU metric (and thus the MAC contention) is kept constant because of the dynamic adjustment of the CW size. In the same Figure, we also depict (on the x1-y2) axis the number of active vehicles as estimated through Equation 9.25. It is easy to see that the proposed method provides a realistic approximation of N, based on the current value of the CW size and of the SU.

Figure 9.10: The PDR as a function of λ for the Analysis II.

Figure 9.11: The MAC Collision Risk for the Analysis II.

Figure 9.12: The PDR and the N estimation for the Analysis III.

Figure 9.13: The SU and the N estimation for the Analysis III.

Chapter 10

Conclusion and Future Works

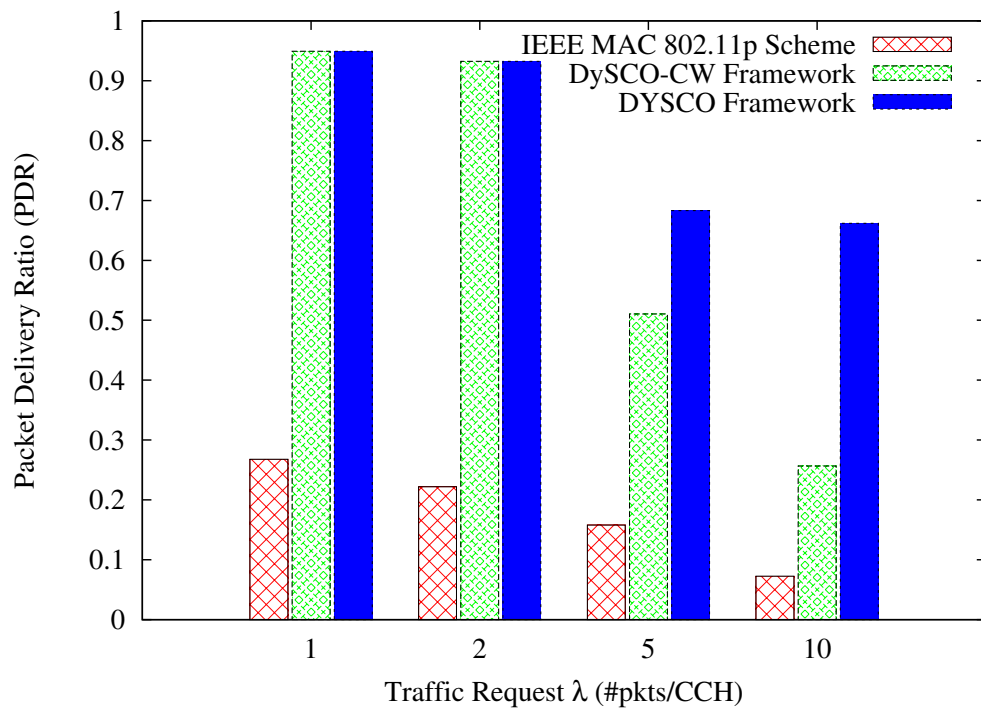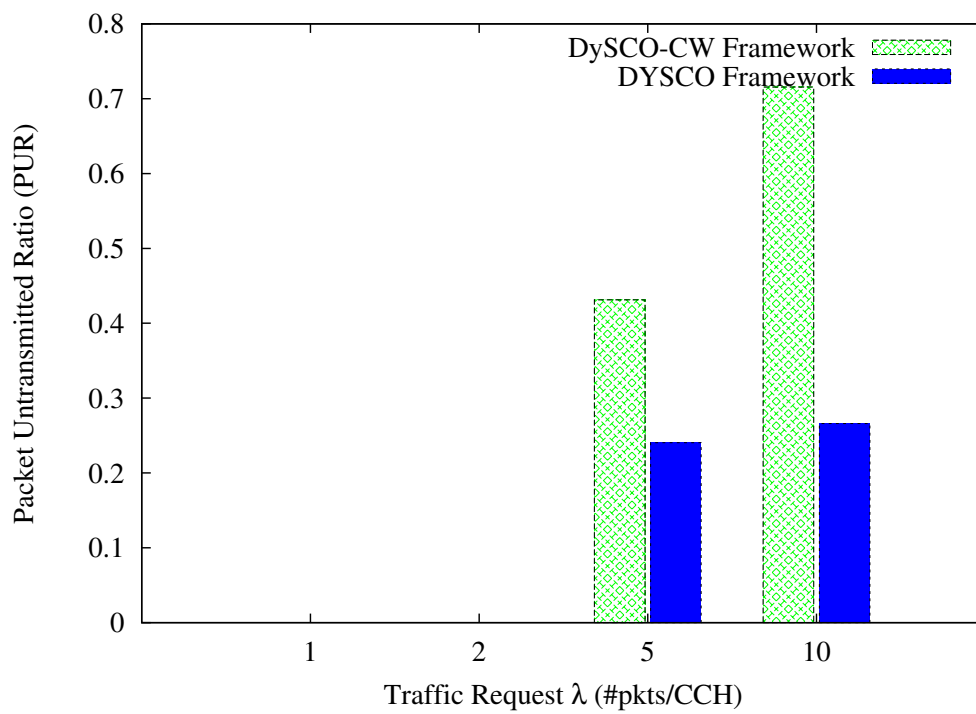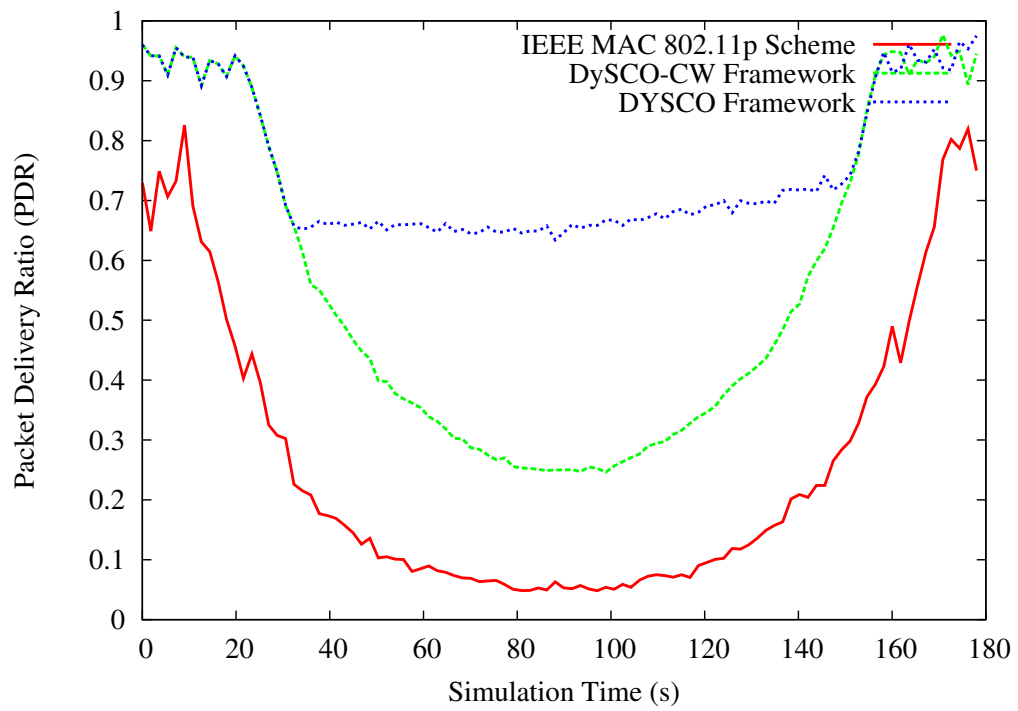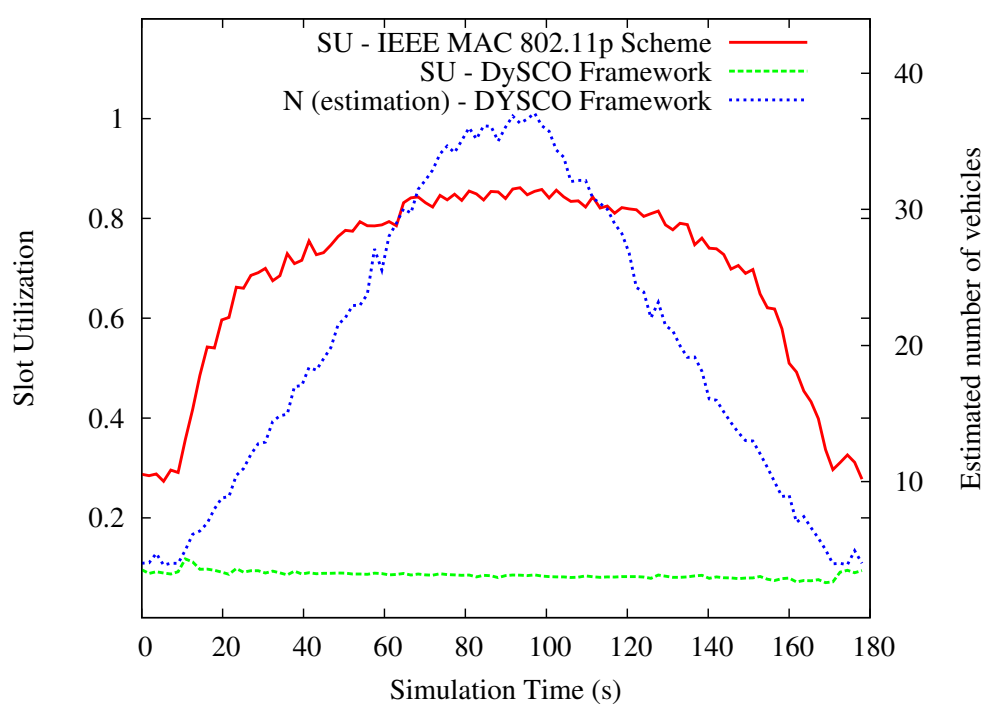Wireless communication is certainly one of the most used technologies in everyday's life. Either for working or for entertainment, several devices are now equipped with wireless capabilities, that keep them connected to the internet on the move. This created new services, with a restless growing demand for new spectrum and for high data rates. This trend pushed research efforts to provide new standards and methods to progress towards a more efficient spectrum utilization. Among all the possibilities, which ranges from LTE networks, to femtocell, and the last WiFi standards, in this thesis we studied Cognitive Wireless Networks, with a specific focus on TVWS communication opportunities.

A deep literature review has been performed in Part I, where both scientific works as well as regulations and standards have been taken into account. Then, in Part II all the contributions to the state of the art have been presented and discussed.

Then we moved to the main contributions of this work in Part II, where the different topics taken into account have been explained and documented. In Section 4, new spectrum measurements have been presented, carried out in Germany and in Italy. Those measurements were done in order to study the different reception of the singal when moving from outdoor to indoor scenarios. Results have shown that, as previosuly theorized, indoor secondary networks can benefit from a negligible noise floor induced by the primary network, and thus communication may be possible.

Then, we moved to a deep comparison of currently standards operating in TVWS, like the IEEE 802.11af and the IEEE 802.15.4m, in Section 5. For the former, we have shown that the most beneficial effects come when IEEE 802.11af networks are combined with other technologies, like IEEE 802.11n [11], where both networks leverage on the other strengths. IEEE 802.15.4m has been compared against the 433 MHz and 868 MHz. Here, we have shown

that IEEE 802.15.4m networks offer better data rates and duty cycles, at the cost of a higher uncertainity in spectrum availability, due to the presence or not of TVWS.

In Section 6 we presented the per-floor spectrum sharing, which extends classical 2D spectrum sharing models by considering also the height of the device. We have shown that by adding the height from the floor, indoor devices can benefit of a much increased channel availability. A theoretical model, as well as simulation results with real city scenario, has been provided and commented. Certainly, 3D spectrum sharing models, although more complex, are far more precise and thus less communication opportunities are lost.

Section 7 focused on M2M communication, and to the TVWS networks that can be deployed to support it. Again, IEEE 802.15.4m have been studied, and quantitative results for TVGS deployments have been provided for Germany. We have shown that for highly populated areas, TVGS present severe constraints. The interference coming from the primary network is too high to be eliminated by the secondary device, and thus these kind of networks present poor performance.

Section 8 presented the Mobile Femto Database framework, needed to extend the availability of Master devices to Slave devices. Here, we have shown that by caching the information which comes from the remote spectrum database, and eventually deliver it to the interested Slave device, more communication opportunities can be found.

Finally, Section 9 has shown the application of Cognitive Radio techniques to VANETs. We have shown improvements of the IEEE 802.11p protocol, which is the amendment of IEEE 802.11 for vehicular communications.

To conclude, TVWS networks are fairly new, but present some unique characteristics that are hard to be obtained with other technologies. Thanks to the lower spectrum bands used to communicate, the communication range is greatly increased, and also indoor environments present better coverage, mostly due to a better obstacle penetration. However, much work have still to be done in order to bring TVWS networks to life. In the following, some key aspect and possible future research directions are identified and commented.

- **Additional measurements**: although it is possible to find several spectrum measurements studies in literature, there is a need for more focused results, particularly looking at the indoor scenario. Most measurements studies for TVWS focus on the outdoor scenario, and recently some studies have also been done for the indoor scenario. However, different materials and terrains make hard to derive general rule of thumbs.

- **Testbeds**: almost all the works that study TVWS communication are done with either analytical models or simulation models. Some exception can be found, but certainly research has to move towards real testbeds, which will offer a clearer picture on the potentials of TVWS operated networks.

- **Large scale studies**: Up to now, many studies focused on homogeneous scenario, with the notable exception of [55] and [111], which instead provide results for the U.S. and Europe, respectively. In fact, to really bring to light TVWS networks, the whole ecosystem of standards, spectrum bands, devices, have to work in different environments, and for various scenarios. This result have still to be achieved, with particular respect to the availability of TVWS in densely populated areas, where the scarcity of channels could make TVWS networks completely unusable.

The principal outcome of this work is that even though TVWS present some interesting characteristics, and good performance, their principal use can be foreseen as an offload technology, due to the limitation already presented. TVGS can be employed where TVWS are hard to be found, but this behavior is currently not envisioned by regulators.

Bibliography

[1] https://www.sbireports.com/Smart-Grid-Utility-2496610/.

[2] a Abbasi and M Younis. A survey on clustering algorithms for wireless sensor networks. *Computer Communications*, 30:2826–2841, 2007.

[3] Andreas Achtzehn, Ljiljana Simic, Marina Petrova, Petri Mahonen, Valentin Rakovic, Pero Latkoski, and Liljana Gavrilovska. Software tool for assessing secondary system opportunities in spectrum whitespaces. In *2013 IEEE 14th International Symposium on "A World of Wireless, Mobile and Multimedia Networks" (WoWMoM)*, pages 1–3. IEEE, June 2013.

[4] Ian F. Akyildiz, Brandon F. Lo, and R. Balakrishnan. Cooperative spectrum sensing in cognitive radio networks: A survey. *Physical Communication*, 4(1):40–62, March 2011.

[5] Karol Andersson and Carlson Wireless Technologies. Super Wi-Fi. 2011.

[6] Raamkumar Balamurthi, Harshit Joshi, Cong Nguyen, Ahmed K Sadek, Stephen J Shellhammer, and Cong Shen. A TV white space spectrum sensing prototype. *2011 IEEE International Symposium on Dynamic Spectrum Access Networks DySPAN*, pages 297–307, 2011.

[7] S. Bandyopadhyay and E.J. Coyle. An energy efficient hierarchical clustering algorithm for wireless sensor networks. In *Infocom '03. 22nd Annual Joint Conference of the IEEE Computer and Communications.*, volume 3, pages 1713–1723, 2003.

[8] A. Bartoli, J. Hernandez-Serrano, M. Soriano, M. Dohler, A. Kountouris, and D. Barthel. Secure Lossless Aggregation for Smart Grid M2M Networks. In *Smart Grid Communications SmartGridComm 2010 First IEEE International Conference on*, pages 333–338. IEEE, 2010.

[9] Tuncer Baykas, M. Kasslin, M. Cummings, Joe Kwak, R. Paine, A. Reznik, R. Saeed, and Stephen J. Shellhammer. Developing a standard for TV white space coexistence: technical challenges and solution approaches. *IEEE Wireless Communications*, 19(1):10–22, February 2012.

[10] Luca Bedogni, Andreas Achtzehn, Marina Petrova, and Petri Mähönen. Smart meters with TV gray spaces connectivity: A feasibility study for two reference network topologies. In *Proceedings of SECON 2014*, 2014.

[11] Luca Bedogni, Marco Di Felice, Fabio Malabocchia, and Luciano Bononi. Cognitive Modulation and Coding scheme Adaptation for 802.11n and 802.11af networks. In *Globecom 2014 Workshop - Telecommunications Standards - From Research to Standards (GC14 WS - TCS)*, 2014.

[12] Luca Bedogni, Marco Di Felice, Fabio Malabocchia, and Luciano Bononi. Indoor Communication over TV Gray Spaces based on Spectrum Measurements. In *Proceedings of WCNC 2014*, 2014.

[13] Luca Bedogni, Angelo Trotta, and Marco Di Felice. On 3-Dimensional Spectrum Sharing for TV White and Gray Space Networks. In *submitted for publication*, 2015.

[14] Luca Bedogni, Angelo Trotta, Marco Di Felice, and Luciano Bononi. Machine-to-Machine Communication over TV White Spaces for Smart Metering Applications. In *Proceedings of ICCCN13*, 2013.

[15] Giuseppe Bianchi. Performance analysis of the IEEE 802.11 distributed coordination function. *Selected Areas in Communications IEEE Journal on*, 18(3):535–547, 2000.

[16] Luciano Bononi, Marco Conti, and Lorenzo Donatiello. Design and Performance Evaluation of a Distributed Contention Control (DCC) Mechanism for IEEE 802.11 Wireless Local Area Networks. *Journal of Parallel and Distributed Computing*, 60(4):407–430, April 2000.

[17] Athina Bourdena, George Kormentzas, Charalabos Skianis, Evangelos Pallis, and George Mastorakis. Real-time TVWS trading based on a centralized CR network architecture. In *2011 IEEE GLOBECOM Workshops, GC Wkshps 2011*, pages 964–969, 2011.

[18] Athina Bourdena, George Mastorakis, Evangelos Pallis, A. Arvanitis, and George Kormentzas. A dynamic spectrum management framework

for efficient TVWS exploitation. In *Proceedings of CAMAD 2012*, pages 51–55. IEEE, September 2012.

[19] O. Boyinbode, H. Le, A. Mbogho, M. Takizawa, and R. Poliah. A Survey on Clustering Algorithms for Wireless Sensor Networks. *Network-Based Information Systems (NBiS), 2010 13th International Conference on*, 2010.

[20] Spectrum Bridge. Spectrum Database - http://whitespaces-canada.spectrumbridge.com/.

[21] T X Brown and D C Sicker. Can Cognitive Radio Support Broadband Wireless Access?, 2007.

[22] D Cabric, S M Mishra, and R W Brodersen. Implementation issues in spectrum sensing for cognitive radios, 2004.

[23] Angela Sara Cacciapuoti, Ian F. Akyildiz, and Luigi Paura. Primary-user mobility impact on spectrum sensing in Cognitive Radio networks. In *2011 IEEE 22nd International Symposium on Personal Indoor and Mobile Radio Communications*, pages 451–456. Broadband Wireless Networking Laboratory, School of Electrical and Computer Engineering, Georgia Institute of Technology, Atlanta, USA, IEEE, 2011.

[24] Cambridge White Spaces Consortium. Cambridge TV White Spaces Trial A Summary of the Technical Findings. Technical report.

[25] Inhyok Cha Inhyok Cha, Y Shah, A U Schmidt, A Leicher, and M V Meyerstein. Trust in M2M communication, 2009.

[26] Hou-Shin Chen Hou-Shin Chen, Wen Gao Wen Gao, and D G Daut. Spectrum Sensing for Wireless Microphone Signals, 2008.

[27] CISCO. The Internet of Things, How the Next Evolution of the Internet Is Changing Everything. 2011.

[28] Pengfei Cui, Hui Liu, Dinesh Rajan, and Joseph Camp. A measurement study of white spaces across diverse population densities. In *2014 12th International Symposium on Modeling and Optimization in Mobile, Ad Hoc, and Wireless Networks (WiOpt)*, number WiNMeE, pages 30–36. IEEE, May 2014.

[29] E. Damosso and L. M. Correia. COST Action 231: Digital Mobile Radio Towards Future Generation Systems: Final Report. European Commission. Technical report, 1999.

[30] Rob Davies and Monisha Ghosh. Field trials of DVB-T sensing for TV White Spaces. In *2011 IEEE International Symposium on Dynamic Spectrum Access Networks (DySPAN)*, pages 285–296. Philips Research, IEEE, May 2011.

[31] M. Dawkins, A.P. Burdett, and N. Cowley. A single-chip tuner for DVB-T. *IEEE Journal of Solid-State Circuits*, 38(8):1307–1317, August 2003.

[32] M. Deruyck, E. Tanghe, W. Joseph, D. Pareit, I. Moerman, and L. Martens. Performance Analysis of WiMAX for Mobile Applications. In *Proceedings of IEEE Wireless Communication and Networking Conference(WCNC)*, pages 1–6, April 2010.

[33] Marco Di Felice, Luca Bedogni, and Luciano Bononi. DySCO: a dynamic spectrum and contention controlframework for enhanced broadcast communication invehicular networks. In *Proceedings of Mobiwac 2012*, page 97, New York, New York, USA, 2012. ACM Press.

[34] Marco Di Felice, Luca Bedogni, and Luciano Bononi. Group communication on highways: An evaluation study of geocast protocols and applications. *Ad Hoc Networks*, 11(3):818–832, May 2013.

[35] Marco Di Felice, Kaushik Roy Chowdhury, Andreas Kassler, and Luciano Bononi. Adaptive Sensing Scheduling and Spectrum Selection in Cognitive Wireless Mesh Networks, 2011.

[36] Ping Ding, JoAnne Holliday, and Aslihan Celik. Distributed Energy-Efficient Hierarchical Clustering for Wireless Sensor Networks. In *First IEEE International Conference, DCOSS 2005*, 2005.

[37] Rahman Doost-mohammady and Kaushik Roy Chowdhury. Enhancing Wireless Medical Telemetry through Dynamic Spectrum Access. pages 1628–1633.

[38] J.P. Eira and A.J. Rodrigues. Analysis of WiMAX data rate performance. Technical report.

[39] ETSI. Electromagnetic Compatibility and Radio Spectrum Matters (ERM); Short Range Devices (SRD); Radio equipment to be used in the 25 MHz to 1 000 MHz frequency range with power levels ranging up to 500 mW; Part 1: Technical characteristics and test methods. Technical report, 2012.

[40] Mauro Fadda, Maurizio Murroni, and Vlad Popescu. A cognitive radio indoor HD1T V multi-vision system in the TV white spaces. *2012 IEEE International Conference on Consumer Electronics (ICCE)*, pages 27–28, 2012.

[41] FCC. Section 15.247 Operation within the bands 902 - 928 MHz, 2400 - 2483.5 MHz, and 5725 - 5850 MHz. 1996.

[42] FCC. NOTICE OF PROPOSED RULE MAKING. 2004.

[43] Federal Communications Commission (FCC). Second Report and Order and Memorandum Opinion and Order, 2009.

[44] Laura Marie Feeney. An energy consumption model for performance analysis of routing protocols for mobile ad hoc networks. *Mobile Networks and Applications*, 6:239–249, 2001.

[45] L.M. Feeney and M. Nilsson. Investigating the energy consumption of a wireless network interface in an ad hoc networking environment. *Proceedings IEEE INFOCOM 2001. Conference on Computer Communications. Twentieth Annual Joint Conference of the IEEE Computer and Communications Society (Cat. No.01CH37213)*, 3, 2001.

[46] Adriana B Flores, Ryan E Guerra, and Edward W Knightly. IEEE 802.11af: a standard for TV white space spectrum sharing. *IEEE Communications Magazine*, 51(10):92–100, October 2013.

[47] R. Funada, F. Kojima, and H. Harada. IEEE 802.15.4m: The first low rate wireless personal area networks operating in TV white space. In *Proceedings of the18th IEEE International Conference on Networks (ICON)*, pages 326–332. IEEE, December 2012.

[48] Liljana Gavrilovska, Jaap Van De Beek, Yong Xie, Erik Lidström, Janne Riihijärvi, Petri Mähönen, Vladimir Atanasovski, Daniel Denkovski, and Valentin Rakovic. Enabling LTE in TVWS with radio environment maps : From an architecture design towards a system level prototype. *COMPUTER COMMUNICATIONS*, (August), 2014.

[49] Ali J Ghandour, Marco Di Felice, Luciano Bononi, and Hassan Artail. Modeling and Simulation of WAVE 1609.4-based Multi-channel Vehicular Ad Hoc Networks. In *Proceedings of SIMUTOOLS*, 2012.

[50] A Ghasemi and E S Sousa. Interference Aggregation in Spectrum-Sensing Cognitive Wireless Networks, 2008.

[51] Chittabrata Ghosh, Sumit Roy, and Dave Cavalcanti. Coexistence challenges for heterogeneous cognitive wireless networks in TV white spaces. *IEEE Wireless Communications*, 18(4):22–31, August 2011.

[52] M Ghosh, V Gaddam, G Turkenich, and K Challapali. Spectrum Sensing Prototype for Sensing ATSC and Wireless Microphone Signals, 2008.

[53] Google. Google TV White Spaces Database - www.google.com/get/spectrumdatabase/channel/.

[54] Ning Han Ning Han, SungHwan Shon SungHwan Shon, Jae Hak Chung Jae Hak Chung, and Jae Moung Kim Jae Moung Kim. Spectral correlation based signal detection method for spectrum sensing in IEEE 802.22 WRAN systems, 2006.

[55] K. Harrison, S.M. Mishra, and A. Sahai. How Much White-Space Capacity Is There? In *Proceedings of IEEE Symposium on New Frontiers in Dynamic Spectrum (DySPAN)*, pages 1–10, April 2010.

[56] T. Henderson, G. Pei, R. Groves, T. Bosaw, M. Rush, C. Ghosh, and S. Roy. Wireless Network Coexistence - Boeing Project Report. Technical report, 2009.

[57] Farzad Hessar, Student Member, and Sumit Roy. Capacity Considerations for Secondary Networks in TV White Space. (June):1–29, 2009.

[58] Http://www.otgtv.it/index2.html. Italian TVWS.

[59] Hesong Huang, Jie Wu, and Boca Raton. A probabilistic clustering algorithm in wireless sensor networks. In *VTC-2005-Fall. 2005 IEEE 62nd Vehicular Technology Conference, 2005.*, volume 3, pages 1796–1798. IEEE, 2005.

[60] IETF. PAWS - Protocol to Access the White Space Database - Available http://datatracker.ietf.org/doc/draft-ietf-paws-protocol/. Technical report, 2014.

[61] Ecma International. Ecma 392. Technical Report June, ECMA International, 2012.

[62] M.H. H Islam, C.L. L Koh, S.W. W Oh, Xianming Qing Xianming Qing, Y.Y. Y Lai, Cavin Wang Cavin Wang, Ying-Chang Liang Ying-Chang Y.C. Liang, B.E. E Toh, F. Chin, G.L. L Tan, and W. Toh.

Spectrum Survey in Singapore: Occupancy Measurements and Analyses. In *in Proceedings of the 3rd International Conference on Cognitive Radio Oriented Wireless Networks and Communications (CrownCom)*, volume May. IEEE, May 2008.

[63] ITU-R. Directivity and polarization discrimination of antennas in the reception of television broadcasting. Technical report, 1992.

[64] Shanjeevan Jayavalan, Hafizal Mohamad, Norazizah Mohd Aripin, Aiman Ismail, and Nordin Ramli. Measurements and Analysis of Spectrum Occupancy in the Cellular and TV Bands. 2(2):133–138, 2014.

[65] Hyunduk Kang, Donghun Lee, Byung-Jang Jeong, and Allen C Kim. Coexistence between 802.22 and 802.11af over TV white space, 2011.

[66] Margot Karam, William Turney, Kevin Baum, Philippe Sartori, Laddie Malek, and Isselmou Ould-Dellahy. Outdoor-indoor propagation measurements and link performance in the VHF/UHF bands. In *IEEE Vehicular Technology Conference*, 2008.

[67] Vivek Katiyar, Narottam Chand, and Surender Soni. A Survey on Clustering Algorithms for Heterogeneous Wireless Sensor Networks. *International Journal of Applied Engingeering Research, Dindigul*, 1:273–287, 2010.

[68] Jussi Kerttula and Riku Jäntti. DVB-T Receiver Performance Measurements Under Secondary System Interference. In *Proceedings of COCORA 2011*, 2011.

[69] P. Kumarawadu, D. J. Dechene, M. Luccini, and A. Sauer. Algorithms for Node Clustering in Wireless Sensor Networks: A Survey. In *2008 4th International Conference on Information and Automation for Sustainability*, pages 295–300, 2008.

[70] A. G. Longley and P. L. Rice. Prediction of tropospheric radio transmission loss over irregular terrain. A computer method. Technical report, NTIS ESSA Tech. Rep. ERL 79-ITS 67, 1968.

[71] Albert Lysko, Moshe Masonta, and Luzango Mfupe. Field measurements done on operational TVWS trial network in Tygerberg. Technical report, 2013.

[72] J. A. Magliacane. Splat!: an RF Signal Propagation, Loss, And Terrain analysis tool [Online]. Available: http://www.qsl.net/kd2bd/splat.html.

[73] Dimitris Makris, Georgios Gardikis, and Anastasios Kourtis. Quantifying TV white space capacity: A Geolocation-Based Approach. *IEEE Communications Magazine*, 50(9):145–152, September 2012.

[74] Geneviève Mange, Ulrico Celentano, Per H Lehne, and Terje Tjelta. Cognitive Architecture and System Solutions to Offload LTE Networks in TVWS. In *Proceedings of the Future Network & Mobility Summit 2013*, pages 1–8, 2013.

[75] Ioana Marcu and Ion Marghescu. Evaluation of Spectrum Occupancy in an Urban Environment in a Cognitive Radio Context. *Advances in Telecommunications*, 3(3):172–181, 2010.

[76] Gustavo Marfia, Marco Roccetti, Alessandro Amoroso, and Giovanni Pau. Safe Driving in LA: Report from the Greatest Intervehicular Accident Detection Test Ever. *IEEE Transactions on Vehicular Technology*, 62(2):522–535, February 2013.

[77] Moshe M.T. Masonta, David L Johnson, and Mjumo Mzyece. The White Space Opportunity in Southern Africa: Measurements with Meraka Cognitive Radio Platform. In *Proceedings of AFRICOMM*, volume 92 of *Lecture Notes of the Institute for Computer Sciences, Social Informatics and Telecommunications Engineering*, pages 64–73. Springer, 2011.

[78] Moshe Timothy Masonta, Mjumo Mzyece, and Ntsibane Ntlatlapa. Spectrum Decision in Cognitive Radio Networks: A Survey. *IEEE Communications Surveys & Tutorials*, pages 1–20, 2012.

[79] M.A. McHenry, P.A. Tenhula, D. McCloskey, D.A. Roberson, and C.S. Hood. Chicago spectrum occupancy measurements & analysis and a long-term studies proposal. In *Proceedings of the first international workshop on Technology and policy for accessing spectrum (TAPAS)*, 2006.

[80] Leonard E Miller. Distribution of Link Distances in a Wireless Network. *Journal Of Research Of The National Institute Of Standards And Technology*, 106(2):401–412, 2001.

[81] Shridhar Mubaraq Mishra and Anant Sahai. How much white space is there? *Department of Electrical Engineering University of California Tech Rep UCBEECS20093*, pages 1–16, 2009.

[82] Jad Nasreddine, Janne Riihijärvi, Andreas Achtzehn, and Petri Mähönen. The World is not flat: Wireless communications in 3D environments. In *2013 IEEE 14th International Symposium on "A World of Wireless, Mobile and Multimedia Networks" (WoWMoM)*, pages 1–9. IEEE, June 2013.

[83] Maziar Nekovee. Quantifying the Availability of TV White Spaces for Cognitive Radio Operation in the UK. *2009 IEEE International Conference on Communications Workshops*, pages 1–16, 2009.

[84] S.-Y. Ni, Y.-C. Tseng, Y.-S. Chen, and J.-P. Sheu. The broadcast storm problem in a mobile ad hoc network. *Proceedings of the 5th annual ACM/IEEE international conference on Mobile computing and networking MobiCom 99*, 8(2/3):151–162, 1999.

[85] NIST. Electromagnetic Signal Attenuation in Construction Materials. Technical report, 1997.

[86] Dusit Niyato, Lu Xiao, and Ping Wang. Machine-to-machine communications for home energy management system in smart grid. *IEEE Communications Magazine*, 49(4):53–59, April 2011.

[87] Thomas Novlan, Kunal Rele, and Srikanteswara Srikathyayani. Coverage and Density Study of Wi-Fi in the TV White Spaces. 2010.

[88] Ofcom. Digital dividend : cognitive access. 2009.

[89] Ofcom. TV white spaces - A consultation on white space device requirements, 2012.

[90] Ofcom. TV white spaces: approach to coexistence. Technical report, 2013.

[91] Ser Wah Oh, Francois Chin, and See Gim Kerk. TV white-space for smart grid. In *Proceedings of the 4th International Conference on Cognitive Radio and Advanced Spectrum Management - CogART '11*, pages 1–5, New York, New York, USA, 2011. ACM Press.

[92] C. Palazzi, S. Ferretti, M. Roccetti, G. Pau, and M. Gerla. How Do You Quickly Choreograph Inter-Vehicular Communications? A Fast Vehicle-to-Vehicle Multi-Hop Broadcast Algorithm, Explained. *Consumer Communications and Networking Conference (CCNC)*, 2007.

[93] J. Perez-Romero, Dominique Noguet, M. Lopez-Benitez, and Fernando Casadevall. Towards More Efficient Spectrum Usage: Spectrum Sensing and Cognitive Radio Techniques. *Radio Science Bullettin*, 7, 2011.

[94] Caleb Phillips, Douglas Sicker, and Dirk Grunwald. A Survey of Wireless Path Loss Prediction and Coverage Mapping Methods. *IEEE Communications Surveys & Tutorials*, 15(1):255–270, January 2013.

[95] S. Pollin, M. Ergen, S. Ergen, B. Bougard, L. Der Perre, I. Moerman, A. Bahai, P. Varaiya, and F. Catthoor. Performance Analysis of Slotted Carrier Sense IEEE 802.15.4 Medium Access Layer. *IEEE Transactions on Wireless Communications*, 7(9):3359–3371, September 2008.

[96] T. Rappaport. *Wireless Communications: Principles and Practice.* Prentice Hall PTR, second edition, 2001.

[97] Jose Jorge Ribeiro, Jonathan Rodriguez, Rogerio Dionisio, Hugo Esteves, Pedro Duarte, Paulo Marques, Digital Video Broad, Program Making, and Special Events. Testbed for combination of local sensing with geolocation database in real environments. *IEEE Wireless Communications*, 19(4):59–66, August 2012.

[98] Yosra Ben Saied, Alexis Olivereau, and Djamal Zeghlache. Energy efficiency in M2M networks: A cooperative key establishment system. In *2011 3rd International Congress on Ultra Modern Telecommunications and Control Systems and Workshops ICUMT*, pages 1–8. CEA, LIST, Communicating Systems Laboratory, 91191 Gif-sur-Yvette CEDEX, France, IEEE, 2011.

[99] Yngve Selen, Hugo Tullberg, and Jonas Kronander. Sensor Selection for Cooperative Spectrum Sensing. Number i, page 2008, 2008.

[100] Stephen J Shellhammer. SPECTRUM SENSING IN IEEE 802.22. *Methodology*, pages 1–6, 2008.

[101] Ljiljana Simic, Marina Petrova, and Petri Mähönen. Wi-Fi , but not on Steroids : Performance Analysis of a Wi-Fi-like Network Operating in TVWS under Realistic Conditions. In *Proceedings of ICC*, pages 1533–1538, 2012.

[102] Christoph Sommer, David Eckhoff, Reinhard German, and Falko Dressler. A computationally inexpensive empirical model of IEEE 802.11p radio shadowing in urban environments. Technical report,

Friedrich-Alexander-Universit{ä}t Erlangen-N{ü}rnberg, Department Informatik, January 2011.

[103] White Spaces and Sharon Hanson. Expanding wireless communications with "white spaces". 2008.

[104] C. Stevenson, G. Chouinard, S. Shellhammer, and W. Caldwell. IEEE 802.22: The first cognitive radio wireless regional area network standard. *IEEE Communications Magazine*, 47(1):130–138, January 2009.

[105] S. Subramani, S. Gormus, P. Kulkarni, and M. Sooriyabandara. WISE-MEN: White Space for Smart Metering. In *Proceedings of the IEEE PES Innovative Smart Grid Technologies (ISGT)*, pages 1–6. IEEE, January 2012.

[106] Chin-Sean Sum, Liru Lu, Ming-Tuo Zhou, Fumihide Kojima, and Hiroshi Harada. Design considerations of IEEE 802.15.4m low-rate WPAN in TV white space. *IEEE Communications Magazine*, 51(4):74–82, April 2013.

[107] Haleh Tabrizi, Golnaz Farhadi, and John M Cioffi. Tethering over TV White-Space: Dynamic Hotspot Selection and Resource Allocation. In *2013 IEEE 78th Vehicular Technology Conference (VTC Fall)*, pages 1–6. IEEE, September 2013.

[108] Tanim M Taher, Roger B Bacchus, Kenneth J Zdunek, and Dennis A Roberson. Long-term spectral occupancy findings in Chicago. In *Proceedings of IEEE International Symposium on Dynamic Spectrum Access Networks (DySPAN)*, pages 100–107, May 2011.

[109] TGn. IEEE 802.11-03-0940-04-000n-tgn-channel- models. Technical report, 2004.

[110] P. Tuset-Peiro, A. Angles-Vazquez, J. Lopez-Vicario, and X. Vilajosana-Guillen. On the suitability of the 433 MHz band for M2M low power wireless communications: propagation aspects. *Transactions on Emerging Telecommunications Technologies*, 2013.

[111] Jaap van de Beek, Janne Riihijärvi, Andreas Achtzehn, and Petri Mähönen. TV White Space in Europe. *IEEE Transactions on Mobile Computing*, 11(2):178–188, February 2012.

[112] Gabriel Villardi, Yohannes Alemseged, Chen Sun, Chin-Sean Sum, Tran Nguyen, Tuncer Baykas, and Hiroshi Harada. Enabling coexistence of multiple cognitive networks in TV white space. *IEEE Wireless Communications*, 18(4):32–40, August 2011.

[113] Jianfeng Wang Jianfeng Wang, Myung Sun Song Myung Sun Song, S Santhiveeran, Kyutae Lim Kyutae Lim, Gwangzeen Ko Gwangzeen Ko, Kihong Kim Kihong Kim, Sung Hyun Hwang Sung Hyun Hwang, M Ghosh, V Gaddam, and K Challapali. First Cognitive Radio Networking Standard for Personal/Portable Devices in TV White Spaces, 2010.

[114] Junyi Wang, Tuncer Baykas, Stanislav Filin, M Azizur Rahman, Chunyi Song, and Hiroshi Harada. Coexistence protocol design for autonomous decision-making systems in TV white space. In *2012 IEEE Wireless Communications and Networking Conference (WCNC)*, pages 3249–3254. IEEE, April 2012.

[115] W. Webb. *Understanding Weightless.* Cambridge University Press, Cambridge, 2012.

[116] W. Webb. Weightless. *International Journal of Interdisciplinary Telecommunications and Networking*, 4(2):30–37, January 2012.

[117] Matthias Wellens, Jin Wu, and Petri Mähönen. Evaluation of Spectrum Occupancy in Indoor and Outdoor Scenario in the Context of Cognitive Radio. In *2007 2nd International Conference on Cognitive Radio Oriented Wireless Networks and Communications (CROWNCOM)*, pages 420–427. IEEE, August 2007.

[118] C Wietfeld, H Georg, S Gr, C Lewandowski, and J Schmutzler. Wireless M2M Communication Networks for Smart Grid Applications. *Energy*, pages 275–281, 2011.

[119] Jie Bang Yan and Jennifer T. Bernhard. Study of digital TV signal reception in domestic indoor environment. In *IEEE Antennas and Propagation Society, AP-S International Symposium (Digest)*, 2009.

[120] Bo Yang, Guangxi Zhu, Weimin Wu, and Youjun Gao. M2M access performance in LTE-A system. *European Transactions on Telecommunications*, 25:3–10, 2014.

[121] Sixing Yin, Dawei Chen, Qian Zhang, Mingyan Liu, and Shufang Li. Mining Spectrum Usage Data: A Large-Scale Spectrum Measurement

Study. *IEEE Transactions on Mobile Computing*, 11(6):1033–1046, June 2012.

[122] Xuhang Ying, Jincheng Zhang, Lichao Yan, Guanglin Zhang, Minghua Chen, and Ranveer Chandra. Exploring indoor white spaces in metropolises. In *Proceedings of the 19th annual international conference on Mobile computing & networking - MobiCom '13*, page 255, New York, New York, USA, 2013. ACM Press.

[123] O. Younis and S. Fahmy. HEED: a hybrid, energy-efficient, distributed clustering approach for ad hoc sensor networks. *IEEE Transactions on Mobile Computing*, 03, 2004.

[124] Adel Youssef, Mohamed Younis, Moustafa Youssef, and Ashok Agrawala. Distributed formation of overlapping multi-hop clusters in wireless sensor networks. In *GLOBECOM - IEEE Global Telecommunications Conference*, 2006.

[125] Y. Zhang, R. Yu, M. Nekovee, Y. Liu, S. Xie, and S. Gjessing. Cognitive machine-to-machine communications: visions and potentials for the smart grid. *IEEE Network*, 26(3):6–13, May 2012.

[126] Yan Zhang, Rong Yu, Shengli Xie, Wenqing Yao, Yang Xiao, and Mohsen Guizani. Home M2M networks: Architectures, standards, and QoS improvement. *IEEE Communications Magazine*, 49(4):44–52, April 2011.